The Effects of Textured Foot Orthoses on Lower Leg and Plantar Foot Intrinsic Muscle Activity during Walking

Kelly Robb
robb8660@mylaurier.ca

The Effects of Textured Foot Orthoses on Lower Leg and Plantar Foot Intrinsic Muscle Activity during Walking

by

Kelly A. Robb

A thesis submitted in partial fulfilment of the requirements for

the degree of Doctor of Philosophy

Graduate Department of Kinesiology and Physical Education

Wilfrid Laurier University

DECLARATION OF CO-AUTHORSHIP / PREVIOUS PUBLICATION

I. Co-Authorship

I hereby declare that this thesis incorporates material that is result of joint research, as follows: Chapters 2, 3, 4 and 5 incorporates unpublished material that is authored by myself (Kelly Robb) under the supervision of Dr. Stephen Perry. In all cases the key ideas, primary contributions, experimental designs, data analysis, interpretation, and writing were performed by myself; however, Dr. Stephen Perry contributed knowledge and guidance throughout each above-mentioned experimental step and created the data analysis programs for each experimental study.

I am aware of the Wilfrid Laurier's Senate Policy on Authorship and I certify that I have properly acknowledged the contribution of other researchers to my thesis, and if written permission from each of the co-author(s) to include the above material(s) in my thesis is required, these documents will get appended to my final thesis submission.

I certify that, with the above qualification, this thesis, and the research to which it refers, is the product of my own work.

II. General

I declare that, to the best of my knowledge, my thesis does not infringe upon anyone's copyright nor violate any proprietary rights and that any ideas, techniques, quotations, or any other material from the work of other people included in my thesis, published or otherwise, are fully acknowledged in accordance with the standard referencing practices. Furthermore, to the extent that I have included copyrighted material that surpasses the bounds of fair dealing within the meaning of the Canada Copyright Act, I certify that I have obtained a written permission from the copyright owner(s) to include such material(s) in my thesis.

I declare that this is a true copy of my thesis, (however final revisions will be made following my dissertation defence), as approved by my thesis committee and the Graduate Studies office, and that this thesis has not been submitted for a higher degree to any other University or Institution.

ABSTRACT

The global foot orthotic industry was estimated around $3 billion in 2017. Biomechanists and clinical researchers have used foot orthoses (FOs) to study their effects on kinetic, kinematic, and muscle activity, although the mechanisms defining how a FO functions remain unclear. Recently, a neuromotor paradigm has been proposed suggesting that a FO augments the sensory feedback from foot sole skin and subsequently reduces muscle activity while optimizing movement. Although this paradigm currently lacks supporting evidence, neurophysiological research has linked foot sole skin to motorneuron pools of the lower extremity. Furthermore, one potential method of intentionally stimulating sensory feedback from the foot sole is to target the activation of cutaneous mechanoreceptors within the design of FOs. Thus, the overall objective of this dissertation was to design a series of experimental studies which uses texture in FO design to intentionally stimulate mechanoreceptors in foot sole skin, and then measure the modulation of lower leg and plantar foot intrinsic muscle activity during locomotor tasks. By studying the effects of textured foot orthoses (FOTs) on muscle activity, this novel approach to FO design will support or refute the defining principles of the neuromotor paradigm, while also providing mechanistic insight into the provision of FOTs.

The results of study 1 confirmed that texture placed under distinct regions of the foot sole can modify lower leg muscle activity during walking. More specifically, distinct regions of tactile feedback demonstrated stimulation-site and gait-phase specificity in the modulation of tibialis anterior, peroneus longus, medial gastrocnemius, extensor digitorum longus, extensor hallucis longus, tibialis posterior, flexor digitorum longus, and flexor hallucis longus during walking. These results support the topographical organization of cutaneous mechanoreceptors in foot sole skin and is the first study exploring how texture can be used in FO design to target the modulation of lower leg muscle activation during locomotion. Study 2 explored the use of texture along the entire length of the foot sole while measuring muscle activity of 4 plantar intrinsic foot muscles (abductor hallucis, transverse head of adductor hallucis, flexor digitorum brevis, and abductor digiti minimi)

during walking. Similar to study 1, results of this study demonstrated phasic modulation of foot intrinsic musculature that was apparent throughout the stance and swing phases of gait. In studies 3 and 4, previously collected data from studies 1 and 2 subdivided the results by foot posture. Using a commonly adopted clinical tool, the Foot Posture Index, results from these studies provided evidence which supports the variability in lower leg and plantar intrinsic foot muscle activation across the foot posture spectrum. Future research exploring texture in FO design is encouraged to consider foot posture when designing experimental protocols.

Overall, this dissertation provides evidence which supports the use of textured materials in FO design while increasing the data available to the scientific community in developing new FO-related research questions. In the interest of distilling the connection between cutaneous mechanoreceptors of the foot sole and muscles' of the lower extremity and foot, this dissertation suggests the following revision to the neuromotor paradigm: "FOs can modify sensory output to the central nervous system (CNS), and subsequently facilitate and/or inhibit motorneuron pool activation of lower extremity and foot intrinsic musculature during movement". Future research is now encouraged to ask new questions and develop new experimental protocols which support or refute this paradigm.

ACKNOWLEDGEMENTS

To Dr. Perry: As I sit down to write these acknowledgements, I can't help but recall a few years back when Katrina and I walked out of your office: KR to KP: "Did he just break up with us?" KP to KR: "Yup! That just happened!". It was a meeting that you called between the three of us, very unexpectedly, and told us that you were stepping back from hand holding, and the remainder of our PhD was our responsibility. I recall feeling frustrated and confused, but admittedly, I slowly began to appreciate the significance of this meeting. Thinking back, I appreciate the independence and personal growth you help guide, rather than control. You allowed me to make mistakes, laughed at them at times, and then allowed me to make more… but you never told me what to do. Although this independence comes with challenges, I appreciate the ability to pave my own academic career alongside your guidance. Thank you.

And.. No, you can't retire, not yet anyways.

To my committee members, Dr. Kalmar and Dr. Bent: I am still in awe of both you ladies! You are both remarkable female scientists in which I feel privileged to have worked with. I have felt challenged, overwhelmed, and cared for… all at the same time. I wouldn't expect anything different, nor would have wanted it any other way. Thank you for being an inspiration throughout this academic journey.

To my profession: This research is as much mine as it is yours. **To M:** Your support throughout this process has been invaluable. I appreciate the calls where you just listen and remind me that it's all worth it. I appreciate your friendship and tireless academic conversations on topics that no one else will engage in.

To HBO: This PhD would have never happened without you. Thank you for the continual reminders that the strongest women in the world lead by example and never stop asking questions. Thank you for holding my motivation when I've needed to walk away and thank you for highlighting the small wins towards the achievement of this larger goal.

And to P: don't ever lose your inquisitiveness and desire to keep learning. I love you monkey.

Table of Contents

LIST OF TABLES

LIST OF FIGURES

LIST OF APPENDICES

GLOSSARY

Afferent	A nerve fiber that carries action potentials to the central nervous system. For example, a sensory afferent nerve carries action potentials from skeletal muscle spindles to the spinal cord.
Base of support	The surface area in which a body is in contact with the ground. The size of area is defined by the distance of each segment. For example, when standing on the ground, the base of support is defined by the distance between both feet, and the length of each foot respectively.
Center of pressure	An arbitrary point on the ground representing the net ground reaction force of a body.
Center of mass	A point which represents the average position of a body's total mass.
Dynamic stability	The continual motion of a body's center of mass within its base of support.
Efferent	A nerve fiber that carries action potentials away from the central nervous system. For example, an efferent motor nerve carries action potentials from the brain and spinal cord to skeletal muscles.
Electromyography	The measure of electrical activity of a skeletal muscle. This measurement can be performed with surface electrodes over the skin surface, or with indwelling (fine-wire) electrodes inserted through the skin, into the muscle belly.
Excitatory pathway	A pre-synaptic nerve depolarizes a post-synaptic nerve, generating an action potential and signal transmission from one nerve to another.
Foot orthoses	A device placed under the foot, with intent of modifying biomechanical alignment, providing cushioning under the foot, or enhancing sensory information to the mechanoreceptors in the skin of the plantar foot sole. A foot orthosis (or foot orthoses) can be a generic prefabricated device matched to a foot posture, and/or a custom-made device individually manufactured for the wearer.
Golgi tendon organ	A receptor located in the tendinous portion of skeletal muscle that is responsive to muscle tension.

Ground reaction force	A force which opposes gravity, generally in the vertical direction when a system is in contact with the ground. The force is equal to the sum of all distributed forces applied to the ground surface.
Inhibitory pathway	A pre-synaptic nerve does *not* depolarize the post-synaptic nerve. No action potential is generated to the post-synaptic nerve.
Kinematics	A branch of study measuring motion of a system. Examples include velocity, acceleration, and angular displacement.
Kinetics	A branch of study measuring forces, or causes of motion, acting on a system. Examples include power, impulse, and momentum.
Meissner corpuscle	A type 1 rapid adapting mechanoreceptor (RAI) located in human skin.
Merkel cell	A type 1 slow adapting mechanoreceptor (SAI) located in human skin.
Mechanoreceptor	A receptor which is sensitive and responds to mechanical pressure/deformation within the tissue it resides. For example, a cutaneous mechanoreceptor is located in the skin. This type of receptor is responsive to various touch modalities, including stroking, skin stretch and vibration.
Microneurography	An electrophysiological tool to measure and record nerve impulse trains through a nerve fiber.
Muscle spindle	A receptor located in skeletal muscle that is responsive to rate and muscle length changes.
Neuromotor paradigm	A foot orthoses paradigm which theorizes the effectiveness of foot orthoses. The paradigm is grounded in the concept that foot orthoses provide enhanced sensory information under the foot, to intentionally modify muscular activity.
Pacinian corpuscle	A type 2 fast adapting mechanoreceptor (SAII) located in human skin.
Pes cavus	A foot posture characterized by a high medial longitudinal arch. Pes cavus feet typically demonstrate supinated subtalar joint positions in static weight-bearing.
Pes planus	A foot posture characterized with a low, or ‘flat’, medial longitudinal arch. Pes planus feet typically demonstrate pronated subtalar joint positions in static weight-bearing.

Pes rectus	A foot posture characterized by a neutral medial longitudinal arch. The subtalar joint is typically aligned with the calcaneus and tibia.
Ruffini ending	A type 2 slow adapting mechanoreceptor (SAII) located in human skin.

LEGEND (acronyms used throughout the chapters)

AP	Anteroposterior
AFO	Ankle Foot Orthoses
BBS	Berg Balance Scale
BOS	Base of support
COM	Center of mass
COP	Center of pressure
CPG	Central pattern generator
CNS	Central Nervous System
EMG	Electromyography
FA	Fast-adapting (receptor)
FAI	Fast-adapting Type 1
FAII	Fast-adapting Type 2
FFI-R	Revised Foot Function Index
FHSQ	Foot Health Status Questionnaire
FO	Foot orthotic
FOs	Foot orthoses
FOT(s)	Textured foot orthosis(es)
FPI	Foot Posture Index
GRF	Ground reaction force
GTO	Golgi tendon organ
ML	Mediolateral
MLA	Medial longitudinal arch
MS	Multiple Sclerosis
MTPJ	Metatarsalphalangeal joint
MVIC	Maximum voluntary isometric contraction
PD	Parkinson’s Disease
PHP	Plantar heel pain
PPT	Pain perceptual thresholds
RMS	Root mean square
sEMG	Surface electromyography
SA	Slow-adapting (receptor)
SAI	Slow-adapting Type 1
SAII	Slow-adapting Type 2
SC	Spinal cord
SOP	Standard Operating Procedures
SP	Superficial peroneal (nerve)
STJ	Subtalar joint
TUG	Timed Up and Go

Muscles:

AbdH	Abductor hallucis
AddH	Adductor hallucis
AddH-T	Adductor hallucis (transverse head)
ADM	Abductor digiti minimi
BF	Biceps femoris
EDL	Extensor digitorum longus
EHL	Extensor hallucis longus
ES	Erector spinae
FDB	Flexor digitorum brevis
FDL	Flexor digitorum longus
FHL	Flexor hallucis longus
GMax	Gluteus maximus
GMed	Gluteus medius
GMin	Gluteus minimus
GR	Gracilis
MG	Medial gastrocnemius
LG	Lateral gastrocnemius
PL	Peroneus longus
PB	Peroneus brevis
RF	Rectus femoris
SOL	Soleus
SR	Sartorius
SM	Semimembranosus
ST	Semitendinosus
TA	Tibialis anterior
TP	Tibialis posterior
VL	Vastus lateralis

CHAPTER 1

1.1 INTRODUCTION

Foot orthoses (FOs) are common medical devices used for people who experience foot discomfort and pain. Orthoses have proven successful in reducing painful symptomology, secondary to conditions such as lower limb arthritis, injury, and impaired walking patterns. Commonly treated conditions include plantar fasciitis/plantar heel pain, offloading of diabetic ulcers, lower limb tendinitis and arthritis, and overall ankle and foot pain. The global foot orthotic industry was estimated around $3 billion in 2017 and assumed to grow by 6% between 2018 and 2023 [1].

The term 'orthotic' predates the 1970s with biomechanical literature predominantly focusing on kinetic and kinematic analyses. The use of FOs has been studied extensively in areas such as biomechanical abnormalities [2], overuse injuries [3], and in the treatment of common pathological conditions [4]. Although commonly studied across scientific literature, authors are summarizing the effectiveness of foot orthoses (FOs) as being 'inconclusive', 'controversial' and thus 'requiring further research' [2,3,5–7]. It is arguable that these conclusions are largely due to a misunderstanding of the mechanistic paradigm supporting the use of FOs [8,9]. Furthermore, it is possible that some of the inconclusive and conflicting results within the FO literature are due to methodologically different experimental designs. Such differences can include discrepancies across interventions, experimental protocols and/or FO designs. Until experimental protocols are harmonized, researchers cannot expect to reach consensus for a mechanism of action supporting FOs use.

Broadly defined, a paradigm should encapsulate the frame of thoughts and previous literature which guides researchers in developing a research hypothesis [10]. Current FOs paradigms fall into three broad classifications: the kinematic, shock attenuation, and neuromotor control paradigms. Each of these paradigms consider the effectiveness of a FOs to be grounded in a distinct mechanism by which researchers assume FOs function. Each paradigm should include details pertaining to the orthotic manufacturing process and unique research-based experimental outcome measures that support the FO's intended purpose. One of the largest problems across FOs literature is the lack of research hypotheses being driven by strong paradigms. Furthermore, a paradigm should be tested, confirmed, refined and/or refuted, based on advancements in the scientific literature [10]. Arguably, today's FOs research is combining theoretical perspectives together and failing to develop hypothesis driven by paradigms, leading to reduced clarity on the mechanisms supporting FOs use.

The aim of this dissertation is to develop a series of studies to grow our understanding of the mechanism behind 'how' FOs function, and to translate these results into improvements in FOs design and knowledge advancements within the FO industry [6]. Two studies (4 different analyses) have been developed under the umbrella of one FO paradigm: the neuromotor paradigm. As this paradigm suggests that FOs function through a sensory change applied to the foot sole, texture has been incorporated into the FO design across all studies. Prior to discussing these FO paradigms, a general description of the gait cycle and normal foot are introduced.

1.2 THE GAIT CYCLE

An understanding of a 'normal' gait cycle in healthy populations is imperative in the foot orthoses industry. Normative gait provides a baseline in which to quantify change. One complete gait cycle consists of the time interval between two consecutive foot falls of the same foot, which is equal to the initial contact of one limb to the subsequent initial contact of this same limb. Additional descriptive components of the gait cycle include the spatial-temporal parameters of gait, kinematic analysis, kinetic analysis, and muscle activity (as measured with electromyography (EMG)). The spatial-temporal parameters of gait include temporal descriptors of stance and swing, cadence, stride length and width, and walking velocity. Kinematic data typically describes the motion of the major joints in the lower leg, including the hip, knee, and ankle joints in the sagittal, frontal, and transverse planes. The most common kinetic measurement is ground reaction force under the foot during stance, and the combination of kinematic and kinetic data allows for the calculation of joint moments and powers [11,12].

1.2.1 Normal Kinetic and Kinematic Movement

The gait cycle is typically divided into two major components: stance and swing. Stance phase occupies 60% of the gait cycle and the remaining 40% is swing. Stance can be further divided into single and double support, with single support being characterized by the contralateral limb moving from toe-off to initial contact. Experimental research commonly focuses on the stance phase of gait, as an individual is most susceptible to balance disturbances while load is transferred across the weighted limb. Consequently, stance is commonly subdivided into three additional phases: initial contact, midstance, and toe-off. The kinematic and kinetic activity of the hip, knee, and ankle, for these major events during stance are summarized below.

During initial contact, following terminal swing, the hip begins to extend, the knee flexes to absorb weight transfer and the ankle moves through plantarflexion. Ankle plantarflexion is accompanied by slight pronation of the subtalar joint and internal rotation of the tibia, although remains supinated throughout the duration of initial contact. There is a subsequent extensor moment at the hip, a flexor moment at the knee, and a dorsiflexion moment at the ankle. Power is generated at the hip and knee. Initial contact occupies approximately 0-12% of the gait cycle. At midstance, the hip continues to extend, the flexed knee transitions into extension, and the ankle moves into dorsiflexion as weight shifts over the tibia. The hip and knee have transitional moments while full load is accepted; the hip transitions from an extensor moment into a flexor moment, and the knee moment moves from flexion into extension, while the ankle continues a plantarflexion moment. The supination moment of initial contact peaks at midstance, transitioning into midfoot pronation, and is accompanied by tibial internal rotation. Midstance occupies approximately 7-32% of the gait cycle. At terminal stance, around 50% of the gait cycle, the limb is preparing to push off into swing. There are increased hip and knee flexor moments as the ankle and triceps surae muscle group produce a plantarflexion moment. The subtalar joint is normally resupinated, with accompanying rearfoot inversion and tibial external rotation. The midtarsal joint locks, increasing stability for push off across the entire forefoot into swing. During swing, the hip reaches maximum flexion mid-swing, where it transitions into flexion moving into initial contact. The knee reaches peak flexion early swing, then moves into extension, whereas the ankle maintains supination throughout the majority of swing. [11,12].

1.2.2 Phasic Muscle Activity during Gait

An indication of muscle function is gained through the study of the profiles of muscle activity during locomotion. Several studies have measured lower leg muscle activity (via electromyography (EMG)) during the gait cycle to establish normative EMG values through stance and swing. Phasic EMG refers to EMG with reference to various phases of the gait cycle; stance vs. swing, or the sub-phases within each. It should be noted that variance across EMG profiles is normal. Specific to healthy young adults, reduced variance has been observed in the distal lower leg muscles, especially those crossing a singular joint, compared to those in the upper leg. The coefficient of variation of distal muscles (tibialis anterior (TA), extensor digitorum longus (EDL) & peroneus longus (PL)) has been reported at 59%, whereas proximal muscles (rectus femoris (RF), sartorius (SR), biceps femoris (BF), semitendinosus (ST)) are 112% [13]. Secondly, there is a direct relationship between EMG amplitude and walking velocity. Although the general timing of muscle activity remains consistent, as walking velocity increases, EMG amplitude similarly increases. Normalized EMG profiles demonstrate an amplitude reduction of 30% in TA, 50% in vastus lateralis (VL), and 70% in RF and hamstrings when comparing between walking velocities of 2.25mph and 1.25mph [14]. This variability is important to recognize in the human locomotion of healthy individuals and should be expected when measuring muscle activity in experimental protocols during gait. Furthermore, this EMG variability reinforces the flexibility and adaptability of our muscular system to locomotor tasks, arguably an advantage of the muscular system [13].

Several authors [13,15,16] have studied the phasic profiles of lower leg musculature throughout the gait cycle. The ensemble averages of normative muscle activity during gait are outlined in Figure 1. An overview of major muscle groups is detailed below:

- The dorsiflexors, including tibialis anterior (TA), extensor digitorum longus (EDL) & extensor hallucis longus (EHL) concentrically contract to dorsiflex the foot and make ground clearance during swing. At initial contact, eccentric contraction occurs to decrease the forefoot to the ground.
- The TA, EDL, rectus femoris (RF), vastus lateralis (VL), hamstrings, gluteal maximus (GMax) & gluteal minimus (GMin) are considered the weight accepting muscles of the leg, with major peaks in muscle activity occurring in the initial 15% of stance.
- The superficial (medial gastrocnemius (MG), lateral gastrocnemius (LG), soleus (SOL) & peroneus longus (PL)) and deep plantarflexors (flexor digitorum longus (FDL), flexor hallucis longus (FHL) & tibialis posterior (TP)) concentrically contract during midstance, raising the heel off the ground in preparation for toe-off. Peak activity of the superficial posterior compartment leg muscles occurs at 50% of stance, corresponding to the push off phase of stance.
- The peroneus brevis (PBP muscle has a single burst of EMG, which peaks just prior to heel lift.
- TP demonstrates two bursts of EMG activity during gait. The first burst occurs immediately prior to initial contact (5% of gait cycle (GC)) and the 2nd burst occurs during midstance (35%GC).
- PL demonstrates an initial EMG peak at foot flat to control subtalar joint inversion (10%GC).
- The GMax and hamstring muscles (biceps femoris (BF) & semitendinosus (ST)) function to decelerate the forward progression of the swinging limb. Peak EMG activity occurs late swing, however continued into the early part of stance.
- The erector spinae (ES) muscle peaks approximately 10% & 60% of the GC. ES functions to control forward trunk rotation over weight acceptance (10% of gait for one limb and 60% of gait for the contralateral limb). [13,15,16]

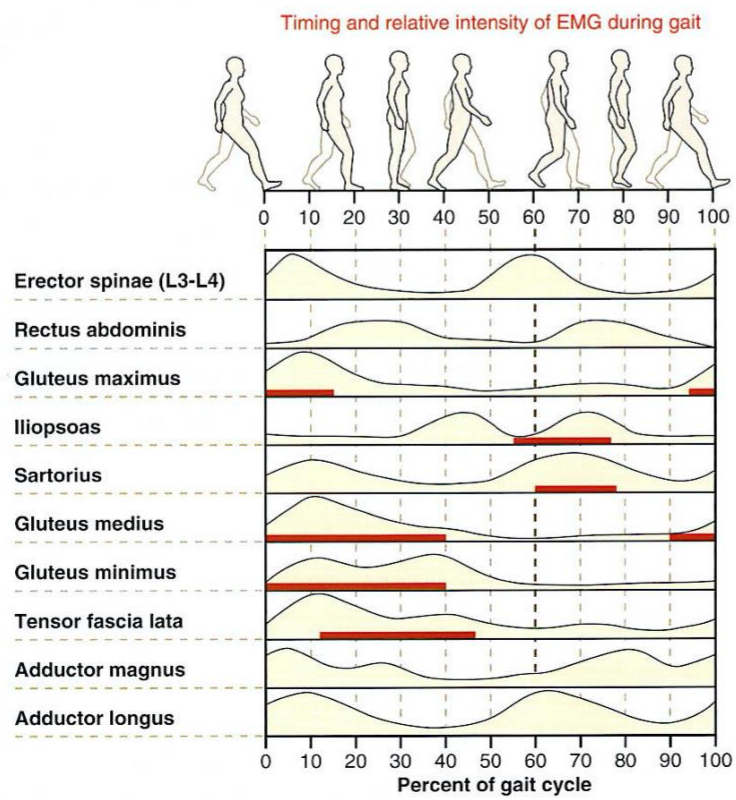

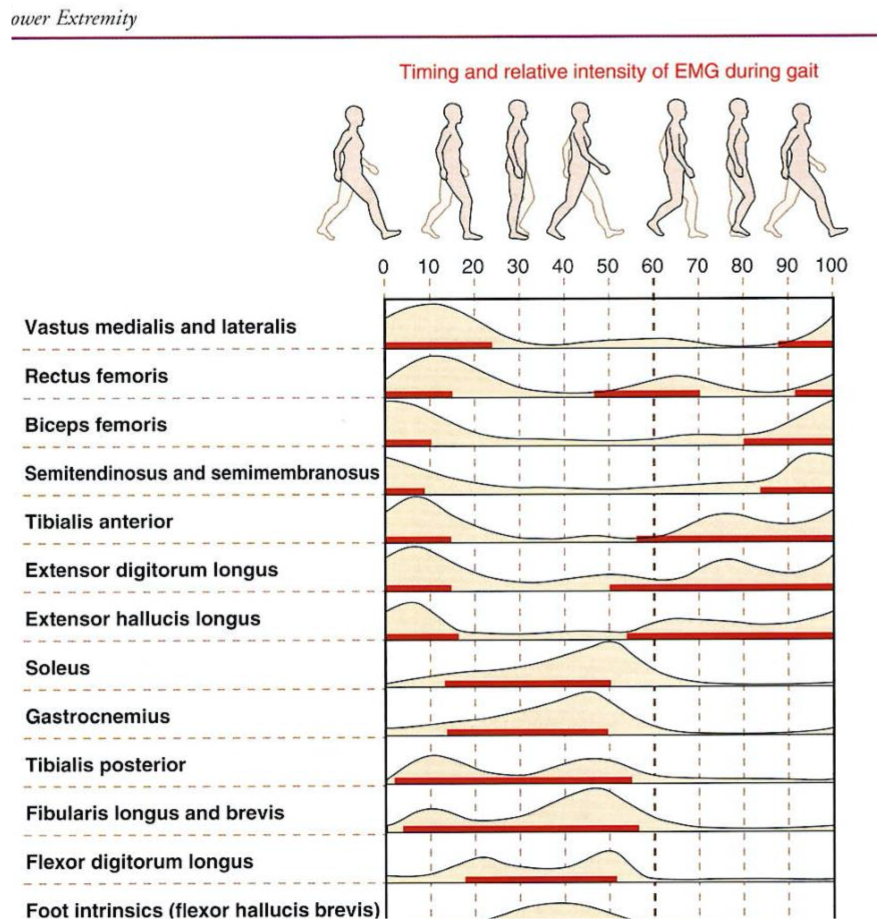

Figure 1. Normative timing of muscle activity throughout the gait cycle, from Kinesiology of the Musculoskeletal System, Donald A. Neumann (2017). Printed with permission from the publisher [17]

1.3 THE NORMAL FOOT

The normal foot is composed of 26 bones, 30 joints and 100+ muscles. These muscles originate internal and external to the foot, stabilize the osseous structures, and passively and actively generate force to produce normal locomotor movement. The foot is commonly divided into two general areas: the ankle and the foot. The ankle, also termed the talocrural joint, is composed of the tibia, fibula, and talus articulations. The foot is comprised of the tarsal bones, including all joints distal to the ankle. There are three general regions to the foot: the rearfoot, midfoot, and forefoot. The rearfoot, also termed hindfoot, consists of the talus, calcaneus and subtalar joint. The midfoot includes the remaining tarsal bones, the medial and lateral longitudinal arches, and the distal transverse arch across the metatarsal heads. The forefoot consists of the metatarsals and phalanges, including metatarsal and tarsometatarsal joints. Together, the bones, joints, and musculature of the foot, functionally interact to absorb shock, support body weight, and transfer load throughout locomotor activities.

1.3.1 Osteology

The tibia and fibula are the two long bones of the leg. The tibia is located on the anteromedial side of the lower leg, superiorly articulates with the femur, and anteriorly articulates with the talus. The tibia is the second largest bone in the body and plays a large role in supporting body weight. The fibula functions as an attachment site of leg muscles and increases stability of the ankle joint. The talus directly articulates with the tibia to receive the weight of the body. The calcaneus, commonly termed ‘heel bone’ is the largest and strongest osseous structure of the foot. When weightbearing, the inferior surface of the calcaneus is in contact with the ground. The calcaneus transfers body weight from the talus to the ground and anteriorly articulates with the cuboid [18].

The tarsal bones of the midfoot include the navicular, cuboid, and medial, intermediate, and lateral cuneiforms bones. The proximal surface of the navicular articulates with the talus forming the talonavicular joint. The medial surface of the navicular is a palpable surface anatomy landmark and is an important distal attachment to the tibialis posterior muscle. The cuboid is a distolateral tarsal bone, which distally articulates with the 4^{th} and 5^{th} metatarsals [18]. The three cuneiform bones contribute to the transverse arch of the foot, contributing to the convexity of the dorsal aspect of the midfoot [19]. This convexity is prominent in pes cavus ("high arch") feet.

The five metatarsals and phalanges of the forefoot are numbered 1 to 5 from the medial to lateral side of the foot. A "ray" consists of each respective metatarsal and accompanying phalange. The first metatarsal bone is the shortest, yet thickest, a reflection of the large distal-medial forces passing through the forefoot during the push off phase of the gait cycle [19]. The first ray has an important functional role during locomotion. As walking terrain and rearfoot positioning varies through stance, the first ray maintains the forefoot in a plantigrade position, assisting hallux dorsiflexion and enabling effective propulsion.

1.3.2 Arthrology

There are three major joints of the foot and ankle: the talocrural, subtalar, and midtarsal joints. Normal movement of these joints occur about three axes of rotation. Ankle dorsiflexion and plantarflexion describes motion that is parallel to the sagittal plane, about the mediolateral (ML) axis of rotation. Ankle inversion/eversion describes motion parallel to the frontal plane about the anteroposterior (AP) axis, and abduction/adduction describes motion parallel to the transverse plane about a vertical axis. The terms pronation and supination are commonly use terms in the foot orthoses industry. Pronation is the combined motion of eversion, abduction and dorsiflexion, whereas supination is inversion, adduction and plantarflexion [19].

The talocrural joint, commonly termed 'ankle joint', is a hinged synovial joint formed between the distal ends of the tibia and fibula, and superior aspect of the talus. The joint is strengthened by a joint capsule, interosseous membrane, and anterior and posterior ligamentous structures. The lateral side of the ankle is reinforced by the anterior talofibular, posterior talofibular and calcaneofibular ligaments. Medially, the deltoid ligament strengthens the joint with distal attachments to the talus, calcaneus and navicular [18]. The talocrural joint has an important functional role during locomotion. In static stance, 90-95% of compressive forces pass through the talus and tibia. Although the lateral malleolus sits slightly inferior and posterior to the medial malleolus, and thus causes slight deviation from the ML axis, the talocrural joint is primarily responsible for dorsiflexion and plantarflexion of the ankle. In open kinetic dorsiflexion (i.e. the foot is unloaded), the talus rolls forward relative to the leg as it simultaneously slides posteriorly. The opposite occurs during ankle plantarflexion. During initial contact of gait, the ankle joint rapidly plantarflexes to lower the forefoot to the ground. By foot flat, the ankle moves through dorsiflexion until toe-off, at which point the joint reaches its most stable position. This is important, as compression forces at propulsion can reach four times one's body weight [19].

The subtalar joint is comprised of the talus and calcaneus. In weight-bearing, the combined motions of pronation and supination occur as the leg and talus move over the relatively fixed calcaneus. Joint stability is provided by the calcaneofibular ligament resisting inversion and the deltoid ligament resisting eversion [19]. The foot orthotic industry places substantial attention on the subtalar joint. During close kinetic chain motion, there is no limitations on frontal plane motion of the subtalar joint. As the foot is fixed on the ground, the joint can easily invert and evert in response to lower leg rotation. Therefore, when a foot orthosis limits subtalar joint motion, there are consequential affects to the range and direction of joints proximal and distal to it. The 'normal foot' is reported to have a 2:1 ratio of supination to pronation of the subtalar joint, although ratios of 3:1 and 4:1 are quite common [20].

The midtarsal joint is a combination of the talonavicular and calcaneocuboid joints. Essentially, these two joints connect the rearfoot to the midfoot. The talonavicular joint is the articulation between the talus and navicular, whereas the calcaneocuboid joint is comprised of the calcaneus and cuboid. Movement of the midtarsal joint is commonly accompanied by subtalar joint movement during weightbearing activities.

1.3.3 Muscles of the Foot and Ankle

Musculature of the foot and ankle are comprised of both extrinsic (proximal attachment of the muscles is in the leg) and intrinsic (proximal and distal attachments are within the foot) muscles. The extrinsic muscles of the leg are divided into four major compartments: anterior, lateral, superficial posterior and deep posterior. The anterior compartment of the leg includes the tibialis anterior (TA), extensor digitorum longus (EDL) extensor hallucis longus (EHL), and fibularis tertius. These muscles are innervated by the deep branch of the fibular nerve. The lateral compartment muscles include peroneus longus and brevis and are also innervated by the fibular nerve. The superficial posterior compartment includes the medial gastrocnemius (MG), lateral gastrocnemius (LG), and soleus (SOL) muscles. The deep compartment includes the tibialis posterior (TP) and both flexors (flexor digitorum longus (FDL) and flexor hallucis longus (FHL)). Both superficial and deep posterior compartments are innervated by the tibial nerve.

There is one intrinsic muscle on the dorsum of the foot: the extensor digitorum brevis. All remaining intrinsic muscles of the foot are commonly described in layers, running superficial to deep on the plantar aspect of the foot. These muscles include: layer 1: flexor digitorum brevis (FDB), abductor hallucis (AbdH) and abductor digiti minimi (ADM); layer 2: quadratus plantae (QP) and lumbricals; layer 3: adductor hallucis (AddH), flexor hallucis brevis (FHB) and flexor digiti minimi; and layer 4: plantar and dorsal interossei. All plantar intrinsic muscles are innervated by the lateral and medial plantar nerves [18,19].

Kinematic, kinetic, and EMG analysis of the lower extremity and foot are common variables of interest in the study of biomechanical gait analysis. In the foot orthotic industry, foot orthoses (FOs) are inserted between the foot sole and walking surface interface to selectively modify these kinematic, kinetic and muscle activity outcome measures. Interestingly, several paradigms have been proposed to explain the mechanisms behind “how” FOs function, with each selectively aiming to modify one (or several) of these outcomes of interest. The literature pertaining to these paradigms is discussed below.

1.4 PARADIGMS SUPPORTING FOOT ORTHOSIS FUNCTION

1.4.1 Kinematic Paradigm

In the late 60s and early 70s, Merton L. Root and associates pioneered the theoretical foundations governing the prescription, casting, and fabrication of foot orthoses. The “Rootean Theory”, now termed ‘traditional kinematic paradigm’, focused on the functional importance of the subtalar joint during gait. Root coined the term “subtalar neutral”, to suggest a subtalar joint position which is neither pronated nor supinated in a non-weightbearing position [21]. Deviations from this “neutral” position, is presumed to increase risk of lower limb overuse and injury. More specifically, if subtalar joint pronation continues past midstance, the foot is unable to convert into a rigid lever for propulsion [22]. This disturbance to the normal temporal sequence of subtalar joint motion imposes functional limitations and/or demand on other joint structures of the lower limb. Consequently, this traditional kinematic paradigm focuses on the reduction and control of subtalar joint motion, achieved by placing a corrective foot orthotic (FO) under the plantar surface of the foot. The orthotic is intended to change the osseous alignment of the subtalar joint, restore the normal biomechanical relationship between the subtalar joint and lower extremities during stance, and subsequently decrease abnormal movement coupling up the kinetic chain [21]. The reduction of subtalar joint motion, coupled by the reduction in tibial rotation, is presumed to decrease the risk of overuse and injury.

Although FO research under this paradigm has been studied extensively, both in locomotion analysis and in various pathological populations [23–25], mixed empirical results have led to questions surrounding its validity. Subtalar joint (STJ) motion is typically measured by the magnitude (total amount of rearfoot eversion) and velocity (rate of calcaneal rearfoot eversion) of 3D calcaneal motion. In 1993, McCulloch et al. [22] reported that wearing FOs significantly reduced the magnitude and rate of calcaneal eversion velocity during 2 and 3mph treadmill walking. This study’s overall conclusions indicated that orthotics reduced calcaneal eversion, considered a positive effect, as these individuals demonstrated improved biomechanics during walking and running. One year later, Eng & Pierrynowski [26] measured subtalar joint mechanics during walking and running using a similar symptomatic population (young adults experiencing activity-related foot and knee pain). These results oppose McCulloch, concluding that FOs had no effects to ankle and/or knee sagittal plane movement during either walking or running. There were two large differences between these two studies: 1) footwear was not standardized across both studies, subjects wore their own footwear in McCulloch [22], whereas it was standardized in Eng & Pierrynowski [26], and 2) the orthoses materials and fabrication processes differed. McCulloch used rigid and semi-rigid FOs to intentionally correct biomechanical alignment. Conversely, Eng & Pierrynowski posted a flat Spenco insole. In both studies, it is unclear if the FOs made full foot contact with the foot sole. The discrepancies between FO material properties and full foot contact makes it unclear how much each device controlled STJ motion. Furthermore, the subjects in McCulloch were routine FO wearers prior to the experiment. It is plausible that these early studies were highlighting the importance of an acclimatization period with prolonged FO wear. In other words, when STJ control is removed following a period of habituation, the overall calcaneal eversion movement appears to be increased – at least temporarily.

Stacoff et al. [27] arguably provided the strongest challenge to the kinematic paradigm with their investigation on the variability of footwear selection and the position of kinematic markers. It has been demonstrated that placing kinematic markers on the exterior of a shoe can overestimate osseous movement of the foot within footwear [27]. To quantify rearfoot and lower leg motion, Stacoff et al. [27] screwed bone pins into the calcaneus and proximal tibia of five male runners. When comparing three orthotic conditions (flat insole, MLA support only, and medial rearfoot wedges only), neither orthosis had an effect on reducing calcaneal eversion from the flat insole. Despite the inability to modify eversion movement, significant reductions in tibial internal rotation were observed when wearing rearfoot posted orthoses. These study results suggest that orthotics do not modify the tibiocalcaneal movement during running, however rearfoot valgus posting can successfully reduce tibial internal rotation.

Following Stacoff's bone pin study, a subsequent series of FO research examined the effects of FOs of various posting levels, with and without MLA support, and in differing footwear. Participant groups were generally limited to pes planus foot types (or "pronators"), with the intent of reducing and/or controlling excessive subtalar joint motion. From 2000, up until a recent 2018 systematic review, overall research conclusions remain controversial. It remains unclear if rearfoot wedging with MLA support increases the total reduction of calcaneal eversion and/or tibial internal movement [25,28–33]. Furthermore, the height, length, and material of the posting has varied across these studies, posing another challenge in interpreting these results. Lastly, Root's entire subtalar joint theory focused on returning the subtalar joint to "neutral". This neutral position is achieved by carefully casting the foot in this 'neutral' position and retaining this position when wearing foot orthotics. Rarely are studies explaining the casting procedures used in designing foot orthotics, if the participants were casted at all. It should be noted that a posted insole is not a foot orthosis, therefore any study using non-casted (i.e. non-custom foot orthoses) are instantly deviating from Root's original theory. Lastly, discrepancies between a weightbearing and non-weightbearing casting position have added to the confusion. When the entire subtalar joint neutral theory is based on the functional importance of the 'neutral' position during gait, and results are suggesting a reduction in calcaneal eversion with and without such 'neutral' position being achieved, researchers are challenging the significance of the STJ neutral position entirely [21].

Despite the continual controversy, there lacks the ability to draw clear conclusions supporting the kinematic paradigm. The optimal combination of casting method, posting, and FOs materials, targeting towards patient-specific outcome measures remains unclear. In the early 2000s, Nester et al. [28] explained that the response to FOs appears beyond kinematic changes. Two alternative suggestions were proposed: 1) FOs may modify the soft tissue and/or passive structures of the lower leg, and/or 2) FOs function by alternating the neurological control of gait [28]. These alternatives are explored in the next two paradigms.

1.4.2 Shock Attenuation Paradigm

The shock attenuation paradigm emphasizes the cushioning properties of foot orthoses (FOs). Under this paradigm, the chosen materials to manufacture a foot orthosis are more important than the casting process, a concept that differs from the previously described kinematic paradigm. FOs function by decreasing ground reaction forces at impact (i.e. initial contact of the gait cycle), which consequently reduces the risk of overuse injuries in healthy populations [34–36]. The underlying rationale suggests that the magnitude of force at impact is the direct cause of injury. Therefore, by reducing the vertical loading rate and impact forces, through FOs and softer materials, the increased shock absorption between the plantar surface of the foot and walking surface reduces the risk of injury.

During gait, transient force occurs between terminal swing and initial contact; as the moving foot contacts the ground, movement is terminated. This ‘impact force’ typically lasts 10-20ms and varies in magnitude and direction between healthy individuals [37]. Walking velocity, footwear type, FOs, and ground surface all contribute to this force vector, by modifying the required time to terminate foot movement. By increasing the compressibility of materials between the calcaneus and ground surface, this serves to reduce the transient forces by extending their application over a longer period of time. Although momentum exchange remains unaltered, a dissipation of force across longer periods minimizes peak force at impact [37]. The term ‘impact attenuation’ was thus defined as the capacity of reducing either the magnitude of the vertical GRF, the loading rate, axial tibial acceleration, and/or peak plantar pressures [37]. Each of these outcome measures have been explored across the footwear and FO literature.

The literature within the shock attenuation paradigm has demonstrated a clear relationship between the peak magnitude of the vertical ground reaction force (GRF) at initial contact and gait velocity in healthy populations. As gait velocity increases, the peak magnitude of the vertical GRF increases [38]. Secondly, the outcome variables of peak GRF and loading rate are closely related, whereby peak GRF magnitude is reduced with the gradual dissipation of transient forces over initial contact. Modifying midsole material and the type of footwear (cushioning vs. neutral vs. motion control) appears to decrease this impact transient [37,38]. Softer material appears to increase compressibility between the shoe and ground surface, and consequently reduces the peak vertical GRF. Conversely, experimental studies comparing the effects of FOs within similar footwear appears to have little effect on transient forces at initial contact [6,37,39,40]. Midfoot pronation appears to be one method of attenuating impact load over longer periods of time, and when wearing FOs, the device functionally reduces this desired midfoot movement. Two experimental studies strengthen this above-mentioned statement. When comparing FOs of various wedging (varus vs. valgus wedging), greater reductions in midfoot pronation during running were observed with higher impact loads [38]. Secondly, the use of lateral rearfoot wedges resulted in increased midfoot pronation and attenuated impact loading over longer periods of time [41]. To clarify, it appears that midfoot pronation is one method to attenuate impact load over longer periods of time. Consequently, studies using FOs to reduce midfoot pronation, may be counterproductive if the intention is to decrease impact load.

The pressure loading response at initial contact differs between various foot orthosis materials. When comparing soft and hard FOs, earlier forefoot load is observed in hard FOs [42]. Results of this study were determined with in-shoe pressure measurements, and arguably, the effect of FOs is a change in plantar pressure distribution rather than a change in loading response. Adding viscoelastic materials under the plantar foot sole, within orthoses design and/or footwear, appears to redistribute plantar pressures [41]. Secondly, recent studies have measured energy absorption of the tibialis posterior tendon, defined as a reduction in subtalar joint (STJ) moment, between footwear with and without custom foot orthoses. During early stance, wearing footwear alone and footwear with orthoses significantly reduced the supination moment and energy absorption at the subtalar joint [43]. As no differences between experimental conditions were observed, athletic footwear alone (rather than adding FOs) may prove sufficient in absorbing energy.

In summary, footwear and FOs alone appear to have minimal effect on loading rate and vertical ground reaction force. The shock attenuation paradigm favors the addition of viscoelastic materials and pressure redistribution, however, these variables do not further our understanding behind the mechanisms supporting FOs use. Adding to the confusion, a reduction in injury rate has been attributed to softer orthoses designs (compared to harder designs), suggesting that softer materials can minimize risk of injury [44]. The relationship between impact characteristics and the functional benefits of FOs appears unclear, and once again, supports research initiatives towards exploring alternative foot orthoses paradigms.

1.4.3 Neuromotor Paradigm

Alternative to the kinematic and shock attenuation paradigms, the neuromotor paradigm suggests that changes to the sensory input from the skin of the plantar surface of the foot may change muscle activity [45]. The concept of neuromotor control, encompasses two important elements: the skin of the foot sole interface and the outcome measure of muscle activity. Benno Nigg et al. [44,46] originally described a preferred movement path theory as a potential alternative paradigm supporting the use of shoe inserts towards the reduction of overuse running injuries. Overuse injuries, and subsequent overuse of muscular activity, is a direct response of skeletal deviation from one's 'preferred movement path'. An obvious outcome measure supporting this paradigm is the amplitude, duration, and fatigue of muscle activity when completing a given task. Interestingly, six years earlier, Nigg et al. [44,46] itemized several propositions related to this new paradigm. Of these, a FO was described as an important filter to the force signals under the plantar surface of the foot. More precisely, it's the soft tissues and cutaneous mechanoreceptors of the foot sole that receive these signals, which are subsequently transferred to the central nervous system (CNS). The CNS programs the output of muscular activity, allowing the individual to perform a given task [46]. Although intriguing, at the time, this proposed paradigm lacked subsequent research to validate these propositions.

When wearing a FO, the foot sole skin remains in contact with the orthotic, creating an influx of mechanical stimuli transmitted via sensory afferents to the spinal cord (SC). Recently, a new wave of research has explored FOs as an intervention tool to facilitate this sensory feedback. This sensory facilitation can be obtained via several mediums, including the addition of texture under the foot sole, electrical stimuli, and/or mechanical vibration. Irrespective of the selected medium, sensory stimulation aims to augment sensory input through decreasing the threshold of afferent firing. Within the context of this paradigm, the purpose of a FO is to modify muscle activity towards a more efficient movement pattern, whereby Nigg specifically states as a reduction in muscle activity. Arguably, excitability changes to a motorneuron pool can be characterized as either an increase or a decrease in muscle amplitude and requires context-specific application when defining “efficiency”. For example, a runner experiencing tibialis anterior (TA) tendinitis may benefit from a reduction in TA amplitude. If EMG recordings indicate a prolonged duration of TA activity over the entire duration of stance, this runner would likely benefit from a reduction in muscle amplitude. A more distinct on/off pattern at initial contact and toe-off is a functionally more appropriate bursting pattern for this muscle, and the reduction in prolonged activity will likely decrease overuse and fatigue. Conversely, an increase in TA activity may benefit an individual suffering from drop foot deformity. If the TA remains functional, although minimally active in electromyography (EMG) recordings, an increase in TA magnitude may increase one’s ability to successfully clear the ground during the swing phase of gait.

In this neuromotor paradigm, Nigg originally proposed that using soft FOs can improve muscle efficiency in running populations [44,46]. That being said, the reflex loop from skin to excite muscle is irrelevant to the orthosis construction itself. Changes in muscle activity may be achievable with both hard and soft FOs. Physiologically, this paradigm is grounded in the neurophysiological effects of skin stimulation on muscle activity, rather than FOs fabrication details, such as soft vs. hard shell materials. If the purpose of the orthosis is to stimulate mechanoreceptor activity, the casting process and material selection should reflect this intention. Suggested methods of accomplishing this goal are to select a casting method which maximizes full foot contact to the plantar surface of the foot, to theoretically increase the opportunity of cutaneous afferent firing, and adding ridges and textured top covers to increase mechanical stimuli. Currently, there isn’t any literature supporting the above-mentioned suggestions, and consequently remains theoretical in nature.

The remainder of this dissertation focuses on the neuromotor paradigm. Section 1.5 introduces basic neurophysiological properties that are important to consider when interpreting and understanding the physiological principles guiding the application of this paradigm. Section 1.6 summarizes the current literature supporting FOs use and sensory facilitation. Sections 1.7 highlights important considerations throughout the FO fabrication process. Lastly, the dissertation's overall objectives are summarized, and individual study details are included in chapters 2-5.

1.5 THE NEUROPHYSIOLOGY OF LOCOMOTION

There are two important elements within the neuromotor control paradigm: the plantar foot sole interface and the outcome measure of muscle activity. Neurophysiology and the neural circuitry between the foot sole and muscle defines the cellular processes by which we move. These processes are important for several reasons: 1) to understand the mechanisms which influence and modify motor output, 2) to understand the role of cutaneous afferents in human locomotion, and 3) to appreciate how motor output may change when afferent input into the spinal cord is modified.

The execution of locomotion consists of the dynamic interaction of three major systems: the descending drive of supraspinal centers, spinal circuitry, and sensory feedback. From a bottom-up approach, sensory organs, which include muscles, tendon, skin afferents, and special senses, provide feedback to the spinal networks. These sensorimotor inputs interact with the ongoing pattern generating networks in the spinal cord. The spinal cord acts as an integration center, receiving incoming afferent feedback and generating the necessary output to perform voluntary movement. Supraspinal centers act as the filter, which modifies, fine tunes, and steers the execution of smooth movement. Although the focus of this dissertation is to study the effect of facilitating foot sole mechanoreceptors (skin afferents) on locomotion, it remains imperative to appreciate all sensorimotor mechanisms at play during walking, therefore, a top-down approach to voluntary movement is also introduced to highlight the complete central nervous system's role in generating voluntary movement.

1.5.1 The Components of Neural Circuitry: An Overview

In the execution of locomotion, somatosensory receptors are responsible for providing afferent feedback to the central nervous system (CNS). The net effect of a sensory afferent is determined by either an excitatory or inhibitory synapse onto an interneuron, or directly onto a motor neuron [47]. The interneuronal selection, consequently varying the excitatory or inhibitory response, is modified according to a given task or phase within the gait cycle. Another important consideration is the role of descending drive from cortical and subcortical pathways which can modulate alpha motorneuron excitability and consequently modify net motor response. The powerful role in which descending systems can influence motor neurons is beyond the scope of this dissertation, yet important to appreciate in considering the modulatory effect on locomotion. Briefly, one of the largest roles of the motor cortex is to receive the multitude of sensory inputs and transform them into appropriate output commands. This coding includes the selective excitation and inhibition of muscle contraction within appropriate levels of force throughout the gait cycle [48]. The sensory inputs reaching supraspinal levels have important modulatory roles on gait initiation, termination, walking velocity, and the refinement of motor patterns [49,50].

In the top-down regulation of voluntary movement, supraspinal structures have monosynaptic (direct) and polysynaptic (indirect) connections to various spinal locomotor networks which can influence these locomotion centers to initiate, terminate, or modulate phase-specific behavior during cyclical movement [49]. For example, the brainstem and forebrain regions of the brain play an important role in the initiation and control of walking. The basal ganglia has direct projections onto the mesencephalic locomotor region (MLR) which is believed to prevent inactivity from this spinal center, specifically by keeping the MLR under tonic inhibition. Although the cerebral cortex is not considered a direct locomotor center, it exerts a powerful influence on locomotion by modulating the excitatory post-synaptic potentials of flexor and extensor muscles during walking [49]. Thus, this top-down regulation of voluntary movement is imperative to recognize in appreciating the diversity and specificity of its influences on spinal locomotor circuitry [51]. In the neuromotor control paradigm, neurophysiological attention remains a bottom-up approach, and although foot sole sensory feedback remains invaluable in responding to external environment changes during walking, top-down regulation should not be disregarded when considering modulatory inputs and spinal integration in the control of human locomotion.

To summarize, sensorimotor integration is dynamic throughout locomotion and mediated by spinal cord synaptic integration and influenced by descending inputs. These sensorimotor inputs are important to appreciate when interpreting the neurophysiological mechanisms which guide the application of the neuromotor paradigm. Sensory afferents, discussed below, consist of the sensory feedback that is relayed to the spinal cord from various sources of afferent sources, including Golgi tendon organs (GTOs), muscle spindles, and skin afferents.

1.5.2 Sensory Afferents

Sensory feedback is essential to maintain phasic motor patterns in walking [14]. There are various sensory receptors that relay information into the spinal cord. There are various sources of incoming sensory feedback, including muscle and joint receptors, and cutaneous mechanoreceptors in the skin. Afferents are classified into groups, ranging from type I to IV, from largest to smallest according to axon diameter. A brief explanation of these receptor type follows, with a larger focus on the mechanoreceptors in skin.

Muscle Spindles

Muscle spindles are sensory receptors encapsulated within and outside the connective tissue capsule of skeletal muscle. Spindles function to signal change in the magnitude and rate of muscle length. As a muscle changes length during joint movement throughout the gait cycle, sensory nerve endings of intrafusal muscle fibers are stretched [47,52]. In response to the muscle length change, the firing rate of sensory nerve endings increase, resulting in increased afferent input to the CNS. Equally important is the role of primary sensory endings in response to the velocity of fiber length change. As primary sensory endings are highly sensitive to velocity change, the transmission of rapid length changes is quick, and of particular importance during unexpected movements and/or balance perturbations [52].

Golgi Tendon Organs

Contrary to spindles, Golgi tendon organs (GTOs) are located in the musculo-tendon junction, between the skeletal muscle fibers and connective tissue. Throughout locomotion, active lengthening of skeletal muscle results in the collagen strands pinching the axons of Ib afferents. The discharge, or excitation, of these Ib afferents increase as muscle and connective tissue is stretched. GTOs monitor ongoing muscle force and the rate of change in force throughout locomotion [47,52].

Cutaneous Mechanoreceptors

Both spindles and GTOs provide feedback to the CNS. One final, albeit most important sensory component in this dissertation is the cutaneous afferent (comprised of the sensory nerve and mechanoreceptor ending). Cutaneous mechanoreceptors, located in the epidermis and dermis of our skin, respond to external information from the environment. As this dissertation focuses on the plantar foot sole interface, sources of external information may include changes in terrain, flooring surface, footwear, and/or foot orthoses. When a mechanical change is detected, the new tactile information causes displacement and indentation of the skin tissues. The mechanoreceptor sensory endings are stimulated, and relay this mechanical stimuli through sensory afferents to the CNS [53]. There are four different receptors which provide tactile feedback from pressure, vibration, and texture. As cutaneous tissue is impinged, Pacinian corpuscles, Meissner's corpuscles, Merkel's disks, and Ruffini endings are the low-threshold cutaneous mechanoreceptors transducing these mechanical forces into nerve impulses [54]. These cutaneous mechanoreceptors are subdivided based on their morphology, innervation pattern and depth within the skin [53]. Each have a unique sensitivity to different vibrotactile frequencies and preferred stimuli. Broadly speaking, they are classified as type I vs. type II based on the depth of receptor ending within the epidermal or dermal layers of the skin, and classified as slow-adapting vs. fast-adapting, based on their adaptation to sustained mechanical stimulation [55,56]. One further classification relates to the receptive field size. The cutaneous receptors closest to the skin surface (Merkel discs and Meissner corpuscles) have smaller receptive fields, whereas those deeper within the dermis (Ruffini endings and Pacinian corpuscles) have larger receptive fields [54].

Merkel disks are slow-adapting type I (SAI) receptors in the basal layer of the epidermis, commonly surrounding the sweat gland ducts of epidermal ridges. SAI's fire continuously during sustained indentation of the skin, with a particular sensitivity to edges, corners, and curvatures. The SAI discharge rate is linearly related to indentation depth [57]. Fast-adapting type I (FAI) receptors, known as Meissner corpuscles, lie in the dermal ridges beneath the epidermis. As fast adapting receptors, Meissner corpuscles will respond during initial and terminal contact of a mechanical stimulus to the skin [54]. They are four times more sensitive to dynamic skin deformation compared to SAIs, with a preferred stimuli response to detecting slip, skin motion, and the detection and discrimination of low frequency vibration [57]. Both SAIs and FAIs have small receptive fields with multiple hot spots.

Type II afferents do not branch within the skin, as do type I afferents. Type II's innervate a single, large mechanoreceptor located in the dermis or subcutaneous tissues of the skin [56]. Slow adapting type II receptors (SAII), known as Ruffini endings, are particularly sensitive to skin stretch. They have large receptive fields and are located in the connective tissue of the dermis. FAII's, or Pacinian corpuscles, lie deep in the dermis. They are a large onion like structure comprised of multiple epithelial layers [57]. They have an on-off response to mechanical stimuli, with a particular sensitivity to vibration. Pacinian corpuscles have large receptive fields with indiscriminate borders, suggesting a stimuli response to skin within and near their receptive field. This unique characteristic accounts for FAII's response to blowing across the skin surface [56].

Beyond this broad overview of cutaneous mechanoreceptor morphology and characteristics, the development of microneurography [58], initially used to study single cutaneous afferents from the skin on the palm of the hand and arm, has provided a tool to further understand skin receptor characteristics specific to the plantar surface of the foot. As to our current knowledge, the breakdown of afferent distribution across the foot sole of healthy adults comprises 48% FAIs, 21% SAIIs, 18% SAIs, and 13% FAIIs [56]. As this dissertation focuses on locomotor movement, the remainder of section 1.5.2 will highlight receptor characteristics pertaining specifically to the foot sole.

The receptive field characteristics of cutaneous afferents from the foot sole are similar to the glabrous skin on the palm of the hand. Type I afferents have small receptive fields (≈78mm^2 in the foot sole), distinct borders, and multiple hot spots. Conversely, type II afferents have larger receptive fields (≈560mm^2 in the foot sole), indiscriminate borders, and a zone of higher sensitivity [56,59]. Following a recent consolidation of several labs' microneurographic recordings, a sample of 364 cutaneous afferents have been extensively analyzed. The receptive field characteristics of each afferent class has been detailed in healthy adults, whereby the mean receptive field size has been reported as follows: FAI: 80.6 mm^2; FAII: 872.7 mm^2; SAI: 76.1 mm$^{2;}$ SAII: 248.1mm^2) [56]. These results align with previously reported values, which clearly demonstrate the differences between type I and II receptive field size. Secondly, these receptive field characteristics have been mapped according to distinct areas of the foot sole. Smaller receptive fields have been observed in the toes compared to the sole of the foot, suggesting the possibility of enhanced resolution of tactile feedback under the forefoot [56].

This research consolidation also divided firing thresholds by afferent class and region under the foot sole. Similar to traditional monofilament testing, regional variation was observed across firing behaviour. The mechanical thresholds of SAII's are higher compared to other afferent classes, FA thresholds are consistently lower than SAs, and thresholds are highest under the calcaneus compared to the lateral midfoot and forefoot. This regional variability in mechanical thresholds has been attributed to the differences in functional demand across various areas of the foot sole [56]. Lastly, three distribution gradients (proximal-distal of the entire foot sole, and medial-lateral of the midfoot and forefoot regions) of afferent class by foot sole region were detailed. FAI's have largest number of sampled afferents across all gradients. Innervation density is greatest in the distal toes and decreases towards the calcaneus. In the medial-lateral direction, the lateral forefoot and midfoot regions have the highest innervation density, which decreases towards the 1st metatarsal phalangeal joint and medial longitudinal arch [56].

The neural firing and afferent characteristics across the foot sole are imperative towards the development of new foot orthotic interventions. These cutaneous afferent details contribute to our understanding of how these receptors influence pressure modulation throughout locomotion. Innervation densities, afferent distribution, and firing characteristics assist in the selection of mechanical stimuli (texture vs. vibration) to facilitate receptor response. More specifically, these afferent characteristics were important details in the development of the textured design used in the experimental studies of this dissertation (described in section 1.7).

1.5.3 Nerve Stimulation Studies during Locomotion

Studies that examine the ways in which locomotor patterns change in response to modifying sensory input provides important insight into their effect on central pattern generator (CPG) organization. More specifically, nerve stimulation delivered during specific times throughout the gait cycle demonstrates locomotor-dependent reflexes which serve to regulate motorneuron activity during walking. From a functional standpoint, the effectiveness of reflexes during locomotion is heightened by their task and phase-dependent modulation [60]. Although much of our understanding of neural circuitry originates from mammalian research, this dissertation only reviews non-noxious nerve stimulation studies in humans. Furthermore, the focus will remain on the modulation of cutaneous reflexes during rhythmical locomotor tasks. Although cutaneous reflexes are not directly studied in any of the experimental protocols, results from these studies provide insight into their functional role during locomotion.

Early studies examining the effect of non-noxious electrical stimulation of cutaneous nerves revealed a task-dependent and phase-dependent response in lower leg muscles [61,62]. Since these studies, research has focused on understanding the functional relevance of cutaneous reflexes [63], the variability in locomotor response based on anatomical location of the stimulated nerve (nerve specific effects) [64], and response modification in diseased populations [65]. Three cutaneous nerves, each innervating distinct skin on the plantar and dorsal regions of the foot, contribute to our understanding of cutaneous feedback during locomotion. These nerves include the posterior tibial nerve (TIB) innervating the calcaneal region of the foot sole, the sural nerve which innervates the lateral border of the foot, and the superficial peroneal nerve (SP) innervating the foot dorsum. Furthermore, the resulting neuromechanical response from electrical stimulation to these nerves can be divided according to their task- and phase-dependent modulation throughout locomotion. Previous research has suggested a low percentage of the human population (only 14%) has a modulatory short-latency reflex response, and therefore, cutaneous reflexes are generally measured as a medium-latency responses (occurring approximately 80-120ms post electrical stimulus) [66].

The skin on the plantar sole of the foot mediates phase-dependent changes in muscle activity. Several studies have measured tibialis anterior (TA) muscle activity while stimulating the tibial nerve during walking. An increase in TA magnitude is typically accompanied by increased ankle dorsiflexion during late stance, which reverses to the suppression of TA activity and an increased ankle plantarflexion during late swing [63,67]. These electromyography (EMG) and kinematic changes provide evidence to support the importance of skin on the plantar sole of the foot during the stance to swing transition phase of gait. During late swing, ground contact is expected once weight is transferred to the limb, therefore the suppression of TA activity has been described as a placing reaction to ensure firm foot contact onto the ground [63].

As previously noted, throughout locomotion there are various sources of afferent information modulating SC excitability. Nakajima et al. (2008) designed an experimental protocol to determine if movement-related or load-related afferent feedback play a more important role in regulating these phase-dependent reflexes. Tibial and superficial peroneal (SP) nerve stimulation was delivered during treadmill walking under various loaded conditions. Study results revealed two interesting observations: phase modulation was absent during unloaded walking, and under the loaded conditions, the magnitude of the medium-latency reflex increased irrespective of the load. These results provide evidence to suggest that the phase-dependent modulation of cutaneous reflexes is independent of changes in motorneuron excitability. In other words, phase-dependent modulation is not simply a product of movement-related afferent feedback (muscles spindle and GTOs), but that the changes in excitability of the reflex pathways are mediated by cutaneous reflexes [68].

The importance of the skin on the dorsum of the foot has been investigated in stimulation studies to the superficial peroneal nerve. Cutaneous afferents from the foot dorsum have functional importance during the swing phase of the gait cycle. In early swing, the electrical stimulation to the SP nerve results in the suppression of TA muscle activity, which consequently suppresses ankle plantarflexion. These EMG changes are further supported by kinematic change; including an increase in ankle dorsiflexion and knee flexion, suggestive of lifting a limb over an obstacle during swing [63,67]. The facilitation of biceps femoris, vastus lateralis and semitendinosus muscles, with accompanying suppression of rectus femoris activity have also been suggestive to assist in knee flexion, hip flexion, or to increase stiffness across the knee joint [63,67]. These combined muscle and kinematics changes appear to mimic movement behaviour as if the dorsum of the foot hit an object during swing. This has been described as a ‘stumbling corrective response’, whereby muscle activity is coordinated to lift the limb in swing over the object and coactivation of antagonistic knee muscles stabilize the leg in stance [60,63,69].

The role of cutaneous afferents from the lateral foot border has been investigated via sural nerve stimulation. The net mechanical actions mimic a withdrawal response to stimuli activating the cutaneous field under this area of the foot. Sural nerve stimulation modulates ankle, knee, and hip kinematics during both stance and swing. In mid-to-late stance, medial gastrocnemius (MG) and TA activity are facilitated with accompanied increases in ankle dorsiflexion and eversion. During swing, muscle activity is similar to those demonstrated during a stumbling corrective response. TA muscle activity is highly correlated with increased ankle dorsiflexion, as vastus lateralis (VL) muscle activity is highly correlated with increased knee flexion [70].

These responses align with a withdrawal behaviour to move the foot away from undesired stimuli. The resultant force vector during stance suggests a flexion-inversion response to move the lateral border of the foot away from the stimuli, whereas in swing, the combined ankle and knee flexion suggests an angular trajectory change as if the lateral border of the foot hit an object, or if the foot prematurely hit the ground [60,70].

In summary, stimulation studies of cutaneous nerves during locomotion have highlighted the functional importance of cutaneous feedback throughout walking. During the stance phase of gait, cutaneous afferent stimulation provides stabilizing reactions while stimulation during swing generates a stumbling corrective response [69]. More recently, research exploring cutaneous reflexes in special populations and injury are slowly emerging [65,71,72]. The functional importance of direct stimulation to the foot sole will be summarized in study 1's introduction. To date, cutaneous afferent response has not been studied using foot orthoses, insoles, and/or texture under the foot sole. Research has predominantly focused on foot orthoses and sensory facilitation, albeit independent of each other, while some protocols have focused on foot posture variance in FO design.

1.6 CURRENT KNOWLEDGE ON FOOT POSTURE, FOOT ORTHOSES, AND SENSORY FACILITATION

1.6.1 The Effect of Foot Posture on Lower Leg Muscle Activity

In experimental protocols, the interaction between foot posture and lower limb biomechanics are traditionally measured with kinetic, kinematic, and EMG analysis. To quantify foot posture, three methods are commonly adopted (the Foot Posture Index (FPI), arch height index, and navicular height), yet these measurements are all performed in static stance to describe midfoot movement during dynamic locomotion. Although expensive and limited in availability, radiographic measurements of load-bearing osseous movement remain the closest to a gold standard in foot posture analysis. To date, between-foot posture analysis has revealed variability across plantar pressures of differing foot postures during walking in healthy adults [73].

Furthermore, comparisons between foot posture and select lower leg muscles have demonstrated variability across different medial longitudinal arch (MLA) heights. More importantly, abnormal foot postures have been associated with a higher risk of lower limb injuries [74]. These three points highlight the importance of understanding the differing biomechanical mechanisms linking foot posture to injury, and thus their effect on improved walking ability, yet this still remains unclear [73]. Skeletal muscle function has an evident role in osseous and joint interactions, however muscle activation may provide a clearer relationship to overuse injury and improved ambulation [75]. To date, the following observations have been reported across foot postures:

- In pes planus feet compared to normal arched feet (pes rectus), peak tibialis anterior (TA), and root mean square (RMS) amplitude are higher during the contact phase of gait. Peak peroneus longus (PL) & tibialis posterior (TP) activity are lower at contact during this same phase of gait.
- During midstance/propulsion, peak PL activity is reduced, whereas peak TP activity is greater in pes planus compared to normal arched feet (pes rectus).
- The magnitude of invertor muscle (TP, TA & flexor hallucis longus (FHL)) activity is greater in pronated (pes planus/flat arched) feet compared to supinated or normal foot posture.
- The magnitude of evertor muscle (PL) activity is reduced in pronated feet compared to supinated or normal (pes rectus) foot posture.
- No between-foot posture differences are observed in medial gastrocnemius (MG) activity.

  [16,75]

1.6.2 The Effect of Foot Orthotics on Lower Leg Muscle Activity

A scoping review was recently conducted to summarize the effects of foot orthotics, both prefabricated and custom devices, on muscle activity during locomotion. The results are summarized in Appendix 1. Most noteworthy is the challenge in making between study comparisons when evaluating the general effects of foot orthotics on muscle activity. The orthotic materials, casting, and fabrication process, window of electromyography (EMG) analysis, the method of EMG normalization, and the temporal and amplitude characteristics of EMG during gait, are all experimental factors which can be manipulated between protocols. Future research in the FO industry is encouraged to understand these between-study differences, acknowledge these differences when reporting results, and compare results only when appropriate.

1.6.3 The use of Textured Insoles as Sensory Facilitation

Currently, the addition of texture in foot orthoses (FOs) manufacturing and design is not common practice. Arguably, based on mixed results across the scientific literature, there still lacks sufficient research for the clinical community to understand its application and use. Various textured materials have been explored in insole design and applied to various populations under differing experimental tasks. A summary of our current understanding is provided below.

Textured Insoles and Postural Control

The largest area of textured insole research is in the domain of postural control. More specifically, the effects of texture on static stance and dynamic stability has been explored in both healthy young [76–79] and healthy older adults [77,80–88]. Four studies have used texture exclusively in healthy young adults [76,78,79,89]. Improvements in static stability are commonly measured by changes in antero-posterior (AP) and medio-lateral (ML) center of pressure (COP) trajectory. In bipedal static stance balance tasks, without visual compromise (i.e. eyes open), the use of texture does not appear to have an effect on AP or ML COP sway in healthy young adults [79]. This study compared two different textured conditions, with both indentation patterns having minimal response to static balance parameters. These results suggest that the absence of balance improvement is not a function of the textured material lacking an effective response, rather the static task itself may not be sufficiently demanding, and healthy young adults do not require this additional cutaneous feedback. A more recent study from this group explored one of these textures under different visual conditions (eyes open vs. eyes closed) and various static balance tasks (bipedal stance, a standard Romberg, tandem

Romberg task, and unipedal stance). Compared to wearing smooth insoles, healthy young adults wearing textured insoles produced a statistically significant reduction in the standard deviation of COP AP sway. Improvements in static balance measures were most pronounced with the removal of vision [89]. Additionally, healthy young adults wearing a similar insole experienced a reduction in the area of COP excursion [76]. Arguably, when using texture on a healthy young adult population, if the experimental task does not sufficiently challenge the balance control system, minimal results should be expected. In a healthy system, there is no need to solely rely on cutaneous feedback for balance control, as a healthy young adult has the ability to effectively reweight their available sensory information, without the need to rely on enhanced cutaneous contributions. Conversely, as we age, our plantar surface sensitivity diminishes [90], and texture has been applied under the foot sole as a method of facilitating this age-related sensory loss.

Research protocols utilizing textured insoles under the foot sole of healthy older adults have furthered our understanding of its application towards improving postural control. When comparing two different textures (the same textures previously used with healthy young adults [79]), improvements in COP range were observed when standing on one pattern and not the other. During double-limb static stance with eyes closed, a texture pattern described as ‘small pyramidal peaks’ under the entire foot sole decreased ML range in healthy older adults by 9.2% compared to stance on smooth material [85]. These balance improvements were not seen with a ‘convex circular patterned’ material, suggesting a pattern-specificity on static balance improvements. This evidence suggests that texture can improve COP ML range in healthy older adults, however these results may be dependent on the pattern of the textured material. Similar improvements in COP-ML range have been reported during static stance and walking trials [83,88]. Healthy older women wearing a modified insole with raised calcaneal and forefoot nodules, along with arch support, showed significant reductions in mean COP standard deviation (SD), velocity and RMS during dynamic walking. When compared to barefoot walking, the greatest improvements to postural stability occurred during a dynamic task when wearing the modified textured insole

[88]. These results suggest that the use of textured material under the foot sole of healthy older adults can positively influence both static and dynamic stability.

The literature using textured insoles on older adult populations also provides insight into its effectiveness under more challenging balance tasks and long-term use. Although not textured material under the entire foot sole, a perimeter ridge insole was designed to facilitate cutaneous feedback when the wearer approaches the limits of their base of support [80,81]. When wearing these insoles, the stepping behaviour to sudden platform perturbations has been documented in older adults. The perimeter ridge addition, providing mechanical facilitation to the boundaries of the plantar surface of the foot, decreased unnecessary postural motion when responding to platform translations. Unnecessary arm movements decreased from 8% to 3% and additional steps decreased from 44% to 37% with mechanical facilitation from the perimeter ridge [80]. Furthermore, this perimeter ridge insole has proven successful in improving lateral stability during uneven gait terrain, without sign of habituation following 12 weeks of wear [81]. In comparison, two 4-week intervention studies have reported mixed results, although reporting different outcome measures. During static stance and walking trials, no change in COP excursion was reported between baseline and 4-weeks of wearing two different textured insole designs [84]. Conversely, Berg Balance Scale (BBS) and Timed Up and Go (TUG) scores significantly improved with 4-weeks of textured insole wear [87]. These mixed results highlight the importance of carefully considering the experimental protocol and the textured material selection under investigation. Similar to young adults, older adults experience the largest benefits to textured insole use when enhanced cutaneous feedback is required. Experimental protocols are described in Maki et al. (1999) and Perry et al. (2008), when older adults experienced platform translations and walked across uneven terrain.

The textured insole research on older adults has provided a few additional insights worth noting. The unfamiliarity with texture may cause temporary deficits to the balance control system. Changes in spatiotemporal gait kinematics, suggestive of a hesitant walking pattern, have been acutely observed in older adults with a history of self-reported falls. The gait kinematic changes included a slower walking velocity, shorter step length, and shorter stride length in this population [86]. Similar results were observed in Parkinson's disease individuals completing a dynamic turn task [91]. This acute impairment, or destabilizing effect, has been limited to high-risk populations. Secondly, one study reported the COP changes following the removal of textured sandals. Interestingly, balance control was similarly impaired with the immediate removal of texture, resulting in increased COP sway parameters in static stance with texture compared to immediate removal [82]. When interpreting these results, two important conclusions have value to clinicians: 1) a destabilizing effect should be cautioned, and monitored, when using texture with high-risk populations, and 2) after wearing texture for any period of time, a similar destabilizing effect may be noted with the immediate removal of texture under the foot sole.

Textured insoles and Kinetic, Kinematic, and Electromyography (EMG)

Spatiotemporal gait parameters and lower limb EMG provides additional value in understanding the effect of textured insoles on dynamic movements. As an aside, no changes in muscle activity during static balance tasks [79,85] have been reported in the literature. Two studies have evaluated the isolation of texture to either the medial and/or lateral sides of the foot sole in healthy young adults. When walking at a self-selected velocity, adding texture under the full medial side of the foot increased subtalar joint supination during the loading and propulsive phases of gait [92]. Secondly, adding dowels under the lateral rearfoot (lateral to the calcaneus) modified the COP-ML trajectory during the 2nd half of stance [78]. Unfortunately, these author's report a rate of COP-ML change during later stance, however the specific location of COP trajectory change is not detailed. A full-length textured insole, with semi-circular mounds 8mm apart, resulted in a slight increase in ankle plantarflexion at initial contact during walking. An 11.8% reduction in peak internal knee moment was further observed with this change, along with decreased SOL and TA EMG when these muscles are most active in stance [93]. More recently, a textured design running perpendicular to the direction of locomotion observed an immediate reduction in vertical loading rate of healthy adults during recreational running. Additional kinematic results include a reduction in stride length, flight and contact time, and an increase in stride rate when running in textured insoles [94]. It remains unclear if runners could tolerate enhanced sensory feedback for the duration of longer runs, however textured insoles may warrant exploration in gait retraining and/or short-term use to facilitate small training adjustments in habitual stride length, rate, and contact time during stance.

<u>Textured Insoles and Special Populations</u>

The textured insole literature pertaining to special populations has predominantly focused on Parkinson's disease (PD) and Multiple Sclerosis (MS). In PD individuals, wearing an insole with a perimeter ridge (intended to facilitate cutaneous sensation around the perimeter of the foot sole) has demonstrated a timing change of TA's peak activity during stance. The onset of TA activity occurred earlier in the gait cycle, suggestive of a more appropriate activation time of muscle activity in this population (PD) [95]. Improvements in gait kinematics have been reported with two different insole designs. Blunted cones stimulating the 1st metatarsophalangeal joint and half-sphere elevations to the forefoot and calcaneus have demonstrated immediate and long-term (1 week) stride length increases in PD participants [96,97]. Elevated granulations along the entire plantar foot sole has decreased COP ML sway (during a static stance with eyes open task) to similar levels of age-matched controls [98]. Lastly, a full length textured orthotic has provided evidence to support long-term improvements to dynamic stability of PD individuals. After 5 weeks of orthotic wear, PD individuals completed a 180^{o} turn task with reduced steps and within a significantly increased COM-ML range [91]. The textured insole research on MS populations has been limited to improvements in static stability. Small spherical projections along the entire plantar foot sole reduced the rate of COP sway velocity after 4 weeks of wear [99]. Secondly, acute Berg Balance Scale (BBS) scores improved after 1 month of textured insole wear. Interestingly, score improvements were also observed after a subsequent month without wearing the textured insoles [100]. Although these results appear promising for MS patients, it should also be noted that several studies have reported inconclusive and/or minimal improvements with textured insole wear [101–103].

Arguably, there is a lack of consistency in experimental protocols, outcome measures and/or textured insole designs to provide an argument for or against PD and MS populations wearing textured devices.

Furthermore, the studies supporting the use of textured insoles have not been replicated by other research groups, enforcing the need for additional research in this area, and stronger experimental protocols using long-term interventions. That being said, this area of research is novel and growing. Recently, textured insoles have proven effective in improving sensory organization tests scores in a population of knee OA participants [104]. Textured insoles, intended to improve cutaneous sensation, should not be deemed ineffective in special populations. The literature simply hasn't evolved enough to understand its application and benefits of use.

<u>Textured Insoles in Sport</u>

The use of textured insoles has recently been explored in various sporting contexts. The use of texture has resulted in greater foot force and contact area under the feet of indoor rowers [105], has improved ankle discrimination scores of elite soccer [106,107], netball players [108], and dancers [109]. Lastly, using a textured lateral wedge reduced frontal plane movement variability during stance in athletes clinically diagnosed with functional ankle instability [110]. Although these results provide evidence to support the use of textured insoles in sport, further research is needed to replicate these results, and should combine other experimental outcome measures to strengthen these findings.

<u>Moving Forward: The Future of Textured Insole Research</u>

The neurological mechanism explaining how textured insoles function remains speculative. Two explanations have been provided. The first, relates to the textured material providing additional stimuli to the mechanoreceptors in foot sole skin. This increased afferent information is then relayed to the spinal cord, see section 1.5 for additional details. An alternative explanation considers the texture as an uncomfortable stimuli, whereby changes in midfoot kinematics is an avoidance behavior to the undesired stimulus [92]. Interestingly, this idea has been explored by one research group using texture under one foot as a method of enhancing unilateral discomfort. Patient's with diseased induced asymmetric gait (example: stroke) have demonstrated a reduced load on the target limb and facilitated locomotion on the contralateral side of texture use [111–113]. This is a novel use of discomfort-induced textured insoles; however, the more common application of textured insoles remains for everyday use. Of importance, this work in stroke patients provides rationale in ensuring a textured device does not induce pain and/or discomfort to the wearer. Perceived level of comfort has been reported across the literature, although mixed results have been reported [81,94,105,114,115]. Furthermore, all but one of these studies are measuring the immediate, short term effects of sensory augmentation on self-perceived comfort [81]. Additional research on the long-term effects of textured insoles on self-perceived comfort warrants attention.

Thus, the neurological mechanism supporting textured insole function requires clarification. Subsequent to this understanding, this growing area of research can confidently apply texture in select demographic/population groups and under specific tasks. Above the replication of many of these independent protocols and experimental results, additional areas of research include: the effects of textured insole use under fatiguing tasks, the effects of psychosocial factors (self-perceived stability and walking confidence) the effect of texture on both physiological and psychological pain reduction, and the effects of long-term use. Furthermore, many lower limb and foot pathologies remain to be explored, and none of these studies have isolated results by foot posture.

1.7 CONSIDERATIONS IN TEXTURED FOOT ORTHOSES DESIGN

Currently, there is no consensus on the ‘best’ texture for an intended purpose. The materials used across the scientific literature have large variation. Most commonly, semi-circular mounds of differing size, density, and durometer has been used under the foot sole. Appendix 2 details the studies, materials & texture currently explored across the literature. Evidently, the current body of literature on textured insoles has provided some foundational insight into its application and effectiveness. Considering the variability across experimental results, strong justification is imperative in the design and use of future textured insoles. Two important factors took precedence in designing the texture used in the studies of this dissertation.

Firstly, there is a large difference between a flat insole and a foot orthotic. A foot orthotic generally takes the shape of the foot, whereby the plantar surface of the foot remains in full contact with the top cover of the orthotic. If a device is prefabricated or custom-made, the contour of a foot shape is typically not present in a flat insole design. Foot posture is a large consideration in foot orthoses manufacturing, and the strongest rationale for clinicians to choose a custom device over one that is prefabricated. For example, a patient with a rigid pes cavus foot structure will rarely find a prefabricated orthotic which makes full plantar sole contact. Furthermore, a custom device provides the opportunity to modify and adjust a device as required, which includes adding special elements (such as metatarsal pads, wedges…etc.) and modifications to decrease pressure and pain. Although these modifications can be added to a flat insole, there is an important distinction to be made between a flat insole and a contoured foot orthotic. The majority of the literature using texture under the plantar foot sole has been added to flat insoles, rather than custom FOs.

Secondly, almost 50% of the cutaneous afferents of the foot sole are fast-adapting, type I receptors (Meissner corpuscles). They are sensitive to the rate of change of mechanical stimuli and fire during dynamic indentation of the skin. In other words, they have an on-off response, whereby firing occurs when the skin is initially exposed to mechanical stimuli, and once again when it is removed [56]. Consequently, to repeatedly stimulate FAI firing, there requires a continual influx of onset-offset mechanical indentation of the skin across the plantar foot sole. This behavioural response is largely due to the layered lamellae organization of Meissner corpuscles. During locomotion, over various phases of the gait cycle, pressure changes under the foot sole causes skin indentation. FAI's are located near the skin surface, nestled within the dermal papillae of the epidermis. As force change indents the skin of the plantar foot sole, force is transduced from collagen fibers connected to lamellar cell edges. FAI axon terminals are bent, compressing the center of the Meissner corpuscle receptor. Action potentials are generated at the onset of compression, and again once relaxed [55].

Understanding this physiology is important. The geometric properties of texture, including the size, shape and density of bumps, grooves, and ridges, is only effective if registered by the cutaneous mechanoreceptors [116]. Research on texture exploration has arrived at two important conclusions supporting textures use in the activation of FAI afferents. The first, is that lateral movement across the skin, as occurs with contact between texture and the skin surface, results in small vibrations within the skin [116]. Secondly, the contact movement between skin and texture causes temporal spiking patterns in fast-adapting cutaneous mechanoreceptor afferents [117]. These results suggest that the application of texture under the plantar foot sole must be sufficient to cause lateral movement of the skin tissue and result in these small minuscule vibrations within the skin.

These above-mentioned factors were instrumental in the development of the textured material used throughout each experimental protocol. The raised indents of the material have abrupt direction changes (zig zag pattern) which run in the medial-lateral direction. This is intended to course perpendicular to the direction of normal locomotion as a method of providing repeated stimulation of FAI firing. As force is transmitted under the foot, the various phases of the gait cycle provide a continual on-off response of mechanical skin indentation. Arguably, this zig-zag pattern has not been previously used in scientific literature (and perhaps these previous textured designs have failed to provide a consistent on-off stimuli), this may explain why previous research has failed to observe consistent changes in muscle amplitude throughout experimental protocols. Previous textured designs have been more uniform in nature, they commonly used semi-circular mounds uniformly placed across a flat insole [79,86,103,110,118–121]. Alternatives include textile fabrics [100,122,123], abrupt pin-like/pointy (intentionally noxious) raised indents [111,112], and a perimeter ridged design [80,95,124]. Furthermore, none of these previous used designs have accounted for the variability in foot shape. Thus, the zigzag texture in this dissertation is used as a top cover over the superficial aspect of the foot orthoses to ensure full foot contact between foot sole skin and texture.

1.8 OBJECTIVES AND HYPOTHESES

The overall objective of this dissertation was to design a series of experimental studies within the neuromotor paradigm to advance scientific literature pertaining to foot orthoses design and to grow our understanding on 'how' foot orthoses function. The individual study objectives are intended to: 1) to provide increased understanding of the immediate effects of sensory facilitation on lower limb and foot intrinsic muscle activity during locomotion, and 2) to understand the immediate effects of varying foot posture on lower leg and foot intrinsic muscle activity when adding texture to foot orthoses design. The chapters of this dissertation are separated by each experimental study. A study-specific literature review is included within each introduction, followed by study methods, results, and conclusion. A final summary, conclusion and suggestions for future research follows.

When adding texture under the foot sole, it is hypothesized that muscle activity in the lower legs will change in a site-specific, functional manner during locomotion. It is further hypothesized that intrinsic foot muscles will similarly change in a functional manner during locomotion. It is hypothesized that foot posture will be an important factor in the provision of textured foot orthoses, by demonstrating modulatory changes in lower leg and foot intrinsic muscle activation across the foot posture spectrum.

CHAPTER 2

THE EFFECT OF TEXTURE UNDER DISTINCT REGIONS OF THE FOOT SOLE ON HUMAN LOCOMOTION

2.1 INTRODUCTION

Sensory feedback from the foot sole plays an important role in shaping human locomotion [69,125]. The functional role of cutaneous afferent feedback has been demonstrated in experimental studies which have electrically stimulated cutaneous nerves [63,64,70,126,127], stimulated discrete skin regions of the foot sole, and mechanically stimulated foot sole cutaneous mechanoreceptors by increasing tactile feedback between the foot sole skin and the walking environment [84,94,119,124,128]. While net EMG and kinematic changes have been correlated with electrical stimulation to five topographical regions of the foot sole [129], it remains unknown if EMG and kinematic responses are similar in response to tactile stimulation under these same foot sole regions. Textured foot orthoses may be an effective method of maximizing foot sole contact while also facilitating tactile stimulation to the foot sole skin.

Stimulation to predominately cutaneous nerves innervating the foot, delivered during specific times throughout the gait cycle, have demonstrated locomotor-dependent reflexes which serve to regulate motorneuron activity during walking [60]. Tibial nerve stimulation during late stance increased the EMG magnitude of tibialis anterior (TA) in parallel with increased ankle dorsiflexion. This electromyography (EMG) response is reversed in late swing, whereby TA EMG is suppressed and an increase in ankle plantarflexion is seen [63,67]. Sural nerve stimulation, which innervates the skin along the lateral border of the foot, generates reflex facilitation of the TA and medial gastrocnemius (MG) during mid- to late stance, and is accompanied with ankle dorsiflexion and eversion [70]. In swing, TA muscle activity has been highly correlated with increased ankle dorsiflexion and accompanied by knee flexion [70]. Thus, when the cutaneous field along the lateral border of the foot is activated, the resultant force vector during stance suggests an ankle plantarflexion-inversion response to move the lateral border of the foot away from the stimuli, whereas in swing, the combined ankle dorsiflexion and knee flexion suggests an angular trajectory change as if the lateral border of the foot hit an undesired object, or if the foot prematurely hit the ground [60,70]. In early swing, superficial peroneal nerve stimulation (which innervates skin to the dorsum of the foot) suppresses TA activity, reduces ankle dorsiflexion, and increases knee flexion [63,130]. These kinematic changes reflect a functional behavioral change which mimics what occurs if the foot dorsum unexpectedly contacted the external environment and the foot and leg must clear the object to maintain smooth leg movement throughout swing [63,67]. In summary, reflex signs (inhibitory or excitatory), and thus the role of cutaneous input, have different functional roles during each phase of the gait cycle. Similar to the locomotor-dependent reflexes observed in these cutaneous nerve stimulation studies, net EMG and kinematic changes also support the contribution of skin from distinct regions of the foot sole and their ability to modify the excitability of motorneurons in a functionally important way.

Direct stimulation to foot sole skin shapes human locomotion through both task (standing vs. walking) and phase (stance vs. swing) specific reflex modulation [60]. Repetitive stroking across an FA1 receptive field, intended to stimulate the low-threshold mechanoreceptors in the foot sole skin, have been linked to motorneuron pools supplying lower extremity musculature [131]. More importantly, a muscle's reflexive response direction (facilitation or suppression), is dependent on the area being stimulated under the foot sole and appears to be reversed around the center of the foot. Running distal to proximal (forefoot to calcaneus), the TA reflex is reversed from facilitation to inhibition, whereas the soleus reflex is reversed from inhibition to facilitation [132]. During gait, stimulation to foot sole skin has demonstrated a modulatory effect between stimulation site, muscle activity, and across the different phases of the gait cycle [129]. For example, during the transition from stance to swing, the TA reflex response is facilitated with medial and lateral forefoot stimulation and medial midfoot stimulation. The PL reflex response in stance is facilitated with lateral forefoot or midfoot stimulation, although suppressed with medial midfoot or forefoot stimulation [129]. It also appears that one's plantar pressures are commonly shifted away from the site of stimulation. Lateral stimulation increases force under the medial aspect of the foot, whereas medial stimulation increases forces under the lateral aspect of the foot [69]. This site and phase dependency in response to non-noxious cutaneous stimulation during locomotion confirms the topographical organization of cutaneous afferents innervating the foot sole. These results are fascinating and validates further study of these neuromechanical outcomes in the functional modulation of gait abnormalities within pathological populations. It remains unknown if alternative stimulation methods, such as adding tactile feedback to distinct regions of the foot sole, shapes locomotor output similarly to cutaneous nerve and skin stimulation studies examining cutaneous reflexes during locomotion.

To capitalize on the physiological properties of FAIs and sufficiently indent the foot sole skin, foot orthoses may be an effective method to maximize full foot contact between the foot sole skin and the walking environment. Although texture has been extensively studied across postural control literature [77,80,82–88,124], minimal research has explored the use of texture within foot orthoses design [91], nor explored the modulatory effects of its application to topographically distinct areas under the foot sole. Furthermore, it remains unclear if tactile stimulation demonstrates similar functional changes during gait as cutaneous nerve and skin stimulation to the foot sole. Almost 50% of the cutaneous afferents of the foot sole are fast-adapting, type I receptors (FAI, Meissner corpuscles) [56]. These receptors are sensitive to the rate of change of mechanical stimuli and fire during dynamic indentation of the skin [56,57]. Consequently, to repeatedly stimulate FAI firing, there requires a continual influx of onset-offset mechanical indentation of the skin across the foot sole. Therefore the geometric properties of texture, if intended to stimulate FAIs, is only effective if registered by these cutaneous mechanoreceptors and sufficiently indents the skin during walking [116]. Small movements between the foot sole skin and texture must cause temporal spiking patterns in the fast-adapting cutaneous mechanoreceptor afferents [117]. More importantly, any texture placed between the skin and foot sole interface must sufficiently cause indentation of skin tissue, generating small minuscule indentations within the skin to have an influence on lower leg motorneuron pools [131].

Consequently, the purpose of this research was to investigate the effects of adding texture to distinct regions of the foot sole on modulating lower limb muscle activity during gait. This study addressed the following research question: Is the amplitude of lower limb muscle activity elicited from tactile facilitation to different regions under the foot sole modulated throughout the gait cycle? It was hypothesized that the direction of EMG response (facilitation or suppression) would modulate across different phases of the gait cycle, as previously observed when electrically stimulating cutaneous fields from distinct skin regions of foot sole skin [129]. Over a series of walking trials, lower limb muscle activity, joint kinematics and location of force application may give us some indication of the locomotor response to facilitating tactile information under distinct regions of the foot sole.

2.2 METHODS

2.2.1 Participants

Fifty-five participants (23.4±4.2years; 19 males, 36 females; 172.2±8.6cm; 70.9±15.7kg) were recruited to participate in this study. A screening questionnaire was provided electronically to all prospective candidates to exclude individuals with known neurological and/or musculoskeletal disorders, balance impairments, and/or ambulatory challenges. Prior to the start of the testing session, all participants were required to read and sign an informed consent. The study was approved by the institutional ethics review board (REB#5583).

All testing sessions lasted between 2.5-3 hours. Participant's foot posture was evaluated using the Foot Posture Index and Semmes-Weinstein monofilaments (North Coast Medical, Inc., Morgan Hill, CA) were used to evaluate tactile sensory thresholds of the foot sole at the start of each testing session. While lying prone, participants were asked to respond "yes" if they felt a light touch applied to their skin. Each monofilament was bowed at a 90^{o} angle against the skin of the foot sole. If a participant did not respond "yes" to the tactile touch of the filament, the next larger filament size was applied to the foot sole region. The five testing sites included the medial and lateral forefoot, medial and lateral midfoot, and calcaneus, which corresponded to the five sensory facilitation areas in this study. Sites were tested at random and continued until the minimum tactile perceptual threshold per area was determined.

2.2.2 Instrumentation

Kinematic data, sampled at 100Hz, and kinetic data, sampled at 1000Hz, were collected using the Optotrak Certus motion capture system (Northern Digital Inc., Waterloo, Ontario, CAN) and 3 force plates embedded flush with the flooring surface (OR6-5-2000; AMTI, Watertown, Massachusetts, USA). Participants were instrumented with 12 IRED markers on twelve anatomical landmarks: bilateral 3rd metatarsals, talocrural joints, superior patella, anterior superior iliac spines, acromions, forehead and xyphoid process. An EMG collection system (Ultium, Noraxon, Scottsdale, AZ, USA) was used to record indwelling fine-wire (iEMG) and surface EMG (sEMG) in 8 lower limb muscles during gait (1000Hz). Legs were divided into 'Leg A' and 'Leg B' to intentionally separate two surface EMG recordings and two fine-wire EMG insertions sites per leg. See Table 1.

Table 1. The distribution of surface and fine-wire EMG sites per leg.

	Surface EMG (sEMG)	**Fine Wire EMG (iEMG)**
LEG A	Tibialis Anterior (TA) Peroneus Longus (PL)	Tibialis Posterior (TP) Extensor Hallucis Longus (EHL)
LEG B	Medial Gastrocnemius (MG) Extensor Digitorum Longus (EDL)	Flexor Digitorum Longus (FDL) Flexor Hallucis Longus (FHL)

All fine-wire electrodes (paired fine-wire needle electrode, Chalgren Enterprises, Inc., [30mm (1.25") x 27g] (000-318-130); 50mm (2.00") x 25g] (000-318-150)) were inserted under ultrasound guidance (Eco 6, CHISON Medical Technologies Co., Ltd) [133]. The division of insertion sites between Leg A and Leg B were separated by their location and depth within the tissues. On Leg A, the fine-wire electrodes were inserted from the anterior aspect of the lower leg into EHL and from the posterior aspect into TP. On Leg B, FDL and FHL were both posterior insertions, although FDL was inserted distal in the lower leg, as FHL was a more proximal insertion. Each insertion site was initially located through surface palpation and the identification of relevant anatomical landmarks. The area was shaven (if required) to ease movement and clarity of the ultrasound probe over the skin and the insertion area was cleaned with alcohol. The probe was placed longitudinally along the muscle fibers. Once the muscle was located, the ultrasound probe was turned in the transverse plane and the doppler function identified neurovascular bundles within the targeted insertion area. While monitoring the needle trajectory on the ultrasound screen, the bipolar fine-wire electrodes were carefully inserted into each muscle of interest.

The fine-wire insertions were always performed in the following order: EHL, FHL, FDL and TP. All insertion sites were initially located via surface palpation of the leg and followed Perotto's fine-wire insertion protocol (with the exception of FHL which we elected for a lateral insertion approach) [133] (Figure 2). The ultrasound confirmed the needle trajectory and insertion accuracy. While the participant lay supine, the EHL muscle was located by palpating three finger breaths above the bimalleolar line, lateral to the anterior crest of the tibia. EHL was located on the ultrasound screen and electrode placement was confirmed with passive and resisted 1st MTP extension while the ankle remained dorsiflexed. The FHL was located by palpating the lateral edge of the tibia, approximately 5 finger breaths (or 10mm) above the Achilles tendon insertion. FHL insertion accuracy was confirmed with passive 1st MTP flexion and extension, while the participant kept the ankle and lesser toes relaxed. The FDL insertion site was located by palpating the medial edge of the tibia, at midshaft. FDL insertion was confirmed with passive flexion and extension of the lesser toes without flexing the ankle. Following a similar protocol as FDL, the TP muscle was located by palpating 1 hand breadth distal to the tibial tuberosity, and one finger breadth off the medial edge of the tibia. The TP was confirmed with resisted subtalar joint inversion and ankle plantarflexion.

A. Extensor Digitorum Longus

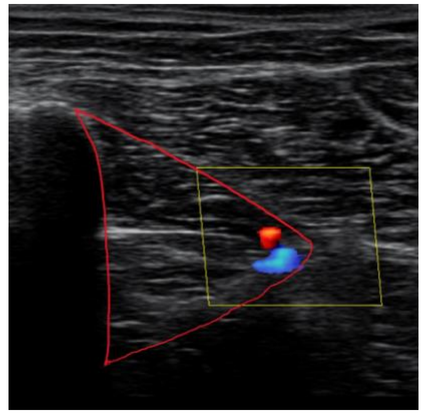

B. Flexor Digitorum Longus

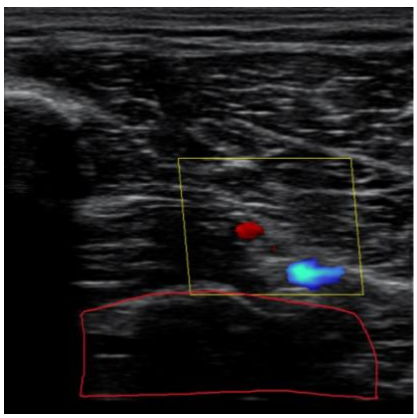

C. Tibialis Posterior

D. Flexor Hallucis Longus

Figure 2. The targeted insertion site of the fine-wire electrodes for each muscle. The muscle of interest is outlined in red. The yellow squares correspond to the ultrasound's doppler function which landmarks the neurovascular bundles of the lower leg. Vascular flow, which indicates the location of a neurovascular bundle is marked by red (flow towards the probe) and blue (flow away from the probe) shaded areas on the ultrasound.

'Leg A' recorded sEMG from TA and PL and 'Leg B' recorded sEMG from MG and EDL. Disposable bipolar surface electrodes (HEX 272S, Ag/AgCL, Noraxon, USA, Inc.) were placed directly over the skin of the muscle belly at an inter-electrode distance of 2cm. Hair and oils were removed, and the skin surface was cleaned with Nuprep abrasive gel. The electrodes were placed on the TA, four finger breaths below the tibial tuberosity, and one lateral to the tibial crest. Proper electrode placement was confirmed with resisted ankle dorsiflexion. The PL electrodes were placed three finger breaths below the fibular head. Electrode placement was confirmed with the combination of resisted ankle plantarflexion and foot eversion. The MG electrodes were placed one hand breath below the popliteal crease on the medial mass of the calf. Electrode placement was confirmed with active ankle plantarflexion while the knee remained straight. The EDL electrodes were placed four finger breaths distal to the tibial tubercle, and two lateral to the tibial crest. Proper electrode placement was confirmed by asking the participant to raise their four lesser toes against resistance. All muscle activity was confirmed by monitoring live EMG signals during active contractions of each respective muscle.

2.2.3 The Textured Foot Orthoses

All participants were fit to a customizable, over-the-counter orthotic (D609561, Sole Thin Sport Footbeds, Edge Marketing Corp; Calgary, AB, Canada) and Rockport casual dress shoe (Rockport WT Classic). All testing was completed barefoot. Medilogic pressure insoles were temporarily placed in participant's footwear and two walking trials confirmed full foot contact between the participant's foot sole and orthotics. Full foot contact was confirmed by a 90% pressure cell distribution.

Each foot orthoses condition included the combination of foot orthoses + top cover (Op-Tek Flex, 1/8" EVA copolymer, Ortho Active, BC, CAN). In the non-facilitated condition, the Op-Tek top cover was smoothly adhered to the entire length of the foot orthotic. In the facilitated conditions, the foot sole was divided into 5 distinct topographical areas: medial forefoot (MF), lateral forefoot (LF), medial midfoot (MM), lateral midfoot (LM), and calcaneus (CALC), each corresponding to a desired location of sensory facilitation. In the facilitated location, the Op-Tek material was replaced with a 3D printed textured material (Flex 45 Thermoplastic Co-Polyester, Shore D 35 hardness, InkSmith) while the remainder of the surface remained covered in smooth Op-Tek material (See Figure 3). One topographical area was facilitated at a time. The smooth Op-Tek material and texture were the same durometer and thickness, which ensured a smooth transition between both materials. See Appendix 3 for a step-by-step description on how each facilitated region was determined.

Figure 3. The five topographical regions of cutaneous facilitation under the foot sole.

The durometer and textured pattern were intentionally designed to trigger the activation of FAI cutaneous mechanoreceptors. The raised indents of the material had abrupt direction changes and ran in the medial-lateral direction. This was intended to course perpendicular to the direction of normal locomotion as a method of providing repeated stimulation of FAI firing during walking. As force was transmitted under the foot, the various phases of the gait cycle provided a continual on-off response of mechanical skin indentation. Secondly, to account for the variability in foot posture, the textured material was used as a top cover in orthoses design, which ensured full foot contact between foot sole skin and textured material.

2.2.4 The Experimental Protocol

Participants completed a series walking trials along a 10m walkway. Starting in quiet static stance, each trial began with the left foot. Two steps were taken before contacting force plate 1, then force plate 3 and participants subsequently continued their forward walking trajectory until the end of the walkway (Figure 4A). Participants experienced two walkway conditions; level walking and a wedged condition, whereby the walkway was modified by adding an inclined wedge onto force plate 3. The orientation of this wedge increased participants subtalar joint eversion (wedge was higher on the lateral side of the foot compared to the medial side) (Figure 4B). Participants completed three level walking trials and three wedged walking trials for each facilitated condition. Non-facilitated walking trials (smooth top cover only) were also included in the beginning, middle, and end of the facilitated trial conditions. A total of 48 walking trials were completed per testing session [3 walking conditions (level gait and wedged gait), 6 orthotic conditions (smooth top cover (3 blocks), 5 different facilitated locations (1 block per region))]. Following each testing session, participants were asked five post-study questions: 1) Were the Rockport shoes comfortable to wear during the walking sessions? 2) Were the orthotics comfortable under your feet? 3) Was there an area of texture that was more comfortable, or less comfortable, compared to the others? 4) Are there any activities that you can speculate in which these orthotics would not be comfortable? 5) Would you care to provide any additional details regarding your testing session experience?.

A.

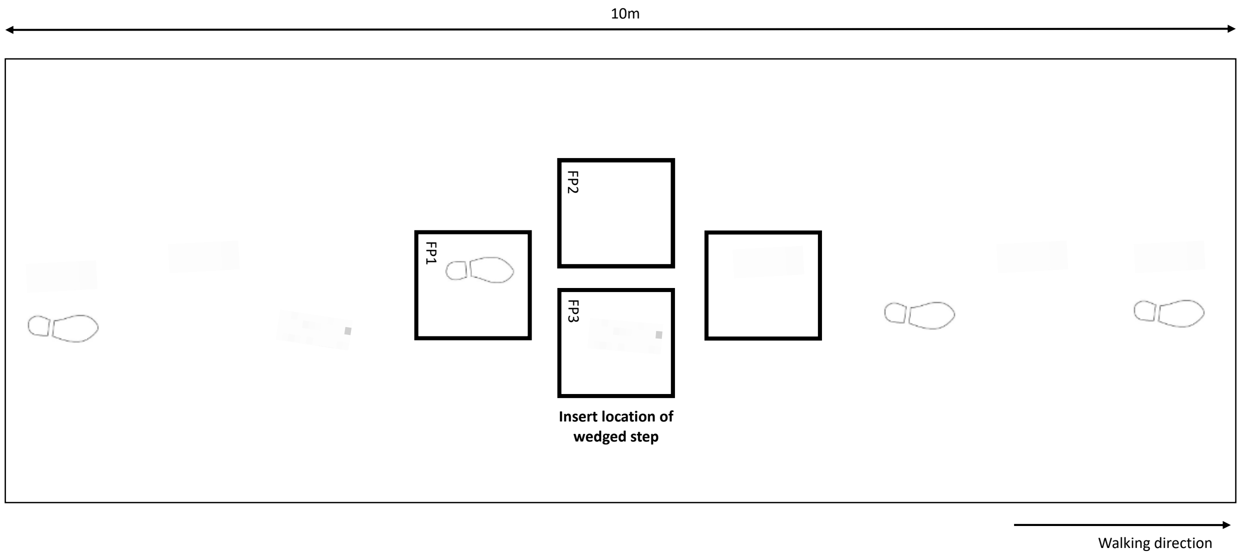

B.

Figure 4. A. A schematic of the 10m walkway. Participants took 2 steps prior to contacting force plate 1 (FP1), and subsequent contact onto force plate 3 (FP3), then continued walking until they reached the end of the walkway. Participants were instructed to continue walking at a consistent velocity until they reached the end of the walkway. FP1, force plate 2 (FP2) and FP3 correspond to the locations of each force plate embedded into the floor along the walkway. During the wedged walking trials, participants were instructed to step onto the wedge (placed on FP3) and continue walking at a consistent velocity until the end of the walkway. **4B**. Wedge used during the study which increased participants subtalar joint inversion across the stance phase of gait.

2.2.5 Data Processing

All EMG was unbiased, full-wave rectified, and linear enveloped with a 40Hz dual-pass Butterworth filter. The raw signals were differentially amplified (gain x500) and band pass filtered (10-500Hz). The gait cycle was divided into 10 equal sized bins within 100% of the gait cycle (each bin represented 10% of the gait cycle).

Bins 1 to 6 corresponded to the stance phase of gait, whereas bins 7 to 10 corresponded to the swing phase of gait. The average EMG (aEMG) during each bin was normalized to the peak EMG (%Pk) of each muscle within the gait cycle. CoP analysis was used to measure the percentage of time in single stance that the COP trajectory remained in each isolated textured area. Each CoP region was calculated from the location of the foot markers in single stance relative to the force plate. The CoP regions were divided into 5 quadrants, each representative of the same facilitated regions of texture used in this study. Raw kinematic data was processed (small gaps in trajectories) with a cubic spline function in a custom-made Optofix software and filtered at 6 Hz low-pass dual-pass Butterworth filter. Sagittal plane kinematics of the hip, knee and ankle was extrapolated from the angular position of the anterior-posterior and vertical coordinates of the IRED markers. Data from a static stance trial was used to standardize the zero-reference position for each joint.

2.2.6 Statistical Analysis

Two-way repeated measures analysis of variance (SAS University Edition, 2.8.1, version 9.4) were performed for each measure (8 x EMG (bins 1-10); % CoP; kinematics and gait parameter data) to compare between within-subject factors of textured location (MF, LF, CALC, MM, MF) and walking condition (level vs. wedge). Analysis bins were divided into the different phases of the gait cycle (Stance: bin 1:initial contact (IC), bin 2:loading response (LR), bin 3:midstance (MS), bin 4:heel rise (HR), bin 5:propulsion (PR), bin 6:toe off (TO); Swing: bin 7:initial swing (ISW), bin 8: early mid-swing (Early MSW), bin 9: late mid-swing (Late MSW), bin 10:terminal swing (TSW)). Two participants were excluded from the analysis due to methodological collection errors. The data was rank-transformed when normality was not met, and Tukey's HSD post hoc comparisons were performed on all data when main effects were significantly different. Any outlier that exceeded ±4SD from the mean was carefully inspected as a potential outlier in the dataset. Outliers and/or missing values were replaced by the mean (averaged 12 x per muscle, per bin across 1980 samples). Fine-wire EMG signals that were saturated with noise or demonstrated poor signal quality were also removed. Statistical significance was determined at $p<0.05$ a priori.

2.3 RESULTS

The Semmes-Weinstein monofilament results confirmed healthy sensation across all participant's foot soles (Right - 1st MTP: 3.22 ± 0.18, 5th MTP: 3.19 ± 0.29, Medial midfoot (MM): 2.95 ± 0.30, Lateral midfoot (LM): 3.15 ± 0.34; Calcaneus (CALC): 3.34 ± 0.34; Left - 1st MTP: 3.20 ± 0.26, 5th MTP: 3.21 ± 0.30, MM: 3.00 ± 0.40, LM: 3.17 ± 0.33; CALC: 3.38 ± 0.32). FPI scores confirmed the sample population included all foot postures.

To evaluate the topographical effects of cutaneous afferent facilitation on lower leg EMG during gait, all 8 muscles recorded by surface EMG and fine-wire EMG were compared across location of texture and walking condition. Each topographically facilitated region was compared to the smooth top covered orthoses. As the primary purpose of this research was to evaluate the effect of cutaneous afferent facilitation on EMG, this results section is focused on the main effects of facilitation rather than walking condition. Complete results for sensory facilitation and walking condition are provided in Appendixes 4A and 4B.

2.3.1 Early Stance

In early stance, texture under the MM and CALC significantly modified the aEMG of EHL, FDL and FHL. Significant main effects of sensory location on EHL were observed at IC ($F_{5,205}$=3.43, p=.004, eta-square=0.83) and LR ($F_{5,205}$=2.81, p=.016, eta-square=0.74), which continued into MS ($F_{5,205}$=4.23, p<.001, eta-square=0.76), and HR ($F_{5,205}$=4.27, p=<.001, eta-square=0.82). (Figure 5). Significant main effects were observed in FDL ($F_{5,195}$=4.55, p=.0004, eta-square=0.85) and FHL ($F_{5,160}$=10.20, p<.0001, eta-square=0.82) at IC, and in FDL during the LR ($F_{5,195}$=6.07, p<.0001, eta-square=0.76). Contrary to these increases in EMG, texture under the CALC at IC (18.42%Pk ± 13.50%Pk) and under both the CALC (26.66%Pk ± 14.31%Pk) and MM during the LR (26.32%Pk ±

15.27%Pk) reduced FDL aEMG in early stance. Texture under the CALC significantly altered knee ($F_{5,240}$=4.76, p=.0003, eta-square=0.91) and ankle joint maximums ($F_{5,1691}$=7.88, p=<.0001, eta-square=0.90) and total ankle joint range of motion ($F_{5,240}$=8.02, p=<.0001, eta-square=0.81) throughout the gait cycle. Cutaneous afferent facilitation under the heel significantly increased knee joint maximum ($54.88^o \pm 4.11^o$) ankle joint maximum ($17.00^o \pm 5.69^o$) and total ankle joint range ($31.07^o \pm 5.09^o$) values during gait (Table 2).

Table 2. Kinematics of the hip, knee, and ankle

Sensory Location	Hip			Knee			Ankle		
	Max (deg)	Min (deg)	Range (deg)	Max (deg)	Min (deg)	Range (deg)	Max (deg)	Min (deg)	Range (deg)
None	21.67 ± 4.07	-23.91 ± 3.97	45.60 ± 4.35	54.57 ± 4.16	-8.26 ± 3.58	62.82 ± 4.37	16.30 ± 4.99	-13.83 ± 5.90	30.08 ± 5.05
MF	21.68 ± 3.93	-23.67 ± 4.35	45.35 ± 4.55	54.20 ± 4.19*	-8.12 ± 3.58	62.32 ± 4.13**	16.54 ± 5.10	-13.74 ± 5.90	30.22 ± 5.17
LF	21.70 ± 4.20	-23.90 ± 3.95	45.60 ± 4.58	54.51 ± 4.28	-8.38 ± 3.68	62.91 ± 4.41	16.44 ± 5.11	-13.83 ± 5.85	30.23 ± 4.95
Calcaneus	21.84 ± 4.03	-23.83 ± 4.12	45.67 ± 4.39	54.88 ± 4.11*	-8.06 ± 3.73	62.88 ± 4.39	17.00 ± 5.69**	-14.09 ± 6.03	31.07 ± 5.15**
MM	21.65 ± 4.09	-23.76 ± 4.07	45.41 ± 4.59	54.83 ± 4.11	-8.15 ± 3.66	62.93 ± 4.35	16.61 ± 5.00	-13.58 ± 5.90	30.19 ± 4.60
LM	21.77 ± 4.15	-23.70 ± 4.21	45.53 ± 4.51	54.64 ± 4.15	-8.09 ± 3.55	62.71 ± 4.24	17.02 ± 5.62**	-13.73 ± 5.81	30.75 ± 5.09**

** = p<.05.   ** = p<.001*

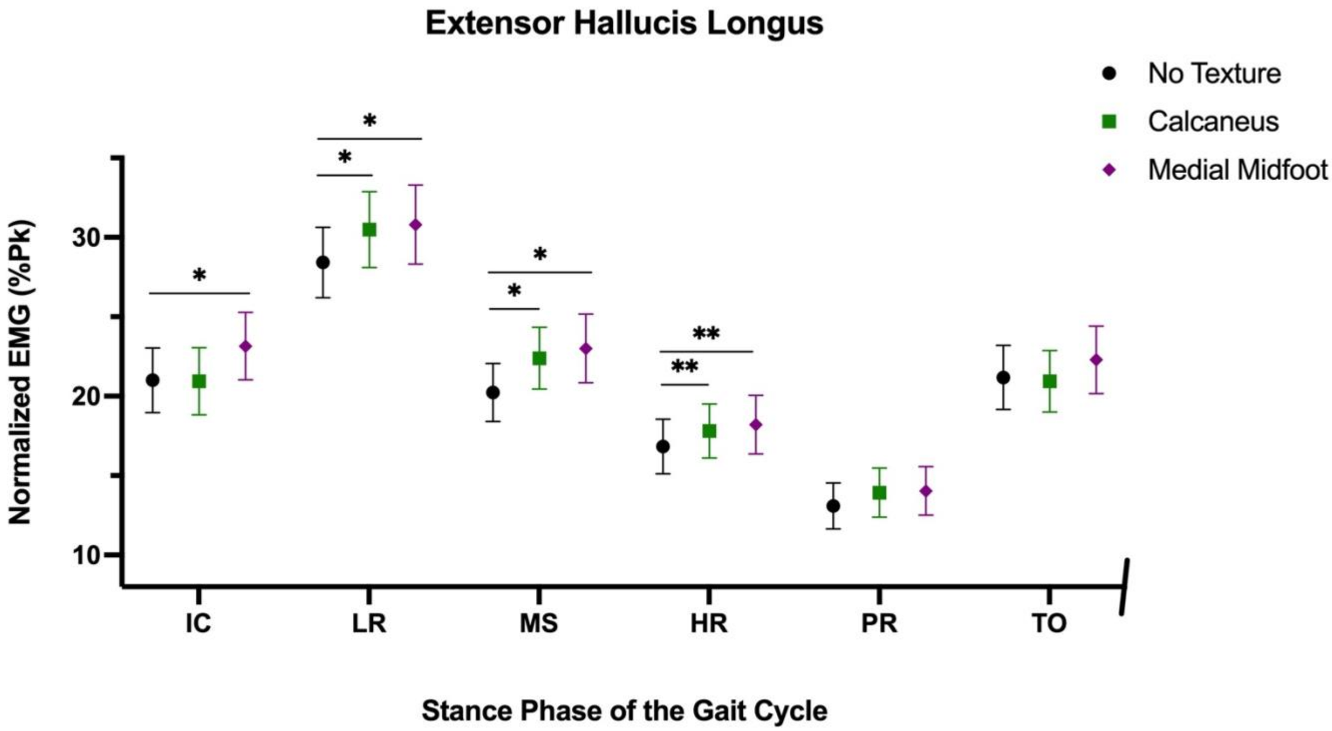

Figure 5. The modulation of extensor hallucis longus (EHL) (normalized EMG) in stance with texture under the calcaneus (CALC, green square) and medial midfoot (MM, purple diamond). The swing phase of gait has been omitted from this figure. Significant main effects of sensory location on EHL were observed at IC ($F_{5,205}$=3.43, p=.004, eta-square=0.83) and LR ($F_{5,205}$=2.81, p=.016, eta-square=0.74), which continued into MS ($F_{5,205}$=4.23, p<.001, eta-square=0.76), and HR ($F_{5,205}$=4.27, p=<.001, eta-square=0.82). Adding texture under the CALC significantly increased EHL aEMG during the LR (30.49%Pk ± 17.24%Pk), MS (22.39%Pk ± 14.00%Pk) and HR (17.81%Pk ± 12.28%Pk) phases of gait. Similar increases in EHL aEMG were observed with texture under the MM: IC (23.15%Pk ± 15.34%Pk), LR (30.80%Pk ± 17.95%Pk), MS (23.01%Pk ± 15.58%Pk) and HR (18.20%Pk ± 13.30%Pk). Significance is denoted by * = p<.05 and ** = p<.001. (IC = initial contact; LR = loading response; MS = midstance; HR = heel rise; PR = propulsion; TO = toe off)

Statistically significant main effects of sensory location on TP aEMG were also observed at initial contact ($F_{5,190}$=8.30, p<.0001, eta-square=0.81) (Figure 6). Interestingly, these significant main effects of cutaneous afferent facilitation were reflected in the %CoP when texture was placed under the MF ($F_{5,230}$=2.38, p=.0364, eta-square=0.85). Facilitation to the MF significantly reduced the %CoP under the LF (6.11% ± 11.16%) and significantly increased the %CoP under the calcaneus (28.17% ± 15.22%) regions of the foot sole. These main effects of sensory facilitation were also accompanied with kinematic changes. Texture under the MF significantly reduced the maximum ($F_{5,240}$=4.76, p=.0003, eta-square=0.91; 54.20°±4.19°) and total range ($F_{5,240}$=5.77, p=<.0001, eta-square=0.88; 62.32° ± 4.13°) of knee joint movement. Texture under the LM significantly increased ankle joint maximum ($F_{5,1691}$=7.88, p=<.0001, eta-square=0.90; 17.02° ± 5.62°; 30.75° ± 5.09°) and total ankle range of motion ($F_{5,240}$=8.02, p=<.0001, eta-square=0.81) throughout the entire gait cycle. Of final note, cutaneous afferent facilitation under either area of the foot sole had no significant effects on the aEMG of the TA, PL and EDL muscles.

2.3.2 Midstance

During the midstance phase of the gait cycle, significant interactions were observed in the superficial (MG) and deep (TP and FHL) posterior muscles (Figure 6). At MS ($F_{5,230}$=3.15, p=.0078, eta-square=0.77), adding texture under the MM (10.06%Pk±9.91%Pk) significantly increased MG activity in the wedged condition, whereas reductions in aEMG remained consistent across all other sensory locations (Figure 6A). During heel rise ($F_{5,235}$=2.31, p=.0419, eta-square=0.81), texture to the MF (15.42%Pk ± 15.59%Pk), LF (14.17%Pk ± 14.57%Pk) and smooth top cover orthoses (13.71%Pk ± 14.51%Pk) increased MG aEMG, whereas texture under the LM reduced MG (12.52%Pk ± 13.09%Pk) aEMG in the wedged condition (Figure 6B). A significant interaction was also observed in the TP muscle between sensory location and walking condition at MS ($F_{5,190}$=3.05, p=.0096, eta-square=0.74) (Figure 6C). In the wedged condition, texture under the LF (21.46%Pk ± 12.87%Pk) and MM (21.35%Pk ± 12.68%Pk) increased TP aEMG, whereas TP aEMG was reduced when texture was placed under the MF (19.80%Pk ± 12.74%Pk). Lastly, a significant interaction was observed in FHL ($F_{5,195}$=2.81, p=.0157, eta-square=0.75) at MS (Figure 6D). Most notably, adding texture to the calcaneus (21.74%Pk ± 11.65%Pk) and LM (21.01%Pk ± 12.46%Pk) increased the FHL aEMG in the wedged condition.

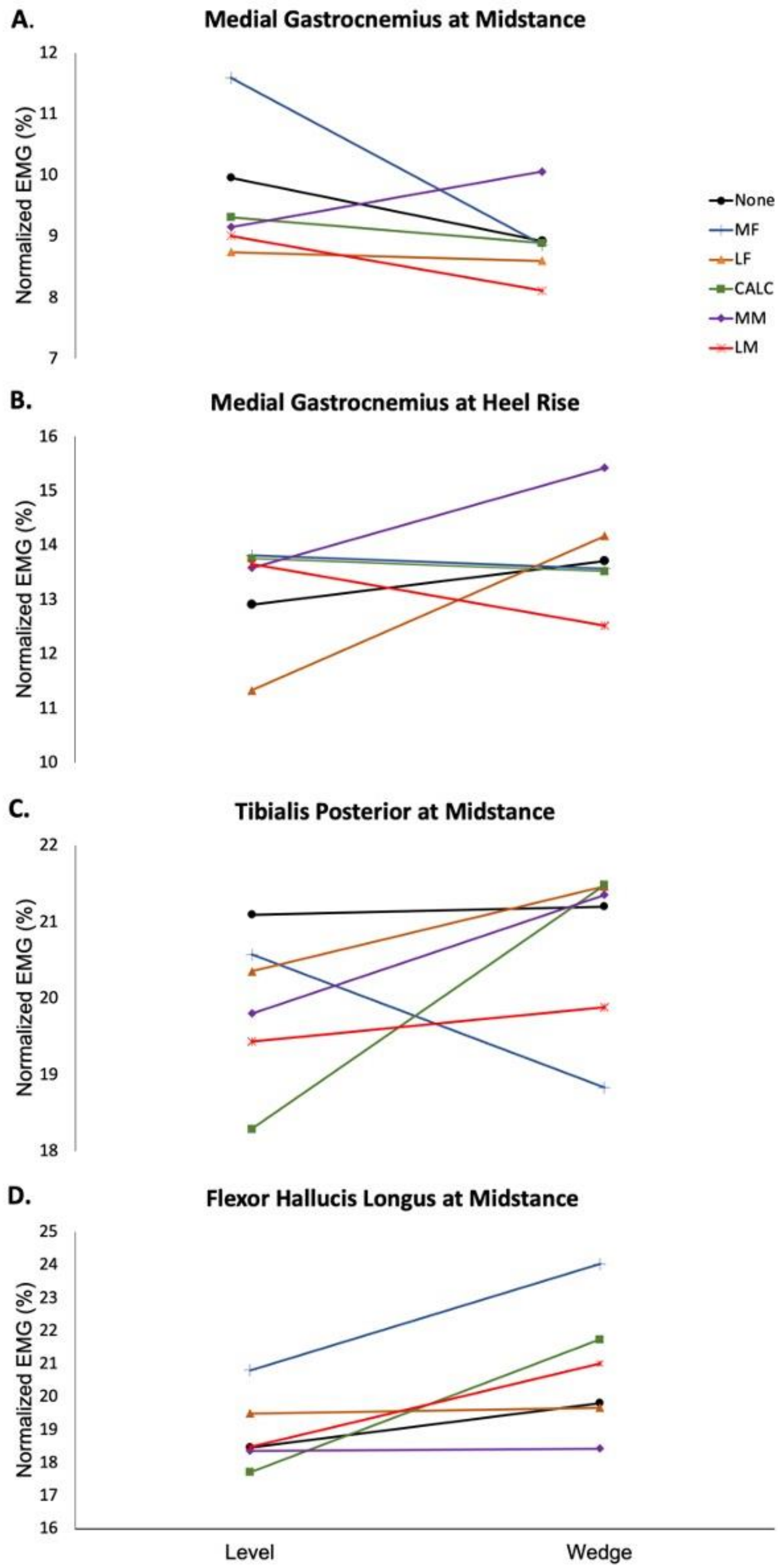

A.
Medial Gastrocnemius at Midstance
Normalized EMG (%)
12
11
10
9
8
7
None
MF
LF
CALC
MM
LM
B.
Medial Gastrocnemius at Heel Rise
Normalized EMG (%)
16
15
14
13
12
11
10
C.
Tibialis Posterior at Midstance
Normalized EMG (%)
22
21
20
19
18
D.
Flexor Hallucis Longus at Midstance
Normalized EMG (%)
25
24
23
22
21
20
19
18
17
16
Level
Wedge

Figure 6. The interaction effects of changing the orientation of the foot (level vs. wedge) across different textured regions under the foot sole during midstance and heel rise. A. Medial Gastrocnemius at midstance, B. Medial Gastrocnemius at heel rise, C. Tibialis posterior at midstance, D. Flexor hallucis longus at midstance. Standard deviations for all muscle and walking condition variables are included in Appendices 4A and 4B.

Significant main effects of sensory facilitation were observed in the TP at heel rise ($F_{5,190}$=4.12, p=.001, eta-square=0.79). (Figure 7). During midstance (TO: $F_{5,195}$=4.12, p=.001, eta-square=0.85; PR: $F_{5,195}$=3.76, p=.0022, eta-square=0.84), aEMG suppression (19.99%Pk ± 13.79%Pk) was observed in FDL with texture under the MF, which similarly continued into propulsion (16.61%Pk ± 11.34%Pk) (Figure 8).

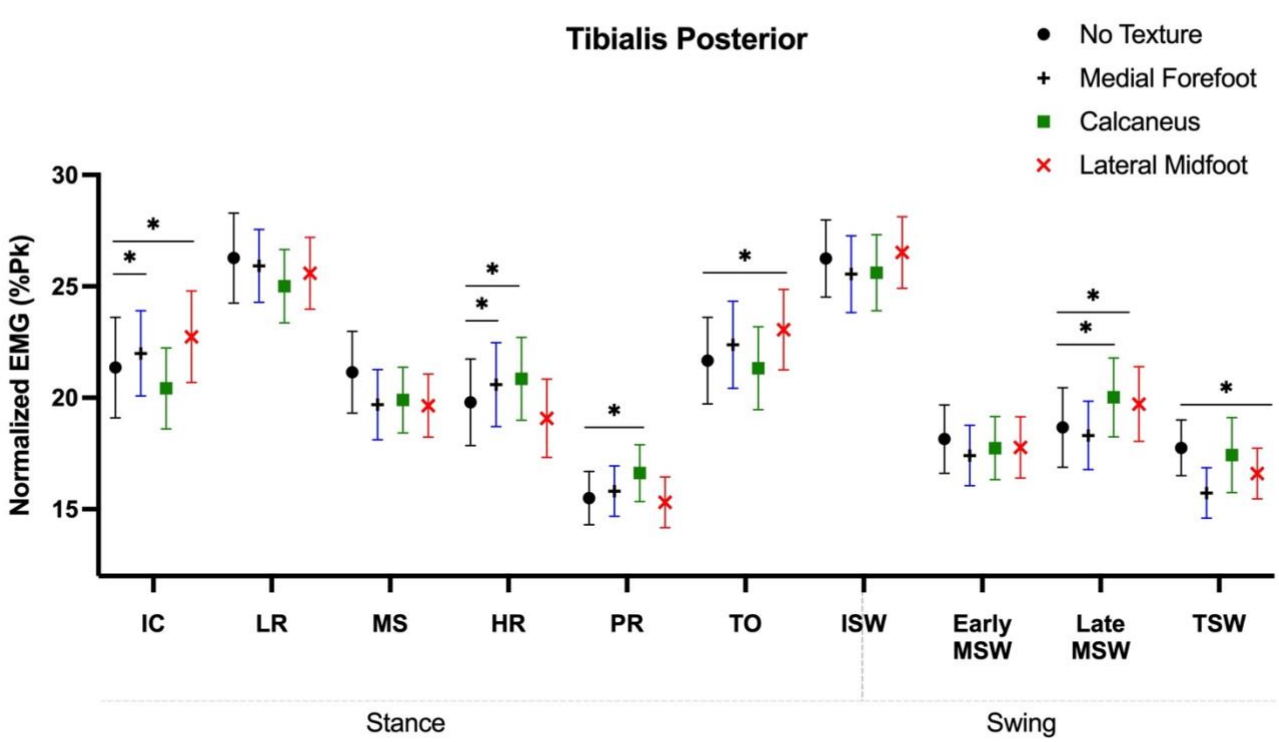

Figure 7. The modulation of tibialis posterior (normalized EMG) throughout the gait cycle with texture under the calcaneus (CALC, green square), medial forefoot (MF, blue +) and lateral midfoot (LM, red X). Statistically significant main effects of sensory location on TP aEMG were observed at initial contact (IC) ($F_{5,190}$=8.30, p<.0001, eta-square=0.81), heel rise (HR) ($F_{5,190}$=4.12, p=.001, eta-square=0.79), and into propulsion (PR)

($F_{5,190}$=2.88, p=.013, eta-square=0.71, 16.62%Pk ± 9.17%Pk). At IC, texture under the MF (20.85%Pk ± 13.39%Pk) and LM increased (22.74%Pk ± 14.81%Pk) TP aEMG. Similarly at HR, texture under the MF (20.59%Pk ± 13.57%Pk) and CALC increased TP aEMG (20.85%Pk ± 13.39%Pk). During swing, TP aEMG ($F_{5,190}$=2.25, p=.0474, eta-square=0.79, 19.72%Pk ± 12.11%Pk), significantly increased with texture under the CALC (20.02%Pk ± 12.77%Pk). In terminal swing $F_{5,190}$=2.22, p=.0499, eta-square=0.72), increases in TP aEMG was reversed to suppression (16.60%Pk ± 8.21%Pk) with LM facilitation. Significance is denoted by * = p<.05. (IC = initial contact; LR = loading response; MS = midstance; HR = heel rise; PR = propulsion; TO = toe off; ISW = initial swing; Early MSW = early mid-swing; late MSW = late mid-swing; TSW = terminal swing).

2.3.3 Terminal Stance

There was a significant interaction in the TA ($F_{5,235}$=2.40, p=.035, eta-square=0.86) between sensory location and walking conditions during the toe-off phase of gait (Figure 9A). Similar to walking in smooth top covered orthoses, texture applied to the MF (20.85%Pk ± 18.42%Pk) and LF (20.96%Pk ± 18.86%Pk) reduced the TA aEMG in the wedged condition. Conversely, the wedged condition increased TA aEMG when texture was applied to the MM (21.90%Pk ± 18.07%Pk) LM (21.71%Pk ± 19.09%Pk) and CALC (20.27 %Pk ± 18.82 %Pk).

In the superficial and deep posterior muscles, significant main effects of sensory location were observed with forefoot facilitation (Figure 8). During propulsion, texture under the MF significantly increased MG ($F_{5,230}$=4.29, p=.0007, eta-square=0.86, 19.99%Pk ± 20.01%Pk) and reduced FDL aEMG ($F_{5,195}$=3.76, p=.0022, eta-square=0.84, 16.61%Pk ± 11.34%Pk). At TO ($F_{5,160}$=20.44, p<.0001, eta-square=0.89), MF texture significantly increased FHL aEMG (28.04%Pk ± 20.24%Pk), with similar results observed with LF facilitation during PR ($F_{5,160}$=5.72, p<.0001, eta-square=0.78, 16.43%Pk±11.01%Pk) and TO (20.90%Pk ± 18.42%Pk). Final observations include two significant phase-specific main effects of sensory location on PL and EDL aEMG. Adding texture to the MM significantly increased PL aEMG ($F_{5,235}$=2.48, p=.030, eta-square=0.66, 10.47%Pk ± 11.34%Pk) while CALC texture significantly increased EDL aEMG ($F_{5,235}$=2.32, p=.040, eta-square=0.72, 12.83%Pk ± 12.45%Pk) at propulsion.

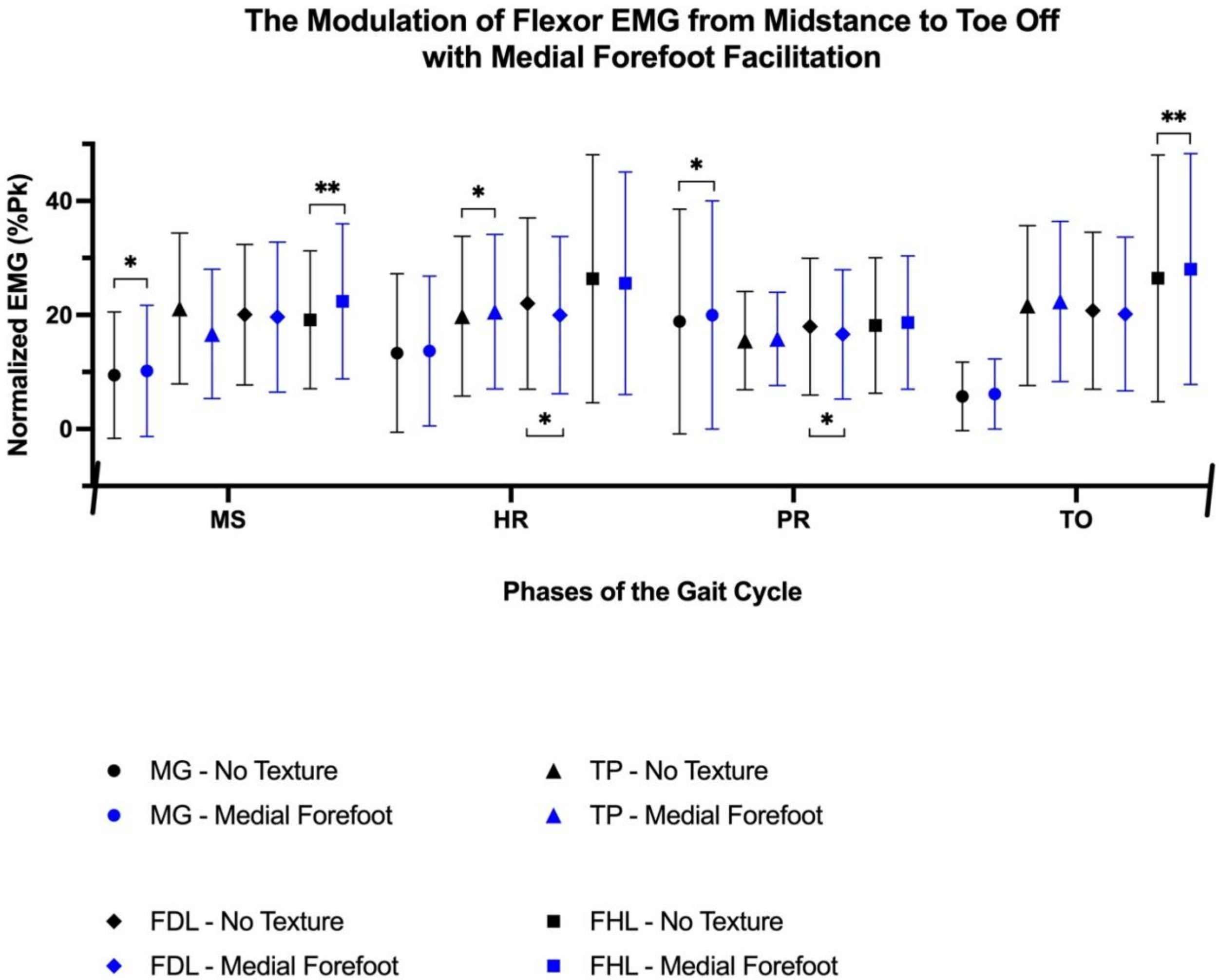

Figure 8. The modulation of posterior compartment musculature's (normalized EMG, %Pk) from midstance to toe off with texture under the medial forefoot (MF, blue diamonds, triangles and squares). Initial contact, loading response and the entire swing phase of gait have been omitted from this figure. During midstance (TO: $F_{5,195}$=4.12, p=.001, eta-square=0.85; PR: $F_{5,195}$=3.76, p=.0022, eta-square=0.84), aEMG suppression (19.99%Pk ± 13.79%Pk) was observed in FDL with texture under the MF, which similarly continued into propulsion (16.61%Pk ± 11.34%Pk). During propulsion, texture under the MF significantly increased MG ($F_{5,230}$=4.29, p=.0007, eta-square=0.86, 19.99%Pk ± 20.01%Pk) and reduced FDL aEMG ($F_{5,195}$=3.76, p=.0022, eta-square=0.84, 16.61%Pk ± 11.34%Pk). At TO ($F_{5,160}$=20.44, p<.0001, eta-square=0.89), MF texture significantly increased FHL aEMG (28.04%Pk ± 20.24%Pk). Significance is denoted by * = p<.05 and ** = p<.001. (MS = midstance; HR = heel rise; PR = propulsion; TO = toe off).

2.3.4 Swing

Across all phases of swing, texture under the LF significantly reduced FHL aEMG (ISW: $F_{5,160}$=7.13, p<.0001, eta-square=0.87, 22.60%Pk ± 15.04%Pk; early MSW: $F_{5,160}$=3.17, p=.0076, eta-square=0.76, 13.60%Pk ± 7.97%Pk, late MSW: $F_{5,160}$=8.97, p<.0001, eta-square=0.75, 15.31%Pk ± 12.48%Pk, TSW: $F_{5,160}$=5.84, p<.0001, eta-square=0.79, 13.80%Pk ± 8.63%Pk), a suppression of FHL amplitude which began in propulsion. Specific to initial swing, texture under the MM significantly increased TA ($F_{5,235}$=2.15, p=.050, eta-square=0.72, 13.64%Pk ± 11.07%Pk) and MG ($F_{5,230}$=4.80, p=.0002, eta-square=0.65, 5,20%Pk ± 5.01%Pk) aEMG.

During mid-swing, texture to the MF significantly increased MG aEMG in early ($F_{5,225}$=2.88, p=.0134, eta-square=0.75, MF:8.18%Pk ± 7.96%Pk) and late MSW $F_{5,230}$=3.52, p=.0036, eta-square=0.81, MF:13.55%Pk ± 12.69%Pk). LM facilitation similarly increased MG (early MSW: 8.33%Pk ± 7.76%Pk, late MSW: 14.10%Pk ± 13.05%Pk) and TP aEMG ($F_{5,190}$=2.25, p=.0474, eta-square=0.79, 19.72%Pk ± 12.11%Pk), with increases also observed with texture under the CALC (20.02%Pk ± 12.77%Pk). In terminal swing $F_{5,190}$=2.22, p=.0499, eta-square=0.72), increases in TP aEMG was reversed to suppression (16.60%Pk ± 8.21%Pk) with LM facilitation (Figure 7). Lastly, a significant main effect was observed in FDL at TSW ($F_{5,195}$=4.41, p=.0005, eta-square=0.83). Adding texture to the calcaneus (15.20%Pk ± 9.17%Pk) significantly reduced FDL aEMG.

Most noteworthy, there was a significant interaction in the TA between sensory location and walking conditions at terminal stance ($F_{5,235}$=2.93, p=.012, eta-square=0.86) (Figure 9B). Compared to walking in smooth top covered orthoses, texture under the LF (14.46%Pk ± 13.97%Pk), MF (14.79%Pk ± 14.53%Pk) and MM (16.21%Pk ± 15.41%Pk) significantly increased TA aEMG when walking in the wedged condition compared to level walking. In comparison, texture under the LM (13.50%Pk ± 12.94%Pk) and CALC (13.42%Pk ± 12.95%Pk) remained less than walking in the smooth top covered orthoses, irrespective of a level or wedged walking condition.

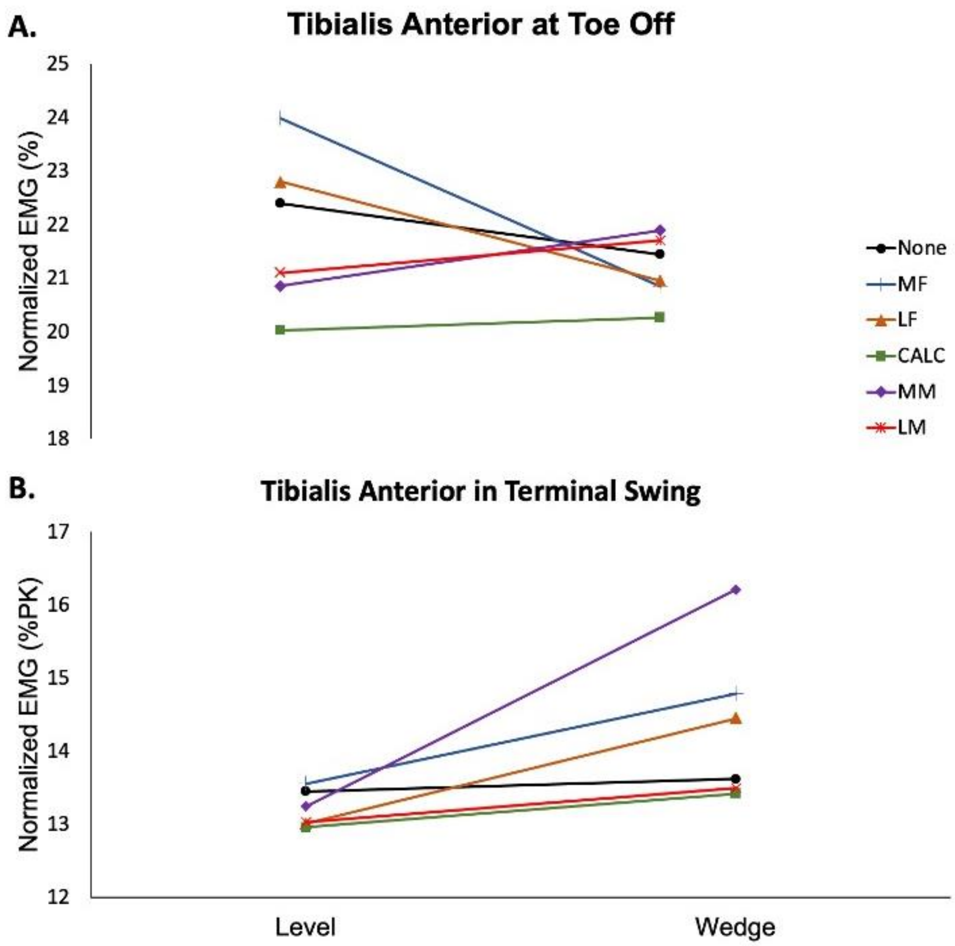

Figure 9. The interaction effects of changing the orientation of the foot (level vs. wedge) across different textured regions under the foot sole of the tibialis anterior during the stance to swing (A. toe off) and swing to stance (B. terminal stance) transition times in the gait cycle. Standard deviations for all muscle and walking condition variables are included in Appendices 4A and 4B.

2.3.5 Gait Parameters Across the Gait Cycle

There were statistically significant main effects of sensory location on step length ($F_{5,230}$=3.66, p=.0027, eta-square=0.86) and walking velocity ($F_{5,230}$=3.14, p=.0079, eta-square=0.94). Adding texture to the MM significantly reduced step length (76.93cm ± 4.57cm) compared to the smooth top cover condition (77.56cm ± 4.70cm). Furthermore, texture to all topographical areas, with the exception of the calcaneus, significantly reduced walking velocity (MF: 1.432m/s ± 0.139m/s; LF: 1.435m/s ± 0.132m/s; MM: 1.426m/s ± 0.131m/s; LM:

1.430m/s ± 0.143m/s) compared to the smooth top covered condition (1.442m/s ± 0.139m/s). There were statistically significant main effects of walking condition on step length ($F_{5,230}$=66.03, p=<.0001, eta-square=0.86), step width ($F_{5,230}$=9.80, p=.0018, eta-square=0.72) and walking velocity ($F_{5,230}$=9.64, p=<.0001, eta-square=0.94). In the wedged condition (compared to the smooth top cover), step length significantly increased (77.77cm ± 4.70cm) while step width (13.44cm ± 3.71cm) and walking velocity was reduced (1.426m/s ± 0.140m/s).

2.3.6 Post-Collection Survey Results

Participants were asked 5 questions following each testing session. On the topic of perceptual comfort, 4 participants reported discomfort walking in the Rockport footwear and 2 participants reported overall discomfort when walking in the textured foot orthoses. Specific to each sensory region, texture under the CALC and MF were reported as the more uncomfortable areas, whereas texture under the MM and LM regions were reported as most comfortable. When asked about wearing textured orthotics during future sporting activities, 8 participants reported that it would be highly unlikely that they would wear the textured orthoses for high impact sports (volleyball, basketball or jumping), 11 shared similar feelings regarding running, and 31 participants had no reservations to wearing the textured orthoses for any sporting activities.

2.4 DISCUSSION

Muscle activity and kinematic changes have been previously correlated with electrical stimulation to five topographical regions of the foot sole. Although these neuromechanical outcomes modify locomotor output, prolonged electrical stimulation to the foot sole may not reflect a viable treatment solution when intentionally modifying pathological gait abnormalities. This study proposed an alternative cutaneous stimulation method which capitalized on the neurophysiological properties of FA1 cutaneous receptors in foot sole skin and enhanced tactile feedback with textured material incorporated into foot orthoses design. Contrary to our hypothesis, the facilitation or suppression of EMG response did not parallel the foot sole site and gait phase modulation previously observed in electrical stimulation research. Despite rejecting this hypothesis, the application of texture to distinct regions of the foot sole did independently modulate lower limb muscle activity during walking. It should also be noted that recent concerns have been raised that fine-wire EMG protocols of lengthy duration (over 30 minutes) may result in EMG amplitude attenuation over time [134]. Despite the evident variability across trials, our EMG signals did not appear to attenuate over the length of a testing session (Figure 10).

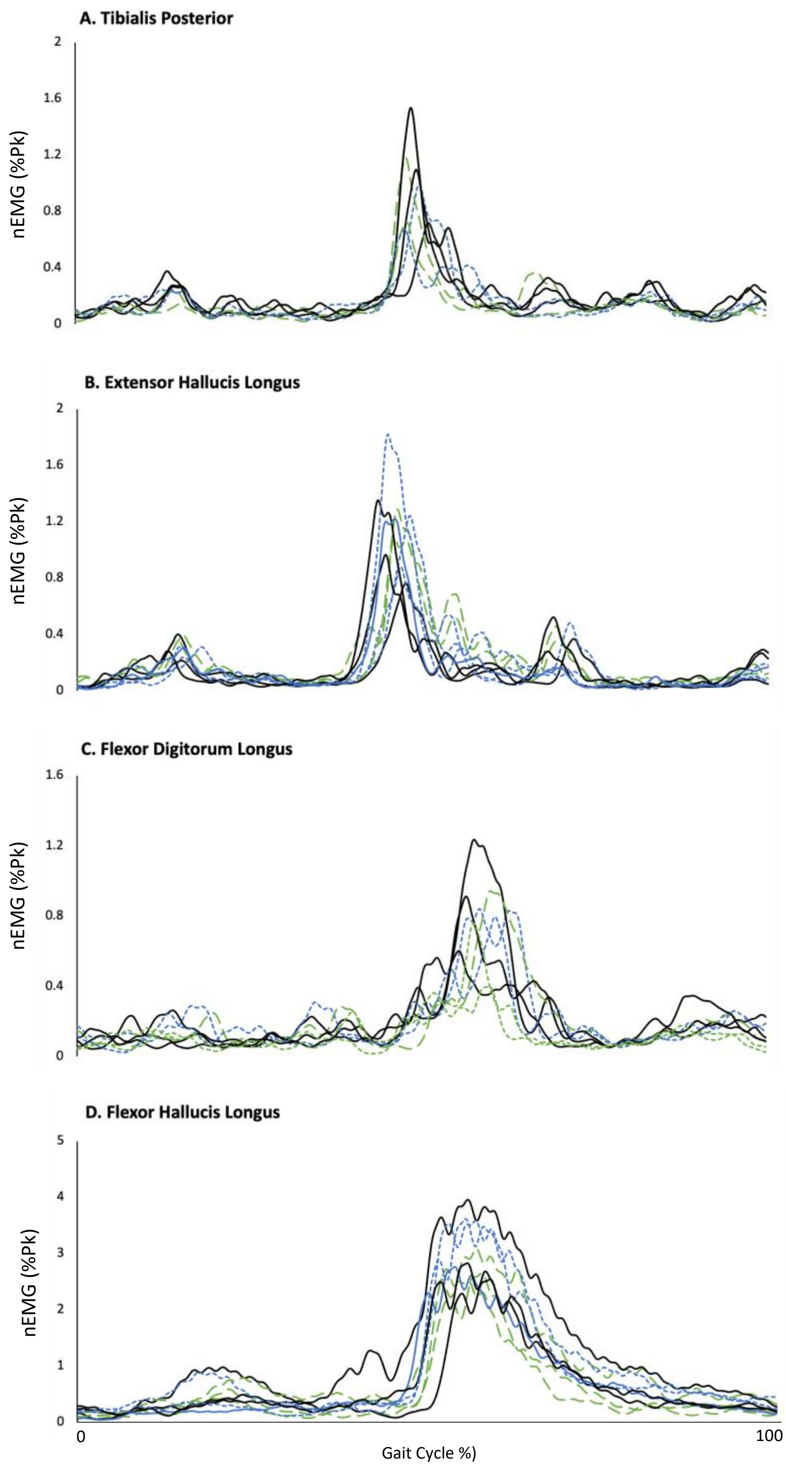

Figure 10. Ensemble averages representing 100% of the gait cycle graphed from four muscles (A. Tibialis Posterior, B. Extensor Hallucis Longus, C. Flexor Digitorum Longus, D. Flexor Hallucis Longus) of the same participant when walking in smooth top covered orthoses. This data represents three time points throughout the testing session: black solid lines: start of session, blue dotted lined: middle of session, green dashed lines: end of session. These were the four muscles recorded via fine-wire EMG.

2.4.1 Different neurophysiological mechanisms between electrical and mechanical stimulation

The neurophysiological mechanisms of electrical stimulation to foot sole skin and mechanical stimulation via tactile feedback are inherently different. A train of electrical stimuli which generates a brief facilitation or suppression of a muscle's EMG is investigating the task and phasic reflex modulation of the polysynaptic cutaneous pathway [60,135]. The stimulation is also applied directly to predominantly cutaneous nerves. Conversely, the use of texture as tactile stimuli is intended to stimulate cutaneous mechanoreceptors in foot sole skin and the EMG response is recorded in muscle. The textured material is intended to mechanically deform FAIs and generate action potential volleys through the cutaneous nerve pathway [69,135]. Although tactile and electrical stimuli travel through similar cutaneous nerves, the initial stimulation is intentionally probing a different area of the cutaneous pathway. Direct stimulation to nerves and end organs are different neurophysiological mechanisms and a likely explanation for their unique locomotor response.

2.4.2 Lower limb modulation is dependent on the phase of gait and site of tactile stimulation

Despite the differences between electrical and tactile stimulation to the foot sole, the results of this study support the ability of texture applied to distinct regions of the foot sole to independently change muscle activity in various lower limb muscles during gait. Overall, texture placed under the LF always generated a suppression of EMG, irrespective of the muscle and/or phase of gait. Texture under the LM always generated a facilitation. Thus, skin on the lateral border of the foot, specifically the midfoot and forefoot, modulated a consistent excitatory or inhibitory motor output. Interestingly, the highest overall density of cutaneous receptors, as well as the density of FAIs receptors specifically, are located in skin from these regions of the foot sole [56]. Additionally, regardless of participant's foot posture, the lateral midfoot and forefoot would always remain in contact with the tactile feedback. It appears that FAI density, coupled with full foot contact between texture and skin, play a large role in altering lower leg motorneuron pool excitability compared to individual muscle responses and phase of the gait cycle.

2.4.3 Early Stance

Texture under the MM or CALC region of the foot sole facilitated extensor muscle activity and suppressed flexor muscle activity in early stance. EHL is typically active in early stance however its activation generally ceases once the forefoot has made contact with the walking environment [15]. As there is no change in TA activation, it can be assumed that the TA is eccentrically contracting and decelerating the forefoot to the ground [11]. The EHL appears to continue resisting 1st metatarsalphalangeal plantarflexion throughout midstance and into propulsion. From the foot's loading response and throughout midstance, EHL activation is accompanied by a significant suppression of both FDL and FHL musculature. Cutaneous afferent facilitation under the MM or CALC may prove valuable in treating medical conditions which could benefit from a suppression of flexors and facilitation of extensors at initial contact and/or loading phases of the gait cycle. Examples include instability of the 1st metatarsal, foot drop and flexor tendinitis. Although the kinematic changes were quite small, it should be noted that texture under the CALC significantly reduced peak knee flexion, peak ankle dorsiflexion and total ankle range of motion. As peak knee flexion typically occurs in early swing and peak ankle dorsiflexion after heel lift [12], these kinematic changes likely don't affect targeted interventions in early stance.

Adding texture under the LM or MF significantly facilitated the activation of TP in early stance. Interestingly, foot orthoses (without cutaneous facilitation) have been previously observed to reduce TP activity [31,32,136–138]. The TP has a large role in decelerating subtalar joint pronation, serves as the primary extrinsic foot muscle that stabilizes the medial longitudinal arch, and is typically active during this phase of the gait cycle [139,140]. A dysfunctional TP muscle and tendon has also been attributed as a main causal factor in the development of adult acquired flat foot [140]. Cutaneous afferent facilitation under the LM or MF regions of the foot sole may prove beneficial in treating this condition assuming the muscle is sufficiently healthy to accommodate increased activation. With texture under the LM, the ankle moves through significantly increased ROM, increased dorsiflexion, and reduced plantarflexion throughout gait. Peak ankle dorsiflexion typically follows heel lift, just prior to the posterior compartment musculature's role in raising the heel for propulsion. This likely contributes to the increased total ankle ROM and may translate to increased demand on the TP muscle. Consequently, in the treatment of tendon dysfunction and/or adult acquired flatfoot, cutaneous afferent facilitation to the MF may prove preferential over the LM. Texture to either region may prove effective in treating conditions aimed at increasing subtalar joint pronation, although careful attention should be placed on the health of the TP muscle and tendon.

2.4.4 Midstance

During midstance, our results suggest that texture to distinct areas of the foot sole have different modulatory effects on lower leg muscle activity when changing the orientation of the foot (Figure 6). When interpreting these results, two details are worth highlighting: 1) the % CoP under the foot sole, and 2) gait cycle timing. Firstly, the wedge used in this experimental protocol increased subtalar joint eversion, which subsequently reduced CoP under the lateral side of the foot and increased CoP under the medial side (Figure 11). Secondly, texture under both midfoot regions are the primary areas that body weight would be loading the textured material. In considering these details, the most interesting result is a modulation of MG and TP muscle activity when facilitating the medial midfoot and changing the orientation of the foot. As the subtalar joint everted when stepping on the wedge, texture under the MF facilitated MG and TP activation compared to walking in the smooth top covered orthoses. The change in the orientation of the foot would naturally shift CoP off the lateral column and increase skin contact onto the textured stimuli. This highlights the need to consider the task and shifts in CoP under the foot sole when selecting the area of tactile facilitation in future experimental designs.

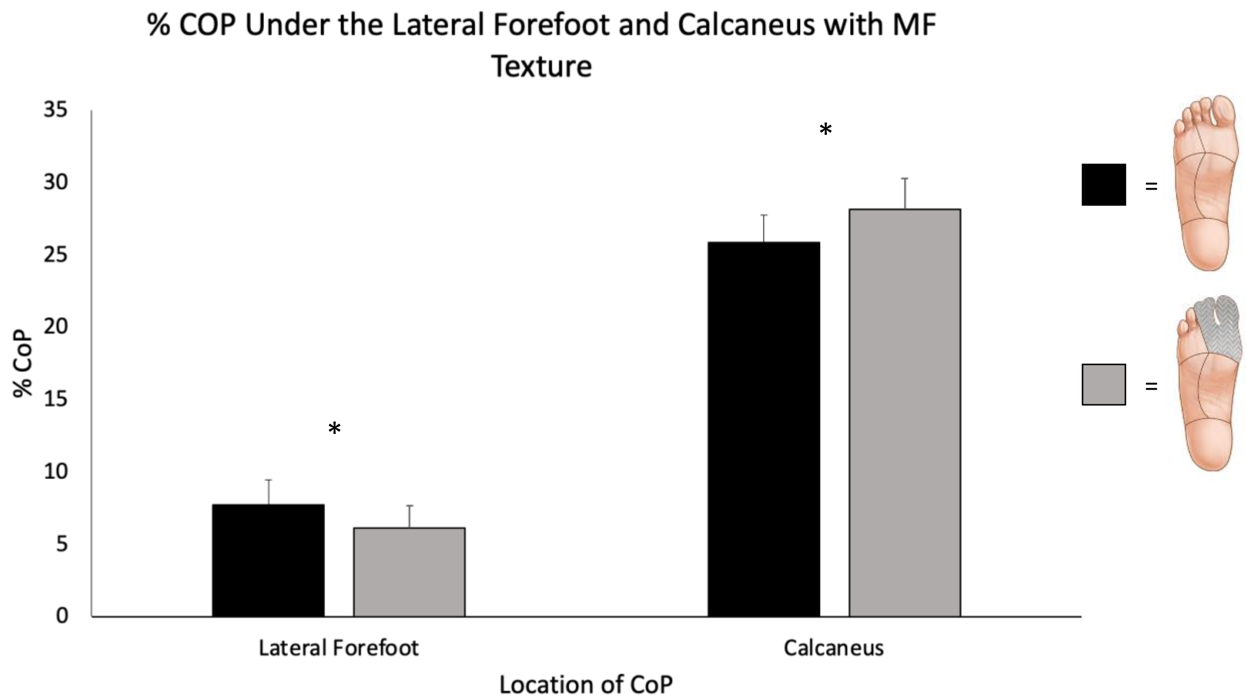

Figure 11. Cutaneous facilitation under the MF significantly reduced CoP under the lateral forefoot and significantly increased CoP under the calcaneus during the gait cycle.

2.4.5 Terminal Stance

Shifting later in stance, texture under the MF (loaded) and CALC (unloaded by this phase in the gait cycle) facilitated TP activity at heel rise, just prior to propulsion (Figure 7). As load is transferred from the midfoot to the textured forefoot, TP muscle activation was facilitated, likely assisting in ankle plantarflexion and inversion at propulsion. These results were accompanied by a significant reduction in knee flexion and total ROM. Furthermore, a significant interaction effect continued between the MG and orientation of the foot. Body weight is now shifting from midfoot to forefoot, supporting the need to consider the effects of midfoot and forefoot cutaneous facilitation. Most notably, texture under the lateral forefoot significantly facilitated MG activity when load increased under the medial aspect of the foot. These results provide a strong indication that tactile feedback generated the strongest MG facilitatory effect when load transitioned from smooth to texture.

The combination of transitional timing (from midstance to heel rise) and smooth to textured material likely caused substantial indentation to foot sole skin and subsequently generated an influx of FAI stimuli.

2.4.6 Swing

During swing, it should be highlighted that each area of textured facilitation would remain in contact with skin, however none of foot sole is loaded. Although this is logical during the swing phase of gait, this distinction is important as modulatory effects to lower limb musculature are likely secondary to the stance phase of gait rather than a direct response to the tactile stimuli. Despite this secondary response, texture under the MF, MM, and LM demonstrated a facilitatory effect on MG muscle activity. Texture under the LF consistently suppressed FHL from propulsion to end of swing. Lastly, in terminal swing, texture under the MM had a larger facilitatory effect on TA activation (compared to no texture) when walking over the wedge compared to level walking. This suggests that texture under the foot in swing is affected by the orientation of the foot in stance. Although not studied here, it remains plausible that the afferent information related to tactile feedback is affecting motorneuron pools across both limbs, highlighting the neurophysiological complexities of spinal interneuronal pathways in the control of human locomotion [141].

2.4.7 Perceived comfort when wearing textured foot orthoses

Ninety-six percent (96%) of participants reported subjective comfort with texture under the foot sole. This is important, as noxious electrical stimuli typically generates a withdrawal reflex in the lower limb [142,143] (which would subsequently alter our net EMG results) while also supporting the translation of textured insoles into clinical intervention studies. Our CoP analysis was intentional in providing an indication of how much participants weighted each area of texture, or conversely, if considered painful, tried to offload the area of texture when walking in each textured condition. Excluding the MF, texture to all other areas had no significant effect on altering CoP. These results suggest that the percentage of time the CoP remained in the region where texture was applied to the LF, CALC, MM, and LM was the same as walking without texture to these areas. These results further confirm participant comfort as normal weight was placed on the texture during load. Specific to the MF region, adding texture under the MF increased CoP under the calcaneus and reduced CoP under the LF. Although these results are irrespective of gait phase, pressure under the calcaneus is typical in early stance and forefoot pressure is typical in late stance. Thus, we can infer that texture under the MF prolonged CoP time at initial contact and shifted CoP from the lateral forefoot onto the textured area (MF), further confirming that participants did not intentionally avoid the tactile facilitation. This is an important distinction with interventions targeted to increase TP activation via MF facilitation in early stance.

There are a few methodological limitations worth highlighting. Participants did not wear socks during the experimental protocol. It is assumed that socks would impede tactile feedback, however it remains unknown if adding socks to the foot sole interface would wash out textured effects. Secondly, this is an acute intervention study and long-term effects of textured foot orthoses remains unknown. Lastly, this study tested the regional application of distinct areas of cutaneous facilitation. We cannot assume that combining results from multiple textured areas would compound the locomotor effects.

2.5 CONCLUSION

In conclusion, the results of this study support the topographic organization of foot sole skin in producing phase and muscle-specific modulation during human locomotion. More importantly, the modulatory response of tactile and electrical cutaneous stimuli do not parallel each other, suggesting independent methods of altering the cutaneous pathway. It is assumed that when force is transferred across the foot during each phase of the gait cycle, these time points within the gait cycle generate the greatest FAI activation and thus maximize the benefits of cutaneous afferent facilitation. Future research is needed to investigate the effects of textured foot orthoses in long-term intervention studies and in pathological or diseased populations.

CHAPTER 3

CAPITALIZING ON SKIN IN FOOT ORTHOSES DESIGN: THE EFFECTS OF TEXTURED FOOT ORTHOSES ON PLANTAR INTRINSIC FOOT MUSCLES DURING LOCOMOTION

3.1 INTRODUCTION

The human foot is complex. Recent scientific advancements have strengthened our understanding of the functional role of plantar intrinsic foot muscles (PIFMs) during locomotion [144–146]. The passive and active structures of the foot can adapt to various static and dynamic loads through the storage and return of elastic energy across the stance phase of gait [147,148]. Foot orthoses (FO) are a commonly prescribed intervention to alter foot function during walking [149–151], although their effects have been primarily studied in the extrinsic muscles of the foot. This is alarming considering foot disorders implicate both extrinsic and intrinsic foot muscles [152,153], and despite this evidence, the role of FOs in modulating muscle activity of PIFMs during gait has yet to be studied. Furthermore, enhancing tactile feedback under the foot sole has been recently shown to alter muscle activity during gait [110,128,154], yet again, these muscular changes have been limited to the study of extrinsic foot muscles. Thus, studying the effects of FOs and tactile facilitation within FO design may be an effective method to capitalize on the functional role of skin and beneficial effects of FOs to intentionally modify PIFMs function during locomotion.

Considering the normal composition of the human foot, including 26 bones, 30 joints, 100+ muscles, and 3 arches [18], it is not surprising that the study of the human foot is complex. Two classic studies [15,155] which measured the phasic electromyography (EMG) of PIFMs during walking shared similar overall conclusions, suggesting that the intrinsic muscles of the foot act as a “functional unit”. Collectively, these papers indicated that EMG of 6 PIFMs (extensor digitorum brevis (EDB), flexor digitorum brevis (FDB), abductor hallucis (AbdH), flexor hallucis brevis (FHB), abductor digiti minimi (ADM) and dorsal interossei) during level walking were active throughout stance while remaining inactive during swing [15,155]. More recently, fine-wire EMG recordings have confirmed that PIFMs have distinct phasic variability during stance and swing [145,146]. The AbdH EMG peaks in early stance, FDB peaks mid- to late stance, and the transverse head of adductor hallucis (AddH) peaks in the early and late stance phases of gait [146]. In swing, the AddH and FDB EMG remain quiet, whereas AdbH and QP burst late in swing [145,146]. This temporal variability between PIFMs challenges the idea that these muscles work as singular unit, and in fact, suggests they may have independent roles (and unique muscle activity) depending on the functional task and/or phase of the gait cycle.

PIFMs demonstrate different EMG activation patterns when the demands of a functional task are altered. As previously highlighted, the AbdH, FDB, AddH, and QP have unique on/off bursting patterns throughout the stance and swing phases of gait [145,146]. The EMG magnitude of AbdH and FDB also increase with greater force requirements during the propulsive phase of gait [156]. Zelik et al. (2015) closely examined the intrinsic forefoot muscles during walking. The antagonistic behaviour of metatarsophalangeal (MTP) flexors and extensors are sequentially active, rather than simultaneously active during walking. During the transition from stance to swing (propulsive phase of gait), the sequential order of muscle activation begins with ankle plantarflexor activity, followed by MTP flexors, MTP extensors, and terminates with ankle dorsiflexors [157]. Thus, the sequential activation of these muscles suggests that they have different bursting patterns contributing to different biomechanical roles when moving through propulsion. Conversely, some functional tasks require simultaneous activation of all PIFMs. For example, the AbdH, FDB, FHB, and ADM are simultaneous active in the maintenance of a heel raise (isometric contraction of standing on toes) and simultaneously inactive during quiet stance [155]. This is further evidence to suggest that PIFMs can independently adapt to the demands of the task and load requirements to meet functional demands.

When the foot experiences load, as occurs during locomotion, the medial longitudinal arch (MLA) lengthens and lowers to the ground. Conversely, as load is removed, a subsequent recoiling occurs at the MLA [145]. During early to mid-stance, as vertical load increases, the MLA is compressed, and the motor-tendon units (AbdH, FDB or QP + plantar aponeurosis) lengthen. Conversely, during mid- to late-stance, as vertical load dissipates, the MLA recoils, and the motor-tendon units shorten [145]. The active lengthening of the PIFMs contribute to the compliant behavior of the MLA. As the muscles spanning the MLA lengthen, as typically occurs in midstance, the stiffness of the arch increases in response to the ground reaction force demands. As ground reaction force profiles change, which occurs between walking and running mechanics, the MLA has demonstrated the ability to adjust its mechanical function. The magnitude of AbdH, FDB, and QP muscle activity increases with increased gait velocity [145] and remains stiffer in shod conditions versus barefoot [158]. This is important, as footwear has been demonstrated to absorb ground reaction force impacts during stance and requires increased PIFM activation (and reduced MLA lengthening) to match foot stiffness requirements moving through stance [158]. This research has highlighted the functional importance of PIFMs spanning the MLA which function to help stiffen the arch in response to changes in the ground reaction forces between the foot and walking environment. Changes to the foot-environment interface requires PIFM adaptability to effectively store and return elastic energy through stance. A FO sits within this interface, makes direct contact to foot sole skin, and typically reduces the active lengthening of the MLA. Research has yet to explore the effects of FOs on PIFM muscle activation during walking.

FOs are a commonly prescribed intervention to alter foot function during walking. Specific to extrinsic foot muscles, FOs have been reported to increase [149,159,160], decrease [138,150,151,161], and/or have minimal effect on musculature [32], all depending on the locomotor or functional task being studied. In contrast, there is a scarcity of research investigating the role of FOs on PIFMs. To date, one single study has reported a reduction in cross-sectional area, while AbdH, ADM, EHB, and EDB EMG remained unchanged after 12 weeks of wear [162]. Recently, adding textured material to the walking surface has emerged as a novel method of stimulating FAI cutaneous mechanoreceptors in foot sole skin to intentionally modify muscle activity [154]. Various methods of tactile enhancement are being incorporated into insoles [77,110,128], and more intriguing, into FO design [91], which maximizes skin-to-texture contact between the foot sole interface. These three areas of research, PIFMs, FOs, and textured FOs have yet to be combined to study the effects of FOs and tactile facilitation on PIFM function during gait.

The cutaneous receptors in foot sole skin, predominantly FAIs [56], are mechanically stimulated when skin is subject to indentation [56,57]. We propose that textured FOs may be an effective method to enhance sensory feedback from foot sole skin, modulate PIFM activity during locomotion, and contribute to the MLA stiffness requirements during stance. Considering the minimal research on FOs and PIFMs, the aim of this study was to investigate the effect of FOs with and without sensory facilitation on PIFM amplitude during locomotion. The specific research questions were as follows: 1) What is the effect of FOs on the amplitude of PIFMs during the gait cycle?, 2) Do textured FOs modulate the amplitude of PIFM differently compared to non-textured FOs throughout the gait cycle?, and 3) How does the compliance of the surface impact the changes seen in the PIFMs with FO condition (non-textured and textured)? It was hypothesized that both non-textured (FOs) and textured FOs (FOTs) would increase the PIFM activity during gait, with the greatest PIFM activation observed in the FOT condition (as a result of increased FAI stimulation). Lastly, when walking on the compliant surface, the largest PIFM amplitude was hypothesized when walking barefoot and in FOTs and reduced in the FO condition. To test these hypotheses, participants completed a series of walking trials on two different surfaces (hard and soft) while kinematics and fine-wire EMG of 4 PIFMs were recorded in two different orthoses conditions (FO and FOT).

3.2 METHODS

3.2.1 Participants

Forty healthy young adults (age: 27 ± 5.2 years, 24 males, 16 females, height: 175.5 ± 10.4cm, weight: 80.2 ± 18.7 kg) with no known neurological and/or musculoskeletal disorders participated in this research study. Semmes-Weinstein monofilaments (North Coast Medical, Inc., Morgan Hill, CA) confirmed that participant's foot soles exhibited normal sensation (Table 3). Informed consent was obtained prior to the start of each testing session and this protocol was approved by the institutional research ethics board (REB#6006).

Table 3. The monofilament scores (touch sensitivity) from participant's bilateral foot soles (n=40 left/right, age: 27 ± 5.2 years). Evaluator filament sizes below 3.22 indicate normal sensory thresholds, filaments of 3.22 and 3.61 indicate diminished light touch, and filaments between 3.84 and 4.31 indicate diminished protective sensation (2011 North Coast Medical, Inc.). Bilateral MLA's demonstrated low levels of diminished light touch, whereas the 4 other areas (1st MTP, 5th MTP, LLA and calcaneus), bilaterally, demonstrated slightly higher levels of diminished light touch. None of the foot sole areas had reduced protective sensation.

Filament Testing Site	Left Foot Sole	Right Foot Sole
1st MTP	3.27 ± 0.30	3.28 ± 0.36
5th MTP	3.36 ± 0.35	3.41 ± 0.35
MLA	3.04 ± 0.35	3.06 ± 0.39
LLA	3.27 ± 0.28	3.26 ± 0.32
Calcaneus	3.50 ± 0.34	3.58 ± 0.37

*MTP: metatarsalphalangeal joint; MLA: medial longitudinal arch; LLA: lateral longitudinal arch

Lastly, participants were asked about their level of perceived comfort on a scale of 1 to 10. This data was collected at the beginning of the testing session (before walking trials started) and at the end of each session (following the last walking trial) to gain insight into participants comfort pertaining to the textured orthoses under their feet.

3.2.2 Instrumentation

Kinematic and Kinetic Data

Kinematic data (100Hz) were collected using the Optotrak motion capture system (Optotrak Certus; Northern Digital Inc., Waterloo, Ontario, CAN). IRED markers were placed on twelve anatomical landmarks: bilateral acromions, anterior superior iliac spines, tibial tuberosities, talocrural joints (ankles) 3rd metatarsals, forehead, and xyphoid process. To maintain consistent marker placement between experimental conditions, careful attention was placed on the markers adhered to the ankles and metatarsals. Landmarking to these sites was critical as socks were removed between conditions to alter orthotic condition exposure (see protocol section). Kinetic data (2000Hz) were collected from 3 force plates (OR6-5-2000; AMTI, Watertown, Massachusetts, USA) embedded into the floor. Gait cycle timing was extrapolated from force plate data to determine initial contact (>10N threshold) through to the terminal swing phase of gait (initial contact of the same limb determined by a <10N threshold).

Electromyography

A wireless EMG system (Ultium, Noraxon, Scottsdale, AZ, USA) recorded muscle activity of four PIFMs during gait (2000Hz). Raw EMG signals were passed through a differential amplifier (gain x500) and band-pass filtered at 10-500Hz. Bipolar fine-wire intramuscular electrodes recorded the EMG signals from the abductor hallucis (AbdH), transverse head of adductor hallucis (AddH), flexor digitorum brevis (FDB) and abductor digiti minimi (ADM). The electrodes were fabricated from 0.005mm formvar coated copper wire (California Wire Company, Grover Beach, USA) and inserted through a 30mm (27g) or 50mm (25g) length single-use hypodermic needle (BD Precision Glide, Franklin Lakes, USA). At the insertion end, 1mm of insulation was stripped from the wire and folded over the needle tip. Two fine-wire insertions were performed per foot. Although the muscle insertions varied between left and right feet, the FDB and AddH recordings were consistently collected from the same foot, as were the AbdH and ADM recordings. All fine-wire electrodes were inserted under ultrasound guidance (HFL50X, SonoSite, Toronto, CAN). Each insertion site was sterilized prior to skin puncture. The fine-wire insertion depth ranged from 8-25mm below the skin dependent on the targeted muscle of interest and individual variations in anatomy. The accuracy of insertions within each respective muscle was confirmed with resisted testing and/or active muscle contractions while monitoring the live EMG signal.

Prior to all insertions, the posterior borders of the medial and lateral sides of the FOs were traced on participant’s feet. This was important to ensure the FO did not touch any insertion site within close proximity to the borders. The AbdH was located by palpating inferior to the medial malleolus and navicular, superior to the medial band of the plantar fascia. The electrode was inserted approximately 1 finger breath below the navicular on the medial aspect of the foot. Insertion accuracy was confirmed with resisted flexion and abduction of the great toe. As the FDB lies deep to the AbdH, this muscle was located by initially palpating and landmarking the

AbdH muscle via ultrasound. Insertion accuracy into FDB was confirmed with active flexion of digits 2-4 and the absence of EMG during resisted abduction. The ADM was located by palpating the cuboid and distal-lateral border of the calcaneus. The electrode was inserted from the lateral border of the foot, approximately equal distance between these two bones. Insertion accuracy was confirmed with resisted abduction of the 5^{th} MTP and active little toe flexion. The ultrasound-guided insertion protocol into the AddH has been previously described in Robb et al. (2021) [146] (Figure 12).

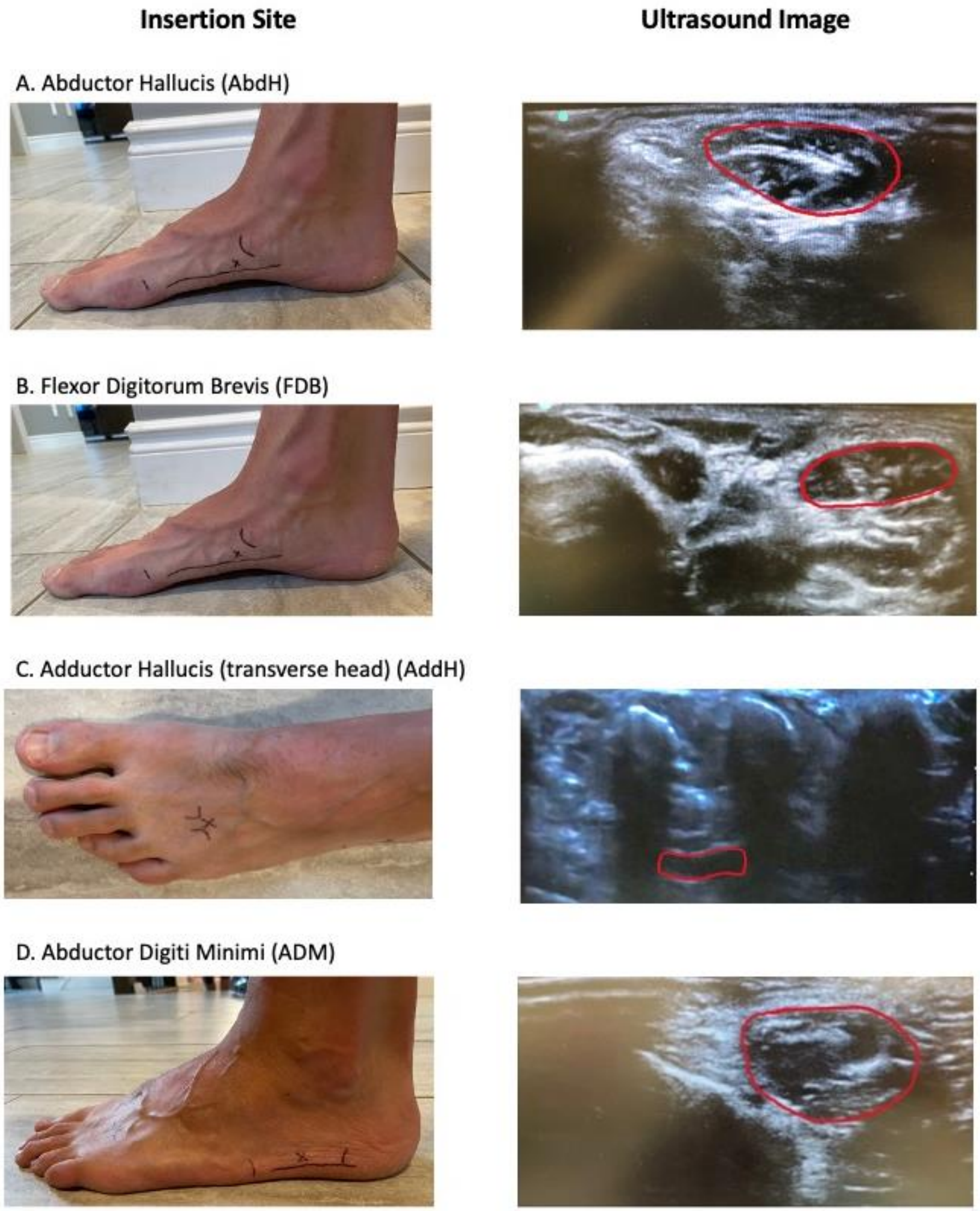

Figure 12. The insertion site and accompanying ultrasound image of the fine-wire insertions for each PIFM in this study. The target insertion site has been marked with an X on the skin surface and outlined in red on the ultrasound image. Orthoses borders and anatomical landmarking's have also been identified on the skin.

Testing Procedures

All participants were tested in each FO conditions (non-textured foot orthoses (FO) and textured foot orthoses (FOT)). The FO condition consisted of participants wearing Sole's 'Active Thin' prefabricated FOs (Sole, Calgary, CAN). The FOT condition included this same FO with an additional textured top cover adhered to its surface (Figure 13). The texture was zigzag patterned running perpendicular to the walking direction. Socks were worn over the FOs and participants feet, which served to secure the FOs during all walking trials. These socks were standardized across all participants (76% polyester, 22% olefine, and 2% rubber; Wal-Mart Canada Corp.).

Figure 13. The foot orthotic conditions. Left image: non-textured foot orthoses (FO); Right image: textured foot orthoses (FOT).

The experimental protocol included three orthotic conditions (barefoot, FO, and FOT) and two flooring surfaces (hard and soft). The walking surface was manipulated with a custom-built platform placed over the force plates embedded flush with the ground. Manipulating the walking environment to a destabilizing surface has been demonstrated to increase the functional demands of shank musculature during gait [163,164]. Although these effects have been minimally studied in PIFM during locomotion [146], as foot stiffness has been attributed to increased PIFM activation [156,158], any surface which dampens ground reaction forces is anticipated to increase PIFM EMG demands. Removeable platform inserts modified the walking surface with two different surfaces (hard and soft), thus modifying the complexity of the walking environment. The hard condition consisted of the same plywood as the remainder of the platform, 90 durometer, shore A. The soft condition was constructed of ½" ethyl vinyl acetate foam, 10 durometer, shore A. Participants were provided the opportunity to practice walking across the custom-built platform and habituate to the inserted fine-wires prior to collection. Each trial started in static stance. When instructed to begin, participants walked at a self-selected velocity from one end of the walking platform to the other (approximately 10m) and stopped in static stance. The steps that occurred over force plates 1 and 2 correspond to the locations where the walking surface was manipulated between the hard and soft surface (Figure 14).

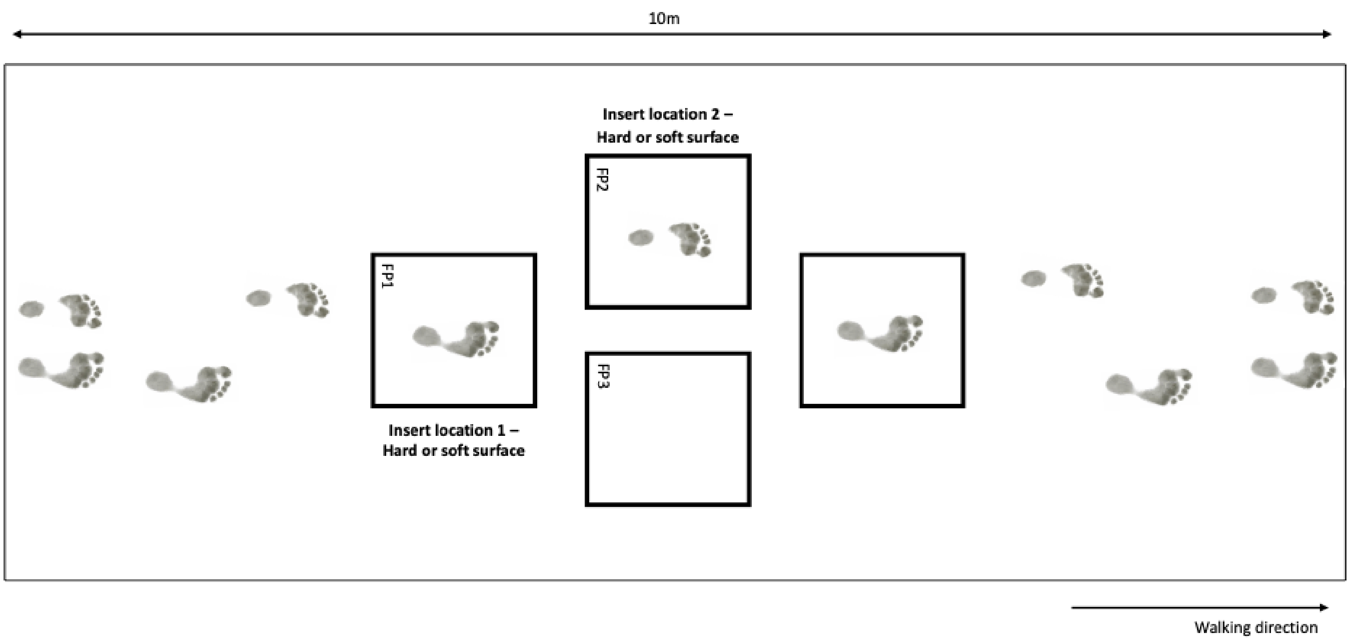

Figure 14. The 10m custom-built platform participants walked over during each trial. Participants took 2 steps prior to making contact with force plate 1 (FP1), and subsequent contact on force plate 2 (FP2). Participants were instructed to continue walking at a consistent velocity until they reached the end of the platform. FP1 and FP2 correspond to the location of a force plate embedded into the floor, underneath the platform. Insert locations 1 and 2 correspond to the locations in which the flooring was removeable, and flooring was either substituted with the hard walking surface (same surface as the rest of the platform), or soft foam. Kinematic, kinetic, and EMG data were extracted from steps 3, 4 and 5.

Each testing session began with five barefoot walking trials on both the hard and soft walking surfaces. The order of FO and FOT exposure then alternated between participants. To secure the orthoses in place, socks were carefully stretched over each foot. The ankle and 3rd metatarsal head markers were adjusted as required. A total of ten walking trials were completed in the first orthotic condition. Participants were asked to take a seat and socks were removed. The current orthotic condition was replaced with the other condition and walking trials were repeated. Fifty walking trials were completed in total [Barefoot: 5 x hard/soft, FO: 10 x hard/soft, FOT: 10 x hard/soft].

3.2.3 Data Processing

All EMG data was full-wave rectified and linear enveloped with a 40Hz dual-pass Butterworth filter. The gait cycle was divided into ten 10% phases of the gait cycle; Stance phase: initial contact (IC), loading response (LR), midstance (MS), heel rise (HR), propulsion (PR), toe off (TR); and Swing phase: initial swing (ISW), early mid-swing (early MSW), late mid-swing (late MSW), and terminal swing (TSW). The average EMG (aEMG) per 10% epoch was normalized to the peak EMG (%Pk) of each muscle within the gait cycle. Raw kinematic data were processed with a cubic spline function in a custom-made Optofix software to correct small gaps in trajectories, then filtered at 6 Hz low-pass dual-pass Butterworth filter. Sagittal plane kinematics of the hip, knee, and ankle were extrapolated from the anterior-posterior and vertical coordinates of the IRED markers. Commonly used references standardized the zero-reference position for each joint [165].

3.2.4 Statistical Analysis

Independent two-way repeated measures analysis of variance (ANOVA) (SAS University Edition, 2.8.1, version 9.4) were performed for each EMG epoch (40 total: 10 EMG epochs/phases of gait x 4 PIFMs) to compare within-subject factors of FO condition (barefoot, FO, FOT) and walking surface (hard, soft). Additional two-way repeated measures ANOVAs compared these same within-subject factors for bilateral kinematic variables (18 total: 3 joints (hip, knee, ankle) x 3 variables (max, min, range) x 2 legs (left, right)) and gait parameters (3 total: walking velocity, step length, and width). Tukey's HSD post hoc comparisons were performed on all data when data were statistically significant. Data were rank-transformed when the Shapiro-wilk test for normality indicated that data did not meet parametric criteria. If a fine-wire EMG signal was saturated with noise or demonstrated poor signal quality it was removed from the dataset. The majority of signal quality concerns were addressed during collection, however two FDB, two AddH, and two AbdH wires tore away from the Fine Wire SmartLeads (842FW, Noraxon, USA) (all different participants) during collection and due to being too short to re-attach during collection they were excluded from the analysis. Data exceeding ±4SD from the mean were visually inspected as a potential outlier by comparing graphed EMG to determine if the signals contained excessive noise and/or motion artifacts. Outliers and/or missing values were replaced by the mean (max 8 replacements per bin of 2000 samples). Statistical significance was determined at $p<0.05$ a priori. An example of raw participant data is provided in Appendix 5.

3.3 RESULTS

3.3.1 Perceived Pain

Participants were asked to rate their perceived level of pain on a numerical scale, from 0-10 (0 - no pain; 10 - worst pain imaginable), at the start and end of the testing session. In 30 of 40 participants, the mean pain score after the first walking trial was 1.4 ± 0.8, and 1.87 ± 1.3 at the end of the last walking trial. As all participant's experienced all conditions, it was not possible to detect differences between experimental conditions. Pain scores were not statistically significant suggesting that participants exhibited minimal pain, which did not change throughout the duration of the protocol.

3.3.2 The differential effects of FOs on PIFMs when changing the walking surface compliance

When walking on different flooring surfaces and when wearing different foot orthoses, the amplitude of each PIFM was modulated differently at initial contact, midstance, heel rise, propulsion, and toe-off phases of the gait cycle. All statistically significant interactions are presented in Figure 15. Complete results are included in appendices 6A-6F.

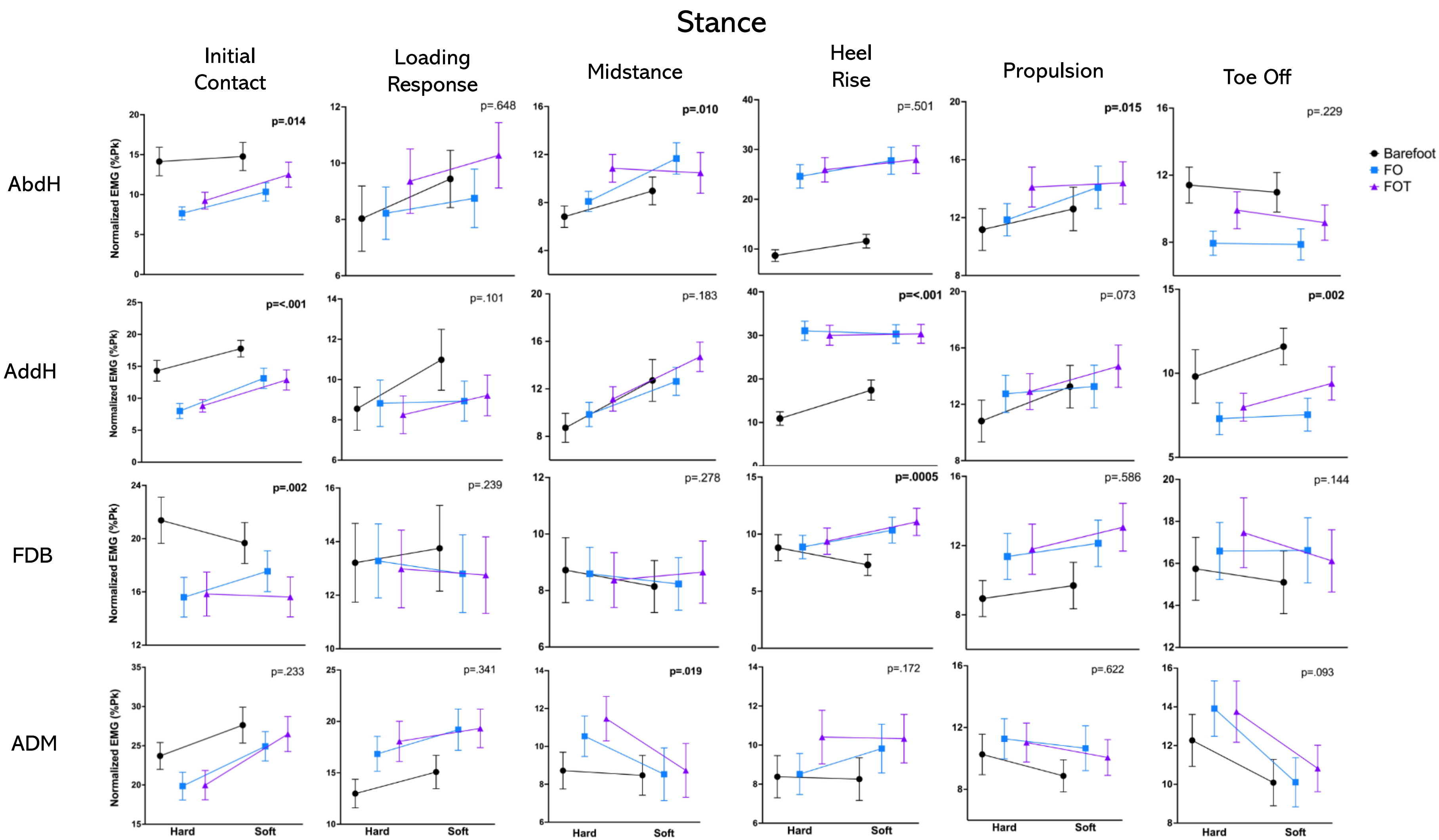

Stance
Initial Contact
Loading Response
Midstance
Heel Rise
Propulsion
Toe Off
AbdH
AddH
FDB
ADM
Normalized EMG (%Pk)
Barefoot
FO
FOT
Hard
Soft
p=.014
p=.648
p=.010
p=.501
p=.015
p=.229
p=<.001
p=.101
p=.183
p=<.001
p=.073
p=.002
p=.002
p=.239
p=.278
p=.0005
p=.586
p=.144
p=.233
p=.341
p=.019
p=.172
p=.622
p=.093

Figure 15. The statistically interactions of each PIFMs when walking on a hard and soft surface, across the stance phases of gait. The p values for all interactions are included, bolded values denote significance. Standard error bars have been included in each graph.

At initial contact (IC), statistically significant interactions were observed in 3 of 4 PIFMs, in AbdH ($F_{2,227}$=4.26, p=.014, eta-square=0.54), AddH ($F_{2,221}$=14.62, p=<.001, eta-square=0.69), and FDB ($F_{2,233}$=6.21, p=.0021, eta-square=0.50). When wearing a FO and FOT, aEMG of AbdH increased when walking over soft foam (FO: 10.34%Pk±7.09%Pk, FOT: 12.49%Pk±9.65%Pk) compared to the hard (FO: 7.65%Pk±4.99%Pk, FOT: 9.24%Pk±6.49%Pk) surface. Larger AbdH aEMG amplitudes were observed in the FOT condition. In AddH, walking in an FO over soft (13.12%Pk±9.82%Pk) foam generated slightly greater AddH aEMG compared to the FOT condition (12.87%Pk±9.72%Pk). On the hard surface, AddH aEMG was higher in FOTs (8.82%Pk±5.99%Pk) compared to FOs (8.01%Pk±7.20%Pk). In FDB, when walking in a FOT, the aEMG amplitude was slightly higher in the hard (15.84%Pk±10.17%Pk) versus soft (15.62%Pk±9.25%Pk) walking condition, whereas the opposite was seen in a FO; the hard surface reduced FDB aEMG (15.60%Pk±9.16%Pk) whereas the soft surface (17.55%Pk±9.45%Pk) increased FDM amplitude.

During midstance (MS) and heel rise (HR), significant interactions were observed in 2 PIFMs within each of these phases of gait. At MS, significant interactions were observed in the AbdH ($F_{2,227}$=4.66, p=.0096, eta-square=0.66) and ADM ($F_{2,239}$=3.99, p=.0187, eta-square=0.53) muscles. The soft walking surface consistently increased AbdH aEMG when barefoot (8.97%Pk±7.12%Pk), in FOs (11.67%Pk±8.10%Pk), and in FOTs (15.38%Pk±10.47%Pk) compared to the hard walking surface (barefoot: 6.82%Pk±8.97%Pk, FO: 8.09%Pk±5.16%Pk, FOT: 10.85%Pk±7.15%Pk). In ADM, walking barefoot generated less aEMG in the hard (8.72%Pk±5.97%Pk) and soft (8.47%Pk±6.45%Pk) walking conditions compared to both FOs. In a FO, walking on the hard (10.54%Pk±6.60%Pk) surface resulted in less ADM aEMG compared to FOTs (11.46%Pk±7.19%Pk), whereas in the soft condition, the ADM aEMG were quite similar between FOs (12.16%Pk±8.53%Pk) and FOTs (12.24%Pk±8.73%Pk). At heel rise, significant interactions were observed in the AddH ($F_{2,221}$=21.22, p=<.001, eta-square=0.75) and FDB ($F_{2,233}$=7.62, p=.0005, eta-square=0.51) muscles. The aEMG of AddH was reduced walking barefoot, on both hard (10.90%Pk±9.58%Pk) and soft (17.43%Pk±14.37%Pk) surfaces compared to both FO conditions. The AddH aEMG was higher walking on the hard surface in FOs (31.05%Pk±13.55%Pk) compared to FOTs (30.03%Pk±14.13%Pk), and conversely on the soft surface, lower in FOs (30.32%Pk±13.28%Pk) compared to FOTs (30.36%Pk±13.16%Pk). In FDB, walking barefoot generated greater aEMG when walking on the hard surface (8.31%Pk±7.02%Pk) compared to soft (7.30%Pk±5.71%Pk). FDB responded similarly to both FO conditions across walking surface. The FO and FOTs reduced FDM aEMG when walking on the hard surface (FO: 8.87%Pk±6.30%Pk, FOT: 9.40%Pk±7.11%Pk) and increased FDM aEMG on the soft surface (FO: 10.35%Pk±6.99%Pk, FOT: 11.07%Pk±7.33%Pk). FDB aEMG was higher in FOTs compared to FOs.

Statistically significant interactions were observed in the AbdH ($F_{2,227}$=4.22, p=.0148, eta-square=0.65) during propulsion (PR) and AddH ($F_{2,221}$=21.22, p=<.001, eta-square=0.75) during toe off (TO). During PR, walking over soft foam barefoot (12.60%Pk±9.26%Pk) and with a FO (14.09%Pk±9.01%Pk) increased AbdH aEMG compared to the hard (barefoot: 11.17%Pk±8.86%Pk, FO: 11.85%Pk±6.93%Pk) walking surface. Walking in the FOT resulted in a smaller increase in AbdH aEMG over the soft foam (14.40%Pk±8.99%Pk) compared to the hard (14.11%Pk±8.49%Pk) surface. At TO, walking barefoot generated greater AddH aEMG compared to both FO conditions. In FOs, a slight increase in AddH aEMG was observed over soft (7.54%Pk±6.05%Pk) foam compared to hard (7.30%Pk±5.87%Pk). Larger increases were observed in FOTs (hard: 7.98%Pk±5.13%Pk, soft: 9.40%Pk±6.08%Pk).

3.3.3 The effect of non-textured FOs on PIFM amplitude throughout the stance phase of gait

The immediate wear of FOs modified the amplitude of PIFMs differently across each phase of stance. Compared to walking barefoot, wearing FOs significantly reduced PIFM aEMG in AbdH, AddH and FDB at IC. These significant aEMG reductions were irrespective of the walking surface (see Figure 15). Similarly at MS, irrespective of the walking surface, wearing FO's significantly increased AbdH aEMG compared to walking barefoot. Lastly at HR, FOs significantly increased all PIFMs aEMG compared to walking barefoot. In AddH and FDB these increases were irrespective of walking condition, whereas significant main effects were observed in AbdH ($F_{2,227}$=527.88, p=<.001, eta-square=0.80) and ADM ($F_{2,239}$=13.98, p=<.001, eta-square=0.50) aEMG (Figure 16a). At propulsion (PR), significant increases in AbdH aEMG, walking in FOs compared to barefoot, were irrespective of walking condition. Significant increases in aEMG were also observed at PR in AddH ($F_{2,221}$=14.53, p=<.001, eta-square=0.71) and FDB ($F_{2,233}$=33.92, p=<.0001, eta-square=0.60) when wearing FOs compared to walking barefoot (Figure 16b). At toe-off (TO), significant aEMG reductions were observed in AbdH ($F_{2,227}$=55.29, p=<.001, eta-square=0.54) (Figure 16c) and AddH (irrespective of walking surface) (Figure 15). In FDB ($F_{2,233}$=4.82, p=.0081, eta-square=0.52), significant aEMG increases continued from PR (Figure 16c) into TO wearing FOs compared to walking barefoot.

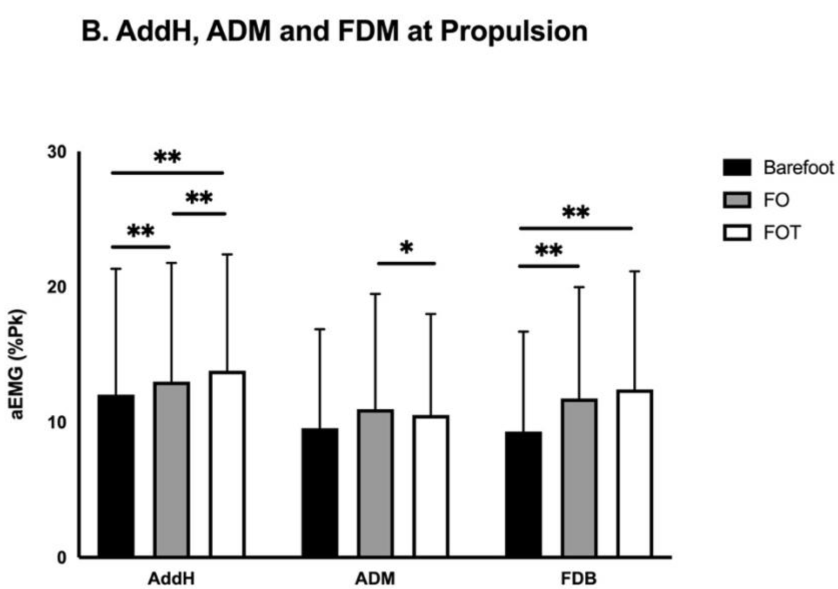

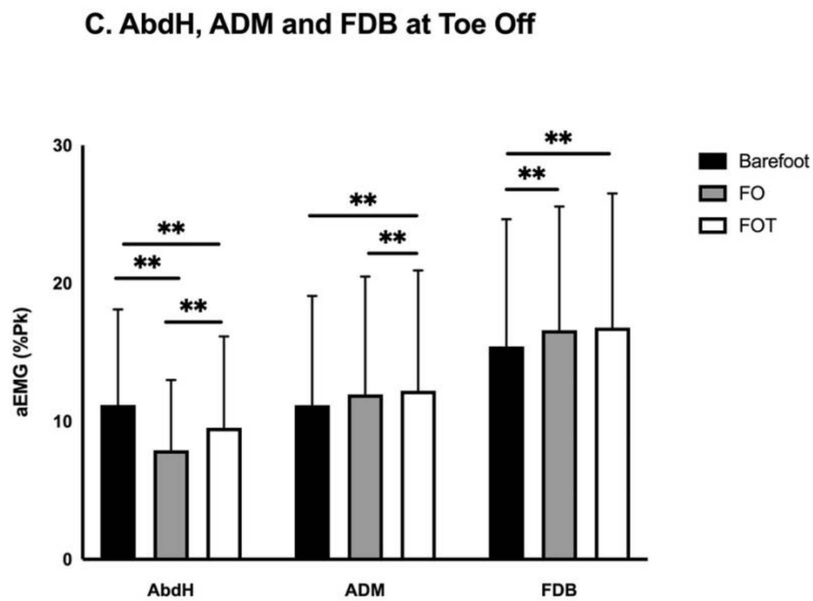

Figure 16. Graphical representation of mean and standard deviations of PIFMs aEMG across heel rise, propulsion, and toe-off phases of gait, divided by foot orthoses condition**. A.** At heel rise, walking in FOs and FOTs significantly increased AbdH aEMG compared to walking barefoot. Similarly, ADM demonstrated significantly greater aEMG magnitude when walking in FOs compared to barefoot, and in FOTs compared to FOs and barefoot. **B.** At propulsion, the AddH aEMG amplitude was significantly greater in FOs compared to barefoot, and in FOTs compared to barefoot and FOs. In FDB, the aEMG amplitude was greater in FOs and FOTs compared to barefoot. ADM aEMG was significantly reduced wearing FOTs compared to FOs. **C.** At toe off, the aEMG of AbdH was significantly reduced walking in FOs compared to barefoot and walking in FOTs. ADM aEMG was significantly greater in FOTs compared to FOs, and in FOs compared to barefoot. Lastly, in FDB, the aEMG was significantly greater in FOs and FOTs compared to walking barefoot. **=p<.05, **=p<.0001*

3.3.4 The effect of textured FOs compared to non-textured FOs

The immediate wear of textured FOs compared to FOs generated reductions in PIFM aEMG at IC, increased PIFM aEMG from LR to HR, and revealed muscle-specific reductions or increases at PR and TO. At IC, significant reductions in AbdH were irrespective of walking surface. ADM aEMG ($F_{2,239}$=12.75, p=<.001, eta-square=0.55) was significantly reduced at IC when walking in FOTs compared to FOs (Figure 17a). During LR, significant increases in AbdH ($F_{2,227}$=12.85, p=<.001, eta-square=0.51) and ADM ($F_{2,239}$=44.67, p=<.001, eta-square=0.61) aEMG were observed in FOTs compared to FOs (Figure 17b). Significant increases in aEMG continued in 3 PIFMs: AbdH, ADM (both irrespective of walking surface), and AddH ($F_{2,221}$=32.38, p=<.001, eta-square=0.63). At HR, significant increases in ADM ($F_{2,239}$=13.98, p=<.001, eta-square=0.50) aEMG were also observed (Figure 17a). At terminal stance, significant increases in aEMG were observed in AbdH (irrespective of walking condition) and AddH ($F_{2,221}$=14.53, p=<.001, eta-square=0.71) at PR. Conversely, wearing FOTs significantly reduced ADM ($F_{2,239}$=8.24, p=.0003, eta-square=0.63) aEMG compared to FOs at PR (Figure 17b). At TO, both AbdH ($F_{2,227}$=55.29, p=<.001, eta-square=0.54) and AddH (irrespective of walking surface) significantly reduced aEMG in FOTs compared to FOs (Figure 17c).

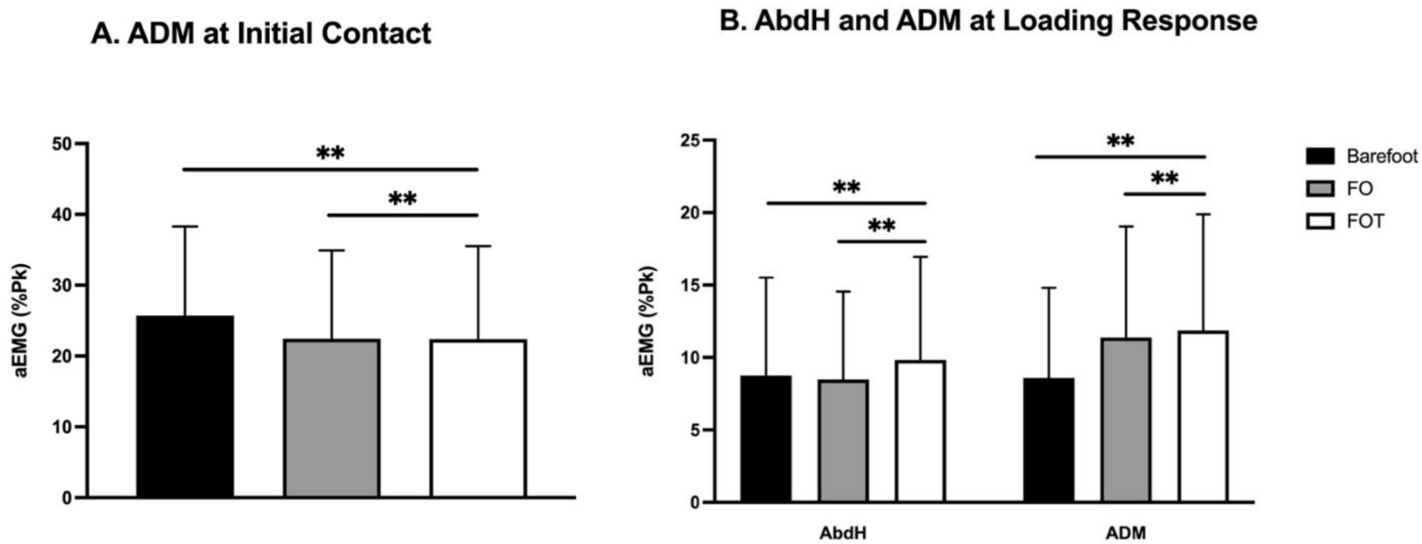

Figure 17. A. Graphical representation of mean and standard deviations of PIFMs aEMG across initial contact and loading response phases of gait, divided by foot orthoses condition. At initial contact, wearing FOTs significantly reduced the ADM aEMG compared to walking in FOs or barefoot. **B.** During the loading response, wearing FOTs significantly increased AbdH aEMG compared to barefoot and FOs. Significant increases were also observed in ADM compared to walking in FOs and barefoot. ***=p<.0001*

3.3.5 Kinematics and Gait Parameters

The most noteworthy kinematic changes were observed at the ankle joint minimum and range values, with minimal changes observed in hip and knee kinematics bilaterally. Significant interactions in ankle joint minimums were observed across FO and walking surface (Left: $F_{2,233}=3.89$, $p=.0206$, eta-square=0.87; Right: $F_{2,233}=5.38$ $p=.0047$, eta-square=0.84). Bilaterally, the ankle joint moved through significantly less plantarflexion in both FO conditions (Left FO: -0.9°±-8.6°, FOT: -0.3°±-7.4°; Right FO: -3.2°±-9.0°, FOT: -2.5°±-9.4°) compared to walking barefoot (Left: -9.6°±-7.7°; Right: -12.0°±-11.4°) on the hard surface. Less ankle plantarflexion was also observed when walking over soft foam. Statistically significant main effects of FOs revealed a reduction in total ankle range (Left: $F_{1,233}=12.12$, $p=.0005$, eta-square=0.81, Right: $F_{1,233}=142.87$, $p=<.0001$, eta-square=0.71) when walking in FOs (Left: 24.9°±7.1°, Right: 25.7°±7.3°) and FOTs (Left: 24.8°±6.2°, Right: 25.4°±7.4°) compared to barefoot (Left: 28.4°±7.0°, Right: 29.6°±5.9°) (Figure 18).

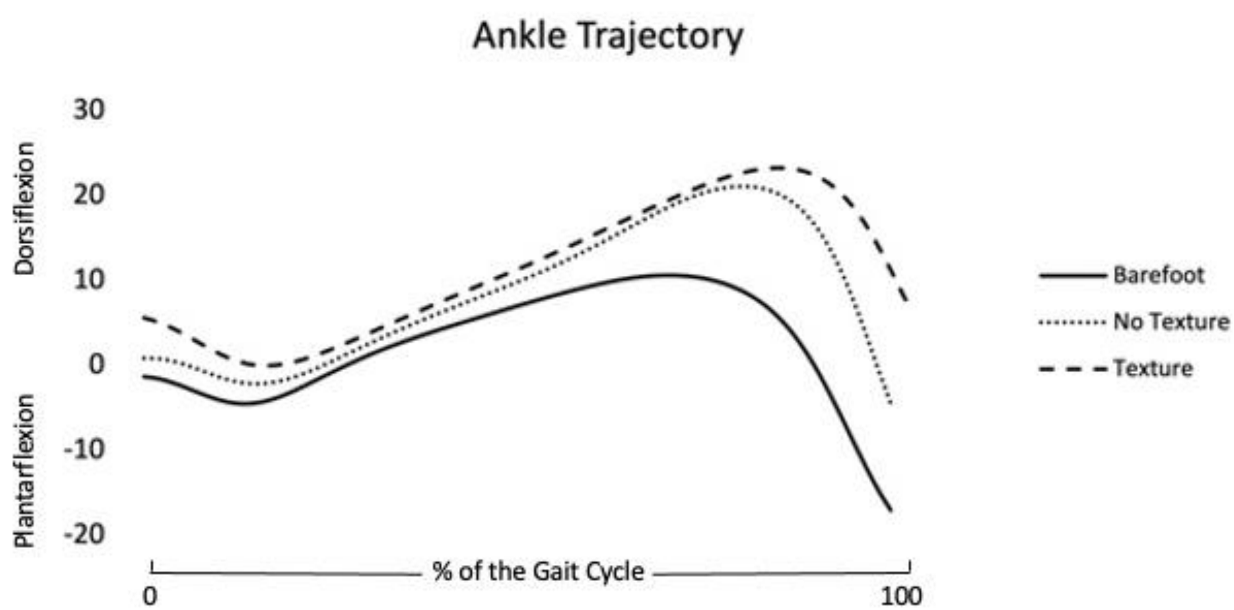

Figure 18. The typical relative ankle joint angle during the gait cycle when walking barefoot, in non-textured orthoses, and in textured foot orthoses.

3.4 DISCUSSION

The primary aim of this study was to understand the effects of adding texture as a top cover in FO design on PIFM function during gait. Prior to answering this research question, it remained important to initially understand how a non-textured FOs modified PIFMs EMG compared to walking barefoot. The results of our study indicate that wearing non-textured FOs immediately modulated PIFM amplitude, reflected as increases and decreases in aEMG, which were gait-phase specific across stance. When adding texture to the FOs, increasing tactile feedback commonly increased aEMG of PIFMs across stance. The modulatory effects of textured FOs on PIFMs aEMG were also gait-phase specific. Lastly, we were interested in understanding the effect of walking surface on PIFMs function. As hypothesized, walking over soft foam increased PIFM aEMG as the unstable surface increased the muscular demand of these small intrinsic foot muscles during walking.

3.4.1 PIFMs activate independent of one another

The results of this study highlight the independent roles of AbdH, AddH, ADM, and FDB muscles throughout the gait cycle. To highlight the validity of this statement, a post-hoc analysis closely examined pair-wise comparisons to demonstrate the significant amplitude variability across each muscle and between the phases of gait within each muscle (Figure 19). Similar to extrinsic foot muscles [13,15,16], our results suggest a modulatory behaviour of PIFMs that is both muscle and gait-phase specific, rather than simultaneous activation of all PIFMs across any particular phase of gait. For example, when walking barefoot on the hard surface, during IC, the magnitude of ADM aEMG is significantly greater than AbdH and AddH, and FDB is also significantly greater than AddH. Within each muscle, the EMG magnitude is greatest at IC and PR, suggesting that the largest muscular demand of PIFMs occurs during the early and late phases of stance. These results are consistent with previous fine-wire EMG studies describing the phasic activity of PIFMs [145,146]. Interestingly, ADM appears to be the most active at IC, followed by FDB, with AbdH and AddH experiencing similar levels of activation. To our knowledge, this is the first experimental study measuring fine-wire EMG in ADM. As the majority of heel strikers contact the walking environment on the lateral aspect of the calcaneus [166], greater activation of ADM at IC may suggests a stabilizing role of the lateral column as the foot plantarflexes into midstance. More importantly, this data provides evidence to support the independent roles of each PIFM and clearly demonstrate individualized amplitudes across muscle and phase of the gait cycle.

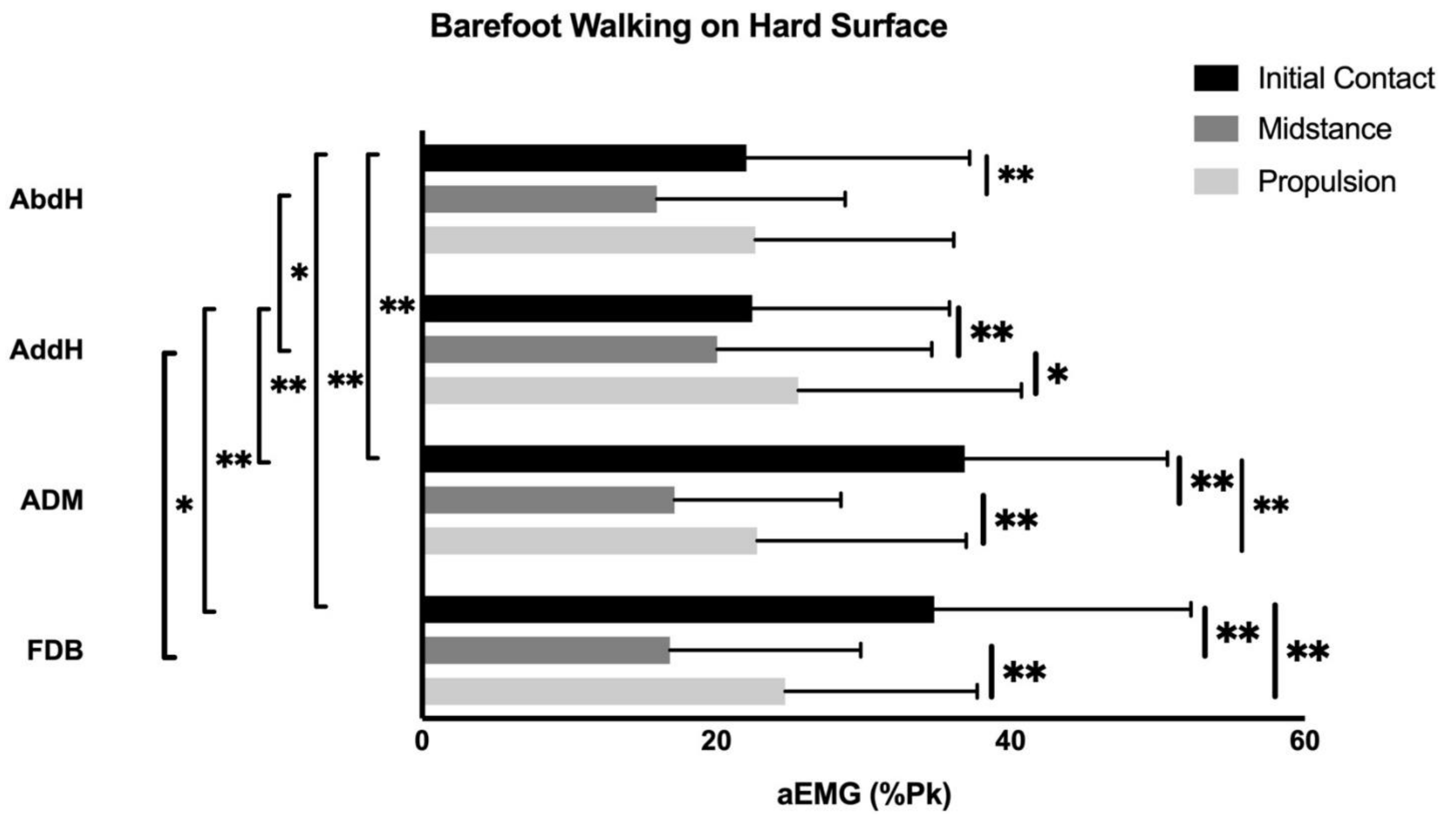

Figure 19. The average EMG (aEMG) of four plantar intrinsic foot muscles (PIFMs) at initial contact, midstance and propulsion when walking barefoot on the hard walking surface. Within each respective muscle, initial contact combined the % of muscle activity data from bins 1 and 2, midstance combined data from bins 3 and 4, and propulsion combined data from bins 5 and 6. Results demonstrated a statistically significant interaction across muscle and phase of gait, $F_{6,467}$=43.98, p=<.001, eta-square=0.68. ** = p=.05, ** =p<.0001*

3.4.2 The muscle activation of PIFMs is maintained when walking in foot orthoses

It is assumed that the MLA exhibits less deformation when wearing a FO compared to not wearing a FO while walking barefoot. As arch skin is in direct contact with the FO, the FO is assumed to increase resistance to muscles spanning the MLA, reducing arch deformation, and reducing the active lengthening of muscles spanning the midfoot. This questions if FOs alter the normal spring-like functioning of the foot [145,158,167] due to limiting the foot's ability to store and return elastic energy throughout the stance phases of gait. Wearing footwear has been similarly shown to limit the amount of MLA compression [168], although motor tendon units of the AbdH and FDB have demonstrated increased stiffness in shod conditions, and thus EMG activation, to effectively maintain the required stiffness levels of the foot during stance. In a FO, our results demonstrate that PIFMs exhibited increased EMG activation at MS and HR (compared to walking barefoot), which is assumed to increase midfoot stiffness during stance. Speculatively, this PIFM aEMG increase suggests that wearing a FO did not impede the storage and return of elastic energy and normal spring-like functioning of the foot was maintained. Not only does this demonstrate the foot's immaculate adaptability to adapt to environmental change, but it also provides evidence to suggest that FOs do not result in disuse of PIFMs. In fact, these results support an opposing view whereby a reduction in MLA compression is mitigated by increased PIFM EMG activation and dissipating concerns of long-term when wearing a FO. To elaborate on Kelly et al.'s (2016) in-series spring analogy, muscles spanning the MLA will adapt their stiffness levels to maintain the total stiffness required for the task (which arguably has task-specificity in itself). When something new is introduced to the foot-environment interface, such as footwear and in this study a FO, the FO alters MLA compression, changes the motor tendon unit length, and thus changes the MLA stiffness at IC [158]. To match the total stiffness requirements and effectively recoil and facilitate propulsion, the PIFMs must adjust its stiffness accordingly (Figure 20). The footwear and FO industry can use this knowledge to potentially manipulate shell material stiffness levels to modify PIFM activation.

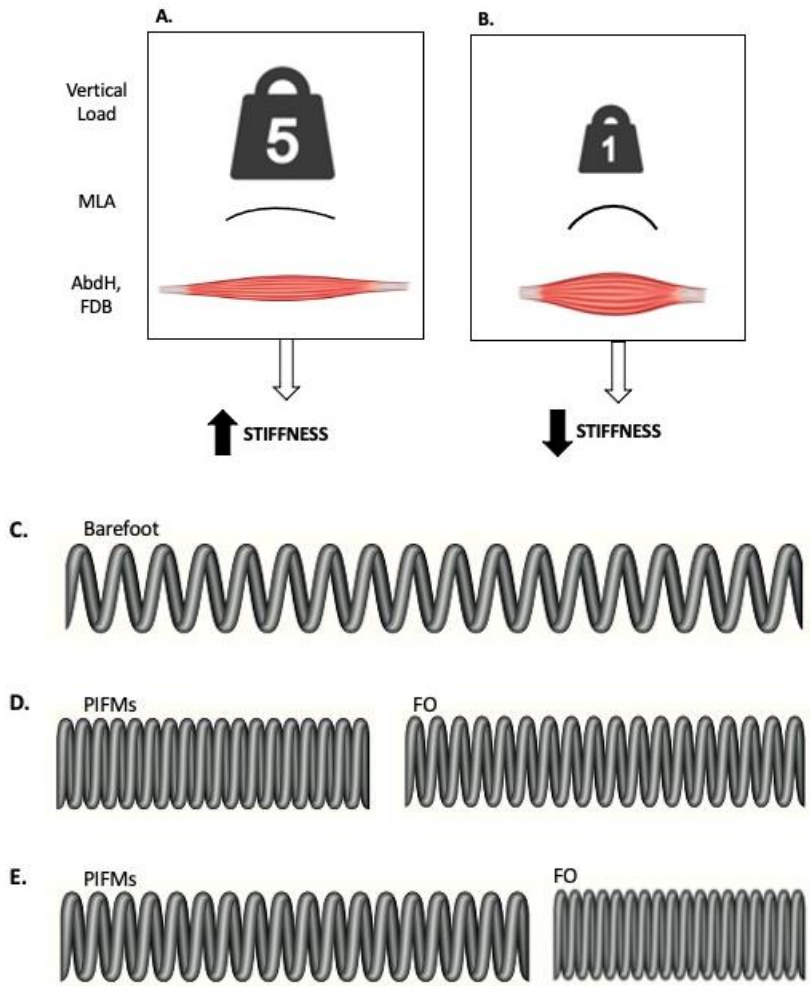

Figure 20. A. As vertical load increases during initial contact, the MLA compresses and the motor tendon units of muscles spanning the MLA (AbdH and FDB) lengthen. MLA compression, and subsequent stiffness of the arch, is maximal during midstance. This increased stiffness stores elastic energy in preparation for propulsion. **B.** Late in stance, as vertical load decreases, the motor tendon units of muscle spanning the MLA shorten (recoil), and stiffness is reduced to facilitate propulsion.

C-E. The total stiffness required to complete the task of walking does not change in conditions C, D, or E. Rather, the amount of lengthening and recoil of the MLA changes, which subsequently alters the total stiffness of the arch. **C.** When barefoot, the spring-like mechanisms of the MLA acts similar to the description provided in A-B. As the arch does not experience resistance from a foot orthotic (FO), the MLA compresses and motor tendon units of muscles spanning the MLA (AbdH and FDB) lengthen at initial contact. Arch stiffness is maximal at mid-stance and recoils at propulsion. **D.** The PIFMs spanning the MLA experience less compression due to the resistance of the FO. To maintain the required rigidity for propulsion, PIFM EMG increases to match the total stiffness requirements of the walking task. **E.** The PIFMs spanning the MLA experience less compression due to the resistance of the FO. This resistance is less compared to condition B, and therefore less PIFM EMG is required to match the total stiffness requirements of the walking task.

At IC and TO, wearing FOs reduced PIFM aEMG compared to walking barefoot. Considering the fatiguing properties of muscle, this amplitude reduction (during time points where PIFMs are most active barefoot) may indicate a mechanism to reduce fatigue over the entire stance phase of gait. As the FO reduced MLA lengthening and PIFMs demand increases in midstance, EMG suppression at IC and TO are likely necessary to store and release energy levels to maintain steady state locomotion.

3.4.3 The role of texture in foot orthoses design

Adding texture to FOs was intentional to maximize full foot contact between foot sole skin and orthoses while additionally stimulating cutaneous mechanoreceptors and targeting the preferential response of FAIs to skin indentation [56,57]. Neurophysiological research supports the importance of cutaneous input in modifying motorneuron pool excitation [69,135]. Furthermore, this modulation can be reflected as either facilitation (increase in EMG) or inhibition (decrease in EMG) in EMG which modulates across different phases of the gait cycle [60]. In comparing FOs to FOTs, the results of this study suggest that adding texture to FOs facilitated aEMG across several stance phase of gait. This is especially evident at midstance with 3 of 4 PIFMs aEMG significantly increasing when wearing FOTs (Figure 21).

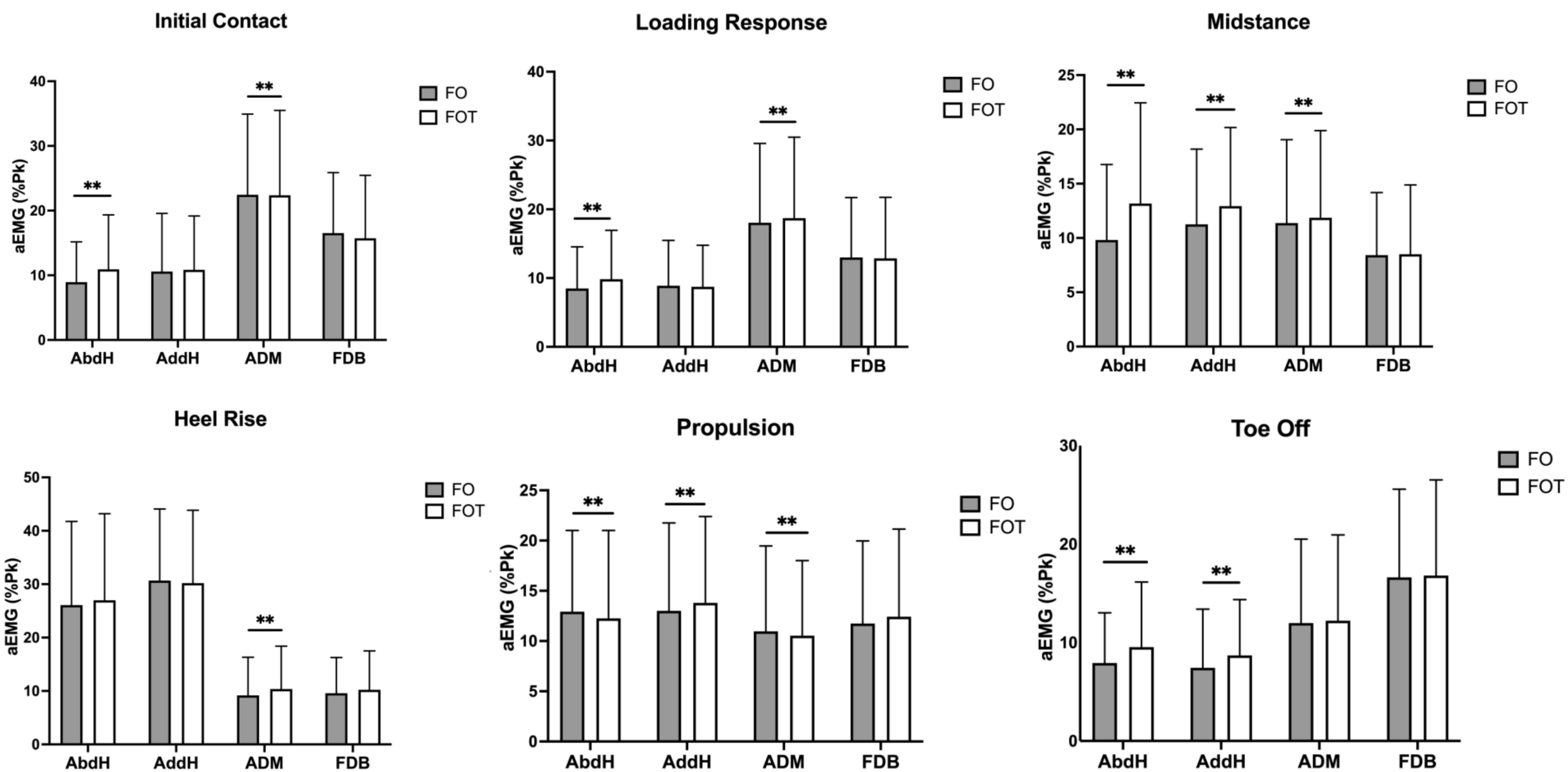

Figure 21. Mean PIFM aEMG (and standard deviations) across each phase of stance: initial contact, loading response, midstance, heel rise, propulsion and toe-off. ***=p<.001*

Thus, adding mechanical stimulation to purposefully stimulate cutaneous mechanoreceptors, through adding texture as a top cover to FOs, appeared to increase motorneuron pool excitation of PIFMs. It should be noted that other neurophysiological factors which were not measured in this study can also contribute to the net excitation of a motorneuron pool. This may include other incoming sensory sources (muscle spindles, GTOs) and pre-synaptic inhibition [49], or variability in center of pressure trajectory under the foot sole. Although important to recognize, our statistical analysis always remained within the same phase of gait, remained within identical tasks (comparing hard-hard or soft-soft), and all participants were tested across both FO conditions (which maintained each participant's foot in a similar position during gait). Therefore, the increases in PIFM aEMG provide strong evidence that the resultant motorneuron pool excitation is a function of tactile facilitation rather than other neurophysiological factors.

In comparing changes in walking surface, PIFMs aEMG responded similarly when participants walked in both FO conditions. In both orthotics, the PIFMs aEMG is reduced at IC and TO and facilitated in MS. The average muscle magnitude (aEMG) in FOTs consistently remains greater than FOs without tactile facilitation, although both FOs aEMG remain above the barefoot walking condition. Thus, these similar observations in net PIFM aEMG supports the notion that FOs, even without tactile facilitation, may also provide cutaneous input that alters motorneuron pool excitation, reflected as a facilitation or suppression, which fluctuated according to the phase of gait and complexity of the walking task. When wearing any type of FO, it can be assumed that there is heightened cutaneous input to the PIFM's motorneuron pools, as a function of minuscular movements and skin indentation between the top cover of the orthoses and foot sole skin. When adding texture to the device, indentation of the skin is heightened, and appears to increase the excitatory effects compared to non-textured FOs. These results open additional questions, for example, why would we want to increase PIFMs EMG during gait, and in which medical conditions would this increased excitability be most beneficial. Future research is encouraged to addressed these open ended questions.

3.4.5 Study Limitation

The kinematic results in this study were important to confirm similar walking profiles between FO conditions. This was especially important as participants in the barefoot condition did not wear socks, although socks were worn when walking in FOs and FOTs. This was intentional, as the addition of socks would have altered the skin-walking surface interface by adding an extra layer between these two surfaces. Consistent with previous literature, both FOs had minimal effect on the kinematics of the hip and knee [28]. These results have been attributed to the likelihood of passive and active soft tissue structures of the foot being a likely contributor to the positive self-reported outcomes when wearing FOs. Our results support this interpretation with clear PIFM modulation across the walking environment and phase in the gait cycle. However, kinematics of the ankle revealed a reduction in ankle plantarflexion when walking in both FOs. Although participants were encouraged to walk similarly across all conditions, the addition of socks, and potential concerns of slipping, cannot be excluded as a contributing factor to these kinematic changes.

3.5 CONCLUSION

The results of this study add to the body of evidence supporting the use of textured materials, specifically in foot orthoses design, to modulate the amplitude of PIFMs across various phases of the gait cycle. Our results suggest that PIFMs demonstrate both phase- and muscle-specific variability across stance. The addition of FOs, both with and without texture, increases cutaneous input from foot sole skin which alters motorneuron pool excitation, and can be reflected as a facilitation or suppression of PIFMs aEMG. Future academics are encouraged to increase our understanding on which pathologies, diseases, and/or medical conditions would best benefit from textured foot orthoses.

CHAPTER 4

THE IMPORTANCE OF FOOT POSTURE WHEN MEASURING LOWER LEG EMG WHEN WALKING IN NON-TEXTURED AND TEXTURED FOOT ORTHOSES

4.1 INTRODUCTION

Anatomical foot posture describes the variance in an individual's overall foot shape, typically classified as pes planus (pronated), pes rectus (neutral), or pes cavus (supinated). Variability in foot posture has been associated with changes in center of pressure (COP), lower limb electromyography (EMG) and limb kinematics during gait [75,169–172]. Foot posture also remains an important consideration in the provision of foot orthoses (FOs), which influences orthosis manufacturing properties, such as shell material durometers and top cover selection. Although FO design could be optimized by considered the topographical organization of fast adapting type I (FAI) cutaneous mechanoreceptors located in foot sole skin, the differential effects of FO designs targeted at facilitating FAI stimuli across varying foot postures remains unknown. Modifying the top cover in FO design, such as adding texture to intentionally indent foot sole skin, may be a mechanism to facilitate receptor activation.

Various methods of foot posture classification have been developed, including visual observations, anthropometric measurements of the foot, and weightbearing radiographs [173]. As radiographs remain limited to hospital and specialized orthopaedic clinics, clinicians commonly rely on visual and anthropometric measurements to characterize a patient's foot morphology. The Foot Posture Index (FPI) [174], a commonly used method of anthropometric evaluation, characterizes foot morphology on a spectrum of pes cavus (high arched or supinated feet), pes rectus (neutral or normal arched feet) to pes planus (low arched or pronated feet) feet. The FPI has demonstrated strong reliability [175] and validity [174] in characterizing the relationship between static foot posture and dynamic midfoot movement [176], thus remains a commonly adopted clinical tool in assessing foot posture variance.

Different foot postures have been associated with changes in the biomechanical functioning of the lower limb. Variance in foot posture has been demonstrated to alter the dynamic reach scores in the Star Excursion balance test [169] and modify the COP trajectory during gait [170]. Peak plantar pressure, contact area, and maximal plantar force are all higher in the medial longitudinal arch (MLA), medial forefoot, and under the hallux in planus compared to cavus feet [73,171]. In planus feet, the COP trajectory is typically more medially deviated under the foot sole and more laterally deviated in cavus feet during walking. Although these outcome measures have been observed across different foot postures, it remains unknown if one foot posture demonstrates greater stability compared to the other. Variation in muscle activity has also been reported across differing foot postures. At initial contact, the amplitude of tibialis anterior (TA) and peroneus longus (PL) muscles are higher in planus compared to individuals with a neutral foot posture. During midstance and propulsion, the amplitude of tibialis posterior (TP) is also higher, accompanied by a reduction in PL [16]. When comparing the foot and ankle kinematics between foot postures, cavus feet have demonstrated greater peak forefoot plantarflexion, forefoot abduction, and rearfoot internal rotation compared to neutral feet [172]. Thus, variance in foot posture has been associated with modified dynamic stability, COP trajectory, EMG of select lower limb muscles and lower limb kinematics during gait, with neither foot posture being considered superior to another. In the prescription of FOs, foot posture remains an important consideration in selecting FO design characteristics uniquely tailored to the intended goal of treatment.

Some FO research has placed careful attention on isolating experimental outcome measures by foot posture or by using foot posture as an inclusion criteria in describing participant characteristics. These studies help differentiate which foot postures and patient populations may best respond to different types of FO design. For example, FOs have been demonstrated to reduce COP excursion in pes planus feet, however remain ineffective in altering COP in pes rectus feet [177]. In pes planus feet, wearing prefabricated and custom orthoses have been shown to reduce tibialis posterior EMG amplitude at initial contact and peroneus longus EMG amplitude during the propulsive phase of gait [178]. Reduced peak dorsiflexion ankle angle and moments have also been reported during walking [179]. In static stance, FOs can effectively reduce the acute sagittal plane 1st metatarsal and calcaneal inclination angle in pes cavus feet [180], a morphological characteristic common to this foot posture. Wearing a FO for 1 month has resulted in a 2% increase in the amplitude of lateral gastrocnemius muscle activity in to the propulsive phase of gait, specifically in pes cavus individuals [161]. Interestingly, reduced ankle and subtalar joint mobility in pes cavus feet has recently been highlighted as an important contributor to the successfulness of FO interventions [181]. In comparing various laterally wedged FO designs, supinated feet were less responsive to all FO designs in reducing the knee adduction moment. Furthermore, pes rectus and planus feet were only responsive to 2 of 6 insole conditions: a laterally wedged FO and a laterally wedged FO including a dual shell material stiffness along the medial longitudinal arch [181]. Although many question remain in attempts to estimate the optimal FO design for differing foot postures, current experimental research speaks to the importance of considering different foot postures in experimental protocols and foot orthoses design. Differentiating results by foot posture remains important and should not be underestimated when interpreting biomechanical and EMG outcomes.

When designing a foot orthosis, the researcher and/or clinician must carefully select which materials to use for the shell, top cover, underlay, and for any additions or modifications. The physiological properties of foot sole skin are not typically considered in these decisions and may be a novel tactic to advance our mechanistic insights supporting FO use. FAI cutaneous mechanoreceptors populate approximately 50% of the receptors in foot sole skin [56]. These receptors preferentially respond to skin indentation [57] are more densely populated in some areas of the foot sole compared to others (higher density in the toes, lateral midfoot and forefoot, lower density in the medial arch and under the heel) [56]. Stroking foot sole skin, to intentionally stimulate FAI cutaneous fields has been linked to motorneuron pools in lower leg muscles [131]. Thus, the use of FO materials, more specifically top covers, to intentionally indent the skin may be a mechanism to facilitate FAI activation. As force is transferred across the foot sole, the on/off skin indentation of foot sole skin may modulate muscle activity throughout different phases of the gait cycle. Furthermore, as the density of FAIs differ across the foot sole, the effect of tactile enhancing materials may have different effects when placed under different areas of the foot.

To date, the effect of foot orthoses designs to enhance skin stimulation across different anatomical foot posture remains unknown. Consequently, the purpose of this research was to answer the following research questions: How does foot posture influence lower leg muscle activity when walking in foot orthoses? Secondly, how does foot posture modify lower leg muscle activity when walking in foot orthoses with tactile facilitation to different regions under the foot sole? It was hypothesized that when the foot is loaded under areas of tactile facilitation, PIFM EMG would increase in magnitude compared to wearing the non-textured foot orthoses.

4.2 METHODS

4.2.1 Participants

Data from this study are extracted from a previous experimental protocol whereby fifty-five (23.4±4.2years; 19 males, 36 females; 172.2±8.6cm; 70.9±15.7kg) healthy young adults completed a series of walking trials on a level and wedged surface (only the level walking data are analyzed here). Study candidates were screened for neurological disorders, balance impairments and/or musculoskeletal injuries prior to participation and normal tactile sensory thresholds of bilateral foot sole were confirmed with Semmes-Weinstein monofilaments (North Coast Medical, Inc., Morgan Hill, CA). The foot posture of each participant was determined by the Foot Posture Index [174]. The distribution of participant's foot posture scores as determined by the Foot Posture Index were n=13:pronated, 7:highly pronated, 24:normal, 4:supinated, and 7:highly supinated. All participants provided informed consent and the study was approved by the institutional research ethics board (REB#5583).

4.2.2. Lower Leg Electromyography (EMG)

Surface and indwelling (fine-wire) EMG (iEMG) (Ultium, Noraxon, Scottsdale, AZ, USA) recorded muscle activity from 8 lower limb muscles during level walking. Four muscles were grouped together into “Leg A” (tibialis anterior (TA), peroneus longus (PL), tibialis posterior (TP) and extensor hallucis longus (EHL)), and the remaining four muscles into “Leg B” (medial gastrocnemius (MG), extensor digitorum longus (EDL), flexor digitorum longus (FDL) and flexor hallucis longus (FHL)) to separate two surface EMG recordings and two indwelling EMG insertions sites per leg.

4.2.3 Surface EMG (sEMG)

sEMG was recorded from the TA, PL, MG and EDL muscles. Disposable bipolar surface electrodes (HEX 272S, Ag/AgCL, Noraxon, USA, Inc.) were placed at an inter-electrode distance of 2cm directly over the muscle belly skin. The skin surface was clean shaven and oils and lotions were removed with Nuprep abrasive gel. sEMG electrode placement followed SENIAM guidelines [182] for the TA, PL and MG muscles. TA electrode placement and signal integrity was confirmed with resisted ankle dorsiflexion, resisted ankle plantarflexion and foot eversion for PL, and active ankle plantarflexion (with a straight knee) for MG. The EDL electrodes were placed four finger breaths distal to the tibial tubercle, two finger breaths lateral to the tibial crest. Proper electrode placement was confirmed by active resistance to the four lesser toes. The integrity of all sEMG signals were monitored live during collection.

4.2.4 Indwelling EMG (iEMG)

Paired fine-wire needle electrodes (Chalgren Enterprises, Inc., [30mm (1.25”) x 27g] (000-318-130); 50mm (2.00”) x 25g] (000-318-150)) recorded iEMG from the TP, EHL, FDL, and FHL under ultrasound guidance (Eco 6, CHISON Medical Technologies Co., Ltd). Each insertion site was initially located through surface palpation, relevant landmarks were identified on ultrasound, and the needle trajectory was determined for each muscle of interest. With the exception of FHL (which we elected for a lateral insertion approach), iEMG insertions followed Perotto's Anatomical Guide for the Electromyographer [133]. Briefly, the EHL electrodes were inserted three finger breaths above the bimalleolar line, lateral to the anterior crest of the tibia, the FHL electrodes were inserted 10mm above the lateral side of Achilles tendon insertion, and the TP and FDL electrodes were inserted one hand breadth distal to the tibial tuberosity, plus one finger breadth off the medial edge of the tibia. EHL insertion accuracy was confirmed with passive and resisted 1st MTP extension (with dorsiflexed ankle), FHL with passive 1st MTP flexion and extension (with ankle and lesser toes relaxed), FDL with passive flexion and extension of the lesser toes (without ankle flexion) and TP was confirmed with resisted subtalar joint inversion and ankle plantarflexion (Figure 22).

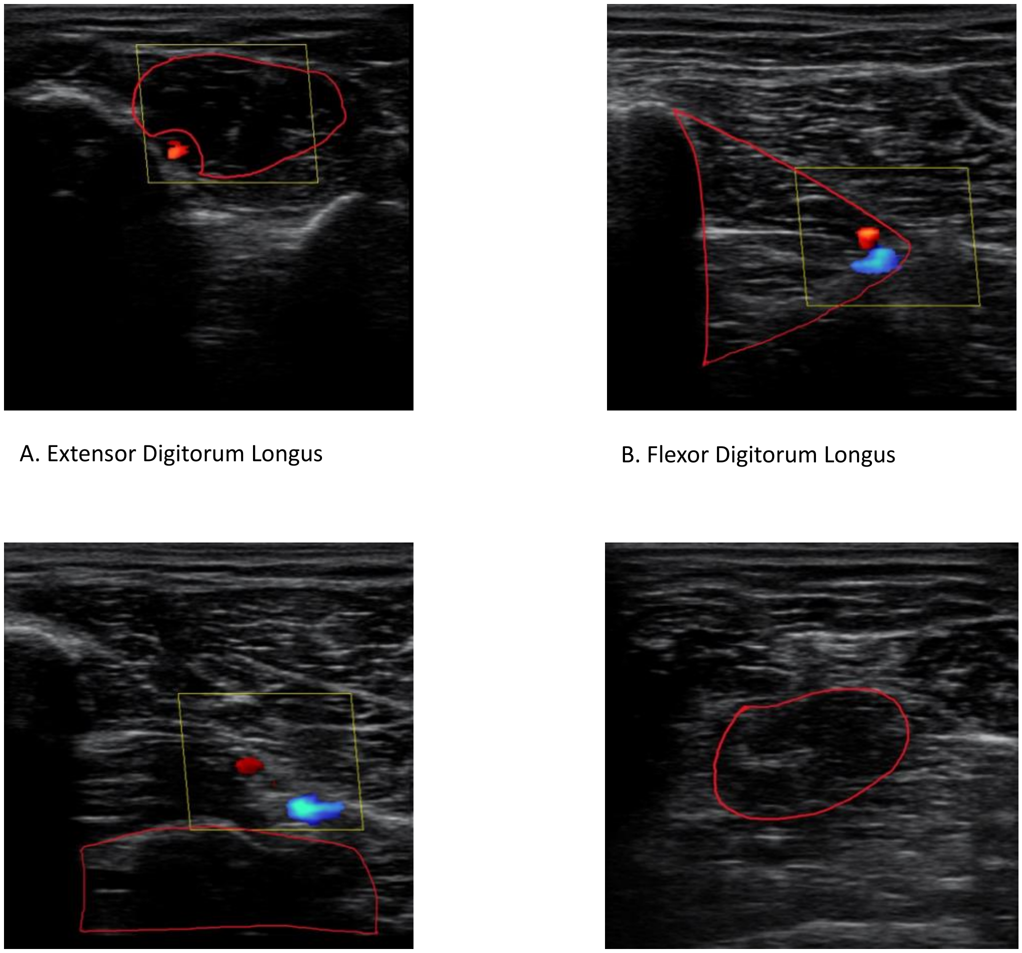

A. Extensor Digitorum Longus

B. Flexor Digitorum Longus

C. Tibialis Posterior

D. Flexor Hallucis Longus

Figure 22. The typical ultrasound view when performing each iEMG insertion. The targeted insertion site for each muscle of interest is outlined in red. When neurovascular bundle landmarking was important, the ultrasound's doppler function was turned on (yellow square). Red (flow towards the probe) and blue (flow away from the probe) vascular flow are identified within the yellow outline. *Note: this image is the same as Figure 2 in this dissertation document.

4.2.5. Footwear and Orthoses

All participants were provided standardized footwear (Rockport WT Classic) and prefabricated orthotics (D609561, Sole Thin Sport Footbeds, Edge Marketing Corp; Calgary, AB, Canada) to wear for the duration of the experimental protocol. Socks were not worn inside footwear. Full foot contact (90% pressure cell distribution) between foot sole skin and the foot orthoses was confirmed by temporarily placing Medilogic pressure insoles into participant's footwear.

This protocol included 6 different foot orthoses (FOs) conditions (1 x non-textured 5 x textured), each corresponding to a different sensory facilitated region that was incorporated into the orthoses design: 1) smooth top cover (Op-Tek Flex, 1/8" EVA copolymer, Ortho Active, BC, CAN); 2) textured medial forefoot (MF); 3) lateral forefoot (LF); 4) calcaneus (CALC); 5) medial midfoot (MM), and 6) lateral midfoot (LM). In each region of texture, the Op-Tek material was replaced with a 3D printed textured material (Flex 45 Thermoplastic Co-Polyester, Shore D 35 hardness, InkSmith) (Figure 23). Only one topographical area had texture at a time and both materials consisted of similar durometer and thickness. The textured material consisted of a zig zag pattern running perpendicular to the walking direction. The design was intended to increase the indentation of foot sole skin and maximize activation of cutaneous mechanoreceptors.

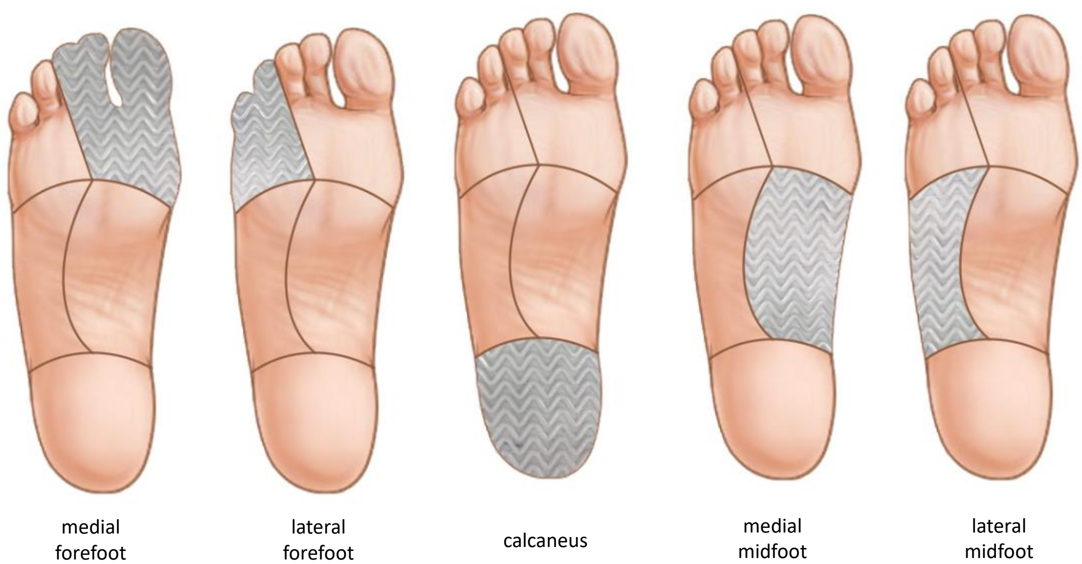

Figure 23. The five topographical regions of texture under the foot sole. *Note: this image is the same as Figure 3 in this dissertation document.

4.2.6. The Experimental Protocol

This experimental protocol is part of a larger research study which included 6 walking trials in each textured condition: 3 level walking and 3 wedged walking trials, as well as 18 non-textured trials (9 x level, 9 x wedge) dispersed randomly across the entire protocol. In this data analysis, only the level walking trials have been included in the analysis. Participants began each walking trial in static stance. All trials began with the left foot and participants were asked to walk at a self-selected walking velocity from one end of the research lab to the other (approximately 10m). On steps 3 and 4 participants walked over two force plates (OR6-5-2000; AMTI, Watertown, Massachusetts, USA) embedded flush with the floor (Figure 24).

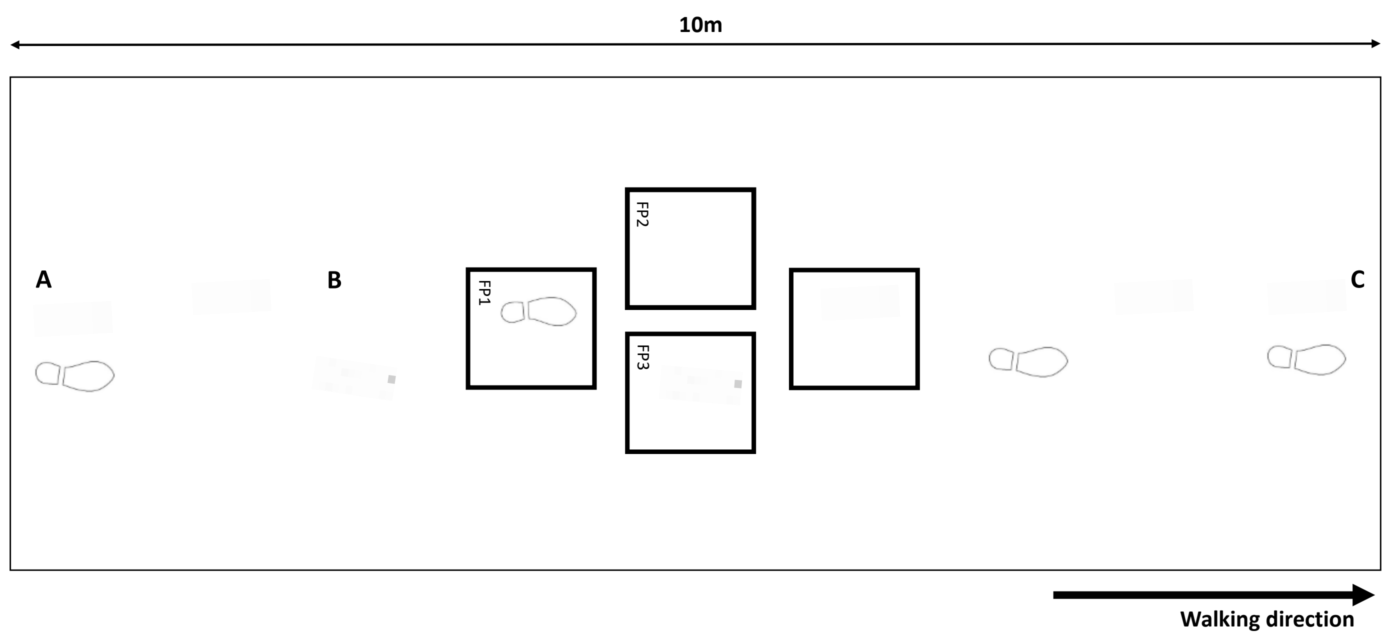

Figure 24. A schematic of the 10m walking protocol. **A.** All participants began each walking trial in quiet static stance. When provided a signal to begin, participants took 2 steps prior to making contact with force plate 1 (FP1), and subsequent contact onto force plate 3 (FP3), then continued walking until they reached the end of the walkway. **B.** Each participants' self-selected velocity was reached before making contact with the force plates. Participants were instructed to continue walking at this consistent velocity until they reached the end of the walkway (**C**), where they were instructed to stop the walking trial in quiet stance. FP1, FP2 and FP3 correspond to the locations of three force plates embedded into the floor along the walkway.

4.2.7 Data Processing

Raw EMG was differentially amplified (gain x500), band-pass filtered 10-500Hz, and sampled at a frequency of 1000 Hz. The temporal characteristics of the gait cycle were identified from the force plates embedded flush with the walking surface. Foot contact on forces plates 1 and 3 (figure 24) determined the gait cycle (GC) timing with the start (0% GC) being initial contact (>10N threshold) on FP1 and the end (100% GC) being toe off (<10 N) from force plate 3, minus the double support time. This defined 0% and 100% of the gait cycle as one foot contact to the next foot contact of that same leg. The signals were full-wave rectified and linear enveloped with a 40Hz dual-pass Butterworth filter. The EMG data was normalized to each participant's peak EMG +/-100ms before and after the gait cycle. Each participant's ensemble averages were initially grouped together for each FO and sensory condition. Overall ensemble averages were then calculated from all participant's normalized EMG (nEMG) for each foot posture (x5) x textured region (x6), derived from the time normalized linear enveloped signals, and then represented as 0 to 100 percent of the gait cycle (GC). Highly supinated and supinated FPI scores were collapsed together into the pes cavus group, highly pronated and pronated FPI scores were collapsed together into the pes planus group, and normal PFI scores defined the pes rectus group. The average EMG (aEMG) of each muscle was calculated by adding each muscle's EMG magnitude data together and dividing by the total number of data points within the stance phase of gait. The aEMG data remained separated into the 5 FPI categories.

4.2.8 Statistical Analysis

Within and between-subject repeated measures analysis of variance (SAS University Edition, 2.8.1, version 9.4) were performed for the within-measures of textured location (MF, LF, CALC, MM, MF) and between-measures of FPI score (normal, pronated, highly pronated, supinated, highly supinated). The data was rank-transformed in instances when normality was not met. When overall means were significantly different, Tukey's HSD post hoc comparisons were run on data to further differentiate between main effects. Outliers exceeding ±4SD from the mean were closely evaluated and removed from the dataset (i.e. closer evaluation of the EMG signal confirmed excess noise generating abnormally high EMG signals and/or poor signal quality generating abnormally low EMG signals) (occurred a maximum 2 x per muscle and FPI score, across 725 samples). Due to methodological errors, two participants were excluded from the analysis. Significance was set at $p<0.05$ a priori.

4.3 RESULTS

Fifty-one participants were included in the final analysis. The division of participants within each FPI score was as follows: 10 pes cavus (6 highly supinated, 4 supinated), 21 pes rectus, and 21 pes planus (6 highly pronated, 15 pronated). To answer our first research question, a closer examination of the planned pair-wise comparisons identified the statistically significant differences in each muscle's aEMG when comparing supinated and pronated foot postures compared to normal foot posture (as identified by FPI scores), when walking in non-textured FOs.

4.3.1 The effect of foot posture on lower leg EMG when walking in foot orthoses

When walking in FOs, different foot postures revealed significantly different lower leg aEMG during the stance phase of gait (Figure 25A). In pronated feet, the aEMG of PL, EDL and FHL were significantly reduced compared to participants with a normal foot posture. In highly pronated feet, the aEMG was significantly reduced in TA and FHL, and conversely, significantly greater in PL, EDL, EHL, MG, FDL and TP compared to a normal foot posture. In supinated feet, a significant reduction in EHL was observed compared to normal feet, whereas the aEMG of TA, EDL and MG was significantly greater. In highly supinated feet, TA, FDL, FHL and TP aEMG was significantly reduced compared to a normal foot posture.

25A.

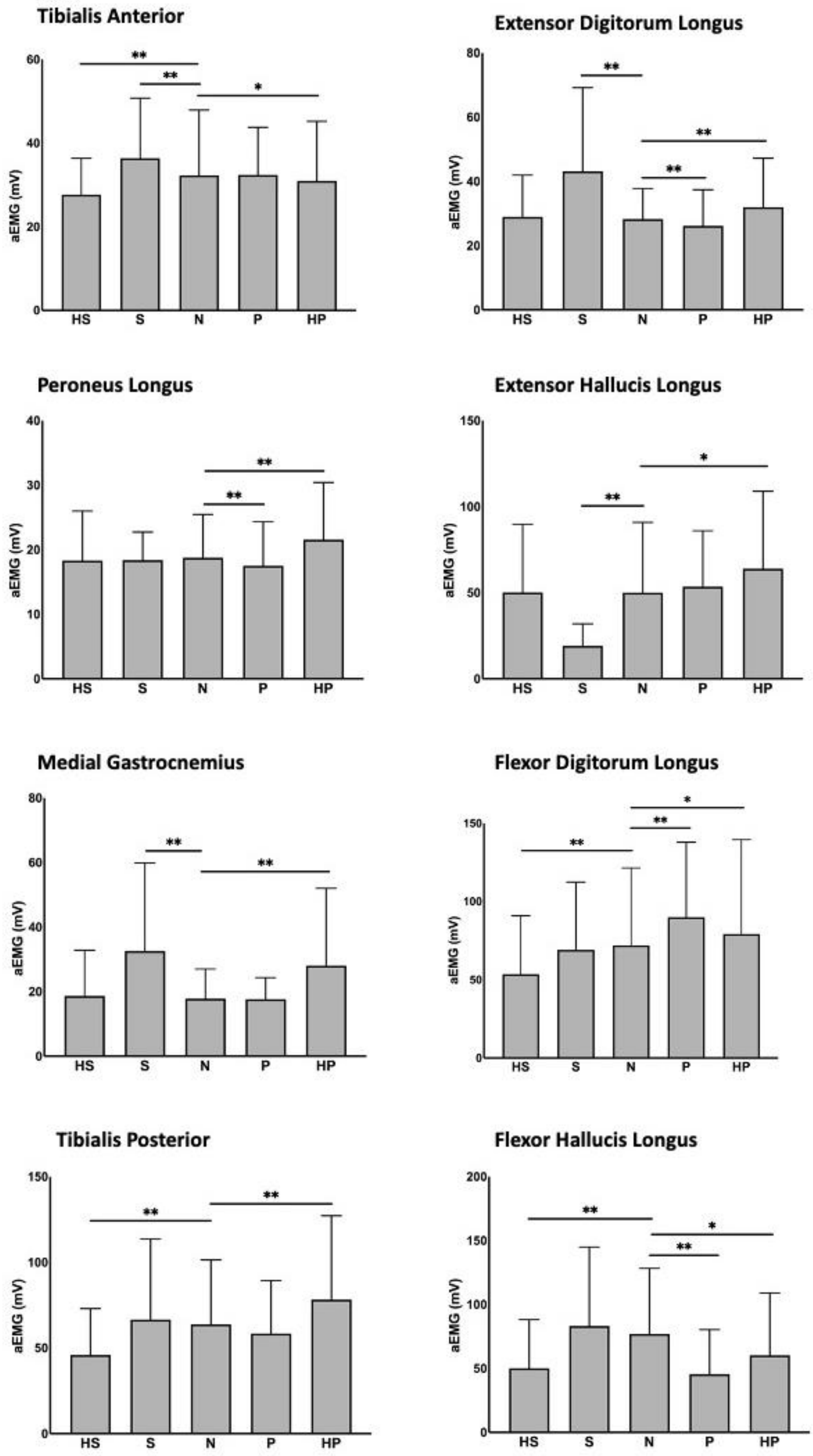

Tibialis Anterior
Extensor Digitorum Longus
Peroneus Longus
Extensor Hallucis Longus
Medial Gastrocnemius
Flexor Digitorum Longus
Tibialis Posterior
Flexor Hallucis Longus
aEMG (mV)
HS
S
N
P
HP

25B.
No Texture:

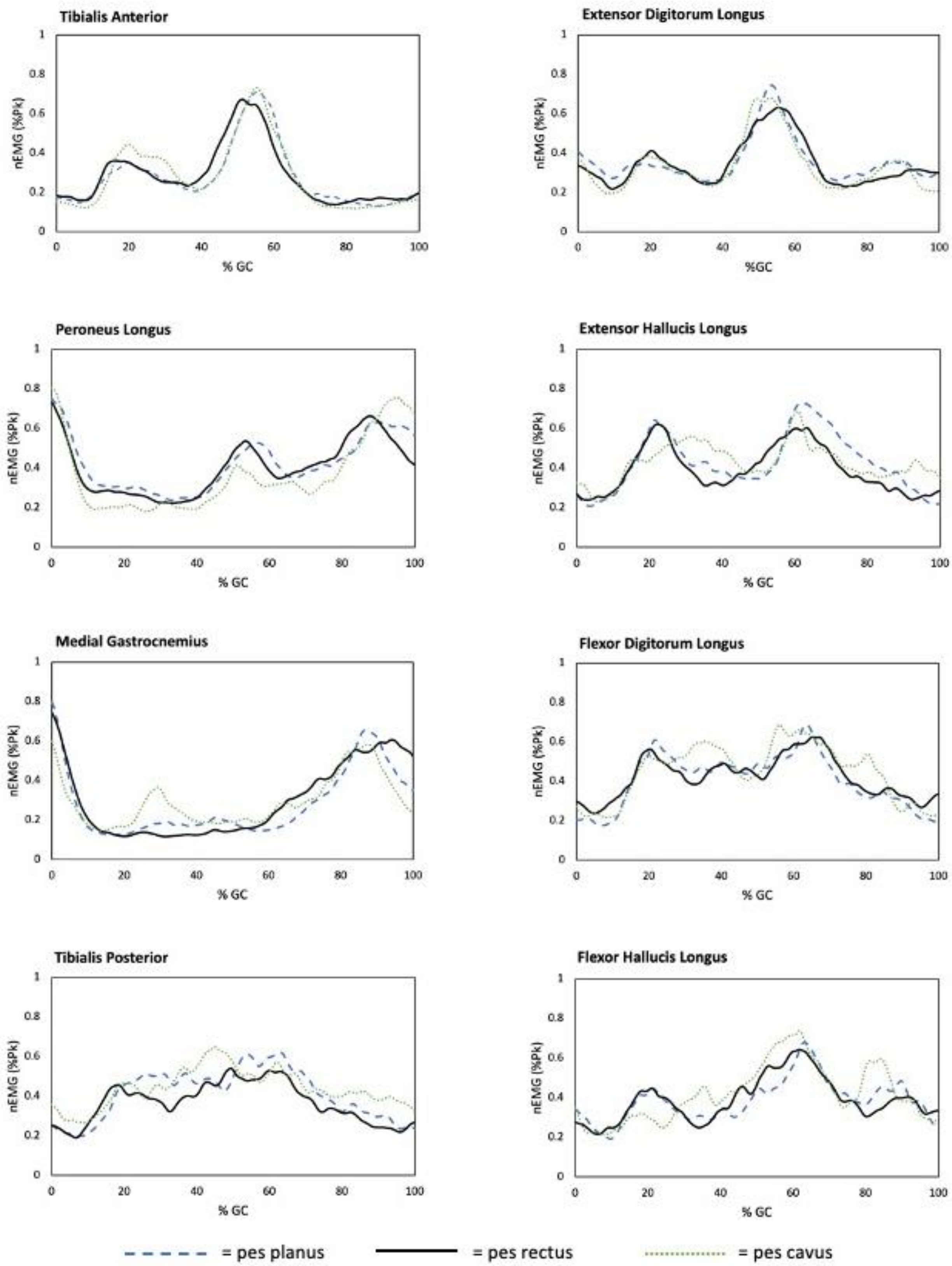

Figure 25. A. The average EMG (aEMG) of each muscle by foot posture across the stance phase of gait (HS: highly supinated/cavus, S: supinated/cavus, N: normal/pes rectus, P: pronated/planus, HP: highly pronated/planus) *=p<.05, **=p<.0001.

B. The time normalized ensemble averages of each lower leg muscle across foot posture when walking in non-textured foot orthoses.

The ensemble averages comparing normalized EMG (nEMG) of lower leg musculature when walking in non-textured FOs are presented in Figure 25B. Most notably, cavus feet demonstrated greater peak nEMG activation levels in TA and MG between 20-40%GC compared to rectus and planus feet. Between 30-40%GC, greater nEMG is observed in EHL, FDL, and FHL compared to planus and rectus feet. Furthermore, flexor musculature in cavus feet reveal increased nEMG activity approaching the toe-off phase of gait (TP: 50%GC, FDL: 50-60%GC, FHL: 55-65%GC) compared to planus and rectus feet. In PL, the aEMG in cavus feet remains lower than planus and cavus feet from 10-90%GC.

In planus feet, TP nEMG remains greater than planus feet from 20-40%GC and 50-90%GC. Additionally, planus feet demonstrate a trend of delayed muscle activation, followed by greater peak nEMG activation near toe-off, compared to both cavus and rectus foot postures; EDL peaks at 50%GC, EHL at 60%GC, and FDL and FHL around 65%GC.

4.3.2 The effect of foot posture on lower leg EMG when texture is added to distinct regions of foot orthoses

Statistically significant interactions were observed in each muscle's average EMG (aEMG) across textured location and FPI score (Figure 26): TA ($F_{19,298}$=7.62, p=<.0001, R^2=0.96), PL ($F_{19,298}$=17.22, p=<.0001, R^2=0.94), EDL ($F_{19,295}$=1.94, p=.0082, R^2=0.96), EHL ($F_{19,255}$=3.46, p=<.0001, R^2=0.92), MG ($F_{19,292}$=2.12, p=.0029, R_2=0.89), TP ($F_{19,223}$=2.31, p=<.0001, R^2=0.91), FDL ($F_{19,238}$=2.01, p=.0057, R^2=0.89) and FHL ($F_{19,190}$=1.65, p=.0379, R^2=0.90), suggesting that the average amplitude of extrinsic muscle activation in stance is modulated by the location of texture and across different FPI scores . The time normalized ensemble averages for each textured location are presented in Figure 27A-E.

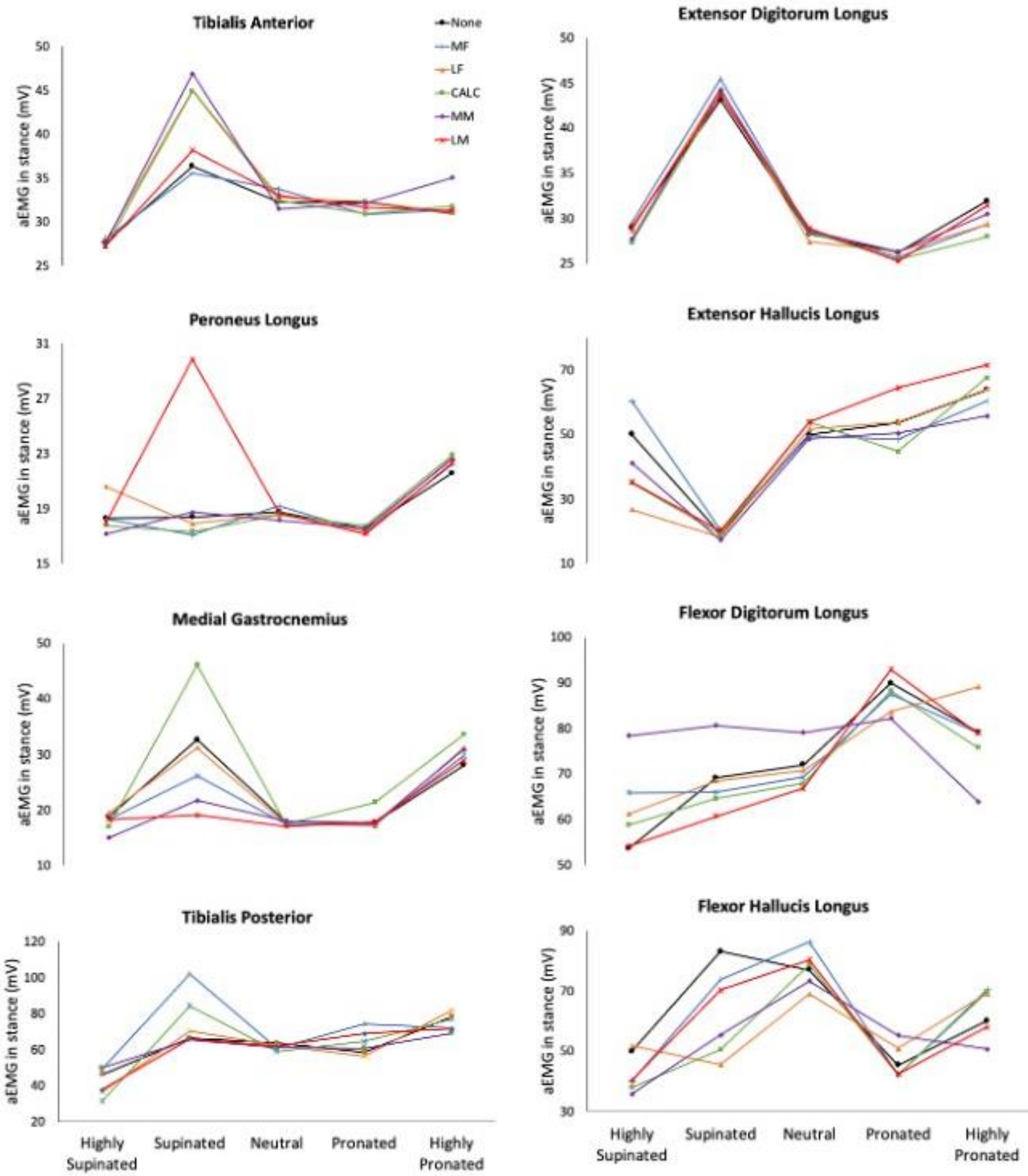

Figure 26. The interaction plots for 8 lower limb muscle's aEMG across differing foot postures and textured locations. Standard deviations for all muscle by FPI classifications are included in Appendix 7.

27A.
Medial Forefoot Texture:

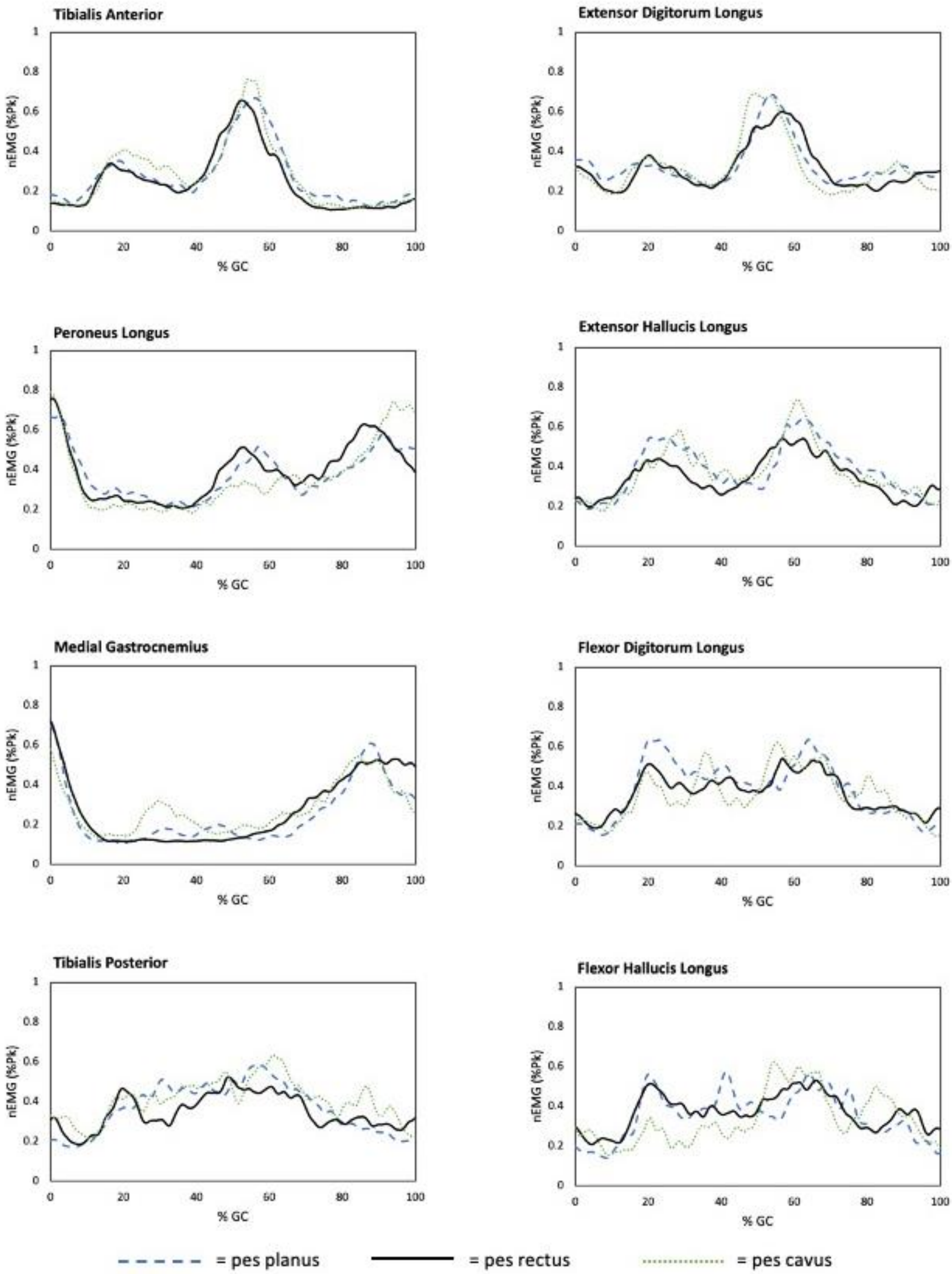

27B.
Lateral Forefoot Texture:

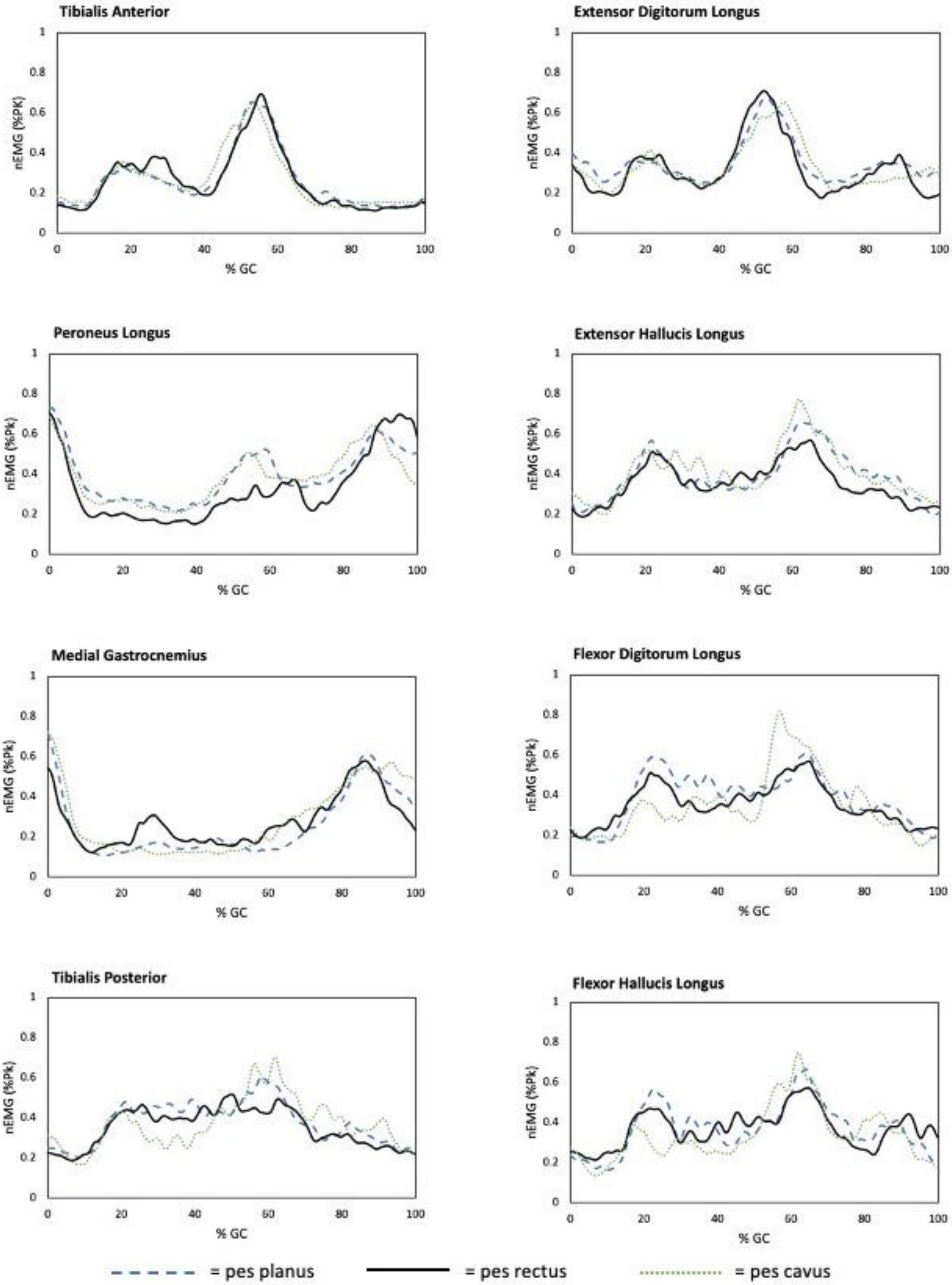

27C.
Calcaneus Texture:

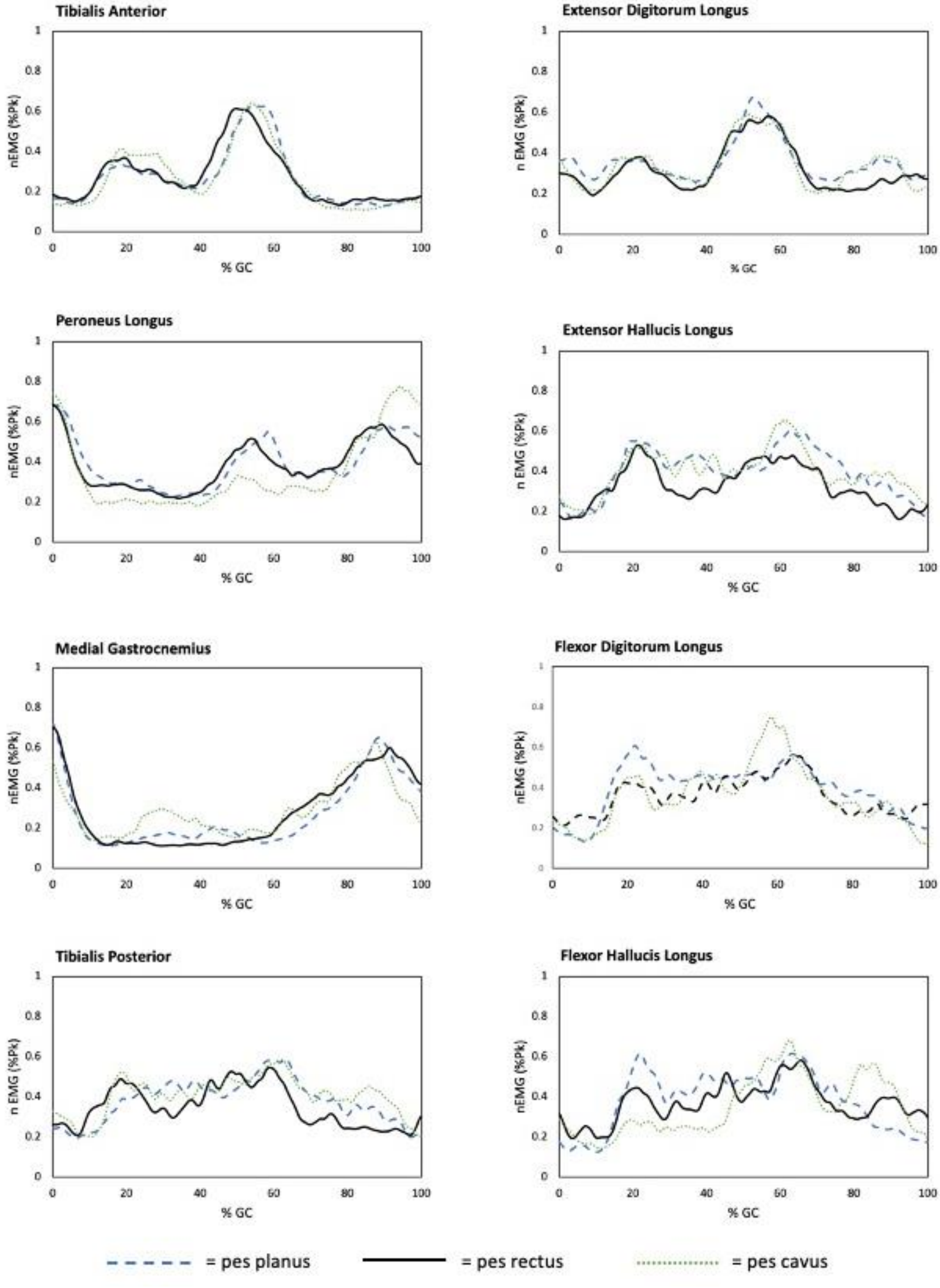

27D.
Medial Midfoot Texture:

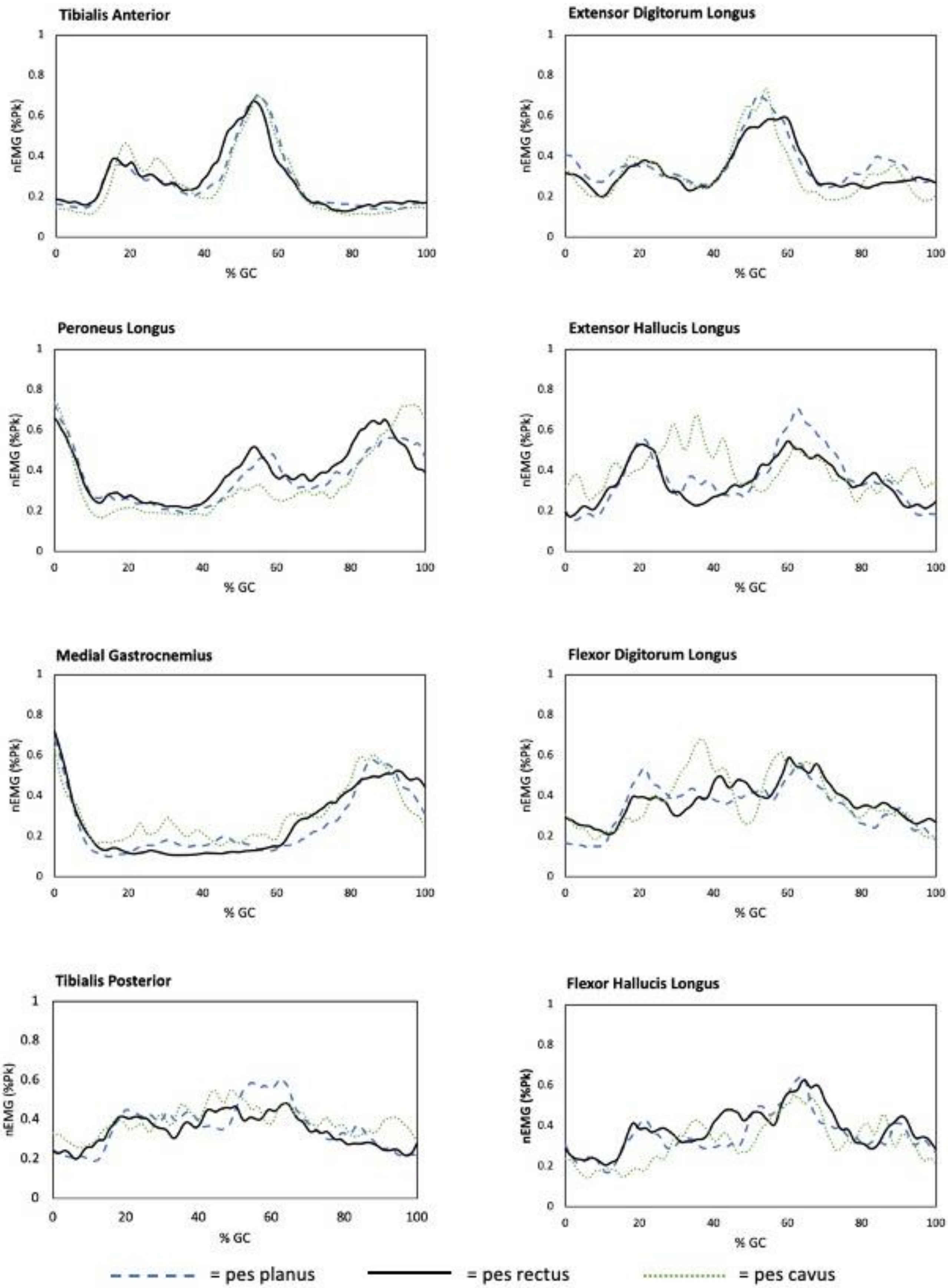

6E.
Lateral Midfoot Texture:

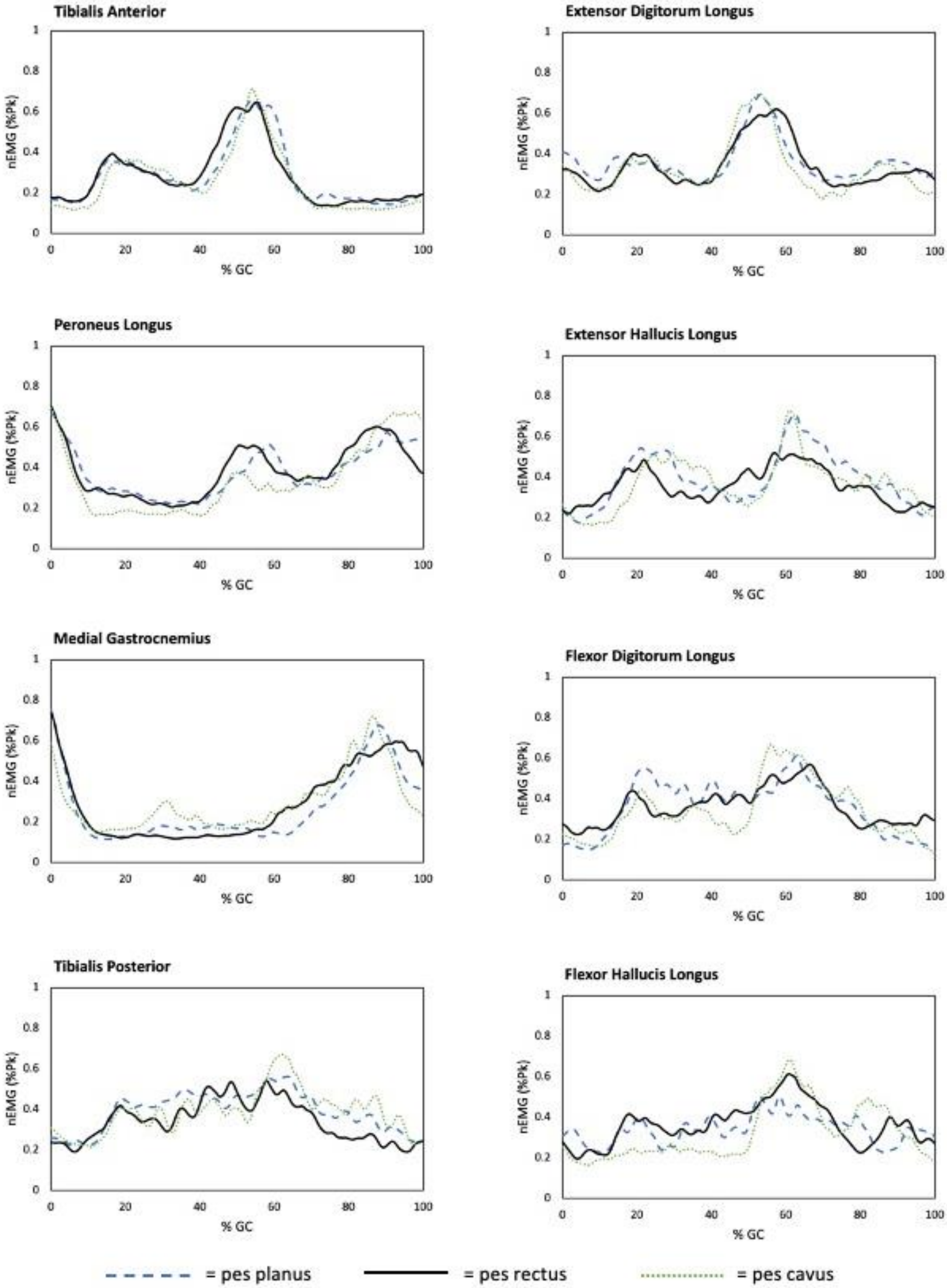

Figure 27. The time normalized ensemble averages of each lower leg muscle across foot posture when walking in textured foot orthoses **A:** medial forefoot (MF) texture, **B:** lateral forefoot (LF) texture, **C:** calcaneus (CALC) texture, **D:** medial midfoot (MM) texture, and **E:** lateral midfoot (LM) texture.

4.4.3 Supinated/Pes Cavus Foot Posture

In supinated feet, the highest amplitudes of TA aEMG were observed with texture to the MM (46.92mV ± 23.50mV), LM (38.17mV ± 16.12mV), CALC (44.92mV ± 22.69mV), and LF (45.00mV ± 22.69mV), compared to rectus and planus feet. The time normalized ensemble averages reveal evident nEMG peaks in TA between 20-35%GC with MM and CALC texture. PL aEMG in supinated feet was significantly greater with texture under the LM (29.83mV ± 3.03mV) compared to other textured locations and/or other foot postures. The ensemble averages, which collapsed highly supinated and supinated foot postures together, interestingly revealed a reduction in nEMG in pes cavus feet across stance. Texture under the CALC in supinated feet increased aEMG of MG (26.10mV ± 16.67mV) and TP (84.37mV ± 77.08mV) compared to rectus and planus foot postures. Both MG (46.17mV ± 42.28mV) and TP (102.18mV ± 86.39mV) aEMG was also greater with texture under the MF. The ensemble averages reveal that both MG and TP activity is greater in pes cavus feet between 20-40%GC when texture is placed under the CALC. Adding texture to the LF (31.18mV ± 20.16mV), LM (19.08mV ± 14.16mV), and MM (21.67mV ± 11.63mV) reduced MG aEMG compared to the non-textured orthotics. The LF ensemble average graph also demonstrates reduced MG nEMG in pes cavus feet between 20-55%CG.

In highly supinated feet, FDL aEMG was highly modulated by textured location. Texture to the MF (58.84mV ± 49.93mV), LF (61.21mV ± 58.76mV), and CALC (65.95mV ± 61.00mV) all increased FDL aEMG compared to non-textured FOs, although the FDL aEMG remained less than pes rectus and planus feet. Texture under the MM (78.39mV ± 72.46mV) also increased FDL aEMG in highly supinated feet, although demonstrated greater amplitudes compared to the highly pronated foot posture. With the exception of texture to the LF (51.81mV ± 48.29mV) in highly supinated feet, FHL aEMG was reduced in all supinated and highly supinated foot postures when texture was applied to each area under the foot (compared to walking in non-textured orthotics). These FHL results are consistent with the time normalized ensemble average graphs.

4.4.4 Pronated/Pes Planus Foot Posture

In general, pes planus feet appear less affected by texture under the foot sole compared to pes cavus feet. Texture under the MM increased TA aEMG (35.06mV ± 17.09mV) in highly pronated feet, although amplitude values remained significantly less than pes cavus feet. Texture under the MF increased MG aEMG in pronated (21.36mV ± 15.24mV) and highly pronated (33.56mV ± 31.70mV) feet compared to the other textured locations. The time normalized ensemble averages revealed MG nEMG increases between 20-50%GC. Although texture under the LF (53.91mV ± 35.54mV) resulted in similar EHL aEMG compared to walking non-textured orthoses, texture under the LM increased EHL aEMG in pronated (64.53mV ± 47.91mV) and highly pronated (71.66mV ± 51.87mV) feet, and decreased EHL aEMG when texture was placed under the MF (48.64mV ± 29.15mV) and MM (50.53mV ± 27.09mV) in pronated feet. Ensemble averages of LM texture reveal EHL nEMG increases between 20-40%GC and again between 60-90%GC. In TP, aEMG was greater in pronated feet when texture was placed under the MF (74.27mV ± 32.79mV), LM (68.86mV ± 42.23mV), and CALC (64.41mV ± 44.46mV) compared to the non-textured orthotics. These increases are consistently observed between 20-40%GC in the graphed ensemble averages. Texture under the LF (56.35mV ± 30.83mV) revealed a reduction in TP aEMG compared to non-textured orthotics, although reversed in highly pronated feet (81.62mV ± 48.02mV) (LF texture increased TP aEMG compared to non-textured FOs). A similar response was observed in FDL aEMG whereby texture to the LF (83.69mV ± 44.90mV) in pronated feet was reduced compared to non-textured orthoses, however greater in highly pronated feet (89.11mV ± 62.95mV). In FHL, texture under two areas (LF (51.07mV ± 42.99mV) and MM (55.39mV ± 29.97mV)) increased aEMG compared to non-textured FOs in pronated feet and reduced aEMG under two areas (LM (42.61mV ± 38.85mV) and CALC (42.27mV ± 33.33mV)).

4.5 DISCUSSION

The purpose of this study was two-fold: 1) to compare the influence of anatomical foot posture on lower leg EMG responses to foot orthoses (FOs), and 2) to explore the effects of foot posture on lower leg EMG responses to FOs with regional application of texture incorporated into the FO design. It was hypothesized that average PIFM aEMG would increase during stance with the addition of texture under the foot sole. Prior to discussing the results, it should be noted that the aEMG data and graphed ensemble averages provide different information to the reader. The ensemble averages comparing normalized EMG (nEMG) of lower leg musculature provides a descriptive analysis of the varying activation levels of each muscle across the gait cycle (GC) and subdivides the data across different foot postures. Although these graphs provide a clear visual comparison of the effect of foot posture on overall lower leg EMG, the data has been collapsed together (highly supinated and supinated as pes cavus, and highly pronated and pronated as pes planus), and this descriptive data has not undergone the same statistical scrutiny as observed in our aEMG results. The aEMG results provide a deeper dive into the amplitude of each muscle within each FPI foot posture classification. Although the division of participants within each FPI score is unequal, these results provide a more precise analysis and will thus remain the focus of this discussion.

4.5.1 EMG activation levels vary across the foot posture spectrum

To our knowledge, this is the first study that takes a comprehensive look at the EMG activation differences of all lower leg muscles (with the exception of lateral gastrocnemius, soleus and plantaris) across different foot postures when immediately walking in FOs. Our results indicate that muscles respond differently to FOs across all 5 FPI classifications. In pes cavus feet/supinated foot posture, the aEMG of TA, EDL, and MG during stance were significantly greater compared to individuals with a pes rectus/normal foot posture (Figure 25A). More specifically, TA and MG appear to co-contract between 20-40% GC (Figure 25B). Pes cavus feet are typically accompanied with greater hindfoot inversion [183] which may account for the increased levels of TA activation. A FO that immediately contacts the plantar foot sole of the cavus foot is an interface contact that likely did not occur without the FO inside participant's footwear. This increased contact on the medial aspect of the foot may trigger increased subtalar joint eversion as the foot relaxes onto the surface of the FO; a movement that is commonly correlated with increased TA activation [184]. Considering the characteristically tight gastrocnemius muscles in pes cavus feet [185], this immediate MG increase to FOs may be undesirable. In exploring the link between subtalar joint position and muscle function, TA and MG co-contraction upon immediate wear increases in subtalar joint eversion has been demonstrated to increases the MG and TA muscle potential in flexing the knee and dorsiflexing the ankle during stance [184]. Consequently, although this immediate co-contraction may initially appear undesirable, TA and MG activation may represent improved ability to maximize their mechanical roles during stance. In pes cavus feet, a secondary observation to immediate FOs was a statistically significant reduction in EHL aEMG (Figure 25A). As FOs have been proven to immediately reduce the 1st metatarsal inclination angle in pes cavus feet [180], this joint position change is a likely explanation for the reduction in EHL activation. Lastly, in the highly supinated foot posture compared to normal/pes rectus, a significant aEMG reduction was observed in TA, FDL, TP, and FHL muscles (Figure 25A), with none of the lower leg EMG experiencing significant increases in muscular activation. Lower FPI values (more cavus feet) are associated with reduced foot mobility compared to higher FPI values (more planus feet) [176]. When placing a FO under a foot that already has reduced mobility, tibial, rearfoot, and midfoot movement control is likely unnecessary, and consequently reduces muscular demand of the lower extremity.

A pes planus foot, compared to pes cavus and/or pes rectus, is commonly accompanied by increased hindfoot valgus, a lower medial longitudinal arch, increased midfoot plantar pressures, reduced forefoot plantar pressures, and greater midfoot movement during stance [73,183]. The results of our study indicate that FOs under pronated feet experienced a significantly reduced PL, EDL, and FHL aEMG, accompanied with increased FDL activation during stance (Figure 25A). Conversely in highly pronated feet, significant reductions in TA and FHL aEMG were accompanied by increased PL, MG, TP, EDL, EHL, and FDL muscular activity. Previous comparisons by Murley et al. (2009) reported opposing EMG results [16], however their EMG analysis window isolated muscle activation by initial contact, midstance, and propulsion, rather than reporting aEMG across the entire stance phase of gait. Furthermore, both studies adopted different foot posture classification tools, therefore, our study populations may have been on different foot posture spectrums. Lastly, peak plantar pressures under the lateral forefoot (4^{th} and 5^{th} metatarsalphalangeal joints) are typically lower in planus feet compared to normal/pes rectus feet. A FO that controls midfoot movement earlier in stance will redistribute forefoot pressures more equally across the forefoot at toe off [186]. This plantar pressure change unsurprisingly alters the flexor muscle demand, increasing FDL and reducing FHL activation, as demonstrated in our results. Overall, these results highlight the importance of considering foot posture when clinicians immediately dispense FOs to patients. EMG activation levels vary across the foot posture spectrum and it's important to recognize this muscular variability to accurately treat underling medical concerns and biomechanical abnormalities.

4.5.2 Foot Posture and Textured Orthotics

The application of texture to distinct regions of the foot sole was intended to stimulate the activation of cutaneous mechanoreceptors under 5 different areas of the foot sole. Furthermore, we were interested in exploring how different foot postures would alter the EMG responses to each textured location. The lower leg EMG responses in highly supinated feet responded similarly to each textured location. The amplitude levels within each respective muscle demonstrated slight amplitude variability, although there was not one textured location that was drastically different, that generated large increases and/or decreases in aEMG amplitude, compared to the others. In pes cavus feet compared to normal (pes rectus), texture under the CALC generated greater aEMG of the TA, MG, and TP muscles; three muscles with important functional roles throughout the stance phase of gait. Texture under the MM also increase TA aEMG, whereas texture under the LM significantly increased PL aEMG. Texture under the MM increased FDL aEMG whereas texture to all locations reduced the magnitude of FHL aEMG compared to wearing non-textured FOs. Lastly, the amplitude of both extensor muscles was not altered by textured location. In pronated feet, the regional application of texture had the largest effect on both flexor muscles. Greater magnitudes of FDL aEMG are evident with texture to each location under the foot sole in comparison to pes rectus feet. In highly supinated individuals, LF texture further increased FDL aEMG levels, whereas the remaining textured locations reduced FDL activation. In FHL, highly pronated feet revealed the highest variability with CALC and LF texture increasing FHL aEMG, and MM and LM reduced FHL aEMG.

The results of our study clearly indicate that EMG amplitudes of all lower limb muscles are affected by both textured location and foot posture classification. As this is the first study of its kind, it remains challenging to compare our results to previous literature. Despite this challenge, our results can provide benchmark data for future experimental protocols to advance knowledge pertaining to sensory augmentation and foot orthoses design. The ensemble averages (Figures 27A-27E) represent the average EMG of all participants trials, which are then averaged together across all participants. These graphs provide a visual snapshot to rapidly compare pes cavus, rectus, and planus foot postures within each textured location.

4.5.3 Limitations

There are a few limitations worth noting. Firstly, this data is collected on healthy individuals and does not represent a pathological and/or diseased population. Individuals seeking FO treatment are commonly experiencing pathology, injury and/or pain, which increases the value in adopting these FO designs into experimental protocols which include non-healthy populations. Secondly, the number of participants within each foot posture classification are not equal. The pes cavus foot posture, which demonstrated the largest fluctuations in EMG response, had the lowest number of participants.

4.6 CONCLUSION

The results of this study provide strong evidence, which supports the importance of considering foot posture when dispensing FOs, both with and without texture to distinct regions under the foot sole. Further research should focus on connecting these muscle changes across foot posture to specific pathology and/or risk of injury. Future experimental protocols are encouraged to continue studying the effects of different textured designs in understanding their modulatory effect on muscle activation during walking.

CHAPTER 5

THE RELATIONSHIP BETWEEN FOOT POSTURE AND PLANTAR INTRINSIC FOOT MUSCLE ACTIVITY DURING GAIT

5.1 INTRODUCTION

The shape of the medial longitudinal arch (MLA) is a common visual characteristic on the medial aspect of the foot which defines the range of variance in foot postures. Plantar intrinsic foot muscle's (PIFMs) span the MLA and recent research has begun exploring how PIFM function changes across different foot postures. Anecdotally, foot posture remains an important consideration when dispensing foot orthoses (FOs), although limited research has explored the effect of foot orthoses on PIFMs across different foot postures. In neurophysiology research, experimental studies have linked cutaneous mechanoreceptors in plantar foot sole skin to motorneuron pools in the lower extremities [131]. The foot orthotic industry has yet to capitalize on the plausibility of using different foot orthoses designs to facilitate cutaneous mechanoreceptor activation as a method of modulating PIFMs activity.

The MLA is a well-defined morphological structure of the human foot. The overall MLA height, in reference to the ground surface, can be visually quantified by the calcaneal inclination angle [173], navicular height from the ground [187], or hindfoot position of the calcaneus in reference to the talus bone (subtalar joint position) [188]. Foot posture runs along a spectrum of pes planus feet, characterized by a flatter arch shape, to pes cavus feet, characterized by a higher arch shape. The MLA is a dynamic structure that changes in height and width as force is transferred under the foot across different phases of the gait cycle. Despite speculations surrounding the effectiveness of static MLA evaluations as a reliable measure of dynamic foot function [188], the Foot Posture Index (FPI), a commonly adopted clinical measure of static foot posture, has proven to be a strong predictor of dynamic MLA movement [176]. Measures of foot posture such as the FPI are important, as different foot postures have been demonstrated to alter MLA mechanics, and subsequent foot function, during walking.

Kinematic and PIFM EMG changes have been reported across different foot postures when walking [183,189,190]. For example, planus feet experience a higher MLA frontal plane eversion moment during midstance compared to rectus (normal arched) feet [189]. Pes cavus feet remain more dorsiflexed and have a greater peak hindfoot inversion moment during stance [191]. Studies measuring the cross-sectional area of AbdH and FDB have generated conflicting results. Some researchers have suggested that AbdH muscle thickness is greater in planus feet compared to rectus feet [192–194]. This muscle hypertrophy has been attributed to the repetitive lengthening of the muscle and assumed to suggest the dynamic function of the AbdH under load (a larger cross sectional area of a muscle is assumed to suggest increased muscle strength due to increased forces during gait) [190]. Despite this interpretation, other researchers have found opposing results whereby AbdH cross sectional area is reduced in planus feet [195], and/or unchanged between varying severity of planus feet [196]. Although foot posture and PIFM cross-section area remains unclear, a recent study correlating FPI scores to cross-sectional area has provided additional insight.

When correlating foot posture with muscle thickness of AbdH and FDB, reduced thickness has been associated with increased FPI scores [190]. Musculature on the medial aspect of the foot has been assumed to have a larger effect on foot posture variance compared to muscles on the lateral aspect of the foot, suggesting that muscle proximity to the medial arch may be more important to overall foot posture. It has been suggested that variance in foot posture and subsequent variability in cross sectional area muscle size may not be a reflection of altered muscle strength, but rather a failure of sensorimotor interactions between PIFMs ability to produce sensory information about changes in foot posture [192,197]. Although more research is required to confirm these speculations, it offers one plausible explanation for the lack of consistency in muscle's cross-sectional area as it correlates with foot posture variance.

In the foot orthotic industry, foot posture remains an important consideration when trying to maximize foot sole contact with the top cover of the device. The effects of FOs on kinetic and kinematic outcomes [6,28,33,198,199], as well as extrinsic foot muscle's EMG [32,200–203] have been extensively researched, however minimal attention has been given to their effect on PIFMs [162]. Furthermore, recent advancements in neurophysiology have linked foot sole cutaneous mechanoreceptors with motorneuron pools in the lower leg [131]. Although this work has yet to get extended to PIFMs, cutaneous reflex literature has emphasized the important role of skin in determining overall motorneuron pool excitability during walking [60,69]. It remains unknown if we can capitalize on this cutaneous mechanoreceptor-motorneuron pool excitability link and integrate receptor stimulation methods into FOs design. Thus, the purpose of this research was to explore two questions: 1) How does foot posture modify PIFM's muscle activity when walking in a FO and a textured FO (FOT)? and 2) What is the relationship between foot posture and PIFM activity? It was hypothesized that PIFM aEMG will be greater in lower FPI scores (pes planus feet) compared to higher FPI scores (pes cavus feet).

5.2 METHODS

5.2.1 Participants

The data from this study was derived from a previously collected dataset whereby PIFM EMG was recorded in forty healthy young adults (age: 27 ± 5.2 years, height: 175.5 ± 10.4cm, weight: 80.2 ± 18.7 kg) completing a walking protocol. All participants confirmed the absence of known neurological and/or musculoskeletal disorders prior to participation. Participant's anatomical foot posture was categorized with the Foot Posture Index (FPI). The distribution of participants by foot posture was as followed: highly supinated=8, supinated=4, normal=11, pronated=11, highly pronated=6. Normal tactile sensation from bilateral foot soles (5 sites) was confirmed with Semmes-Weinstein monofilaments (North Coast Medical, Inc., Morgan Hill, CA) and informed consent was obtained by all participants. The protocol was approved by the institution's research ethics board (REB#6006).

5.2.2 Instrumentation

Fine-Wire Electromyography

Muscle activity was recorded (2000Hz, Ultium, Noraxon, Scottsdale, AZ, USA) from four PIFMs; abductor hallucis (AbdH), transverse head of adductor hallucis (AddH), flexor digitorum brevis (FDB) and abductor digiti minimi (ADM) during gait. Bipolar fine-wire electrodes were custom-made with two formvar copper wires (0.005mm, California Wire Company, Grover Beach, USA) inserted through a single-use hypodermic needle (27G, 25G, BD Precision Glide, Franklin Lakes, USA). A millimeter of insulation was stripped from the insertion end of each wire and folded over the needle tip. All insertions were performed under ultrasound-guidance (HFL50X, SonoSite, Toronto, CAN) with two insertions per foot. FDB and AddH were consistently recorded from one foot, whereas AbdH and ADM were consistently recorded from the opposite foot. Insertions into the left and right foot varied across participants.

The medial and lateral posterior borders of each foot orthotic were traced on participants' skin. All fine-wire insertion sites were landmarked above these borders to ensure the FOs did not contact the wires during gait. The insertion sites were sterilized with alcohol and each muscle was initially landmarked on ultrasound prior to skin puncture. The AbdH electrode was inserted 1-2mm below the navicular bone and confirmed with resisted flexion and abduction of the 1st digit. The FDB electrode was also inserted 1-2mm below the navicular and confirmed with voluntary flexion of digits 2-4. The ADM was inserted equal distance between the cuboid and distal border of the calcaneus bone. Active flexion and resisted 5th digit abduction confirmed the insertion accuracy into the muscle. Insertion into AddH followed a previously described ultrasound-guided approach (Figure 28) [146].

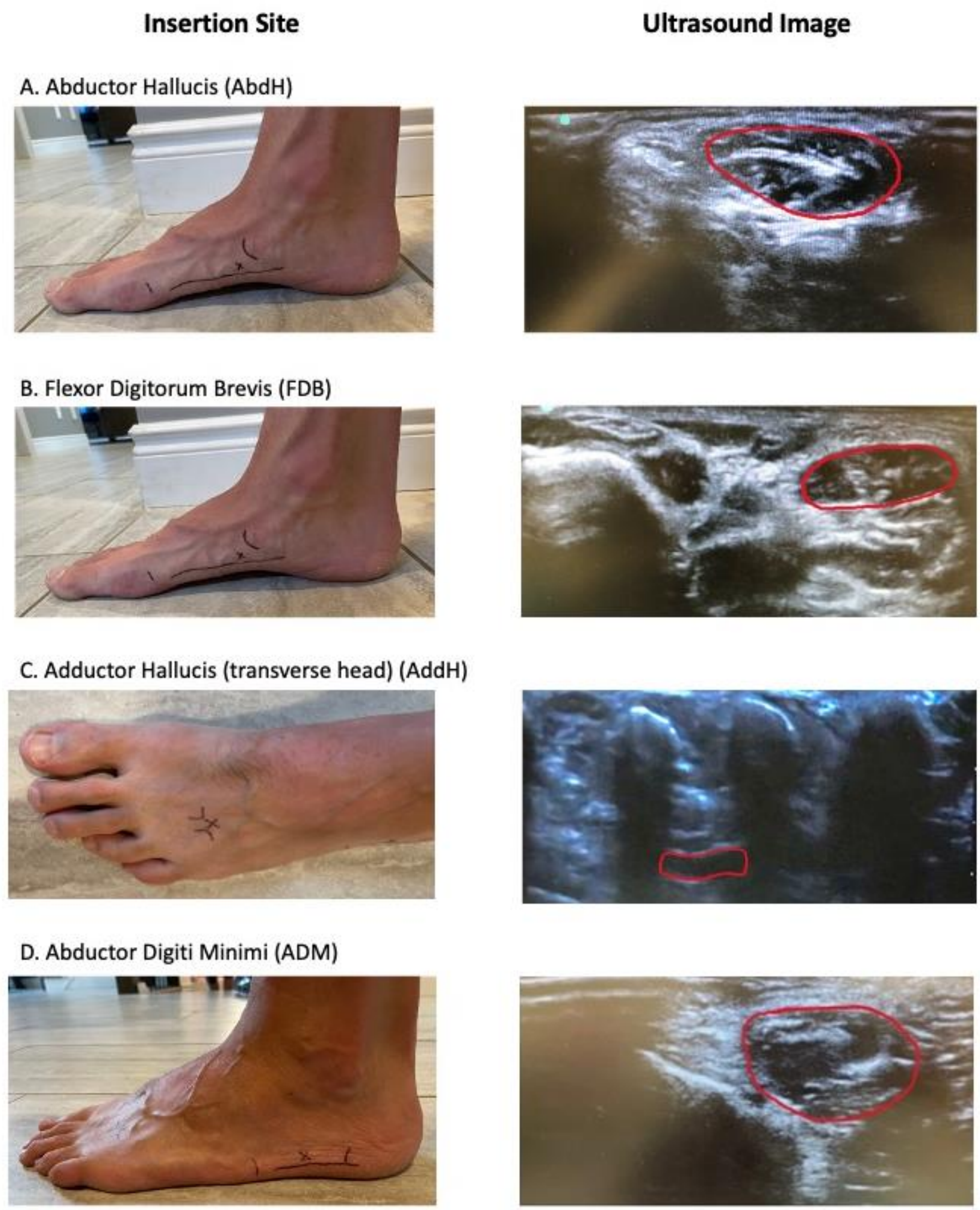

Figure 28. Left images: Surface landmarks prior to fine-wire insertions. The FOs border and targeted insertion sites ("X") are identified. Right images: Ultrasound images identifying each muscle of interest. Each PIFM (the target insertion site) has been outlined in red. *Note: this image is the same as Figure 12 in this dissertation document.

Kinematics and Kinetics

Two 3D motion capture cameras (Optotrak Certus; Northern Digital Inc., Waterloo, Ontario, CAN) captured kinematic data (100Hz) from 12 IRED markers located on each participant's xyphoid process, forehead, and bilateral acromions, anterior superior iliac spines, tibial tuberosities, anterior ankle joints, and 3rd metatarsals. It should be noted that kinematic data was not used in this data analysis although noted here to document all the instrumentation on participants during collection. Kinetic data (2000Hz) was collected with three force plates (OR6-5-2000; AMTI, Watertown, Massachusetts, USA) embedded into the walking surface.

The Foot Orthotics

All participants completed the experimental protocol in two FO conditions (non-textured foot orthoses (FO) and textured foot orthoses (FOT)). The non-textured foot orthoses (FO) were a prefabricated device (Active Thin, Sole, Calgary, CAN) that was matched to each participants' foot length. The textured foot orthoses (FOT) consisted of the identical Active Thin Sole footbed with added textured material serving as a top cover to the orthotics (Figure 29). The zigzag pattern ran medial to lateral with a 7mm peak-to-peak distance and 5mm spacing between horizontals. All participants wore socks (76% polyester, 22% olefine, and 2% rubber; Wal-Mart Canada Corp.) over the FOs to secure them in place. To be clear, socks were worn in both FO conditions (FO and FOT) and not worn in the barefoot walking trials (see protocol below).

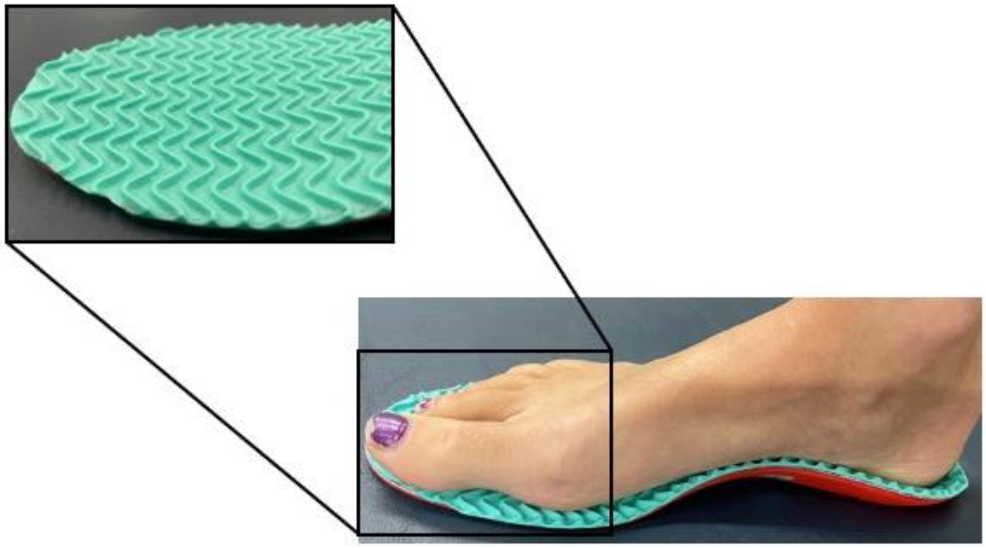

Figure 29. The textured foot orthoses (FOT) used in the experimental study. The top left image provides a close-up view of the zigzag pattern in the textured material.

Experimental Protocol

Data from this study has been extracted from a larger experimental protocol which manipulated the walking surface between hard and soft foam. This dataset and analysis only include the hard, level walking conditions. All participants completed a series of level walking trials in three orthotic conditions: barefoot, FOs, and FOTs. The order of orthotic exposure alternated between participants. Each trial began in static stance. When provided the command ‘go’, participants walked at a self-selected velocity from one end of the walkway to the other. Two steps were taken before contacting force plate 1, then force plate 2, and then walking the remainder of the trial. Each participant completed 25 trials (5 x barefoot, 10 x FO, 10 x FOT). As socks were stretched over participant’s feet and FOs, careful attention was placed on resecuring IRED markers over the ankles and 3rd metatarsal heads when alternating between FO conditions.

5.2.3 Data Processing

The Raw EMG signals were processed with a differential amplifier (gain x500) and band-pass filtered between 10-500Hz. Signals were full-wave rectified and linear enveloped (40Hz dual-pass Butterworth filter). The stance to terminal swing phases of gait were extrapolated from force plate data to outline initial contact to the next initial contact of the same limb. 0% of the gait cycle was identified as initial contact on the 1st force plate (>10N threshold) and 100% being toe-off (<10N on 2nd force plate). EMG averages initially grouped all walking trials for each participant's FO condition and PIFM. Participant averages were then normalized to the peak EMG of each PIFM within the gait cycle. Ensemble averages across participants were calculated and then graphed as 0 to 100% of the gait cycle for each FO condition and PIFM.

5.2.4 Statistical Analysis

To discern the relationship between foot posture and PIFMs nEMG, a correlation (Microsoft Excel, version 16.53) was run between FPI score and each PIFMs when walking barefoot, in FOs and in FOTs. The correlational coefficient results were evaluated according to the following criteria: .90 to 1.00 (-90 to -1.00) = very high positive (negative) correlation, .70 to .90 (-.70 to -.90) = high positive (negative) correlation, .50 to .70 (-.50 to -.70) = moderate positive (negative) correlation, .30 to .50 (-.30 to -.50) = low positive (negative) correlation, and .00 to .30 (.00 to -.30) = negligible correlation [204]. Statistical significance was set at an alpha of p=.05.

5.3 RESULTS

Thirty-two participants were included in the analysis. The division of participants within each FPI score was: 10 pes cavus (6 highly supinated, 4 supinated), 10 pes rectus, and 12 pes planus (9 pronated, 3 highly pronated). The correlation graphs are presented in Figure 30 which compared the relationship of PIFMs aEMG and foot posture (along the entire spectrum of -12 (highly supinated) to +12 (highly pronated). The ensemble graphs for walking barefoot, in FOs and in FOTs are presented in Figure 31. These graphs collapsed the highly supinated and supinated participants together, and the highly pronated and pronated participants together.

5.3.1 The relationship between foot posture and PIFMs nEMG

When walking barefoot, there was a significantly low positive relationship between FPI score and AddH nEMG, r=.34, p<.0001 (Figure 30A). Pronated feet generated higher magnitudes of AddH nEMG compared to supinated feet when barefoot. AbdH, ADM, and FDB nEMG were not significantly correlated with foot posture when walking barefoot. In FOs, none of the PIFMs' nEMG were significantly correlated with foot posture (Figure 30B). Lastly, when walking in FOTs, there was a significantly low positive relationship between FPI score and AbdH nEMG, r=.29, p=<.0001 (Figure 30C). Pronated feet generated higher magnitudes of AbdH nEMG compared to supinated feet when walking in textured FOs.

5.3.2 Walking Barefoot

When barefoot (Figure 30A), there was a reduction in AbdH aEMG during stance (10-60%GC) and in AddH aEMG between 20-50%GC in planus feet compared to rectus and cavus feet. There was also an increase in peak FDB aEMG at toe-off (50-60%GC) in planus feet compared to rectus and cavus feet. Lastly, in ADM, aEMG was reduced in cavus feet at initial contact (0-10%GC) compared to rectus and cavus feet.

A. Walking Barefoot:

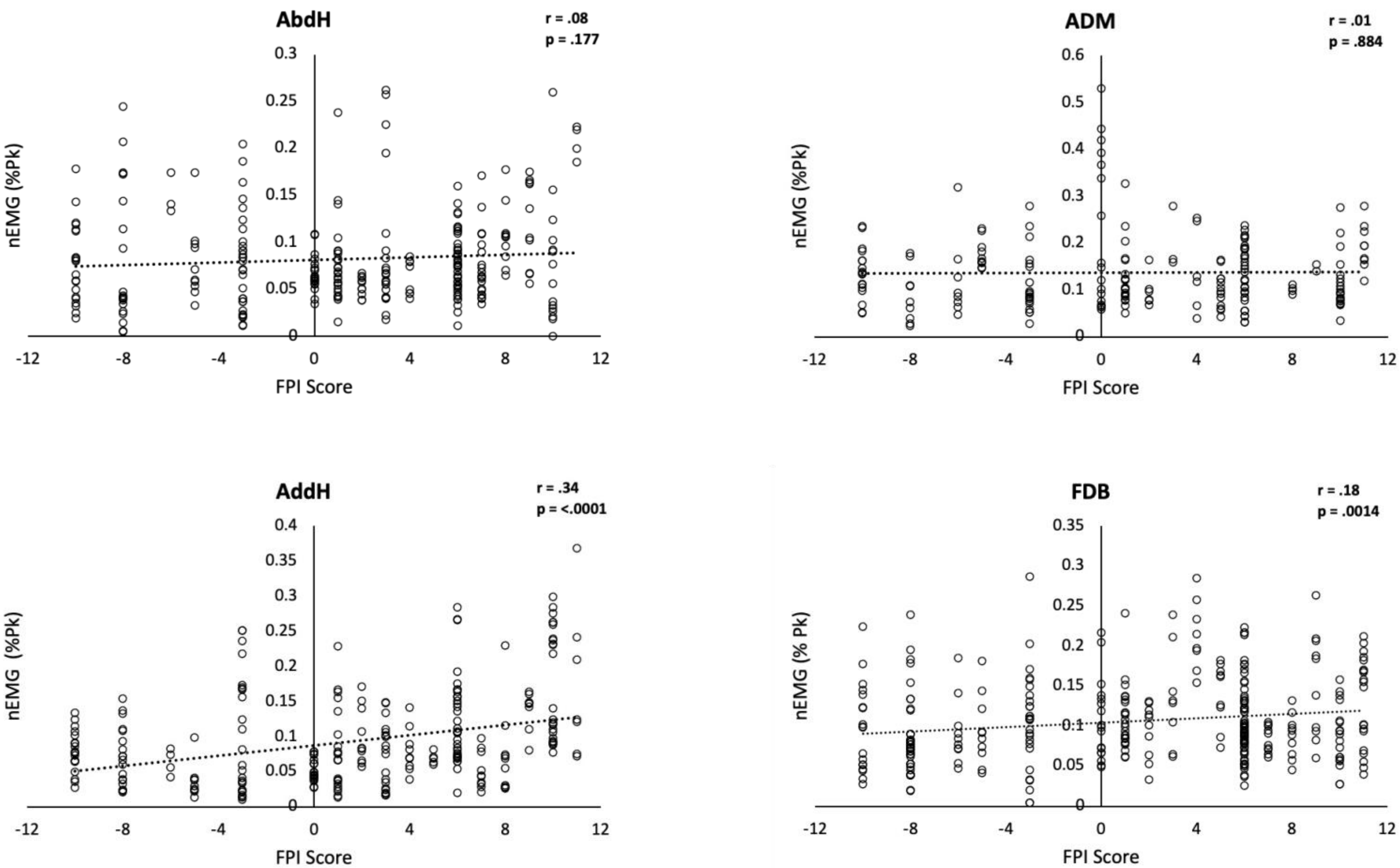

B. Walking in FOs:

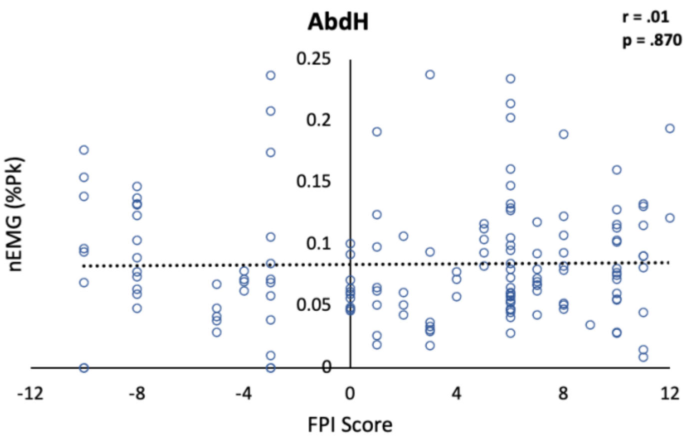

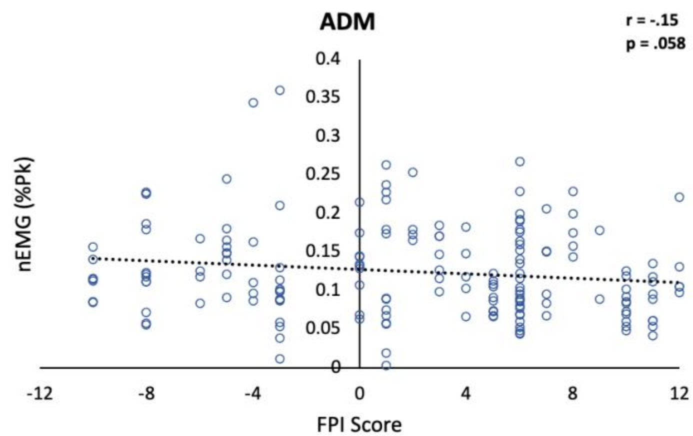

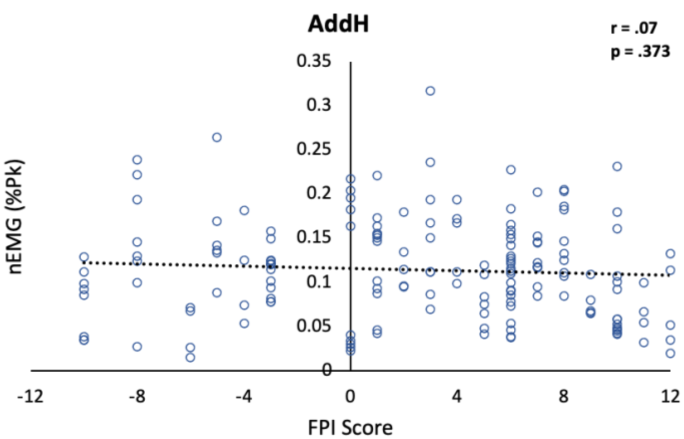

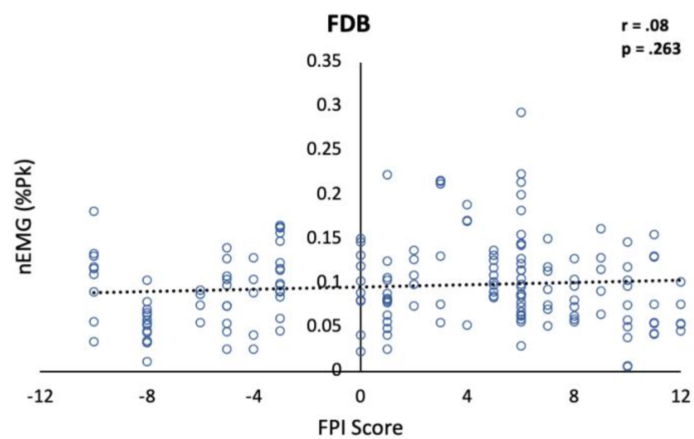

C. Walking in FOTs:

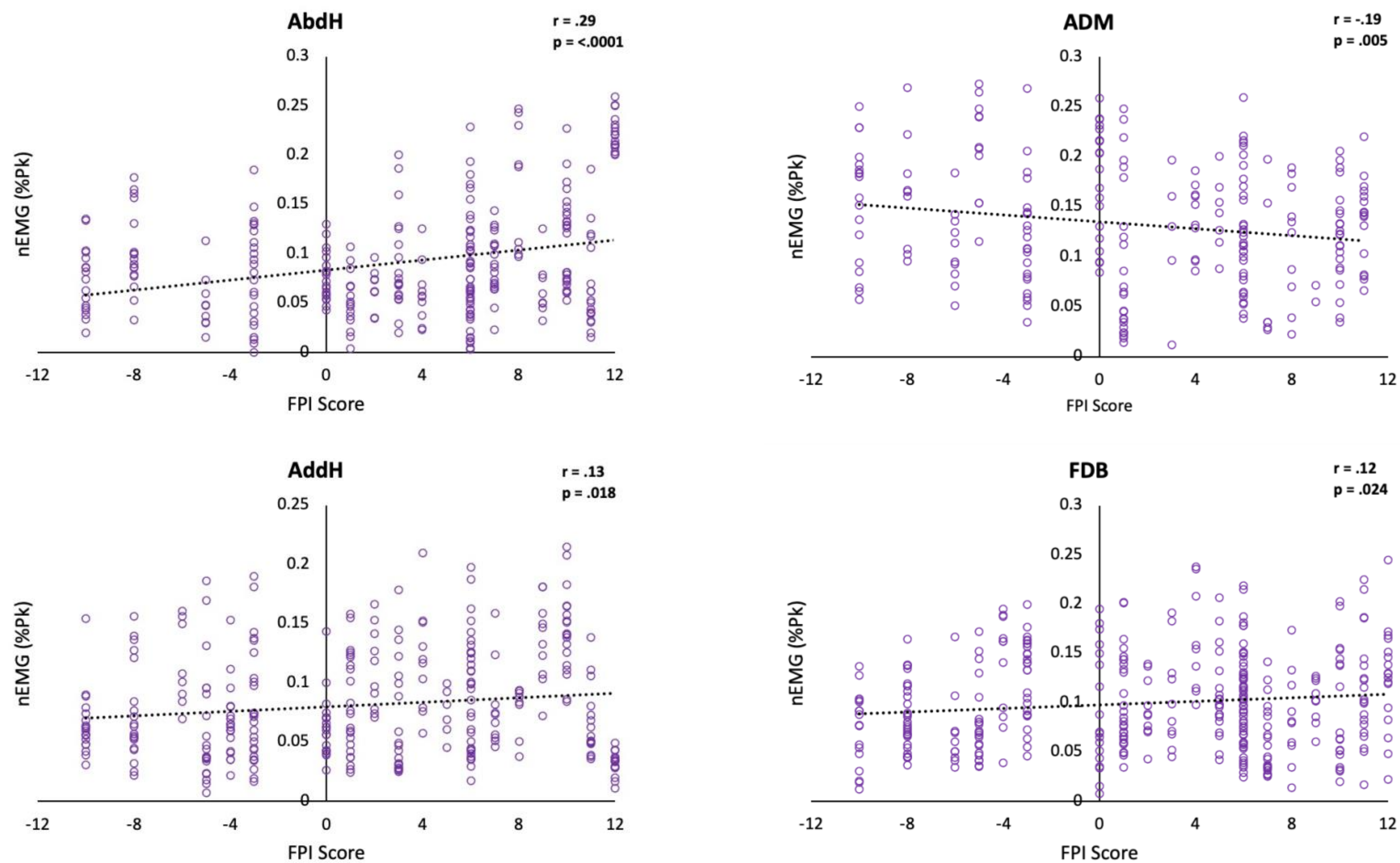

Figure 30. The relationship between Foot Posture Index (FPI) score and 4 plantar intrinsic foot muscles (PIFMs) when walking barefoot (A), in non-textured foot orthoses (FOs) (B) and in textured foot orthoses (FOTs) (C). Muscles of interest: AbdH = abductor hallucis; AddH = transverse head of adductor hallucis; ADM = abductor digiti minimi; FDB = flexor digitorum brevis, nEMG = normalized EMG

A. Walking Barefoot:

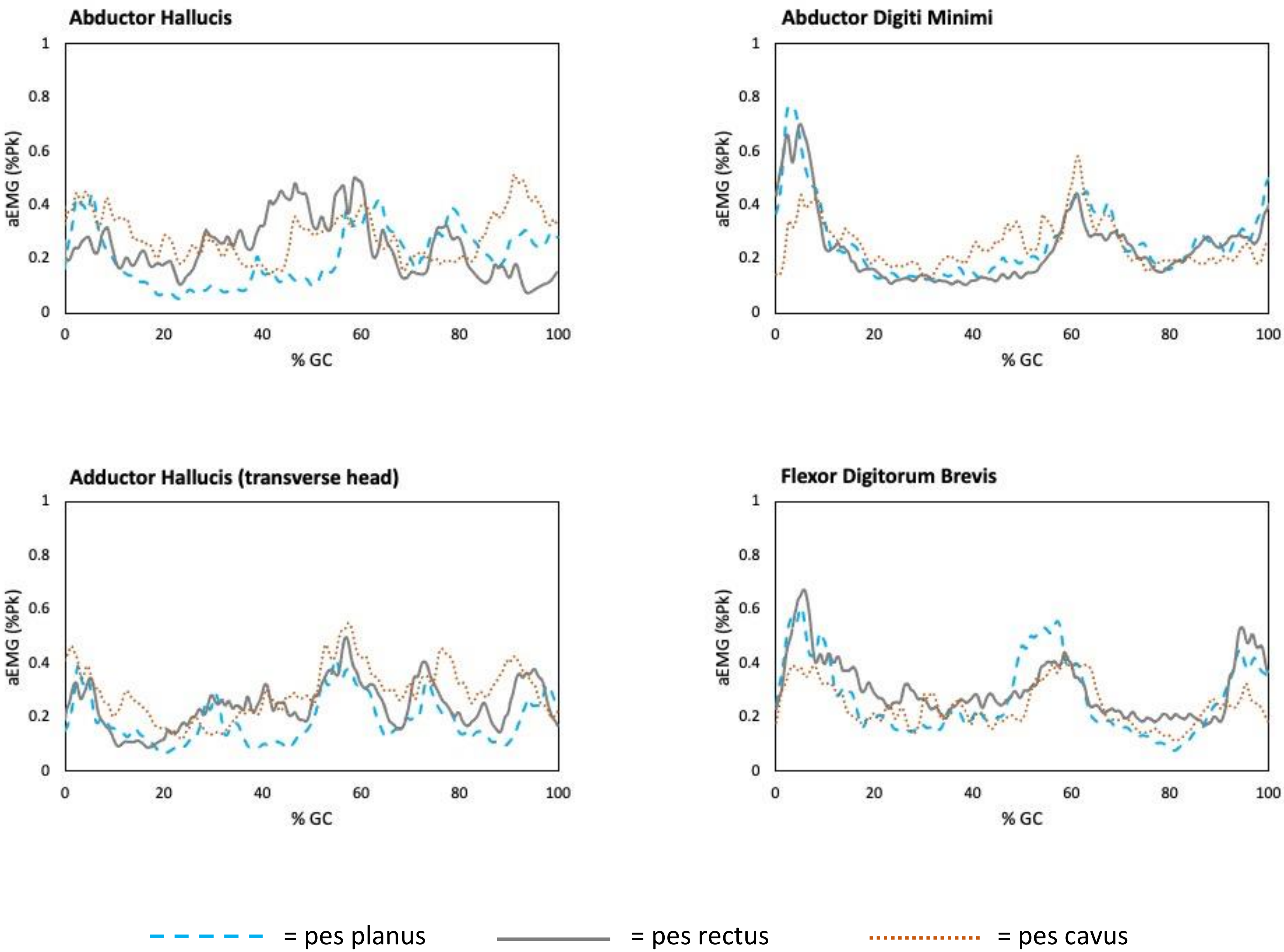

B. Walking in FOs:

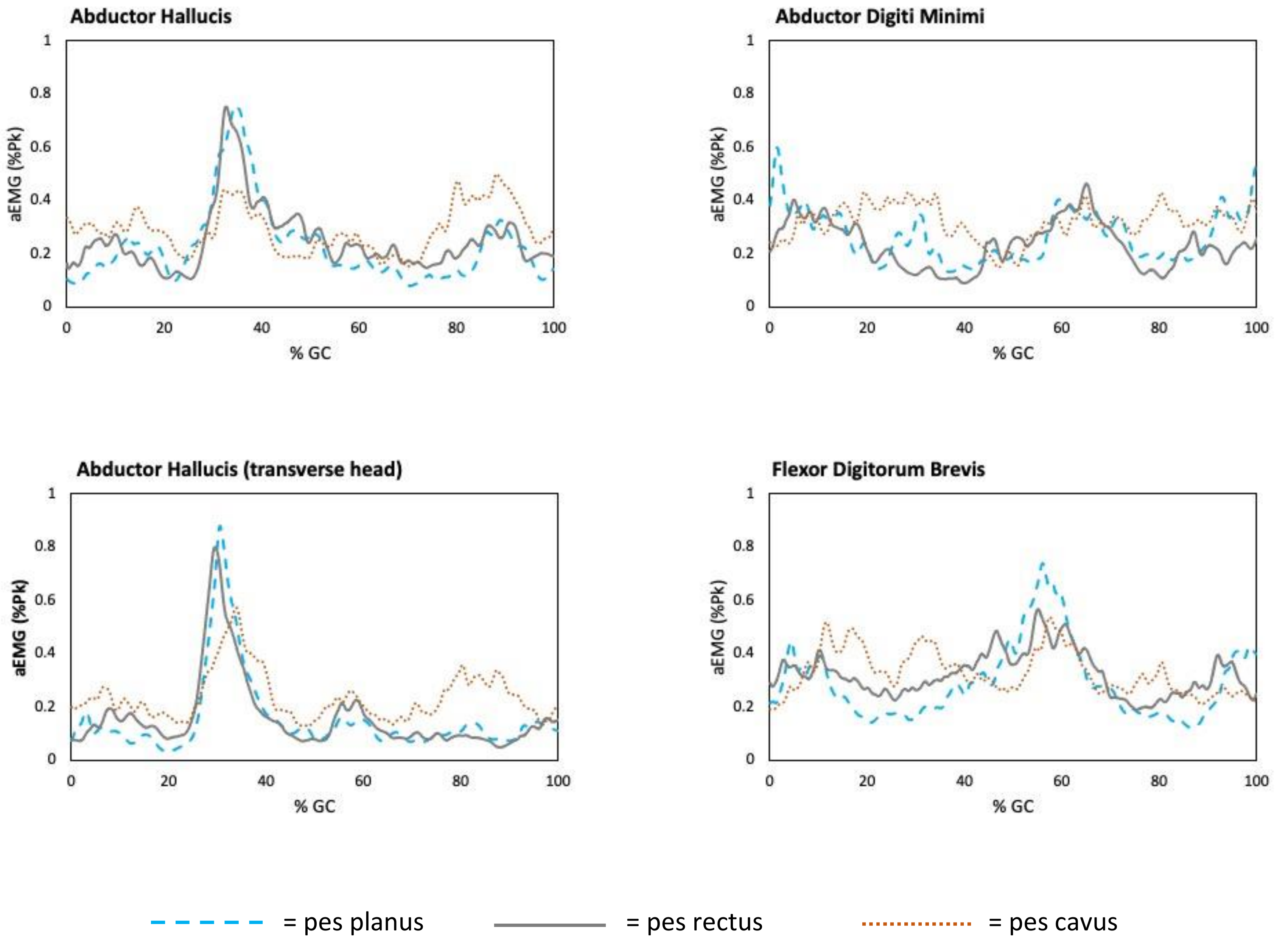

C. Walking in FOTs:

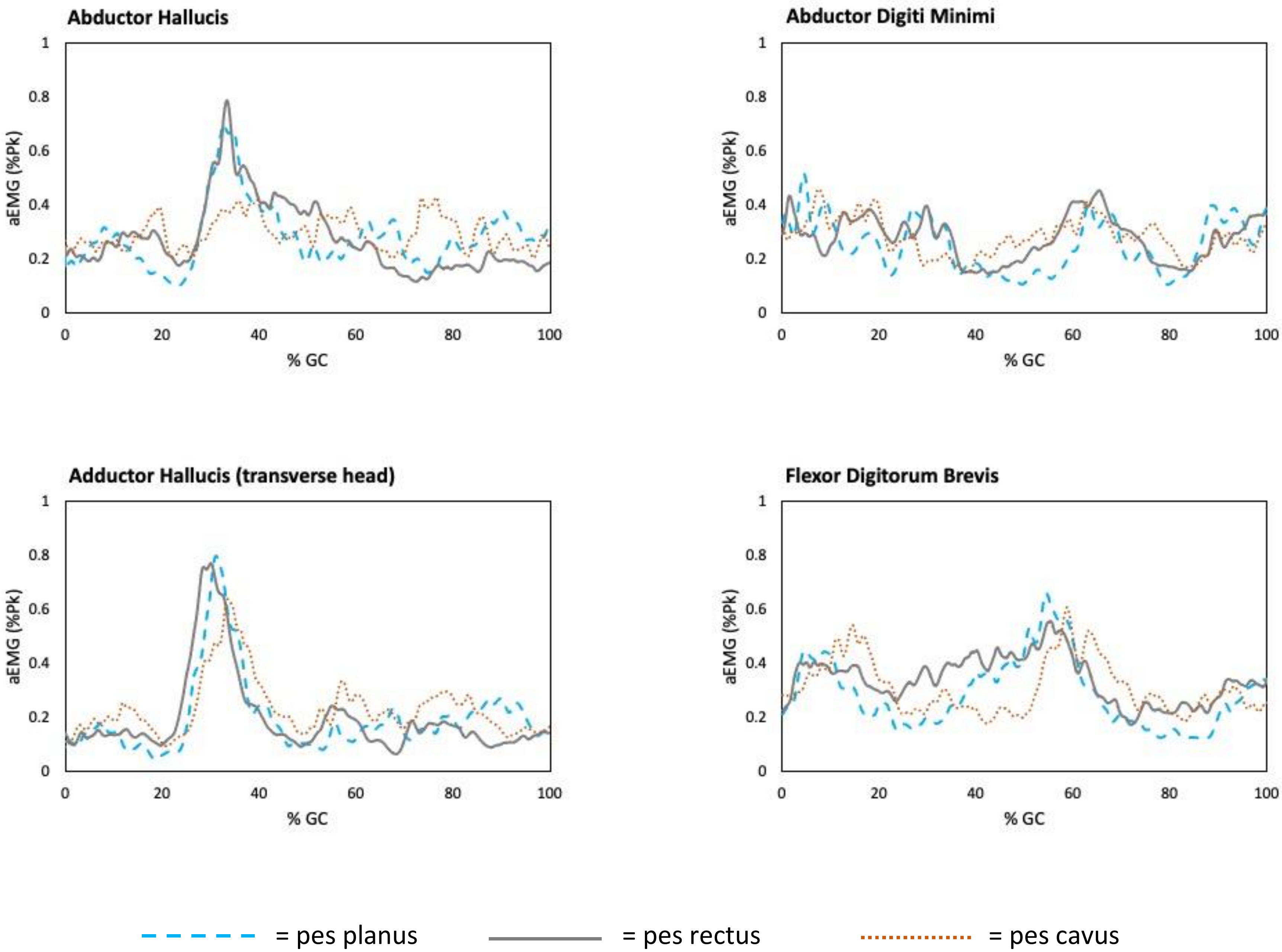

Figure 31. The time normalized ensemble averages of each lower leg muscle across foot posture when walking in textured foot orthoses **A:** Walking barefoot **B:** Walking in non-textured foot orthoses (FOs) **C:** Walking in textured foot orthoses (FOTs).

5.3.3 Walking in FOs

When walking in FOs, peak FDB aEMG at toe-off (50-60%GC) was greater in planus compared to rectus and cavus foot postures, although FDB aEMG was reduced overall during stance (16-40%GC). AbdH (75-100%GC) and AddH (60-100%GC) generated greater aEMG during swing in cavus feet compared to planus and rectus foot postures. Between 20-45%GC, ADM aEMG was also greater in cavus feet compared to planus and rectus feet.

5.3.4 Walking in FOTs

In FOTs, AbdH aEMG was reduced between 25-30%GC and FDB aEMG was reduced between 40-50%GC in cavus feet compared to planus and rectus foot postures.

5.4 DISCUSSION

The main findings of this study were that AddH aEMG was correlated with FPI score when walking barefoot and AbdH aEMG was correlated with FPI score when walking in FOTs. When participants walked barefoot, a more pronated foot posture (higher FPI score) was correlated with greater magnitudes of AddH aEMG during stance compared to a cavus foot posture (lower FPI score). These results suggest that the AddH, a muscle spanning the distal transverse arch of the foot, has greater functional demands when the MLA of the foot is lower to the walking surface. Also to consider, planus feet typically demonstrate larger amounts of MLA movement, they are a more dynamic and flexible foot, compared to cavus feet [183,205]. It has been previously reported that the AddH has a functional role of stabilizing the forefoot at initial contact and toe-off of gait [146]. Thus, in a flexible foot structure (planus foot posture), it is not surprising that the muscular demands of this stabilizing PIFM increases its muscle activation. As the planus foot tends to be more unstable, muscular demand increases to ensure adequate control of the foot as it transitions through different phases of stance. Interestingly, our ensemble averages do not support this interpretation and demonstrate reductions in AddH aEMG between 20-50%GC. This reduction occurred when the AddH is minimally active during stance [146] and the opposing results are likely a reflection of analysis differences between running a correlation and reporting amplitude averages which collapsed foot postures across the gait cycle.

It has been previously suggested that muscles spanning the MLA have a supporting role in dynamic arch mechanics [206–209] and may [190] or may not [196] be correlated with foot posture variance. Furthermore, it remains unclear if pronated feet have weaker PIFMs, as demonstrated by a reduced cross-sectional area in static stance [190,210]. In our study, AbdH and FDB were not correlated with FPI when walking barefoot or in FOs, and thus, the severity of foot posture variance was not related to PIFM activation levels. These results appear consistent with AbdH and FDB roles in controlling midfoot kinematics, rather than amplitude increases reflecting static foot posture. Furthermore, static foot posture, as measured by the FPI, does not appear to be a strong predictor of PIFM activation levels during walking. These details are important to elucidate as many researchers are interested in using PIFM strengthening exercises to modify static foot posture [197,211,212], especially in light of foot posture's link to increasing risk factors to certain foot disorders [213]. Our results suggest that static foot posture should not be used as an indicator of PIFM strength, and when interested in understanding how static foot alignment correlates with the amplitude of muscles spanning the MLA, the focus should lie in dynamic midfoot kinematics rather than static alignment.

When walking in textured FOs, the amplitude of AbdH aEMG increased with greater FPI scores. These results suggest that the addition of tactile stimulation, by adding texture under the foot sole, generates greater AbdH aEMG in planus feet compared to rectus and cavus foot postures. This is of interest to academics and clinicians in support of the neuromotor paradigm [214] of foot orthoses, as these results may suggest that altered cross-sectional area of PIFMs is in fact the inability of PIFMs to produce sensory information about changes in dynamic foot posture. This disconnect between the sensorimotor system and PIFMs has been previously speculated [192,197], although this is the first study to augment cutaneous feedback and measure PIFM response. Our results also suggest muscle dependency in this relationship between FPI score and PIFM aEMG, as AddH, ADM, and FDM generated negligeable results. In the interest in exploring this connection between cutaneous sensory feedback, future experimental protocols should be designed to add tactile feedback under the foot sole, specifically when heightened sensory information may be required, and then measure PIFM modulation across differing foot postures. This is an interesting avenue for future academic research to explore tactile feedback in foot orthoses design.

This study has three limitations that should be acknowledged. Firstly, the participant numbers within each FPI group were not equal. Secondly, the ensemble averages provide an interesting visual comparison of PIFM aEMG across foot posture, however it should be highlighted that these group averages do not undergo statistical analysis. These graphs should be used for visual comparisons only and to guide academics and clinicians to appreciate the amplitude variability across different phases of the gait cycle when walking barefoot, in FOs, and in FOTs. Lastly, participants wore socks for both FO protocols, however, they did not wear socks in the barefoot condition. This difference in surface environment should be acknowledged when comparing PIFM results across walking conditions.

5.5 CONCLUSION

The results of this study demonstrate muscle specificity when correlating PIFMs activation during walking and foot posture variance. Interestingly, increases in AbdH aEMG when walking in textured FOs may be preliminary evidence to suggest PIFMs inability to produce sensory information about changes in dynamic foot posture. This study opens an interesting line of research exploring the link between foot orthoses design, tactile feedback, and PIFM activation during gait.

6.0 FINAL CONCLUSION

The global foot orthotic industry, estimated around $3 billion dollars, requires clarity on the mechanisms supporting foot orthoses use. When a clinician places a foot orthosis under a patient's foot, is he or she confident in explaining to their patient "how" the foot orthoses (FOs) will alleviate their discomfort? The scientific literature supporting the kinematic and shock attenuation paradigms have failed to provide consistent, reliable evidence to support the use of any specific FO casting methods, posting, and FO materials, to effectively target patient-specific outcome measures and consistently reduce pain and discomfort. This remains surprising, as anecdotally, patients commonly report symptom improvement following immediate and long-term wear of FOs. Alternative to the kinematic and shock attenuation paradigms, the neuromotor paradigm highlighted the importance of sensory input from the skin on the plantar surface of the foot. It was proposed that a FO may stimulate the activation of cutaneous mechanoreceptors in foot sole skin, these signals would transfer to the central nervous system (CNS), and subsequently alter motor output when completing a certain task. Until recently, this neuromotor paradigm remained theoretical in nature and lacked experimental research to validate these assumptions.

The purpose of this dissertation was to design a series of studies which would support or refute the design of FOs in support of the neuromotor paradigm. Texture was used as a FO top cover to intentionally stimulate cutaneous mechanoreceptors in foot sole skin during walking. Texture was applied to the FO in one of two ways: to 1 of 5 locations under the foot sole (medial forefoot, lateral forefoot, medial midfoot, lateral midfoot, and calcaneus) or along the entire length of the foot sole. Each study measured muscle activity of the lower leg or foot to evaluate the immediate muscle changes to the textured design during locomotor tasks.

The results of study 1 provide evidence to support the use of texture to modify lower leg electromyography (EMG) during walking. The study also confirms that tactile feedback, by adding texture to the foot-sole interface, modifies lower leg EMG differently than electrical stimulation to foot sole skin. Conversely, it was demonstrated that tactile stimulation, as previously proven with electrical stimulation to the foot sole, experiences stimulation site and phase-specific modulation across different time points throughout the gait cycle. Texture to certain areas under the foot sole generated consistent EMG responses to lower leg musculature and may prove beneficial to clinicians targeting specific motor changes. As an example, texture under the lateral forefoot consistently suppressed lower leg EMG, whereas texture under the lateral midfoot consistently facilitated EMG. Additionally, texture to certain areas under the foot sole appears to modify motor output within specific phases of the gait cycle. For example, texture under the medial forefoot facilitated tibialis posterior activity in early stance, whereas texture to the medial forefoot, medial midfoot, or lateral midfoot each facilitated medial gastrocnemius activation during swing. Capitalizing on the topographical organization of cutaneous mechanoreceptors in foot sole skin and neurophysiological connection between skin and lower leg motorneuron pools, texture to distinct areas under the foot sole can produce phase and muscle-specific modulation during human locomotion.

In study 2, texture was applied along the entire length of the foot sole while EMG was measured in the plantar intrinsic foot muscles (PIFMs) during locomotion. Study results support the use of texture under the foot sole to modify PIFM EMG during different phases of the gait cycle. More specifically, texture facilitated EMG activity of abductor hallucis, the transverse head of adductor hallucis, and abductor digiti minimi during the midstance phase of the gait cycle. Similar observations were evident across different phases of stance: abductor hallucis was also facilitated at initial contact, loading response, propulsion, and toe-off, and similarly, abductor digiti minimi was facilitated from initial contact through to propulsion. In comparison to study 1, texture along the entire length of the foot sole reflects a more consistent facilitatory response to PIFMs across stance compared to distinct areas of tactile feedback to lower leg EMG across the entire gait cycle. Reflecting on the results of these two studies, it is arguable that the observed differences in muscle activity is a result of textured location, rather than differences in the muscles that were recorded. As opposed to consistency in the muscles being active, as observed in study 2's PIFMs, the consistent cutaneous input generated a more uniform response in muscle activation. This was also equally observed in Study 1's EMG data during the stance phase of gait. During swing, when force was not applied to the plantar foot sole, a more uniform, consistent EMG response was observed in all lower leg muscles. These results strengthen the argument that consistent input generated a consistent EMG response, regardless of which muscles were being recorded (lower leg or PIFMs). Conversely, when texture was applied to distinct areas under the foot sole, a phasic EMG response was evident throughout various phases of the gait cycle. This final observation is consistent with previous research that electrically stimulated skin during walking [215].

When electrically stimulating skin during gait, the excitatory impulse is generated acutely, and abruptly, which has been demonstrated to modulate the independent activation of muscle during specific phases of the gait cycle. For example, during the transition from stance to swing, electrical stimulation to the medial forefoot, lateral forefoot, or medial midfoot facilitates the activation of the tibialis anterior muscle. During swing, the peroneus longus muscle is facilitated with lateral forefoot or lateral midfoot stimulation, although the muscle is suppressed with medial midfoot and forefoot stimuli. Calcaneal stimuli facilitates the activation of plantar flexors [215]. In comparing these results with studies 1 and 2 of this dissertation, there is one glaring similarity and one glaring difference. It is clear that both electrical and tactile stimulation (via texture) to distinct areas under the foot sole generate a phasic EMG response throughout the gait cycle. Thus, both the location of stimuli and timing of the gait cycle matter when interpreting muscle amplitude changes during walking. Conversely, both stimulation methods, electrical vs. tactile, produce different EMG responses. In other words, not only does the stimuli location and phase of gait matter, the type of stimuli also requires consideration when interpreting EMG results. It should be acknowledged that this interpretation is only taking account a comparison between two protocols: Zehr et al. 2014 [215] and this dissertation (Of further note, this is a result of minimal research in this area and not a function of only preferentially selecting one study for comparison). Furthermore, the EMG analysis between both protocols is slightly different (ACRE150 method which binned EMG in 12 epochs across the gait cycle vs. this dissertation which binned data in 10 epochs). Regardless of the analysis window discrepancy, the literature also supports the concept that different textures generate different muscle responses. Textures consisting of pyramidal peaks, convex circular patterns, wooden dowel cones, and hard plastic domes have each failed to demonstrate changes in EMG during static stance tasks, locomotion, and/or functional tasks (stairs) [79,93,216–219]. Alternatively, semi-circular mounds has been demonstrated to reduce tibialis anterior amplitude at initial contact and soleus amplitude at propulsion [93]. A checkered textured pattern has reduced tibialis anterior amplitude in terminal stance and into initial swing [219]. Thus, although electrical and tactile stimuli each generate differential responses in motor output, there is also value in highlighting the variability in EMG response as a function of different tactile stimuli. In considering the four types of cutaneous mechanoreceptors in foot sole skin, each with a preferred response to different stimuli, these results provide evidence to suggest that variations in tactile designs can preferentially target the activation of different cutaneous afferents during locomotion. Future research is warranted to confirm this interpretation.

Lastly, in study 3 and 4, data from study 1 and 2's experimental protocols were further analyzed by subdividing results by foot posture. Foot care professionals value the importance of foot posture in the provision of FOs, especially when selecting manufacturing properties, such as material durometers and top cover designs. Results of study 3 confirm that lower leg EMG varies across the foot posture spectrum. Furthermore, the addition of texture to distinct regions under the foot sole modified lower leg EMG differently across various foot postures. In highly supinated feet, texture under the foot sole had minimal effect on lower leg EMG during gait. Conversely in pronated feet, texture under each area of the foot generated a large facilitatory response to flexor muscle EMG. In study 4, contrary to our expectations, the effect of texture on all PIFM EMG was not consistently correlated with foot posture. Most noteworthy, abductor hallucis EMG was greater in pronated feet compared to normal and supinated foot postures when walking in the textured FOs, thus suggesting that abductor hallucis's muscular contribution during gait changes across different foot posture. Previous research has proposed that reduced PIFMs cross-sectional area in pronated feet may reflect intrinsic foot muscles' inability to produce sensory information about changes in dynamic foot posture. When adding cutaneous stimulation to foot sole skin, AbdH, a muscle spanning the MLA, interestingly increased muscle activation. Thus, the results of our study, that PIFMs aEMG increased when adding texture to the FO, supports this interpretation, whereby planus feet may demonstrate an altered ability to provides sensory cues from the walking environment. It appears that adding cutaneous input, via the addition to texture under the foot sole, helps regulate and/or bring sensory information back to baseline levels. This opens a new research avenue to further explore the effects of tactile feedback on increasing the cross-sectional area of PIFMs that span the medial longitudinal arch, or by measuring PIFM modulation under the facilitation and suppression of sensory information from foot sole skin. It appears that it may be possible to offset muscle atrophy via the addition of cutaneous input to the foot sole. Future research that explores the use of texture and tactile feedback in FOs design appears warranted in planus foot postures. Lastly, PIFMs increased activity during midstance and heel rise (study 2) when wearing FOs compared to walking barefoot. The presence of significant activation of key muscles during different phases of gait suggests that FOs do not promote the disuse of PIFMs when wearing a FO, a concern that has been previously speculated across foot orthotics research.

Returning to the original purpose of this dissertation, the results of these studies support future FO research in support of the neuromotor paradigm. This dissertation provides benchmark data to the larger scientific community to develop new research questions and further distill the connection between cutaneous mechanoreceptors of the foot sole and lower extremity/foot muscle activity. Based on the results of this dissertation, the original neuromotor paradigm merits slight modification. Originally, the paradigm proposed that FOs change sensory input to the CNS, and consequently changes motor activation patterns towards movement optimization. Conceptually, “movement optimization” is quite vague. The following is suggested: FOs can modify sensory input to the CNS, and subsequently facilitate and/or inhibit motorneuron pool activation of lower extremity and foot intrinsic musculature during movement. Future research is encouraged to refine, support and/or refute this paradigm, and to grow our understanding on the mechanisms supporting FO use.

The results of these studies open multiple possibilities for future experimental protocols. Firstly, it is unclear if these immediate results will persist long-term. Long-term interventions are needed to confirm the lasting effects of textured FOs on lower extremity/foot muscle activity or to confirm the presence of habituation from prolonged tactile exposure. It would be interesting to explore the effects of textured FOs in older adults susceptible to falls, and/or in pathology-specific populations who commonly seek FO treatment. These studies focused on the effects of textured FOs during locomotor tasks, including functional tasks, such as stairs, jumping, and landing remain unknown. From the results of this dissertation, we can confirm that adding texture under the foot sole, and specifically within FO design, does modify lower extremity and foot muscle activity during walking, and provides support to a ‘modified’ neuromotor paradigm of FO use.

APPENDICES

Appendix 1 Summary of orthotics studies included in a previously conducted scoping review

Study	**Subject Characteristics** (sample size; mean age; inclusion)	**Methodological Details**								**EMG**		**Results**
		Condition	**Foot Type considered?**		**Footwear standardized?**			**Intervention Details**		**Muscles**	**Outcome Measures**	
			Y	**N**	**BF**	**Y**	**N**	**Orthotic Type**	**Details**			
Akuzawa et al. 2016	n=10; 25±5.0 healthy	W		X		X		pre-fabricated	S=EVA, TC=microsuede 3 conditions: barefoot, footwear only & orthotics	PL, TP, FDL	Amplitude in stance (subdivided into IC, MS &TOFF) +/- 10N above/below GRF	1) TP: significant difference in the % MVIC among three conditions in midstance & propulsion 2) TP: no significant difference in the total stance and contact phase 3) FDL & PL: no changes to amplitude between the 3 conditions
Barn et al. 2014	n=10; 50±9.0 pathological	W	X			X		CFO	S=polypropylene; P=RF&FF; TC=poron/vinyl 5 trials/condition 2 conditions: barefoot & shod+CFO	TA, PL, MG, SOL, TP	Temporal & Amplitude in stance phase	1) MG: later peak of contraction in shod+CFO compared to barefoot 2) Soleus: later peak of contraction in shod+CFO compared to barefoot 3) TA: increased magnitude in shod+CFO compared to barefoot 4) TP: trend towards reduced magnitude during contact period
Baur et al. 2011	n=99; 2 groups pathological control: 37.1±8.3 orthotic: 37.3±8.2	R		X		X		modified insole	S=polyurethane foam; P=FF lateral post LT intervention (8 weeks)	PL	Temporal & Amplitude In stance (subdivided into Apre, Awa, Apo phases)	1) PL timing did not change between groups or after 8 weeks of foot orthotics wear 2) PL amplitude was higher after 8week foot orthotic intervention
Bonifacio et al. 2018	n=16; 25.7±5.8 healthy	TS	X			X		modified insole	P: EVA stair descent (6x20 descents) 3 conditions: flat insole, 5° medial RF insole & 5° medial FF + RF posting	TA, PL, MG, AbdH	Amplitude during single limb descent phase of stair descent	1) AbdH: both wedged insoles reduced EMG magnitude 2) TA: reduced magnitude with the medial RF insole
Burke & Papuga 2012	n=6; healthy 32.3± 10.07	TR		X			X	CFO	Treadmill running at increasing speeds 2 conditions: normal insoles + CFOs	TA, MG, VL, BF	Amplitude EMG envelope for each running cycle	CFOs resulted in no consistent EMG changes

Choi et al. 2015	n=10; pathological 23.7±3.4	TW	X					CFO	S=polypropelene; P=polyurethane; TC=leather 3 conditions: footwear only, 3/4 insole & 1/1 length insole	TA, MG, BF, RF	Amplitude in stance (subdivided into IC, LR, MS & TS)	Compared to footwear only: 1) RF: magnitude decreased by 1.74% (3/4 insole) & 1.75% (full length insole) 2) TA: magnitude decreased by 5.61% (3/4 insole) & 5.32% (full length insole) 3) BF: magnitude decreased by 3.01% (3/4 insole) & 3.12% (full length insole) 4) MG: magnitude decreased by 6.38% (3/4 insole) & 6.25% (full length insole)
Dedieu et al. 2013	n=15; healthy 23.7±3.4	W	X				X	CFO	P= RF, EVA 2 conditions: barefoot & CFOs 5 trials/condition	TA, PL, MG, LG, SOL	Temporal Expressed as % of gait cycle	1) duration of EMG activity reduced in TA, SOL, MG, LG & PL when wearing CFO 2) SOL, MG: delayed muscle onset with CFO
Dingenen et al. 2015a	n=15; healthy 20.2±1.4	SS	X			X		pre-fabricated & CFO	S=EVA 4 conditions: barefoot, footwear only, footwear+pre-fabricated & footwear+CFO eyes open and eyes closed 3 trials/condition	TA, PL, MG, VM, GMAX; GMED; ADDL; TFL;	Temporal transition from double leg stance to single leg stance	1) PL: earlier onset time in footwear & footwear+orthoses 2) TA, MG: no onset time change 3) no changes in knee or hip musculature
Dingenen et al. 2015b	n=15; pathological 21.8±3.0	SS	X			X		pre-fabricated & CFO	S=EVA 4 conditions: barefoot, footwear only, footwear+pre-fabricated & footwear+CFO eyes open and eyes closed 3 trials/condition	TA, PL, MG, TFL, GMAX, GMED	Temporal transition from double leg stance to single leg stance	1) PL: earlier onset with footwear+pre-fabricated orthoses and CFO 2) TA: earlier onset in footwear+pre-fabricated 3) VMO, VL: earlier onset in footwear+pre-fabricated
Garbalosa et al. 2015	n=26/group pathological group1: 22±6.3 group2: 20±1.5	TW	X			X		CFO	2 orthotics: Type1: maximal arch stabilization (S=semi-rigid thermoplastic, TC: EVA+ultrasuede) Type2: full contact (S=polypropylene; P= polypropylene; TC=poron+vinyl) 3 conditions: barefoot, sandal only & sandal+orthotic	TA, PL, TP	Amplitude Expressed as % of gait cycle	TP: peak EMG magnitude decreased from sandal to sandal-orthotic (maximal arch stabilization), but magnitude increased when wearing the full contact orthotic
Hertel et al. 2005	n=30; healthy 21.1±1.6	TS	X				X	pre-fabricated	4 orthotic conditions: no orthotic, P=7°	VM, VL, GMED	Amplitude max RMS values during each functional	1) VM & GM: all orthotics increased EMG magnitude during the single leg squat & lateral step down

									medial RF, P=4° lateral RF & P=neutral (7° medial & 4° lateral RF) 3 functional tasks: single-leg squat, lateral stepdown exercise & max vertical jump 3 trials per condition		task	2) VL: orthotics decreased VL magnitude in vertical jump
Kelly et al. 2011	n=12; healthy 31.2±3.8	TR		X			X	pre-fabricated	Heat molded to enhance full foot contact to orthotics 2 conditions: no orthotics & orthotics	TA, PL, MG, VM	Temporal & amplitude burst onset/offset identified by RMS amplitude exceeded a threshold - defined as the average rectified activity during the control run	1) PL: decreased magnitude with time, independently of the condition 2) TA: decreased duration with time, independent of the condition When wearing orthoses: 3) VM & MG: decreased RMS 4) PL: increased duration
Lack et al. 2014	n=20; pathological 28.5±4.2	TS	X			X		pre-fabricated	P=6° varus Step up task 2 conditions: no orthotics & with orthotics 5 trials per condition	VM, VL, GMED	Temporal & Amplitude 0.5s prior & and 0.5s post IC	1) GMED: no change in onset time, reduction in peak amplitude with pre-fabricated orthoses 2) VM: no change in onset times or peak amplitude 3) VL: no change in peak amplitude
Lo et al. 2018	n=12; healthy 23.0±4.3	W		X			X	CFO	3 orthotic conditions: S=AMFIT base+TC1=nora lunairflex; TC2&3=spacer fabrics 5 trials per condition	TA, LG, VL	Amplitude during stance phase	No significant changes to EMG amplitude
Maharah et al. 2018	n=18; healthy 26.0±5	TR	X			X		CFO	S=polypropelene; P=medial skive at 15° & 5° RF; TC=vinyl 3 conditions: barefoot, footwear only & footwear+orthotics	TP	Amplitude time normalized to 3 strides	TP: magnitude reduced in footwear & footwear+orthotics

Mills et al. 2012	n=30; 2 groups pathological mobile group: 28.67±6.13 less mobile group: 31.15±4.41	TR	X				X	pre-fabricated	3 orthotic conditions: hard (Shore A 75°); medium (Shore A 60°); soft (Shore A 52°) & control (3mm Shore A 52° flat insole) 3min. running intervals per orthotic condition	TA, MG, SOL, RF, VM, VL, BF, GMED	Temporal & amplitude time normalised to 100 points for each stride - averaged to 1 representative stride	1) VL: magnitude increased in activity when wearing the least comfortable orthotics 2) MG: delay in offset with individuals with less mobile feet
Moisan & Cantin 2016	n=21; healthy 21.9±2.5	W	X			X		CFO	3 orthotic conditions: footwear only (control), CFO with and without lateral bar S=polypropylene; P: EVA 6 trials per condition 2 sessions: acute (baseline) & LT (30 days)	TA, PL, MG, LG, VL, GMED	Amplitude static stance averaged from 10 trials	After 30days of wearing foot orthotics: 1) PL: CFO + lateral bar decreased peak amplitude & mean activity during combined MS/TS phase 2) TA: CFOs decreased peak amplitude & mean activity during the contact phase compared to a control condition
Moisan & Cantin 2017	n=1; healthy age=26	W	X					CFO	7 orthotic conditions: P=none; P=external oblique RF; P=internal oblique RF; P=straight RF; P=RF & FF; P=RF&FF at 2° varus; P= RF&FF at 5° varus 5 x familiarization trials 3 trials per orthotic condition	TA, PL, MG, LG, BF, VM, VL, GMED	Amplitude static stance averaged from 10 trials	As frontal place inclination of the extrinsic & intrinsic posts increased, EMG magnitude increased
Moisan et al. 2018	n=15; healthy 27.7±9.0	W	X			X		CFO	3 orthotic conditions: footwear only (control), CFO with and without lateral bar S=polypropylene, ¾ length; P: EVA 2 walking speed (normal & fast) 15 strides per condition 2 sessions: acute (baseline) & LT (30 days)	TA, PL, MG, LG, BF, VM, VL, GMED	Amplitude strides normalized to 100% of stance duration	With CFOs, LG magnitude increased during propulsion
Mundermann et al. 2004	n=21; healthy 25.4±5.6	R	X			X		modified insole + CFO	4 orthotic conditions: control (flat Soleflex EVA, Shore C: 50-55), P=6mm EVA; CFO, CFO+P=6mm EVA) TC=Spenco (all orthotics)	TA, PL, MG, BF, RF, VM, VL	Amplitude global, low, and high intensities averaged to pre-IC (50 ms)	Acute EMG results did not change from baseline to 3 weeks post-baseline

									12 trials per condition LT intervention – tested 3 times per week, for 3 weeks)		) post-IC (50 ms), and Phase 3 (30 to 100% of stance phase)	
Mundermann et al. 2006	n=21; healthy M:27.4±1.8 F:23.9±1.6	R	X			X		modified insole + CFO	4 orthotic conditions: control (flat Soleflex EVA, Shore C: 50-55), P=6mm EVA; CFO, CFO+P=6mm EVA) TC=Spenco (all orthotics) 12 trials per condition LT intervention – tested 3 times per week, for 3 weeks)	TA, PL, MG, BF, RF, VM, VL	Amplitude global, low, and high intensities averaged to pre-IC (50 ms)) post-IC (50 ms), and Phase 3 (30 to 100% of stance phase)	1) orthotics increased global EMG magnitude 2) PL, BF: posting produced the highest EMG magnitude pre- and post-IC 3) PL, MG, BF: molding produced the highest EMG magnitude increases pre- and post-IC 4) PL, MG, BF: posting+molding produced the smallest increases in EMG magnitude
Murley & Bird, 2006	n=15; healthy 23.0±5.0	W	X			X		CFO	4 orthotic conditions: barefoot (control), P=RF 0°, P=RF 15° & P=RF 30° 6 trials per condition	TA, MG, PL, SOL	Amplitude averaged over four seconds within the gait cycle	1) TA: magnitude increased in all orthotic conditions (footwear only by 30%, 0° CFO by 33%, 15° CFO by 38% & 30° CFO by 30%) 2) PL: 15° CFO increased max amplitude by 19% during walking 3) MG, SOL: no changes to EMG
Murley et al. 2010	n=30; healthy 21.8±4.3	W	X			X		pre-fabricated & CFO	Pre-fabricated: S=polyethylene ¾ length, P=6mm heel wedge CFO: S=polypropylene ¾ length, P=20° inverted post 4 orthotic conditions: barefoot, footwear only, pre-fabricated & CFO	TA, PL, MG, TP	Amplitude four average gait cycles derived from 8 ipsilateral steps	1) TP: pre-fabricated orthotic decreased EMG magnitude by 19% in contact phase & 12% with CFO 2) PL: pre-fabricated orthotic increase EMG magnitude by 21% in MS/propulsion & 24% with CFO
Nawoczenski & Ludewig, 1999	n=12; pathological 27.2±9.9	R	X			X		CFO	S=polypropylene, TC=spenco 2 conditions: no orthotics & with orthotics	TA, MG, VL, VM, RF	Amplitude First 50% of stance	1) TA: increase (37.5%) in EMG magnitude when wearing CFO 2) BF: reduction (11.1%) in EMG magnitude with CFO
Rose et al. 2002	n=17; healthy 20.6±1.8	SS	X				X	CFO	2 perturbations – designed to cause internal & external rotation in single stance 5 trials per condition	MG, LG, MQ, LQ, MH, LH	Temporal reflex response (delay from perturbation onset to onset of long latency reflex)	Muscle response times were not significantly different between orthotic conditions.
Saeedi et al. 2014	n=1	SS & W	X				X	CFO	2 orthotic conditions: barefoot & CFO	TA, PL, MG	Amplitude normalized peak amplitude during stance	With CFO compared to barefoot: 1) TA: 1% magnitude decrease 2) PL: 7% magnitude increase 3) MG: 1% magnitude increase

Tomaro & Burdett, 1993	n=10; pathological range: 25-30	W	X				X	CFO	2 orthotic conditions: footwear only & CFO	TA, PL, LG	Temporal & amplitude in stance	1) TA: EMG duration increased when wearing CFOs 2) no significant differences in EMG amplitude
Vanicek et al. 2004	n=6; healthy 29±10.5	TS		X			X	pre-fabricated	2 orthotic conditions: Superfeet 'blue' and Superfeet 'green' Isometric contraction in skier's squat	VL	Amplitude (myoelectrical fatigue) first & last 20sec. of each skiers' squat	Green superfeet significantly reduced medial frequency near the end of contraction compared to blue superfeet & no orthotics condition

*M=males; F=females; SS=static stance; W=walking; TW=treadmill walking; TR=treadmill running; R=running; TS=task specific; CFO=custom foot orthotic; S=orthotic shell material; TC=orthotic top cover material; P=orthotic posting materials/details; RF=rearfoot; FF=forefoot; EVA=ethyl vinyl acetate; LT=long-term; IC=initial contact; LR=loading response; MS=midstance; TS=terminal stance; TOFF=toe off; GRF=ground reaction force; Apre=pre-activation phase; Awa=weight acceptance phase; Apo=push off phase; RMS=root mean square

*Muscles: TA=tibialis anterior; PL=peroneus longus; MG medial gastrocnemius; LG=lateral gastrocnemius; TP=tibialis posterior; SOL=soleus; RF=rectus femoris; VM; vastus medialis; VL=vastus lateralis; BF=biceps femoris; ST=semitendinosus; MQ= medial quadriceps; LQ=lateral quadriceps; MH=medial hamstring; LH=lateral hamstring; ADDL=adductor longus; IS=iliopsoas; GR=gracilis; GMAX=gluteus maximus; GMED=gluteus medius; TFL=tensor fascia latae; AbdH=abductor hallucis

Appendix 2 The research studies, insole material details, and texture images previously explored across the textured insole literature. The studies are listed in alphabetical order by first author (unless multiple studies used the same textured insole across several experimental protocols).

Study	Textured Insole **(materials, properties, fabrication)**	Image (if provided)
Aruin & Kanekar 2013 [111] Ma et al. 2016 [113] Curuk et al. 2018 [112]	- polyvinyl chloride embedded with small pyramidal peaks (height = 3mm) with centre-to-centre distance = 10mm - base of insole: 1mm in height - total height of insole: 4mm - designed to elicit a slightly painful/unpleasant stimuli	
Bapirzadeh et al. 2014 [220] Jamali et al. 2019 [110]	- pattern of 10 hemisphere projections per cm2 - 1mm thick top cover	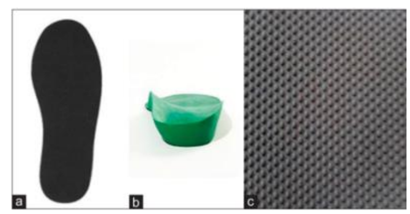
Brognara et al. 2020 [97]	- 3D scanned custom devices, casted by a podiatrist - mechanical stimulation provided by 2 blunted cones located under the distal phalanx of the big toe and below the head of the 1st MTPJ - cones: 5mm x 2mm x 7mm	
Chen et al. 1995 [114]	- coarse sand sock: 5-6mm gravel glued to bottom of sock - midfoot sand sock: same course gravel but only in middle 3rd of foot length - small sand sock: smaller gravel, 2-3mm in diameter	n/a
Clark et al. 2014 [221]	- thin semi-plastic with firm raised nodules, 1.5mm in height - nodules spaced 1.5cm apart in a grid pattern - average insole had approximately 60 nodules	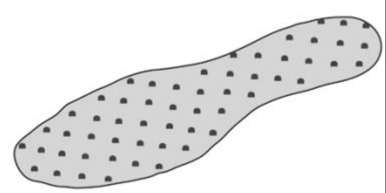
Collings et al. 2015 [78]	- 1.5mm round wooden dowels of 3 different heights (2, 4 & 6mm cones) @ 10mm intervals - each dowel angled 45degrees under leather cover - medial dowels run medial calcaneus to distal navicular - lateral dowels run lateral calcaneus to styloid process	

Corbin et al. 2007 [76]	- thin floor matting from hardware store - round plastic nubs, raised 1/4" off plastic surface	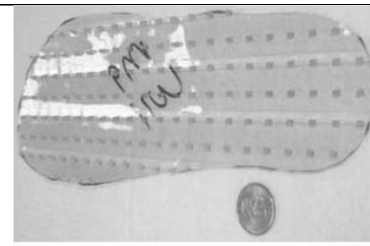
de Morais et al. 2018 [87]	- 3mm thick, EVA, Shore A 40 dur. - small pyramidal peaks with center-to-center distance = 2mm	
Dixon et al. 2014 [102]	Texture 1: Evalite Pyramid EVA, 3 mm thickness, Shore value A50 -- small pyramidal peaks --> 2.5mm centre-to-centre distance between peaks Texture 2: commercially available insoles (Crocs) with small nubs of approx. 1mm in height & 2mm in diameter, shore value A25, curved arch & heel cup	
Elvan et al. 2017 [99]	- EVA, 4 semi-spherical projections per cm2 - each protrusion was 2mm in height	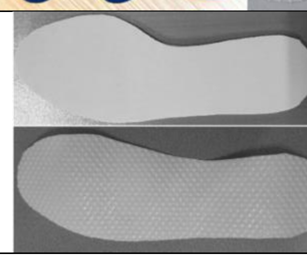
Gomes et al. 2017 [100]	Texture - expanded polyurethane (antiallergic) with thickness of 10.28mm & weight of 3800 g/m2	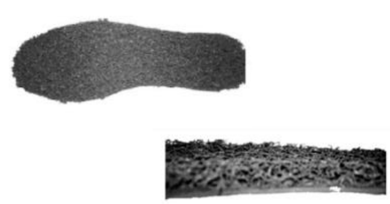
Hatton et al. 2009 [79] Hatton et al. 2011 [217]	Texture 1: Evalite Pyramid EVA, 3 mm thickness, Shore value A50 -- small pyramidal peaks Texture 2: Nora Lunasoft Mini Non Slip, 3 mm thickness, Shore value A50 -- convex circular patterning	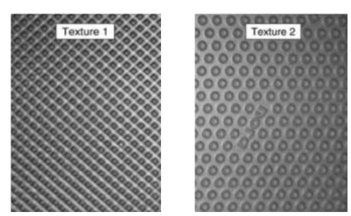
Hatton et al. 2012 [86] Kenny et al. 2019a [77] Kenny et al. 2019b [89]	Evalite Pyramid EVA, 3 mm thickness, Shore value A50 -- small pyramidal peaks	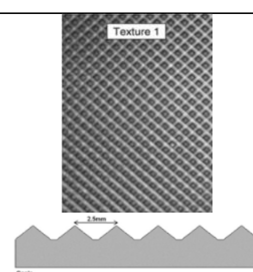

Jenkins et al. 2009 [95] Perry et al. 2008 [124] Maki et al. 1999 [80]	perimeter ridge with flexible polyethelyne tubing (3mm outer diameter, 1mm inner diameter) - tubing runs around 1st, 5th MTP heads and around calcaneus	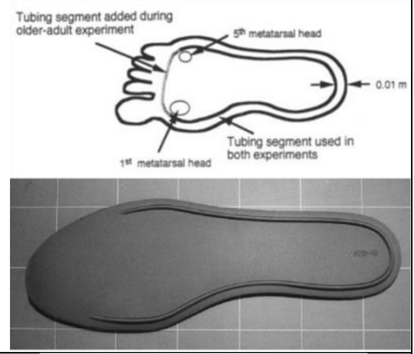
Kalron et al. 2015 [222]	3mm thick elastic rubber & plastic material - full length grid pattern	
Kelleher et al. 2010 [101]	Fine leather insoles with grade P80 Wet & Dry sandpaper	n/a
Li et al. 2019 [88]	- insole + arch support - raised nodules made of silicone - 8 protrusions of equal size, placed around boundaries of metatarsal heads & toe crest (5 protrusions), & lateral heel (3 protrusions)	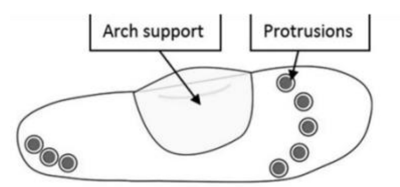
Lirani-Silva et al. 2015 [223]	2mm thick, medium density <u>Half sphere insole</u>: half-sphere elevations, 9mm in diameter - elevations placed distal to the phalanx, heads of MTP joints & heel <u>Raised ridge insole</u>: 3mm high perimeter ridge, external areas of the insole	
Lirani-Silva et al. 2017 [121]	half-sphere elevations, 9mm in diameter - elevations placed distal to the phalanx, heads of MTP joints & heel	

Lo et al. 2016 [224] Lo et al. 2017 [122]	<u>Texture 1</u>: Amfit base, poron midlayer, spacer X material <u>Texture 2</u>: Amfit base, spacer X midlayer, spacer Y top layer - outer layers of spacer materials: 150/48D polyester & nylon/spandex 70D/20D yarn	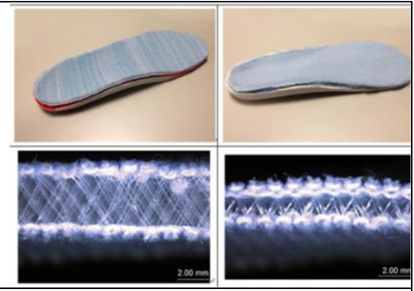
Nurse et al. 2005 [128]	- 3mm EVA, semi-circular mounds, 8mm apart, full insole length	
Park, 2018 [104]	- flexible PVC, 3mm thick - small, round peaks with center-to-center distance of approx. 4mm	
Palluel et al. 2008 [83] Palluel et al. 2009 [82]	Area NewMarco sandals - spikes uniformly covered entire foot - semi-rigid PVC, density: 4 spikes/cm2; height of a spike: 5 mm; diameter: 3 mm - spikes under the MLA are larger - density: 2 spikes/cm2; height: 1 cm; diameter: 5 mm	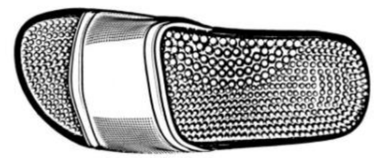
Qiu et al. 2013 [98]	1.5mm thick, 270density EVA granulations: 5mm in diameter, 3.1mm in height distributed evenly over upper surface - 2 raised ridges, 3.1mm in height & width --> around lateral perimeter and around the heel	
Ritchie et al. 2011 [119]	- small 4mm domes of hard plastic, covered with thin cotton material, between dome distance = 12mm, only in medial midsole of the shoe - domes run full length of insole, about 1/2 width of insole	
Steinberg et al. 2016 [225]	rubber insoles with four nodules (3mm high & 1mm in diameter) per square cm	

Stern et al. 2012 [219]	Checker pattern	n/a
Vieira et al. 2017 [105]	3 mm height nodules over a medical, bio-compatible photopolymer - same material for each insole, changes are based on density of nodules <u>HD insole</u>: 1.7cm between adjacent nodules <u>LD insole</u>: 2.8cm between adjacent nodules	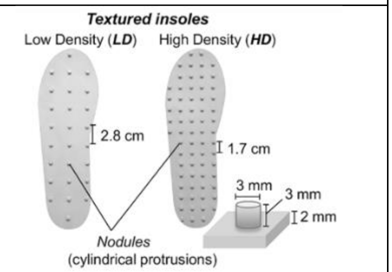
Waddington & Adams 2000 [108]	7mm deep nodules at 4 per cm2	n/a
Waddington & Adams 2003 [106]	- rubber sheeting with four nodules (3mm high, 1mm diameter per square centimetre)	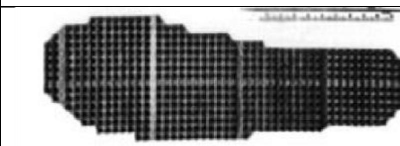
Wilkinson et al. 2018 [94]	- made of rubber, pattern of grooves and ridges aligned perpendicular to the long axis of the foot - grooves: 1mm deep, pattern pitch of 3mm - total insole thickness: 3mm	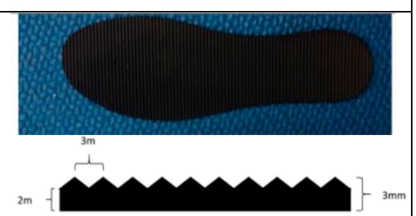
Wilson et al. 2008 [226]	<u>dimple texture</u>: 1mm raised circles, 3mm diameter dimples, 5cm apart <u>raised grid texture</u>: 1mm raised square pyramid shapes, side length two point 5mm, peaks two points 5mm apart)	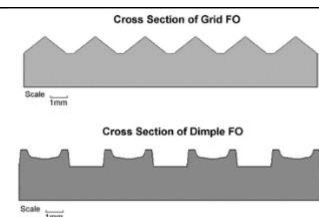

Appendix 3 The step-by-step process of the topographical organization of textured locations under the plantar foot sole

<u>Step 1</u>: The length, forefoot width, and midfoot width was measured for each insole size.

<u>Step 2</u>: This is the rationale as to why each section of the insole was divided as it was:

- Forefoot → divided according to the dermatome regions of the foot
- Midfoot to forefoot → divided proximal to metatarsal heads – as this is where most shells terminate in foot orthoses designs
- Midfoot → from approximately the center of the calcaneus to dermatome split of the forefoot – the curvature to follow the natural curvature of the MLA
- Calcaneus → to follow the contour of the heel cup and considered the transition point between the heel region and the MLA

<u>Step 3</u>: finalizing locations:

<u>Approximate forefoot location determined:</u> marked the termination of the MLA and LLA curvatures on the orthotic, and drew out the approximate location of the midfoot to forefoot curvature
Measured each length (of heel to marked location), summed and averaged this value = 61.5% of total foot length (from calcaneus)
<u>Calcaneus to MF transition determined:</u> visual approximation of the transition from calcaneus to midfoot - based on curvature of MLA and LLA locations
Measured each length (of marker location of transition point), summed and average value = 20.5% of total foot length (from calcaneus)
<u>Dividing forefoot into medial and lateral components:</u> split distal forefoot between the lateral and medial plantar nerve – approximately located between the 3rd and 4th digits
Marked the approximate location of webspace 1-2, and divided remaining width into equal parts (making the assumption that the width of digits 4-5 is approximately the same as digits 2-3)

Lines drawn on orthotic – orthotic image shows divisions between calcaneus and midfoot, medial forefoot and forefoot, and 1st to 2, and 3rd to 4th metatarsals	

Ruler placement to determine division between 3rd-4th metatarsals Ruler placed from mid-calcaneus to metatarsal division	
Line drawn with ruler from center of the calcaneus to marking of 3rd-4th division Angled line drawn between midfoot and forefoot - Used markings on the MLA and LLA of orthotic, and measurement from distal heel to proximal MLA (61.5% of total foot length)	

Rearfoot (calcaneus) to midfoot division drawn – angled approximately the same shape as the midfoot to forefoot curved line Calcaneus to midfoot division at 20.5% of total foot length	
Following the MLA shape, and rearfoot and forefoot lines, the midfoot division was drawn out, angled approximately the same shape of midfoot Start and end points of line are approximated to middle of midfoot-forefoot divisions and middle of calcaneus to midfoot divisions	

Appendix 4A Mean data for each lower leg muscle by tactile facilitated region, divided across each phase of the gait cycle

Muscle	Sensory Location	Bins (%Pk)									
		Initial Contact (IC)	Loading Response (LR)	Midstance (MS)	Heel Rise (HR)	Propulsion (PR)	Toe Off (TO)	Initial Swing (iSW)	Mid Swing (MSW)		Terminal Swing (TSW)
Tibialis Anterior	None	21.33 ± 19.51	14.34 ± 11.11	11.24 ± 8.57	7.86 ± 5.84	15.86 ± 13.39	21.91 ± 19.19	12.41 ± 10.13	9.85 ± 8.57	7.95 ± 6.72	13.54 ± 12.44
	MF	20.61 ± 19.36	15.03 ± 11.54	12.14 ± 8.88	7.89 ± 5.74	16.18 ± 13.52	22.41 ± 19.62	12.51 ± 10.67	10.13 ± 8.96	8.31 ± 7.11	14.18 ± 13.39
	LF	21.26 ± 19.27	15.30 ± 11.67	12.04 ± 8.91	7.79 ± 5.78	16.02 ± 13.86	21.87 ± 19.76	12.13 ± 9.65	9.58 ± 8.47	7.77 ± 6.50	13.74 ± 12.81
	Calcaneus	20.29 ± 19.27	13.84 ± 11.61	11.25 ± 9.38	7.57 ± 6.45	15.28 ± 14.01	20.15 ± 19.60*	12.14 ± 10.49	10.00 ± 9.36	7.88 ± 6.90	13.19 ± 12.41
	MM	21.67 ± 20.14	14.78 ± 10.71	11.62 ± 8.37	7.98 ± 5.90	16.39 ± 14.32	21.38 ± 19.10	13.64 ± 11.07*	10.52 ± 9.11	8.69 ± 7.63	14.73 ± 14.07*
	LM	20.96 ± 18.33	14.23 ± 10.87	11.14 ± 8.05	7.56 ± 5.39	16.00 ± 12.66	21.41 ± 19.16	11.79 ± 9.07	9.49 ± 7.82	7.70 ± 6.08	13.27 ± 12.09
Peroneus Longus	None	9.82 ± 10.81	8.18 ± 9.18	8.49 ± 9.60	15.53 ± 15.88	18.62 ± 20.54	8.98 ± 10.26	7.52 ± 8.36	7.59 ± 8.80	10.18 ± 12.86	13.75 ± 15.26
	MF	9.84 ± 10.27	9.13 ± 10.50	8.34 ± 9.69	11.30 ± 14.23	18.60 ± 20.95	10.20 ± 12.13	8.04 ± 9.01	7.75 ± 8.89	9.69 ± 12.00	13.24 ± 13.89
	LF	9.92 ± 11.29	8.67 ± 9.76	8.83 ± 9.76	12.06 ± 14.68	17.71 ± 19.84	9.20 ± 11.16	7.51 ± 8.98	7.35 ± 9.31	9.41 ± 11.96	13.82 ± 15.43
	Calcaneus	10.04 ± 12.71	7.58 ± 9.10	7.22 ± 8.67	11.68 ± 14.94	17.64 ± 20.60	8.39 ± 9.98	7.72 ± 9.35	7.20 ± 8.59	8.98 ± 11.66	12.87 ± 15.32
	MM	11.22 ± 11.67	9.27 ± 9.87	9.34 ± 9.71	12.64 ± 14.75	20.69 ± 21.03	10.47 ± 11.34*	8.53 ± 8.82	8.28 ± 9.11	10.26 ± 12.41	14.88 ± 15.74
	LM	10.46 ± 11.80	8.12 ± 9.12	8.17 ± 9.37	11.92 ± 14.88	18.19 ± 20.16	9.29 ± 10.89	8.31 ± 9.47	8.54 ± 10.06	10.53 ± 13.51	14.42 ± 15.62
Extensor Digitorum Longus	None	17.00 ± 17.80	11.12 ± 10.66	9.35 ± 9.12	8.02 ± 7.78	14.44 ± 13.43	16.27 ± 18.34	10.64 ± 10.56	9.46 ± 9.36	9.07 ± 9.13	15.11 ± 14.45
	MF	17.22 ± 18.05	12.12 ± 11.59	9.96 ± 9.59	8.49 ± 8.71	14.69 ± 13.57	16.10 ± 17.72	11.17 ± 10.74	9.49 ± 9.27	8.79 ± 8.65	15.41 ± 14.46
	LF	15.98 ± 17.60	11.20 ± 10.63	9.38 ± 9.18	7.69 ± 7.19	14.61 ± 13.61	16.21 ± 18.19	10.33 ± 10.36	9.03 ± 9.51	9.50 ± 9.17	15.19 ± 14.34
	Calcaneus	15.73 ± 17.99	10.08 ± 10.39	8.49 ± 8.56	7.45 ± 7.39	12.83 ± 12.45*	15.68 ± 18.08	10.36 ± 10.80	9.13 ± 9.30	9.14 ± 9.63	14.15 ± 14.57
	MM	17.01 ± 17.73	11.80 ± 11.19	9.68 ± 8.99	8.16 ± 7.17	15.14 ± 13.86	16.67 ± 17.56	11.64 ± 11.34	10.01 ± 9.91	9.91 ± 9.71	15.57 ± 14.90
	LM	16.30 ± 17.55	11.09 ± 10.64	9.34 ± 9.01	8.01 ± 8.02	14.02 ± 13.17	15.74 ± 17.80	10.81 ± 10.63	9.24 ± 9.25	8.55 ± 8.50	14.49 ± 13.74
Extensor Hallucis Longus	None	21.01 ± 14.67	28.42 ± 16.00	20.23 ± 13.15	16.83 ± 12.37	13.09 ± 10.45	21.18 ± 14.58	26.35 ± 12.83	15.56 ± 12.42	15.49 ± 10.17	12.11 ± 7.63
	MF	21.31 ± 14.89	29.46 ± 17.52	20.73 ± 15.27	16.21 ± 11.96	12.60 ± 10.13	19.83 ± 14.66	25.43 ± 12.54	19.75 ± 13.12	14.70 ± 9.68	11.59 ± 7.88
	LF	20.74 ± 14.15	27.01 ± 14.91	21.23 ± 14.12	16.12 ± 10.92	12.44 ± 9.79	20.57 ± 14.70	25.59 ± 12.81	19.73 ± 11.69	15.36 ± 8.78	11.88 ± 7.19
	Calcaneus	20.94 ± 15.21	30.49 ± 17.24*	22.39 ± 14.00*	17.81 ± 12.28**	13.93 ± 11.20	20.94 ± 14.01	25.43 ± 12.11	19.14 ± 12.65	16.04 ± 10.23	12.40 ± 7.89
	MM	23.15 ± 15.34*	30.80 ± 17.95*	23.01 ± 15.58*	18.20 ± 13.30**	14.04 ± 11.06	22.29 ± 15.33	27.12 ± 11.97	20.57 ± 13.02	15.86 ± 9.92	12.77 ± 8.01
	LM	22.03 ± 14.85	28.74 ± 15.00	20.74 ± 12.44	15.67 ± 10.50	12.75 ± 9.07	22.07 ± 14.93	26.84 ± 13.41	19.48 ± 13.12	16.19 ± 11.28	12.79 ± 8.08
Medial Gastrocnemius	None	4.22 ± 3.17	5.29 ± 5.36	9.43 ± 11.09	13.32 ± 13.91	18.85 ± 19.71	5.72 ± 6.01	4.58 ± 4.62	7.80 ± 8.25	13.06 ± 13.46	13.28 ± 13.90
	MF	4.15 ± 2.81	5.13 ± 4.75	10.21 ± 11.51*	13.69 ± 13.13	19.99 ± 20.01*	6.15 ± 6.14	4.54 ± 4.11	8.18 ± 7.96*	13.55 ± 12.69*	13.62 ± 13.02
	LF	3.76 ± 3.19*	4.86 ± 5.26	8.67 ± 10.03	12.78 ± 13.40	17.84 ± 18.40	5.69 ± 6.05	4.02 ± 3.92	7.61 ± 8.26	13.09 ± 12.76	13.04 ± 13.59
	Calcaneus	4.36 ± 4.01	5.49 ± 6.38	9.10 ± 10.87	13.64 ± 14.29	18.81 ± 19.25	5.13 ± 4.64	4.48 ± 4.41	8.04 ± 7.73	13.57 ± 13.28	13.75 ± 13.30*
	MM	4.71 ± 3.60	5.75 ± 7.06	9.61 ± 10.10	14.51 ± 15.47	18.38 ± 18.89	5.88 ± 5.65	5.20 ± 5.01*	8.10 ± 8.03	13.80 ± 13.28	14.24 ± 13.50*
	LM	4.34 ± 3.74	5.09 ± 5.33	8.56 ± 9.67	13.08 ± 13.44	28.37 ± 18.51	5.54 ± 4.71	4.66 ± 4.28	8.33 ± 7.76*	14.10 ± 13.05*	13.77 ± 13.23
Tibialis Posterior	None	21.36 ± 16.27	26.27 ± 14.57	21.15 ± 13.24	19.80 ± 14.01	15.50 ± 8.61	21.67 ± 14.02	26.25 ± 12.47	18.15 ± 11.07	18.67 ± 12.85	17.75 ± 9.01
	MF	21.99 ± 13.79*	25.92 ± 11.76	19.69 ± 11.36	20.59 ± 13.57*	15.81 ± 8.16	22.38 ± 14.06	25.55 ± 12.41	17.41 ± 9.75	18.31 ± 11.03	15.73 ± 8.12
	LF	19.49 ± 13.47	25.75 ± 14.21	20.90 ± 12.49	19.57 ± 13.67	15.10 ± 7.95	21.15 ± 12.98	26.00 ± 12.22	18.26 ± 11.18	18.42 ± 11.08	15.60 ± 8.42
	Calcaneus	20.42 ± 13.12	25.01 ± 11.90	19.90 ± 10.60	20.85 ± 13.39*	16.62 ± 9.17*	21.33 ± 13.40	25.61 ± 12.32	17.74 ± 10.21	20.02 ± 12.77*	17.43 ± 12.09
	MM	21.70 ± 15.89	26.04 ± 16.81	20.57 ± 12.71	20.18 ± 13.35	14.95 ± 8.31	21.28 ± 13.50	25.94 ± 14.51	19.48 ± 13.94	20.86 ± 15.91	16.63 ± 10.32
	LM	22.74 ± 14.81*	25.59 ± 11.61	19.65 ± 10.20	19.08 ± 12.69	15.31 ± 8.19	23.06 ± 13.01*	26.52 ± 11.54	17.77 ± 9.92	19.72 ± 12.11*	16.60 ± 8.21*
Flexor Digitorum Longus	None	20.55 ± 14.37	29.09 ± 15.57	20.50 ± 12.32	22.01 ± 15.01	17.96 ± 11.99	20.75 ± 13.76	26.76 ± 13.94	20.25 ± 10.88	21.40 ± 15.77	16.70 ± 10.79
	MF	20.42 ± 14.20	29.07 ± 15.34	19.64 ± 13.15	19.99 ± 13.79*	16.61 ± 11.34*	20.17 ± 13.48	26.27 ± 13.64	18.63 ± 9.16*	20.39 ± 13.94	17.37 ± 11.62
	LF	20.73 ± 14.91	27.60 ± 14.74	19.06 ± 10.88	21.89 ± 16.09	16.85 ± 11.14	20.37 ± 13.52	26.39 ± 13.58	20.74 ± 11.55	20.83 ± 16.19	16.55 ± 10.58
	Calcaneus	18.42 ± 13.50*	26.66 ± 14.31*	18.92 ± 10.53	21.34 ± 14.90	17.90 ± 13.07	20.48 ± 13.90	26.66 ± 15.59	20.19 ± 11.82	20.19 ± 15.43	15.20 ± 9.17*
	MM	19.92 ± 15.60	26.32 ± 15.27*	17.75 ± 9.24**	20.56 ± 15.01	16.92 ± 11.61	22.00 ± 14.67	28.04 ± 16.04	19.44 ± 10.79	20.86 ± 15.79	15.93 ± 10.07
	LM	20.52 ± 14.02	29.47 ± 16.29	19.92 ± 12.57	21.42 ± 14.49	17.48 ± 11.97	21.17 ± 14.69	26.62 ± 13.75	20.37 ± 11.19	20.11 ± 14.42	16.47 ± 10.57
Flexor Hallucis Longus	None	22.06 ± 16.23	24.95 ± 17.44	19.15 ± 12.10	26.37 ± 21.76	18.16 ± 11.89	26.44 ± 21.65	27.37 ± 19.65	16.21 ± 11.60	20.30 ± 19.06	15.99 ± 10.69
	MF	21.74 ± 15.90	27.53 ± 16.64**	22.41 ± 13.60**	25.58 ± 19.51	18.69 ± 11.69	28.04 ± 20.24**	26.26 ± 18.50	16.35 ± 12.48	19.48 ± 17.79	15.61 ± 10.39
	LF	23.29 ± 16.92	24.67 ± 15.25	19.57 ± 10.80	26.20 ± 20.69	16.43 ± 11.01**	20.90 ± 18.42**	22.60 ± 15.04**	13.60 ± 7.97*	15.31 ± 12.48**	13.80 ± 8.63**
	Calcaneus	23.35 ± 17.36	25.10 ± 16.77	16.69 ± 11.44	27.59 ± 21.69	19.19 ± 11.80	25.78 ± 20.63	27.43 ± 17.90	16.50 ± 10.81	21.03 ± 18.36**	17.50 ± 12.65
	MM	22.22 ± 16.02	22.88 ± 17.16**	18.39 ± 13.23	26.01 ± 20.95	18.42 ± 14.28	25.46 ± 20.95	25.33 ± 18.21	16.38 ± 11.93	19.02 ± 17.72	14.66 ± 9.79
	LM	23.63 ± 15.89	26.10 ± 16.83	19.76 ± 11.29	27.45 ± 20.91*	18.47 ± 10.78	23.99 ± 17.37	24.78 ± 15.51	15.60 ± 9.73	19.69 ± 16.63	16.00 ± 10.42
		IC			HEEL RISE		TOE OFF	Initial Swing		Mid-Swing	Terminal Swing

LOADING RESPONSE ---------------------- MIDSTANCE -------------------------------- PROPULSION -------------------------------- ---------------------------------------SWING---------------------------------------

** = p<.05.   ** = p<.001*

Appendix 4B Mean data for each lower leg muscle by walking condition, divided across each phase of the gait cycle

Muscle	Walking Condition	Bins (%Pk)									
		Initial Contact (IC)	Loading Response (LR)	Midstance (MS)	Heel Rise (HR)	Propulsion (PR)	Toe Off (TO)	Initial Swing (iSW)	Mid Swing (MSW)		Terminal Swing (TSW)
TA	Level	20.65 ± 19.22	13.09 ± 10.16	10.54 ± 8.05	7.84 ± 5.89	15.85 ± 13.96	21.99 ± 20.23	11.74 ± 9.67	9.58 ± 8.34	7.23 ± 5.69	13.27 ± 11.77
	Wedge	21.53 ± 19.48*	15.94 ± 12.00**	12.47 ± 9.14**	7.76 ± 5.81	15.93 ± 13.19	21.26 ± 18.44	13.12 ± 10.64**	10.24 ± 9.01*	8.81 ± 7.68**	14.18 ± 13.70**
PL	Level	9.52 ± 11.09	7.47 ± 8.74	7.54 ± 8.88	10.56 ± 14.09	15.49 ± 17.39	8.91 ± 10.94	7.37 ± 8.51	7.85 ± 9.40	10.81 ± 13.97	15.30 ± 17.30
	Wedge	10.72 ± 11.48**	9.37 ± 10.13**	9.30 ± 10.02**	13.67 ± 15.93**	21.66 ± 22.81**	9.73 ± 10.71*	8.31 ± 9.16**	7.66 ± 8.70**	9.07 ± 10.86	12.36 ± 12.71**
MG	Level	4.11 ± 3.43	5.31 ± 5.88	9.71 ± 11.34	13.12 ± 13.55	15.86 ± 16.91	4.99 ± 4.87	4.96 ± 4.76	8.68 ± 8.37	14.56 ± 13.78	15.46 ± 14.96
	Wedge	4.39 ± 3.33*	5.23 ± 5.44	8.92 ± 10.00	13.80 ± 14.32**	21.57 ± 20.94**	6.39 ± 6.30**	4.22 ± 4.11**	7.25 ± 7.66**	12.30 ± 12.45	11.66 ± 11.69**
EDL	Level	15.72 ± 17.50	10.05 ± 9.83	8.32 ± 8.00	7.43 ± 7.43	13.26 ± 12.87	15.70 ± 18.36	9.72 ± 9.71	8.96 ± 9.19	8.78 ± 9.31	14.86 ± 14.10
	Wedge	17.59 ± 18.00**	12.35 ± 11.60**	10.38 ± 9.93**	8.53 ± 8.00**	15.37 ± 13.78**	16.59 ± 17.69*	11.83 ± 11.49**	9.86 ± 9.61*	9.50 ± 8.96*	15.18 ± 14.73
TP	Level	21.55 ± 15.39	25.70 ± 13.69	20.17 ± 11.81	18.99 ± 12.48	15.65 ± 9.03	21.51 ± 13.41	27.77 ± 12.64	19.14 ± 11.40	21.01 ± 13.23	16.75 ± 9.76
	Wedge	21.06 ± 14.62	26.04 ± 13.97	20.81 ± 12.47	20.94 ± 14.43**	15.41 ± 7.85	22.05 ± 13.81	24.33 ± 12.30**	17.17 ± 10.74**	17.43 ± 12.09**	15.60 ± 8.98**
EHL	Level	21.35 ± 14.96	28.39 ± 15.85	20.68 ± 13.31	15.92 ± 10.77	13.15 ± 10.01	21.52 ± 14.92	27.45 ± 12.71	20.54 12.61	17.15 ± 11.06	12.69 ± 7.76
	Wedge	21.49 ± 14.68	29.58 ± 16.91*	21.57 ± 14.53**	17.69 ± 13.12**	13.12 ± 10.66	20.79 ± 14.46*	24.95 ± 12.51**	18.83 ± 12.56**	14.04 ± 8.72**	11.78 ± 7.72**
FDL	Level	16.68 ± 13.73	28.17 ± 14.96	19.25 ± 11.47	20.51 ± 14.71	17.55 ± 11.90	21.39 ± 14.23	29.06 ± 14.13	21.74 ± 11.06	22.36 ± 15.54	17.26 ± 10.11
	Wedge	20.71 ± 15.08*	28.37 ± 15.75	19.87 ± 11.99*	22.23 ± 15.34**	17.33 ± 11.89	20.24 ± 13.65**	25.54 ± 14.19**	18.31 ± 10.51**	19.27 ± 15.06**	15.65 ± 10.94**
FHL	Level	22.41 ± 15.40	25.10 ± 16.24	18.79 ± 11.64	26.03 ± 19.84	19.84 ± 12.68	24.16 ± 20.55	28.22 ± 18.53	17.50 ± 11.95	21.66 ± 19.41	17.21 ± 10.94
	Wedge	22.71 ± 17.23	25.17 ± 17.52	20.55 ± 12.61**	26.95 ± 22.26	16.61 ± 11.00**	24.68 ± 20.25**	23.83 ± 17.38**	14.38 ± 9.86**	17.16 ± 15.39**	14.16 ± 9.97**

** = p<.05.   ** = p<.001*

Appendix 5 Ensemble averages of the raw AbdH EMG signals of subject 24 walking in FOs and FOTs. Each graph includes 10 walking trials in both conditions (FO and FOT) demonstrating strong signal quality from start to finish of the testing session.

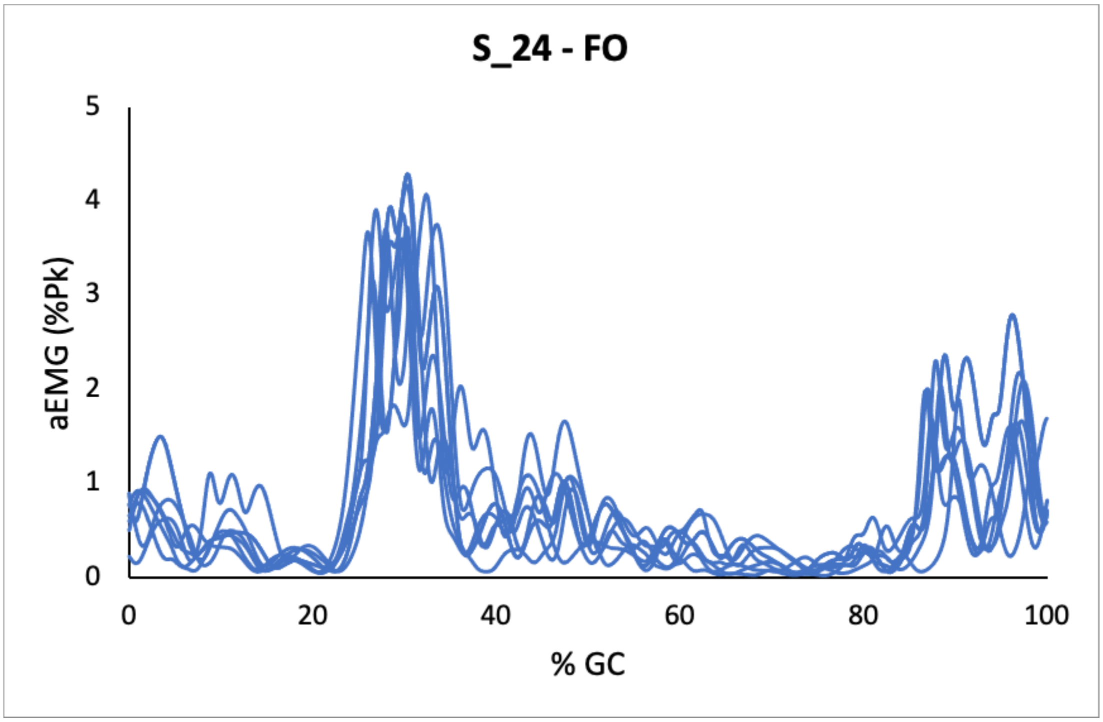

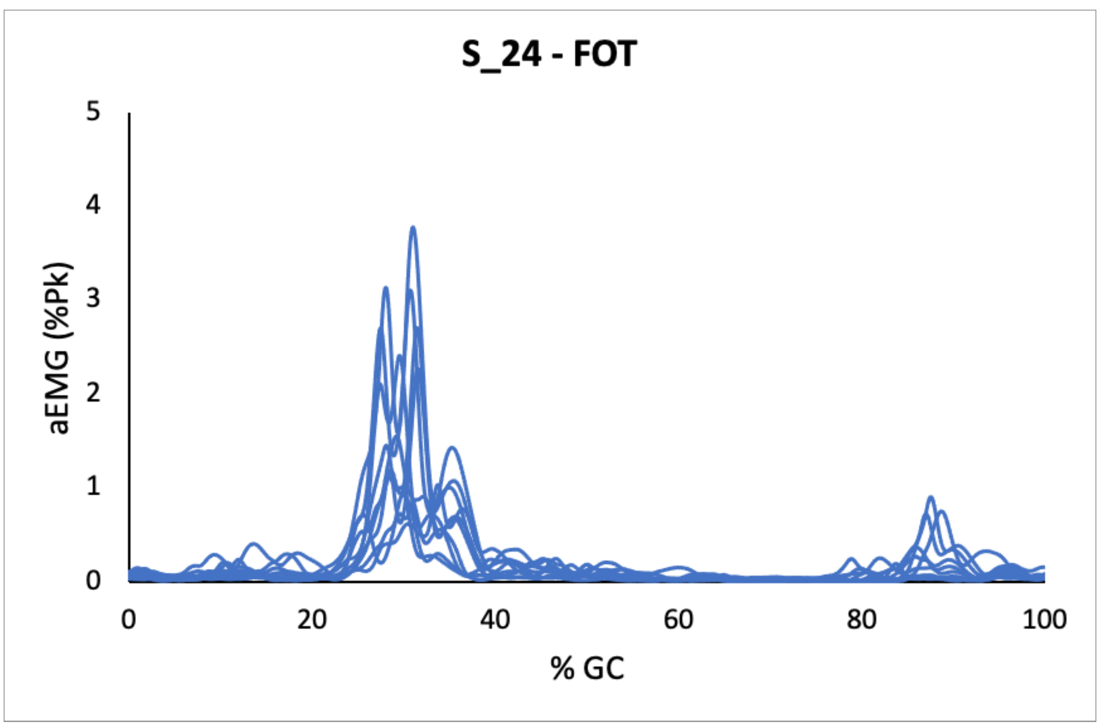

Appendix 6A Mean data for each foot intrinsic muscle by orthotic condition, divided across each phase of the gait cycle

Muscle	Orthotic Condition	Bins (%Pk)									
		Initial Contact (IC)	Loading Response (LR)	Midstance (MS)	Heel Rise (HR)	Propulsion (PR)	Toe Off (TO)	Initial Swing (iSW)	Mid Swing (MSW)		Terminal Swing (TSW)
Abductor Hallucis	Barefoot	14.46 (10.94)	8.75 (6.77)	7.90 (6.44)	10.16 (7.98)	11.89 (9.08)	11.19 (6.93)	11.88 (9.20)	9.20 (7.25)	10.24 (7.64)	8.90 (7.88)
	Non-textured FO	8.94 (6.23)**B	8.48 (6.07)	9.81 (6.96)**B	26.08 (15.67)**B	12.93 (8.07)**B	7.91 (5.09)**B	8.04 (6.00)**B	7.18 (4.87)**B	12.43 (9.18)**B	8.92 (6.34)
	Textured FO	10.92 (8.43)**B,FO	9.83 (7.12)**B,FO	13.17 (9.28)**B,FO	26.98 (16.23)**B	14.26 (8.75)**B,FO	9.53 (6.62)**B,FO	10.31 (7.63)**B,FO	8.06 (5.51)**B,FO	13.75 (10.70)**B,FO	11.11 (8.17)**B,FO
Adductor Hallucis (transverse head)	Barefoot	15.99 (11.40)	9.76 (8.15)	10.72 (9.54)	14.19 (12.64)	12.03 (9.30)	12.99 (8.48)	15.36 (10.61)	11.26 (7.67)	13.92 (10.31)	9.10 (6.64)
	Non-textured FO	10.59 (8.98)**B	8.88 (6.59)	11.25 (6.94)	30.68 (13.41)**B	13.00 (8.76)**B	7.42 (5.96)**B	8.08 (7.28)**B	6.61 (5.39)**B	12.13 (11.22)**B	8.13 (6.45)**B
	Textured FO	10.85 (8.32)**B	8.73 (6.04)	12.94 (7.23)**B, FO	30.20 (13.64)**B	13.80 (8.60)**B,FO	8.69 (5.67)**B,FO	10.05 (8.59)**B,FO	7.22 (4.96)**B,FO	13.04 (9.72)**B,FO	8.82 (5.80)**FO
Abductor Digiti Minimi	Barefoot	25.70 (12.59)	14.04 (9.35)	8.59 (6.21)	8.32 (6.66)	9.56 (7.30)	11.17 (7.92)	13.53 (9.41)	9.15 (7.08)	9.57 (7.63)	11.45 (7.88)
	Non-textured FO	22.45 (12.47)	18.05 (11.53)	11.37 (7.68)	9.18 (7.14)**B	10.96 (8.51)	11.96 (8.53)	15.08 (11.49)**B	8.88 (6.41)	10.72 (7.35)**B	16.32 (10.74)**B
	Textured FO	22.37 (13.12)**B,FO	18.71 (11.78)**B, FO	11.86 (8.03)**B, FO	10.37 (8.03)**B,FO	10.53 (7.47)*B, FO	12.22 (8.72)*B	16.19 (11.22)**B,FO	9.71 (6.82)*FO	11.43 (7.78)**B,FO	16.41 (11.04)**FO
Flexor Digitorum Brevis	Barefoot	20.55 (10.13)	13.47 (9.45)	8.43 (6.44)	7.81 (6.42)	9.31 (7.38)	15.43 (9.22)	16.71 (11.00)	9.00 (6.13)	7.12 (6.28)	8.53 (5.83)
	Non-textured FO	16.53 (9.35)**B	13.00 (8.71)	8.42 (5.77)	9.59 (6.68)**B	11.74 (8.23)**B	16.61 (8.96)*B	18.03 (9.94)**B	10.16 (7.55)*B	8.26 (6.06)**B	9.98 (7.23)*B
	Textured FO	15.73 (9.72)**B	12.86 (8.88)	8.50 (6.39)	10.23 (7.27)**B	12.42 (8.73)**B	16.80 (9.72)*B	20.16 (12.42)**B,FO	9.97 (6.67)*B	7.93 (5.97)**B	8.97 (6.57)*FO

** = p<.05. ** = p<.001. B=comparisons to barefoot, FO=comparisons to FO*

Appendix 6B Mean data for each foot intrinsic muscle by walking condition, divided across each phase of the gait cycle

Muscle	Walking Condition	Bins (%Pk)									
		Initial Contact (IC)	Loading Response (LR)	Midstance (MS)	Heel Rise (HR)	Propulsion (PR)	Toe Off (TO)	Initial Swing (iSW)	Mid Swing (MSW)		Terminal Swing (TSW)
Abductor Hallucis	Hard	9.55 (7.51)	8.62 (6.57)	8.90 (6.26)	21.92 (15.15)	12.58 (8.05)	9.39 (6.01)	10.91 (8.10)	7.95 (5.80)	10.59 (8.20)	8.87 (6.83)
	Soft	12.12 (9.18)**	9.51 (6.74)**	12.62 (9.30)**	24.48 (16.91)**	13.90 (9.07)**	9.04 (6.47)*	8.51 (6.72)**	7.93 (5.65)	14.44 (10.52)**	10.69 (8.02)**
AddH-T	Hard	9.64 (7.83)	8.54 (6.48)	10.13 (6.63)	26.46 (15.31)	12.40 (8.26)	9.05 (7.17)	11.35 (9.72)	8.02 (6.22)	12.63 (10.30)	8.61 (6.42)
	Soft	13.96 (10.53)**	9.47 (6.98)**	13.47 (8.31)**	27.66 (14.44)*	13.83 (9.30)**	9.13 (6.38)*	9.39 (8.07)**	7.61 (5.86)**	13.10 (10.63)	8.60 (6.07)
ADM	Hard	20.78 (11.18)	16.43 (10.88)	10.48 (6.77)	9.22 (7.38)	10.95 (7.93)	13.47 (9.09)	18.00 (12.07)	10.72 (7.13)	11.08 (7.63)	16.00 (10.20)
	Soft	26.15 (13.68)**	18.34 (11.66)**	11.38 (8.34)**	9.68 (7.50)	10.03 (7.78)*	10.38 (7.55)**	12.47 (9.07)**	7.88 (6.01)**	10.42 (7.59)*	14.94 (10.75)*
FDB	Hard	16.85 (10.12)	13.11 (8.77)	8.53 (6.14)	8.96 (6.77)	11.05 (8.23)	16.76 (9.35)	19.56 (11.86)	10.22 (7.02)	7.77 (5.83)	8.99 (6.35)
	Soft	17.18 (9.49)	12.97 (9.08)	8.38 (6.17)	10.03 (7.03)**	12.02 (8.44)*	16.12 (9.31)*	17.63 (10.52)**	9.47 (6.87)*	8.04 (6.32)	9.61 (7.15)

**** = p<.05. ** = p<.001***

Appendix 6C Mean kinematic data of the hip, knee and ankle across each orthotic condition

LEFT LEG KINEMATICS									
Orthotic Condition	Hip			Knee			Ankle		
	Max (deg)	Min (deg)	Range (deg)	Max (deg)	Min (deg)	Range (deg)	Max (deg)	Min (deg)	Range (deg)
Barefoot	29.82 (4.56)	-11.74 (5.30)	41.52 (4.69)	32.33 (7.40)	0.37 (3.66)	31.93 (6.95)	18.91 (5.40)	-9.74 (7.25)	28.44 (6.99)
Non-textured FO	29.85 (4.75)	-12.43 (5.53)**B	42.25 (5.02)**B	31.53 (8.03)**B	0.85 (4.00)**B	30.72 (7.94)**B	23.48 (4.81)**B	-1.38 (8.45)**B	24.88 (7.06)**B
Textured FO	29.95 (4.56)	-12.11 (5.51)**B,FO	41.99 (4.66)**B,FO	32.13 (8.18)**FO	0.89 (3.98)**B	31.21 (7.74)**B,FO	23.99 (4.53)**B,FO	-0.88 (7.03)**B,FO	24.78 (6.22)**B

** = p<.05.   ** = p<.001. B=comparisons to barefoot, FO=comparisons to FO*

RIGHT LEG KINEMATICS									
Orthotic Condition	Hip			Knee			Ankle		
	Max (deg)	Min (deg)	Range (deg)	Max (deg)	Min (deg)	Range (deg)	Max (deg)	Min (deg)	Range (deg)
Barefoot	31.08 (4.98)	-9.85 (5.42)	40.98 (4.34)	35.27 (8.87)	1.26 (3.56)	34.07 (8.41)	18.74 (4.47)	-12.42 (11.23)	29.64 (5.94)
Non-textured FO	30.81 (5.19)**B	-10.25 (6.17)**B	41.07 (4.81)	33.78 (9.11)**B	1.81 (3.52)**B	32.03 (8.50)**B	22.00 (5.52)**B	-4.13 (9.29)**B	25.70 (7.26)**B
Textured FO	30.95 (5.11)	-10.33 (5.95)**B	41.26 (4.68)*B	34.40 (9.37)**B,FO	2.24 (3.71)**B,FO	32.16 (8.54)**B	22.72 (4.73)**B,FO	-3.16 (0.10)**B,FO	25.36 (7.36)**FO

** = p<.05.   ** = p<.001*

Appendix 6D Mean kinematic data of the hip, knee, and ankle across each walking surface

LEFT LEG KINEMATICS									
Walking Condition	Hip			Knee			Ankle		
	Max (deg)	Min (deg)	Range (deg)	Max (deg)	Min (deg)	Range (deg)	Max (deg)	Min (deg)	Range (deg)
Hard Surface	29.83 (4.61)	-12.01 (5.51)	41.76 (4.92)	30.86 (8.07)	0.83 (3.94)	30.01 (7.99)	23.48 (4.91)	-2.32 (8.67)	25.74 (7.07)
Soft Surface	29.94 (4.67)	-12.31 (5.45)**	42.24 (4.71)**	33.00 (7.72)**	0.71 (3.92)	32.32 (7.09)**	22.08 (5.38)**	-3.30 (8.10)**	25.35 (6.67)*

** = p<.05.   ** = p<.001*

RIGHT LEG KINEMATICS									
Walking Condition	Hip			Knee			Ankle		
	Max (deg)	Min (deg)	Range (deg)	Max (deg)	Min (deg)	Range (deg)	Max (deg)	Min (deg)	Range (deg)
Hard Surface	30.74 (5.01)	-10.17 (5.94)	40.93 (4.85)	32.76 (8.53)	1.57 (3.46)	31.22 (8.24)	22.15 (5.27)	-4.61 (10.31)	26.06 (7.30)
Soft Surface	31.11 (5.21)**	-10.23 (5.95)	41.33 (4.47)**	35.90 (9.55)**	2.18 (3.75)**	33.77 (8.63)**	21.14 (5.13)**	-6.12 (10.12)	26.60 (7.18)*

** = p<.05.   ** = p<.001*

Appendix 6E Mean gait parameter data across each orthotic condition

Orthotic Condition	GAIT PARAMETERS		
	Walking Velocity (m/s)	Step Length (cm)	Step Width (cm)
Barefoot	1.32 (0.11)	72.69 (4.45)	14.41 (4.05)
Non-textured FO	1.30 (0.16)**B	72.39 (4.61)	13.02 (3.76)**B
Textured FO	1.30 (0.11)**B,FO	72.18 (4.89)	12.72 (3.86)**B,FO

** = p<.05.   ** = p<.001. B=comparisons to barefoot, FO=comparisons to FO*

Appendix 6F Mean gait parameter data across each walking surface

Walking Condition	GAIT PARAMETERS		
	Walking Velocity (m/s)	Step Length (cm)	Step Width (cm)
Hard Surface	1.29 (0.13)	71.45 (4.90)	13.00 (3.81)
Soft Surface	1.31 (0.13)**	73.28 (4.29)**	13.37 (4.00)*

** = p<.05.   ** = p<.001*

Appendix 7 aEMG data of eight lower limb muscles during the stance phase of gait, divided by FPI classifications

SENSORY LOCATION	Average EMG (mV) in Stance by Foot Posture				
	Highly Supinated	Supinated	Neutral	Pronated	Highly Pronated
Tibialis Anterior (TA)					
None	27.63 (8.68)	36.35 (14.40)	32.27 (15.65)	32.35 (11.45)	30.96 (14.26)
MF	28.11 (8.62)	35.58 (13.57)	33.70 (16.46)	30.89 (11.93)	31.39 (14.59)
LF	27.89 (9.50)	45.00 (22.69)	32.79 (16.38)	32.38 (10.77)	31.06 (12.16)
Calcaneus	27.17 (9.38)	44.92 (22.69)	32.46 (16.69)	30.92 (11.37)	31.78 (15.60)
MM	27.67 (8.84)	46.92 (23.50)	31.51 (14.46)	32.15 (11.98)	35.06 (17.09)
LM	27.28 (8.08)	38.17 (16.12)	33.02 (15.05)	31.64 (11.13)	31.33 (15.39)
Peroneus Longus (PL)					
None	18.31 (7.68)	18.39 (4.35)	18.78 (6.70)	17.51 (6.81)	21.58 (8.84)
MF	18.28 (8.08)	17.08 (3.37)	19.19 (6.75)	17.33 (7.00)	22.22 (8.95)
LF	20.61 (8.49)	17.92 (4.12)	18.56 (6.26)	17.36 (7.26)	22.72 (10.39)
Calcaneus	17.78 (7.91)	17.33 (3.23)	18.54 (6.59)	17.75 (7.40)	22.89 (10.27)
MM	17.17 (6.25)	18.75 (3.86)	18.17 (6.32)	17.59 (7.14)	22.56 (9.87)
LM	18.00 (6.67)	29.83 (3.03)	18.73 (6.26)	17.15 (7.13)	22.33 (9.92)
Extensor Digitorum Longus (EDL)					
None	28.98 (12.96)	43.11 (26.08)	28.27 (9.56)	26.19 (11.21)	31.94 (15.28)
MF	29.50 (13.52)	45.50 (28.77)	28.57 (10.24)	25.69 (12.00)	30.11 (14.52)
LF	28.67 (13.48)	44.42 (28.37)	27.44 (10.39)	26.29 (13.09)	29.39 (12.76)
Calcaneus	27.33 (13.44)	43.75 (30.82)	28.47 (10.62)	25.44 (12.01)	28.00 (11.50)
MM	27.72 (12.86)	44.25 (29.20)	28.68 (11.01)	26.31 (11.37)	30.50 (13.02)
LM	29.00 (13.63)	43.67 (28.26)	28.89 (10.90)	25.31 (11.27)	31.44 (16.50)
Extensor Hallucis Longus (EHL)					
None	50.16 (39.67)	19.17 (12.79)	50.02 (40.88)	53.62 (32.41)	64.01 (44.93)
MF	60.38 (46.99)	20.50 (11.87)	49.61 (40.02)	48.64 (29.15)	60.58 (46.03)
LF	26.81 (18.98)	18.13 (11.97)	51.80 (49.55)	53.91 (35.54)	64.19 (38.29)
Calcaneus	34.89 (28.93)	19.09 (8.59)	53.85 (53.29)	44.83 (25.86)	67.72 (48.37)
MM	41.18 (28.50)	17.23 (12.07)	48.77 (41.42)	50.53 (27.09)	55.78 (41.98)
LM	35.28 (27.08)	20.19 (12.94)	53.91 (51.22)	64.53 (47.91)	71.66 (51.87)
Medial Gastrocnemius (MG)					
None	18.69 (14.16)	32.63 (27.25)	17.81 (9.22)	17.65 (6.69)	28.04 (23.97)
MF	16.89 (9.65)	46.17 (42.28)	17.45 (9.04)	21.36 (15.24)	33.56 (31.70)
LF	19.39 (14.92)	31.18 (20.16)	17.40 (7.86)	17.13 (5.85)	31.22 (28.19)
Calcaneus	18.33 (13.34)	26.10 (16.67)	17.37 (8.37)	17.46 (6.03)	29.78 (23.41)
MM	14.94 (6.31)	21.67 (11.63)	18.05 (8.35)	17.62 (6.26)	30.83 (27.93)
LM	18.28 (13.78)	19.08 (14.16)	17.07 (8.51)	17.80 (6.94)	28.89 (23.97)
Tibialis Posterior (TP)					
None	45.93 (27.11)	66.53 (47.07)	63.78 (37.69)	58.48 (30.95)	78.19 (49.05)
MF	48.87 (32.31)	102.18 (86.39)	60.71 (33.64)	74.27 (32.79)	71.94 (47.49)
LF	36.49 (24.31)	70.08 (40.05)	62.31 (49.36)	56.35 (30.83)	81.62 (48.02)
Calcaneus	31.08 (17.95)	84.37 (77.08)	59.04 (41.12)	64.41 (44.46)	76.77 (53.48)
MM	49.60 (26.06)	65.54 (46.55)	60.92 (49.54)	60.65 (39.77)	68.99 (45.03)
LM	37.51 (24.54)	65.92 (45.72)	61.81 (39.36)	68.86 (42.23)	71.42 (45.85)
Flexor Digitorum Longus (FDL)					
None	53.61 (37.23)	69.06 (42.35)	71.98 (49.44)	89.89 (47.97)	79.21 (60.23)
MF	58.84 (49.93)	64.62 (44.45)	67.90 (46.66)	88.27 (60.35)	75.81 (59.29)
LF	61.21 (58.76)	68.49 (36.73)	70.74 (51.91)	83.69 (44.90)	89.11 (62.95)
Calcaneus	65.95 (61.00)	65.99 (36.51)	69.30 (50.03)	87.50 (44.25)	79.03 (55.30)
MM	78.39 (72.46)	80.68 (61.75)	79.10 (55.76)	82.18 (33.53)	63.91 (55.59)
LM	54.11 (40.30)	60.72 (32.25)	66.89 (47.50)	92.94 (55.11)	78.94 (50.04)
Flexor Hallucis Longus (FHL)					
None	50.01 (38.12)	83.14 (61.80)	76.96 (51.22)	45.45 (34.83)	60.21 (48.69)
MF	40.25 (32.67)	73.77 (41.37)	86.16 (56.44)	42.13 (33.19)	70.45 (60.23)
LF	51.81 (48.29)	45.67 (30.07)	69.03 (50.97)	51.07 (42.99)	69.24 (58.00)
Calcaneus	38.11 (29.22)	50.60 (25.42)	78.84 (60.03)	42.27 (33.33)	69.62 (58.87)
MM	35.88 (26.95)	55.41 (31.53)	73.32 (52.94)	55.39 (29.97)	50.79 (41.81)
LM	40.31 (31.01)	70.26 (31.29)	80.30 (63.67)	42.61 (38.85)	58.07 (38.54)

REFERENCES

[1] K. Walia, Global Foot Orthotic Insole Market Report , 2018 to 2025, 2019.

[2] M. Razeghi, M.E. Batt, Biomechanical analysis of the effect of orthotic shoe inserts. A review of the literature, Sport. Med. 29 (2000) 425–438.

[3] N. Collins, L. Bisset, T. Mcpoil, B. Vicenzino, Foot orthoses in lower limb overuse conditions: A systematic review and meta-analysis, Foot Ankle Int. 28 (2007) 396–412. https://doi.org/10.3113/FAI.2007.0396.

[4] R.T. Lewinson, D.J. Stefanyshyn, Wedged insoles and gait in patients with knee osteoarthritis: A biomechanical review, Ann. Biomed. Eng. 44 (2016) 3173–3185. https://doi.org/10.1007/s10439-016-1696-1.

[5] G.S. Murley, K.B. Landorf, H.B. Menz, A.R. Bird, Effect of foot posture, foot orthoses and footwear on lower limb muscle activity during walking and running: A systematic review, Gait Posture. 29 (2009) 172–187. https://doi.org/10.1016/j.gaitpost.2008.08.015.

[6] A. Mcmillan, C. Payne, Effect of foot orthoses on lower extremity kinetics during running : a systematic literature review, J. Foot Ankle Res. 1 (2008) 19–21. https://doi.org/10.1186/1757-1146-1-13.

[7] R. Ferber, The influence of custom foot orthoses on lower extremity running mechanics, Int. Sport. J. 8 (2007) 97–106.

[8] A. Hatton, J. Dixon, K. Rome, D. Martin, Effect of foot orthoses on lower limb muscle activation: a critical review, Phys. Ther. Rev. 13 (2008) 280–293. https://doi.org/10.1179/174328808X252037.

[9] K. Mills, P. Blanch, A.R. Chapman, T.G. McPoil, B. Vicenzino, Foot orthoses and gait: a systematic review and meta-analysis of literature pertaining to potential mechanisms, Br. J. Sports Med. 44 (2010) 1035–1046. https://doi.org/10.1136/bjsm.2009.066977.

[10] J. Dankasa, Developing a Theory in Academic Research: A Review of Experts' Advice, J. Inf. Sci. Theory Pract. 3 (2015) 64–74. https://doi.org/10.1633/jistap.2015.3.3.4.

[11] M.W. Whittle, Normal Gait, in: Gait Anal. An Introd., Fourth, Butterworth Heinemann Elsevier, Philadelphia, PA, 2007: pp. 47–100.

[12] M.W. Whittle, Clinical gait analysis: A review, Hum. Mov. Sci. 15 (1996) 369–387. https://doi.org/10.1016/0167-9457(96)00006-1.

[13] D.A. Winter, H.J. Yack, EMG profiles during normal human walking: stride-to-stride and inter-subject variability, Electroencephalogr. Clin. Neurophysiol. 67 (1987) 402–411. https://doi.org/10.1016/0013-4694(87)90003-4.

[14] D.A. Winter, Biomechanical motor patterns in normal walking, J. Mot. Behav. 15 (1983) 302–330. https://doi.org/10.1080/00222895.1983.10735302.

[15] F. Sheffield, J. Gersten, A. Mastellone, Electromyographic study of the muscles of the foot in normal walking, Am. J. Phys. Med. 35 (1956) 223–236.

[16] G.S. Murley, H.B. Menz, K.B. Landorf, Foot posture influences the electromyographic activity of selected lower limb muscles during gait, J. Foot Ankle Res. 2 (2009) 1–9. https://doi.org/10.1186/1757-1146-2-35.

[17] D.A. Neumann, Figure 15.29 A & B, in: Kinesiol. Musculoskelet. Syst. Found. Rehabil., Third, Elsevier, St. Louis, Missouri, 2017: pp. 676–678.

[18] K.L. Moore, A.F. Dalley, A.M.R. Agur, Lower Limb, in: Clin. Oriented Anat., Eighth, Wolters Kluwer, Philadelphia, PA, 2018: pp. 666–828.

[19] D.A. Neumann, Ankle and Foot, in: Kinesiol. Musculoskelet. Syst., Third, Elsevier, St. Louis, Missouri, 2017: pp. 595–652.

[20] R.L. Valmassy, Lower Extremity Function and Normal Mechanics, in: Clin. Biomech. Low. Extrem., Mosby, St. Louis, Missouri, 1996: pp. 2–57.

[21] K.A. Ball, M.J. Afheldt, Evolution of foot orthotics - Part 1: Coherent theory or coherent practice?, J. Manipulative Physiol. Ther. 25 (2002) 116–124. https://doi.org/10.1067/mmt.2002.121415.

[22] M.U. Mcculloch, D. Brunt, D. Vander Linder, The effect of foot orthotics and gait velocity on lower limb kinematics and temporal events of stance, J. Orthop. Sport. Phys. Ther. 17 (1993).

[23] A. Mundermann, B.M. Nigg, R.N. Humble, Foot orthotics affect lower extremity kinematics and kinetics during running, Clin. Biomech. (Bristol, Avon). 18 (2003) 254–262.

[24] B.M. Nigg, P. Stergiou, G. Cole, D.J. Stefanyshyn, A. Mundermann, R.N. Humble, Effect of shoe inserts on kinetics, center of pressure, and leg joint moments during running., Med. Sci. Sport. Exerc. 35 (2003) 314–319.

[25] A. Stacoff, I.K. de Quervain, M. Dettwyler, P. Wolf, R. List, T. Ukelo, E. Stüssi, Biomechanical effects of foot orthoses during walking, Foot. 17 (2007) 143–153. https://doi.org/10.1016/j.foot.2007.02.004.

[26] J.J. Eng, M.R. Pierrynowski, The effect of soft foot orthotics on three-dimensional lower-limb kinematics during walking and running, Phys. Ther. 74 (1994) 836–844. https://doi.org/10.1093/ptj/74.9.836.

[27] A. Stacoff, C. Reinschmidt, B.M. Nigg, A.J. Van Den Bogert, A. Lundberg, J. Denoth, E. Stussi, Effects of foot orthoses on skeletal motion during running, Clin. Biomech. 15 (2000) 54–64.

[28] C.J. Nester, M.L. van der Linden, P. Bowker, Effect of foot orthoses on the kinematics and kinetics of normal gait, Gait Posture. 17 (2003) 180–187. https://doi.org/10.1163/156854096X00033.

[29] K. Mills, P. Blanch, A.R. Chapman, T.G. McPoil, B. Vicenzino, Foot orthoses and gait: a systematic review and meta-analysis of literature pertaining to potential mechanisms, Br. J. Sports Med. 44 (2010) 1035–1046. https://doi.org/10.1136/bjsm.2009.066977.

[30] S.C. Cobb, L.L. Tis, J.T. Johnson, Y.T. Wang, M.D. Geil, Custom-molded foot-orthosis intervention and multisegment medial foot kinematics during walking, J. Athl. Train. 46 (2011) 358–365. https://doi.org/10.4085/1062-6050-46.4.358.

[31] R. Barn, M. Brandon, D. Rafferty, R.D. Sturrock, M. Steultjens, D.E. Turner, J. Woodburn, Kinematic, kinetic and electromyographic response to customized foot orthoses in patients with tibialis posterior tenosynovitis, pes plano valgus and rheumatoid arthritis, Rheumatology. 53 (2014) 123–130. https://doi.org/10.1093/rheumatology/ket337.

[32] J.C. Garbalosa, B. Elliott, R. Feinn, R. Wedge, The effect of orthotics on intersegmental foot kinematics and the EMG activity of select lower leg muscles, Foot. 25 (2015) 206–214. https://doi.org/10.1016/j.foot.2015.07.005.

[33] G. Desmyttere, M. Hajizadeh, J. Bleau, M. Begon, Effect of foot orthosis design on lower limb joint kinematics and kinetics during walking in flexible pes planovalgus: A systematic review and meta-analysis, Clin. Biomech. 59 (2018) 117–129. https://doi.org/10.1016/j.clinbiomech.2018.09.018.

[34] R. Butler, I. Davis, C. Laughton, M. Hughes, Dual-function foot orthosis: effect on shock and control of rearfoot motion, Foot Ankle Int. 24 (2003) 410–414.

[35] C. Miller, E. Laskowski, V. Suman, Effect of corrective rearfoot orthotic devices on ground reaction forces during ambulation., Mayo Clin. Proc. 71 (1996) 757–762.

[36] B.M. Nigg, W. Herzog, L. Read, Effect of viscoelastic shoe insoles on vertical impact forces in heel-toe running, Am. J. Sports Med. 16 (1988) 70–76.

[37] M.W. Whittle, Generation and attenuation of transient impulsive forces beneath the foot: A review, Gait Posture. 10 (1999) 264–275. https://doi.org/10.1016/S0966-6362(99)00041-7.

[38] S. Perry, M. Lafortune, Influences of inversion/eversion of the foot upon impact loading during locomotion, Clin. Biomech. 10 (1995) 253–257.

[39] M. Ho, L. Chong, V. Kong, G. Lam, The effects of foot orthosis on ground reaction force and comfort in flat-footed individuals during sprints, J. Sci. Med. Sport. 21 (2018) S68. https://doi.org/10.1016/j.jsams.2018.09.154.

[40] G. Gijon-Nogueron, I. Palomo-Toucedo, A. Gil-Tinoco, A.B. Ortega-Avila, P.V. Munuera-Martínez, Effect produced on ground reaction forces by a prefabricated, weight-bearing and non-weight-bearing foot orthosis in the treatment of pronated foot, Med. (United States). 97 (2018). https://doi.org/10.1097/MD.0000000000010960.

[41] A.A.A. El Megeid Abdallah, Effect of unilateral and bilateral use of laterally wedged insoles with arch supports on impact loading in medial knee osteoarthritis, Prosthet. Orthot. Int. 40 (2016) 231–239. https://doi.org/10.1177/0309364614560942.

[42] M.W. Cornwall, T.G. McPoil, The effect of foot orthotics on the initiation of plantar surface loading, Clin. Biomech. 12 (1997) S4.

[43] J.N. Maharaj, A.G. Cresswell, G.A. Lichtwark, The immediate effect of foot orthoses on subtalar joint mechanics and energetics, Med. Sci. Sports Exerc. 50 (2018) 1449–1456. https://doi.org/10.1249/MSS.0000000000001591.

[44] B.M. Nigg, J. Baltich, S. Hoerzer, H. Enders, Running shoes and running injuries: Mythbusting and a proposal for two new paradigms: “Preferred movement path” and “comfort filter,” Br. J. Sports Med. 49 (2015) 1290–1294. https://doi.org/10.1136/bjsports-2015-095054.

[45] K. Mills, P. Blanch, A.R. Chapman, T.G. McPoil, B. Vicenzino, Foot orthoses and gait: a systematic review and meta-analysis of literature pertaining to potential mechanisms, Br. J. Sports Med. 44 (2010) 1035–1046. https://doi.org/10.1136/bjsm.2009.066977.

[46] B.M. Nigg, M.A. Nurse, D.J. Stefanyshyn, Shoe inserts and orthotics for sport and physical activities, Med. Sci. Sport. Exerc. 31 (1999) S421–S428. https://doi.org/10.1097/00005768-199907001-00003.

[47] R. Enoka, Chapter 7: Voluntary Movement, in: Neuromechanics Hum. Mov., Fifth, Human Kinetics, Champaign, IL, 2015: pp. 255–313.

[48] P.D. Cheney, Role of cerebral cortex in voluntary movements. A review, Phys. Ther. 65 (1985) 624–635.

[49] S. Rossignol, R. Dubuc, J.P. Gossard, Dynamic sensorimotor interactions in locomotion, Physiol. Rev. 86 (2006) 89–154. https://doi.org/10.1152/physrev.00028.2005.

[50] D.G. Amaral, The functional organization of perception and movement, in: Princ. Neural Sci., Fifth, McGraw Hill Education, 2013: pp. 356–369.

[51] M.J. Ferreira-Pinto, L. Ruder, P. Capelli, S. Arber, Connecting Circuits for Supraspinal Control of Locomotion, Neuron. 100 (2018) 361–374. https://doi.org/10.1016/j.neuron.2018.09.015.

[52] K.G. Pearson, J.E. Gordon, Spinal Reflexes, in: Princ. Neural Sci., fifth, n.d.

[53] E. Gardner, K. Johnson, Touch, in: Princ. Neural Sci., Fifth, McGraw Hill Companies, Inc., United States of America, 2013: pp. 498–529.

[54] F. McGlone, D. Reilly, The cutaneous sensory system, Neurosci. Biobehav. Rev. 34 (2010) 148–159. https://doi.org/10.1016/j.neubiorev.2009.08.004.

[55] A. Zimmerman, L. Bai, D.D. Ginty, The gentle touch receptors of mammalian skin, Science (80-.). 346 (2014) 950–954. https://doi.org/10.1126/science.1254229.

[56] N.D.J. Strzalkowski, R.M. Peters, J.T. Inglis, L.R. Bent, Cutaneous afferent innervation of the human foot sole: what can we learn from single-unit recordings?, J. Neurophysiol. 120 (2018) 1233–1246. https://doi.org/10.1152/jn.00848.2017.

[57] K.O. Johnson, The roles and functions of cutaneous mechanoreceptors, Curr. Opin. Neurobiol. 11 (2001) 455–461.

[58] K.. Hagbarth, B. Vallbo, Mechanoreceptor activity recorded percutaneously with semi-microelectrodes in human peripheral nerves, Acta Physiol. Scand. 69 (1967) 121–122. https://doi.org/10.1111/j.1748-1716.1967.tb03498.x.

[59] P.M. Kennedy, J.T. Inglis, Distribution and behaviour of glabrous cutaneous receptors in the human foot sole, J. Physiol. 538 (2002) 995–1002. https://doi.org/10.1013/jphysiol.2001.013087.

[60] E.P. Zehr, R.B. Stein, What functions do reflexes serve during human locomotion?, Prog. Neurobiol. 58 (1999) 185–205. https://doi.org/10.1016/S0301-0082(98)00081-1.

[61] J. Duysens, C.M. Bastiaanse, B.C.M.M. Smits-Engelsman, V. Dietz, Gait acts as a gate for reflexes from the foot, Can. J. Physiol. Pharmacol. 82 (2004) 715–722. https://doi.org/10.1139/y04-071.

[62] D. Burke, H.G. Dickson, N.F. Skuse, Task-dependent changes in the responses to low-threshold cutaneous afferent volleys in the human lower limb., J. Physiol. 432 (1991) 445–458.

[63] E.P. Zehr, T. Komiyama, R.B. Stein, Cutaneous reflexes during human gait: Electromyographic and kinematic responses to electrical stimulation, J. Neurophysiol. 77 (1997) 3311–3325. https://doi.org/10.1152/jn.1997.77.6.3311.

[64] T. Komiyama, E.P. Zehr, R.B. Stein, Absence of nerve specificity in human cutaneous reflexes during standing, Exp. Brain Res. 133 (2000) 267–272. https://doi.org/10.1007/s002210000411.

[65] J. Duysens, B.M.H. Van Wezel, B. Smits-Engelsman, Modulation of cutaneous reflexes from the foot during gait in Parkinson's disease, J. Neurophysiol. 104 (2010) 230–238. https://doi.org/10.1152/jn.00860.2009.

[66] B.C.M. Baken, V. Dietz, J. Duysens, Phase-dependent modulation of short latency cutaneous reflexes during walking in man, Brain Res. 1031 (2005) 268–275. https://doi.org/10.1016/j.brainres.2004.10.058.

[67] B.M.H. Van Wezel, F.A.M. Ottenhoff, J. Duysens, Dynamic control of location-specific information in tactile cutaneous reflexes from the foot during human walking, J. Neurosci. 17 (1997) 3804–3814.

[68] T. Nakajima, K. Kamibayashi, M. Takahashi, T. Komiyama, M. Akai, K. Nakazawa, Load-related modulation of cutaneous reflexes in the tibialis anterior muscle during passive walking in humans, Eur. J. Neurosci. 27 (2008) 1566–1576. https://doi.org/10.1111/j.1460-9568.2008.06120.x.

[69] G.E.P. Pearcey, E.P. Zehr, We are upright-walking cats: Human limbs as sensory antennae during locomotion, Physiology. 34 (2019) 354–364. https://doi.org/10.1152/physiol.00008.2019.

[70] E.P. Zehr, R.B. Stein, T. Komiyama, Function of sural nerve reflexes during human walking, J. Physiol. 507 (1998) 305–314. https://doi.org/10.1111/j.1469-7793.1998.305bu.x.

[71] P.O. Mckeon, A.J. Stein, C.D. Ingersoll, J. Hertel, Altered Plantar-Receptor Stimulation Impairs Postural Control in Those With Chronic Ankle Instability, J. Sport Rehabil. 21 (2012) 1–6.

[72] L.P. Madsen, K. Kitano, D.M. Koceja, E.P. Zehr, C.L. Docherty, Effects of chronic ankle instability on cutaneous reflex modulation during walking, Exp. Brain Res. 237 (2019) 1959–1971. https://doi.org/10.1007/s00221-019-05565-4.

[73] A.K. Buldt, J.J. Allan, K.B. Landorf, H.B. Menz, The relationship between foot posture and plantar pressure during walking in adults: A systematic review, Gait Posture. 62 (2018) 56–67. https://doi.org/10.1016/j.gaitpost.2018.02.026.

[74] J.W.K. Tong, P.W. Kong, Association between foot type and lower extremity injuries: Systematic literature review with meta-analysis, J. Orthop. Sports Phys. Ther. 43 (2013) 700–714. https://doi.org/10.2519/jospt.2013.4225.

[75] G.S. Murley, K.B. Landorf, H.B. Menz, A.R. Bird, Effect of foot posture, foot orthoses and footwear on lower limb muscle activity during walking and running: A systematic review, Gait Posture. 29 (2009) 172–187. https://doi.org/10.1016/j.gaitpost.2008.08.015.

[76] D.M. Corbin, J.M. Hart, P.O. McKeon, C.D. Ingersoll, J. Hertel, The effect of textured insoles on postural control in double and single limb stance, J. Sport Rehabil. 16 (2007) 363–372. https://doi.org/10.1123/jsr.16.4.363.

[77] R.P.W. Kenny, G. Atkinson, D.L. Eaves, D. Martin, N. Burn, J. Dixon, The effects of textured materials on static balance in healthy young and older adults: A systematic review with meta-analysis, Gait Posture. 71 (2019) 79–86. https://doi.org/10.1016/j.gaitpost.2019.04.017.

[78] R. Collings, J. Paton, N. Chockalingam, T. Gorst, J. Marsden, Effects of the site and extent of plantar cutaneous stimulation on dynamic balance and muscle activity while walking, Foot. 25 (2015) 159–163. https://doi.org/10.1016/j.foot.2015.05.003.

[79] A.L. Hatton, J. Dixon, D. Martin, K. Rome, The effect of textured surfaces on postural stability and lower limb muscle activity, J. Electromyogr. Kinesiol. 19 (2009) 957–964. https://doi.org/10.1016/j.jelekin.2008.04.012.

[80] B.E. Maki, S.D. Perry, R.G. Nome, W.E. Mcllroy, Effect of facilitation of sensation from plantar foot-surface boundaries on postural stabilization in young and older adults, Journals Gerontol. - Ser. A Biol. Sci. Med. Sci. 54 (1999) 281–287. https://doi.org/10.1093/gerona/54.6.M281.

[81] S.D. Perry, A. Radtke, W.E. McIlroy, G.R. Fernie, B.E. Maki, Efficacy and effectiveness of a balance-enhancing insole, J. Gerontol. 63 (2008) 595–602. https://doi.org/10.1093/gerona/63.6.595.
[82] E. Palluel, I. Olivier, V. Nougier, The lasting effects of spike insoles on postural control in the elderly., Behav. Neurosci. 123 (2009) 1141–7. https://doi.org/10.1037/a0017115.
[83] E. Palluel, V. Nougier, I. Olivier, Do spike insoles enhance postural stability and plantar-surface cutaneous sensitivity in the elderly?, Age (Omaha). 30 (2008) 53–61. https://doi.org/10.1007/s11357-008-9047-2.
[84] M.L. Wilson, K. Rome, D. Hodgson, P. Ball, Effect of textured foot orthotics on static and dynamic postural stability in middle-aged females, 27 (2008) 36–42. https://doi.org/10.1016/j.gaitpost.2006.12.006.
[85] A.L. Hatton, J. Dixon, K. Rome, D. Martin, Standing on textured surfaces: effects on standing balance in healthy older adults, Age Ageing. 40 (2011) 363–368. https://doi.org/10.1111/j.
[86] A.L. Hatton, J. Dixon, K. Rome, J.L. Newton, D.J. Martin, Altering gait by way of stimulation of the plantar surface of the foot: the immediate effect of wearing textured insoles in older fallers, J. Foot Ankle Res. 5 (2012) O21. https://doi.org/10.1186/1757-1146-5-S1-O21.
[87] C. de Morais Barbosa, M.B. Bértolo, J.Z. Gaino, M. Davitt, Z. Sachetto, E. de Paiva Magalhães, The effect of flat and textured insoles on the balance of primary care elderly people: A randomized controlled clinical trial, Clin. Interv. Aging. 13 (2018) 277–284. https://doi.org/10.2147/CIA.S149038.
[88] P.L. Li, K.L. Yick, S.P. Ng, J. Yip, Influence of textured indoor footwear on posture stability of older women based on center-of-pressure measurements, Hum. Factors. 61 (2019) 1247–1260. https://doi.org/10.1177/0018720819837414.
[89] R.P.W. Kenny, D.L. Eaves, D. Martin, A.L. Hatton, J. Dixon, The effects of textured insoles on quiet standing balance in four stance types with and without vision, BMC Sports Sci. Med. Rehabil. 11 (2019) 1–8. https://doi.org/10.1186/s13102-019-0117-9.
[90] S.D. Perry, Evaluation of age-related plantar-surface insensitivity and onset age of advanced insensitivity in older adults using vibratory and touch sensation tests, Neurosci. Lett. 392 (2006) 62–67. https://doi.org/10.1016/j.neulet.2005.08.060.
[91] K.A. Robb, S.D. Perry, Textured foot orthotics on dynamic stability and turning performance in Parkinson's disease, J. Mot. Behav. July (2019) 1–8. https://doi.org/10.1080/00222895.2019.1639609.
[92] C. Ritchie, K. Paterson, A.L. Bryant, S. Bartold, R.A. Clark, The effects of enhanced plantar sensory feedback and foot orthoses on midfoot kinematics and lower leg neuromuscular activation, Gait Posture. 33 (2011) 576–581. https://doi.org/10.1016/j.gaitpost.2011.01.012.
[93] M.A. Nurse, M. Hulliger, J.M. Wakeling, B.M. Nigg, D.J. Stefanyshyn, Changing the texture of footwear can alter gait patterns, J. Electromyogr. Kinesiol. 15 (2005) 496–506. https://doi.org/10.1016/j.jelekin.2004.12.003.
[94] M. Wilkinson, A. Ewen, N. Caplan, D. O'leary, N. Smith, R. Stoneham, L. Saxby, Textured insoles reduce vertical loading rate and increase subjective plantar sensation in overground running, Eur. J. Sport Sci. 18 (2018) 497–503. https://doi.org/10.1080/17461391.2018.1444094.
[95] M.E. Jenkins, Q.J. Almeida, S.J. Spaulding, R.B. van Oostveen, J.D. Holmes, A.M. Johnson, S.D. Perry, Plantar cutaneous sensory stimulation improves single-limb support time, and EMG activation patterns among individuals with Parkinson's disease, Park. Relat. Disord. 15 (2009) 697–702. https://doi.org/10.1016/j.parkreldis.2009.04.004.
[96] E. Lirani-Silva, R. Vitório, F.A. Barbieri, D. Orcioli-Silva, L. Simieli, L.T.B. Gobbi, Continuous use of textured insole improve plantar sensation and stride length of people with Parkinson's disease: A pilot study, Gait Posture. 58 (2017) 495–497. https://doi.org/10.1016/j.gaitpost.2017.09.017.
[97] L. Brognara, E. Navarro-flores, L. Iachemet, N. Serra-catalá, O. Cauli, Beneficial effect of foot plantar stimulation in gait parameters in individuals with Parkinson's disease, Brain Sci. 10 (2020) 1–12. https://doi.org/10.3390/brainsci10020069.
[98] F. Qiu, M.H. Cole, K.W. Davids, E.M. Hennig, P.A. Silburn, H. Netscher, G.K. Kerr, Effects of textured insoles on balance in people with Parkinson's disease, PLoS One. 8 (2013) 6–13.

https://doi.org/10.1371/journal.pone.0083309.
[99] A. Elvan, M. Selmani, B. Kara, S. Angin, İ.E. Şimsek, E. İdiman, Effects of textured insoles on static balance tests in patients with multiple sclerosis, J. Exerc. Ther. Rehabil. 4 (2017) 111–117. http://scsu.idm.oclc.org/login?url=http://search.ebscohost.com/login.aspx?direct=true&db=s3h&AN=127891524&site=ehost-live&scope=site.
[100] W.D.L. Gomes, T.B. Scalha, L.B. Mota, V.A. Kuroda, J.C. Garrafa, S.M. Chã, G.D.R. Faria, T.M. de Oliveira, E.W.D.A. Cacho, R.D.O. Cacho, N.M.F.V. Lima, Effects of application of texture insoles on the balance of subjects with Multiple Sclerosis, ConScientiae Saúde. 16 (2017) 9–16. https://doi.org/10.5585/conssaude.v16n1.6860.
[101] K.J. Kelleher, W.D. Spence, S. Solomonidis, D. Apatsidis, The effect of textured insoles on gait patterns of people with multiple sclerosis, Gait Posture. 32 (2010) 67–71. https://doi.org/10.1016/j.gaitpost.2010.03.008.
[102] J. Dixon, A.L. Hatton, J. Robinson, H. Gamesby-Iyayi, D. Hodgson, K. Rome, R. Warnett, D.J. Martin, Effect of textured insoles on balance and gait in people with multiple sclerosis: An exploratory trial, Physiother. (United Kingdom). 100 (2014) 142–149. https://doi.org/10.1016/j.physio.2013.06.003.
[103] A. Kalron, D. Pasitselsky, M. Greenberg-Abrahami, A. Achiron, Do textured insoles affect postural control and spatiotemporal parameters of gait and plantar sensation in people with multiple sclerosis?, PM R. 7 (2015) 17–25. https://doi.org/10.1016/j.pmrj.2014.08.942.
[104] H. Park, The effects of textured insoles on balance in individuals with knee osteoarthritis, Int. J. Hum. Mov. Sport. Sci. 6 (2018) 10–18. https://doi.org/10.13189/saj.2018.060102.
[105] T. Vieira, A. Botter, L. Gastaldi, I.C.N.N. Sacco, F. Martelli, C. Giacomozzi, Textured insoles affect the plantar pressure distribution while elite rowers perform on an indoor rowing machine., PLoS One. 12 (2017) e0187202. https://doi.org/10.1371/journal.pone.0187202.
[106] G. Waddington, R. Adams, Football boot insoles and sensitivity to extent of ankle inversion movement, Br. J. Sports Med. 37 (2003) 170–174. https://doi.org/10.1136/bjsm.37.2.170.
[107] H. Hasan, K. Davids, J.Y. Chow, G. Kerr, Changes in organisation of instep kicking as a function of wearing compression and textured materials, Eur. J. Sport Sci. 17 (2017) 294–302. https://doi.org/10.1080/17461391.2016.1241829.
[108] G. Waddington, R. Adams, Textured insole effects on ankle movement discrimination while wearing athletic shoes, Phys. Ther. Sport. 1 (2000) 119–128. https://doi.org/10.1054/ptsp.2000.0020.
[109] N. Steinberg, G. Waddington, R. Adams, J. Karin, O. Tirosh, Should ballet dancers vary postures and underfoot surfaces when practicing postural balance?, Motor Control. 22 (2018) 45–66. https://doi.org/10.1123/mc.2016-0076.
[110] A. Jamali, S. Forghany, K. Bapirzadeh, C.J. Nester, The effect of three different insoles on ankle movement variability during walking in athletes with functinpoal ankle instability, Adv. Biomed. Res. 6 (2019) 1–13. https://doi.org/10.4103/abr.abr.
[111] A.S. Aruin, N. Kanekar, Effect of a textured insole on balance and gait symmetry, Exp. Brain Res. 231 (2013) 201–208. https://doi.org/10.1007/s00221-013-3685-z.
[112] E. Curuk, Y. Lee, A.S. Aruin, The effect of a textured insole on symmetry of turning, Rehabil. Res. Pract. 2018 (2018) 1–6. https://doi.org/10.1155/2018/6134529.
[113] C.C. Ma, Y.J. Lee, B. Chen, A.S. Aruin, Immediate and short-term effects of wearing a single textured insole on symmetry of stance and gait in healthy adults, Gait Posture. 49 (2016) 190–195. https://doi.org/10.1016/j.gaitpost.2016.07.010.
[114] H. Chen, B.M. Nigg, M. Hulliger, J. de Koning, Influence of sensory input on plantar pressure distribution, Clin. Biomech. 10 (1995) 271–274. https://doi.org/10.1016/0268-0033(95)99806-D.
[115] W.-T. Lo, D.P. Wong, K.-L. Yick, S.P. Ng, J. Yip, The biomechanical effects and perceived comfort of textile-fabricated insoles during straight line walking, Prosthet. Orthot. Int. (2017) 030936461769608. https://doi.org/10.1177/0309364617696084.

[116] M. Hollins, S.J. Bensmaa, E.A. Roy, Vibrotaction and texture perception, Behav. Brain Res. 135 (2002) 51–56. https://doi.org/10.1016/S0166-4328(02)00154-7.

[117] A.I. Weber, H.P. Saal, J.D. Lieber, J.W. Cheng, L.R. Manfredi, J.F. Dammann, S.J. Bensmaia, Spatial and temporal codes mediate the tactile perception of natural textures, Proc. Natl. Acad. Sci. U. S. A. 110 (2013) 17107–17112. https://doi.org/10.1073/pnas.1305509110.

[118] M.A. Nurse, B.M. Nigg, The effect of changes in foot sensation on plantar pressure and muscle activity, Clin. Biomech. 16 (2001) 719–727. https://doi.org/10.1016/S0268-0033(01)00090-0.

[119] C. Ritchie, K. Paterson, A.L. Bryant, S. Bartold, R.A. Clark, The effects of enhanced plantar sensory feedback and foot orthoses on midfoot kinematics and lower leg neuromuscular activation, Gait Posture. 33 (2011) 576–581. https://doi.org/10.1016/j.gaitpost.2011.01.012.

[120] R.P.W.W. Kenny, D.L. Eaves, D. Martin, A.L. Hatton, J. Dixon, The effects of textured insoles on quiet standing balance in four stance types with and without vision, BMC Sports Sci. Med. Rehabil. 11 (2019) 1–8. https://doi.org/10.1186/s13102-019-0117-9.

[121] E. Lirani-Silva, R. Vitório, F. Augusto, D. Orcioli-Silva, L. Simieli, L. Teresa, B. Gobbi, F.A. Barbieri, D. Orcioli-Silva, L. Simieli, L.T.B. Gobbi, Continuous use of textured insole improve plantar sensation and stride length of people with Parkinson's disease: A pilot study, Gait Posture. 58 (2017) 495–497. https://doi.org/10.1016/j.gaitpost.2017.09.017.

[122] W.-T.T. Lo, D.P. Wong, K.-L.L. Yick, S.P. Ng, J. Yip, The biomechanical effects and perceived comfort of textile-fabricated insoles during straight line walking, Prosthet. Orthot. Int. 42 (2017) 153–162. https://doi.org/10.1177/0309364617696084.

[123] W.T. Lo, D.P. Wong, K.L. Yick, S.P. Ng, J. Yip, Effects of custom-made textile insoles on plantar pressure distribution and lower limb EMG activity during turning, J. Foot Ankle Res. 9 (2016) 1–13. https://doi.org/10.1186/s13047-016-0154-5.

[124] S.D. Perry, A. Radtke, W.E. McIlroy, G.R. Fernie, B.E. Maki, Efficacy and Effectiveness of a Balance-Enhancing Insole, J. Gerontol. 63A (2008) 595–602.

[125] F.J.F. Viseux, The sensory role of the sole of the foot: Review and update on clinical perspectives, Neurophysiol. Clin. 50 (2020) 55–68. https://doi.org/10.1016/j.neucli.2019.12.003.

[126] E.P. Zehr, R.B. Stein, T. Komiyama, Non-noxious electrical stimulation of cutaneous nerves during human walking, J. Physiol. 1 (1998) 10. https://www.ncbi.nlm.nih.gov/pmc/articles/PMC2230764/pdf/tjp0507-0305.pdf.

[127] B.M.H. Van Wezel, F.A.M. Ottenhoff, J. Duysens, Dynamic control of location-specific information in tactile cutaneous reflexes from the foot during human walking, J. Neurosci. 17 (1997) 3804–3814.

[128] M.A. Nurse, M. Hulliger, J.M. Wakeling, B.M. Nigg, D.J. Stefanyshyn, Changing the texture of footwear can alter gait patterns, J. Electromyogr. Kinesiol. 15 (2005) 496–506. https://doi.org/10.1016/j.jelekin.2004.12.003.

[129] E.P. Zehr, T. Nakajima, T. Barss, T. Klarner, S. Miklosovic, R.A. Mezzarane, M. Nurse, T. Komiyama, Cutaneous stimulation of discrete regions of the sole during locomotion produces "sensory steering" of the foot, BMC Sports Sci. Med. Rehabil. 6 (2014) 1–23. https://doi.org/10.1186/2052-1847-6-33.

[130] E.P. Zehr, K. Fujita, R.B. Stein, Reflexes from the superficial peroneal nerve during walking in stroke subjects., J. Neurophysiol. 79 (1998) 848–858. https://doi.org/10.1152/jn.1998.79.2.848.

[131] J.B. Fallon, L.R. Bent, P. a McNulty, V.G. Macefield, Evidence for strong synaptic coupling between single tactile afferents from the sole of the foot and motoneurons supplying leg muscles, J. Neurophysiol. 94 (2005) 3795–3804. https://doi.org/10.1152/jn.00359.2005.

[132] T. Nakajima, M. Sakamoto, T. Tazoe, T. Endoh, T. Komiyama, Location specificity of plantar cutaneous reflexes involving lower limb muscles in humans., Exp. Brain Res. 175 (2006) 514–525. https://doi.org/10.1007/s00221-006-0568-6.

[133] A. Perotto, Anatomical Guide for the Electromyographer - The limbs and trunk, Fifth, Charles C Thomas, Springfield, Illinois, 2011.

[134] J. Reeves, C. Starbuck, C. Nester, EMG gait data from indwelling electrodes is attenuated over time and changes independent of any experimental effect, J. Electromyogr. Kinesiol. 54 (2020).
[135] D. Purves, G.J. Augustine, D. Fitzpatrick, W.C. Hall, A.-S. LaMantia, R.D. Mooney, M.L. Platt, L.E. White, Lower Motor Neuron Circuits and Motor Control, in: Neuroscience, 6th ed., Oxford University Press, United States of America, 2018: pp. 357–379.
[136] G.S. Murley, K.B. Landorf, H.B. Menz, Do foot orthoses change lower limb muscle activity in flat-arched feet towards a pattern observed in normal-arched feet?, Clin. Biomech. 25 (2010) 728–736. https://doi.org/10.1016/j.clinbiomech.2010.05.001.
[137] J.N. Maharaj, A.G. Cresswell, G.A. Lichtwark, The mechanical function of the tibialis posterior muscle and its tendon during locomotion, J. Biomech. 49 (2016) 3238–3243. https://doi.org/10.1016/j.jbiomech.2016.08.006.
[138] H. Akuzawa, A. Imai, S. Iizuka, N. Matsunaga, K. Kaneoka, Calf muscle activity alteration with foot orthoses insertion during walking measured by fine-wire electromyography, J. Phys. Ther. Sci. 28 (2016) 3458–3462. https://doi.org/10.1589/jpts.28.3458.
[139] R. Semple, G.S. Murley, J. Woodburn, D.E. Turner, Tibialis posterior in health and disease: a review of structure and function with specific reference to electromyographic studies, J. Foot Ankle Res. 2 (2009) 1–8. https://doi.org/10.1186/1757-1146-2-24.
[140] J. Kohls-Gatzoulis, J.C. Angel, D. Singh, F. Haddad, J. Livingstone, G. Berry, Tibialis posterior dysfunction: A common and treatable cause of adult acquired flatfoot, Br. Med. J. 329 (2004) 1328–1333. https://doi.org/10.1136/bmj.329.7478.1328.
[141] M.P. Côté, L.M. Murray, M. Knikou, Spinal control of locomotion: Individual neurons, their circuits and functions, Front. Physiol. 9 (2018) 1–27. https://doi.org/10.3389/fphys.2018.00784.
[142] M.A. Richard, E.G. Spaich, M. Serrao, O.K. Andersen, Stimulation site and phase modulation of the withdrawal reflex during gait initiation, Clin. Neurophysiol. 126 (2015) 2282–2289. https://doi.org/10.1016/j.clinph.2015.01.019.
[143] E.G. Spaich, J. Emborg, T. Collet, L. Arendt-Nielsen, O.K. Andersen, Withdrawal reflex responses evoked by repetitive painful stimulation delivered on the sole of the foot during late stance: Site, phase, and frequency modulation, Exp. Brain Res. 194 (2009) 359–368. https://doi.org/10.1007/s00221-009-1705-9.
[144] J.N. Maharaj, S. Kessler, M.J. Rainbow, S.E. D'Andrea, N. Konow, L.A. Kelly, G.A. Lichtwark, The Reliability of Foot and Ankle Bone and Joint Kinematics Measured With Biplanar Videoradiography and Manual Scientific Rotoscoping, Front. Bioeng. Biotechnol. 8 (2020) 1–11. https://doi.org/10.3389/fbioe.2020.00106.
[145] L.A. Kelly, G. Lichtwark, A.G. Cresswell, A.G. Cresswell, Active regulation of longitudinal arch compression and recoil during walking and running, J. R. Soc. Interface. 12 (2015).
[146] K.A. Robb, H.D. Melady, S.D. Perry, Fine-wire electromyography of the transverse head of adductor hallucis during locomotion, Gait Posture. 85 (2021) 7–13. https://doi.org/10.1016/j.gaitpost.2020.12.020.
[147] L. Welte, L.A. Kelly, G.A. Lichtwark, M.J. Rainbow, Influence of the windlass mechanism on arch-spring mechanics during dynamic foot arch deformation, J. R. Soc. Interface. 15 (2018). https://doi.org/10.1098/rsif.2018.0270.
[148] R. Riddick, D.J. Farris, L.A. Kelly, R. Riddick, The foot is more than a spring : human foot muscles perform work to adapt to the energetic requirements of locomotion, R. Soc. (2019) 5. https://doi.org/10.1098/rsif.2018.0680.
[149] G. Moisan, M. Descarreaux, V. Cantin, Muscle activation during fast walking with two types of foot orthoses in participants with cavus feet, J. Electromyogr. Kinesiol. 43 (2018) 7–13. https://doi.org/10.1016/j.jelekin.2018.08.002.
[150] J.N. Maharaj, A.G. Cresswell, G.A. Lichtwark, The Immediate Effect of Foot Orthoses on Subtalar Joint Mechanics and Energetics, Med. Sci. Sport. Exerc. 50 (2018) 1449–1456. https://doi.org/10.1249/MSS.0000000000001591.

[151] J.K. Choi, E.J. Cha, K.A. Kim, Y. Won, J.J. Kim, Effects of custom-made insoles on idiopathic pes cavus foot during walking, Biomed. Mater. Eng. 26 (2015) S705–S715. https://doi.org/10.3233/BME-151362.
[152] S. Fuglkjær, K.B. Dissing, L. Hestbæk, Prevalence and incidence of musculoskeletal extremity complaints in children and adolescents. A systematic review, BMC Musculoskelet. Disord. 18 (2017). https://doi.org/10.1186/s12891-017-1771-2.
[153] M. Oh-Park, J. Kirschner, D. Abdelshahed, D.D.J. Kim, Painful Foot Disorders in the Geriatric Population: A Narrative Review, Am. J. Phys. Med. Rehabil. 98 (2019) 811–819. https://doi.org/10.1097/PHM.0000000000001239.
[154] K.A. Robb, J.D. Hyde, S.D. Perry, The role of enhanced plantar-surface sensory feedback on lower limb EMG during planned gait termination, Somatosens. Mot. Res. 38 (2021) 146–156. https://doi.org/10.1080/08990220.2021.1904870.
[155] R. Mann, V.T. Inman, Phasic activity of intrinsic muscles of the foot, J. Bone Jt. Surg. 46-A (1964) 469–481.
[156] D.J. Farris, J. Birch, L. Kelly, Foot stiffening during the push-off phase of human walking is linked to active muscle contraction, and not the windlass mechanism, J. R. Soc. Interface. 17 (2020). https://doi.org/10.1098/rsif.2020.0208rsif20200208.
[157] K.E. Zelik, V. La Scaleia, Y.P. Ivanenko, F. Lacquaniti, Coordination of intrinsic and extrinsic foot muscles during walking, Eur. J. Appl. Physiol. 115 (2015) 691–701. https://doi.org/10.1007/s00421-014-3056-x.
[158] L.A. Kelly, G.A. Lichtwark, D.J. Farris, A. Cresswell, Shoes alter the spring-like function of the human foot during running, J. R. Soc. Interface. 13 (2016). https://doi.org/10.1098/rsif.2016.0174.
[159] H. Baur, A. Hirschmueller, S. Mueller, F. Mayer, A. Hirschmüller, S. Müller, F. Mayer, Neuromuscular activity of the peroneal muscle after foot orthoses therapy in runners, Med. Sci. Sports Exerc. 43 (2011) 1500–1506. https://doi.org/10.1249/MSS.0b013e31820c64ae.
[160] J. Hertel, B.R. Sloss, J.E. Earl, Effect of foot orthotics on quadriceps and gluteus medius electromyographic activity during selected exercises, Arch. Phys. Med. Rehabil. 86 (2005) 26–30. https://doi.org/10.1016/j.apmr.2004.03.029.
[161] G. Moisan, V. Cantin, M. G., G. Moisan, V. Cantin, Effects of two types of foot orthoses on lower limb muscle activity before and after a one-month period of wear, Gait Posture. 46 (2016) 75–80. https://doi.org/http://dx.doi.org/10.1016/j.gaitpost.2016.02.014.
[162] K. Protopapas, S.D. Perry, The effect of a 12-week custom foot orthotic intervention on muscle size and muscle activity of the intrinsic foot muscle of young adults during gait termination, Clin. Biomech. 78 (2020) 105063. https://doi.org/10.1016/j.clinbiomech.2020.105063.
[163] M.J. MacLellan, A.E. Patla, Adaptations of walking pattern on a compliant surface to regulate dynamic stability, Exp. Brain Res. 173 (2006) 521–530. https://doi.org/10.1007/s00221-006-0399-5.
[164] D.S. Marigold, A.E. Patla, Adapting locomotion to different surface compliances: Neuromuscular responses and changes in movement dynamics, J. Neurophysiol. 94 (2005) 1733–1750. https://doi.org/10.1152/jn.00019.2005.
[165] J. Hamill, K.M. Knutzen, T.R. Derrick, Angular Kinematics, in: Biomech. Basis Hum. Mov., Fourth, Lippincott Williams & Wilkins, Philadelphia, PA, 2015: pp. 318–345.
[166] M.M. Rodgers, Dynamic biomechanics of the normal foot and ankle during walking and running, Phys. Ther. Rehabil. J. 68 (1988) 1822–1830.
[167] D.J. Farris, L.A. Kelly, A.G. Cresswell, G.A. Lichtwark, D. James, L.A. Kelly, A.G. Cresswell, G.A. Lichtwark, The functional importance of human foot muscles for bipedal locomotion, Proc. Natl. Acad. Sci. U. S. A. 116 (2019) 1645–1650. https://doi.org/10.1073/pnas.1812820116.
[168] R.J. Butler, I.S. Davis, J. Hamill, Interaction of arch type and footwear on running mechanics, Am. J. Sports Med. 34 (2006) 1998–2005. https://doi.org/10.1177/0363546506290401.
[169] K.P. Cote, M.E.B. Ii, B.M. Gansneder, S.J. Shultz, Effects of Pronated and Supinated Foot Postures on Static and Dynamic Postural Stability, J. Athl. Train. 40 (2005) 41–46.
[170] V. Lugade, K. Kaufman, Center of pressure trajectory during gait: A comparison of four foot positions,

Gait Posture. 40 (2014) 719–722. https://doi.org/10.1016/j.gaitpost.2014.07.001.
[171] A.K. Buldt, S. Forghany, K.B. Landorf, G.S. Murley, P. Levinger, H.B. Menz, Centre of pressure characteristics in normal, planus and cavus feet, J. Foot Ankle Res. 11 (2018) 1–9. https://doi.org/10.1186/s13047-018-0245-6.
[172] P. Levinger, G.S. Murley, C.J. Barton, M.P. Cotchett, S.R. McSweeney, H.B. Menz, A comparison of foot kinematics in people with normal- and flat-arched feet using the Oxford Foot Model, Gait Posture. 32 (2010) 519–523. https://doi.org/10.1016/j.gaitpost.2010.07.013.
[173] M. Razeghi, M.E. Batt, Foot type classification: a critical review of methods, Gait Posture. 15 (2002) 282–291.
[174] A.C. Redmond, J. Crosbie, R.A. Ouvrier, Development and validation of a novel rating system for scoring standing foot posture : The Foot Posture Index, 21 (2006) 89–98. https://doi.org/10.1016/j.clinbiomech.2005.08.002.
[175] P. McLaughlin, B. Vaughan, J. Shanahan, J. Martin, G. Linger, Inexperienced examiners and the Foot Posture Index: A reliability study, Man. Ther. 26 (2016) 238–240. https://doi.org/10.1016/j.math.2016.06.009.
[176] M.W. Cornwall, T.G. McPoil, Relationship between static foot posture and foot mobility, J. Foot Ankle Res. 4 (2011) 1–9. https://doi.org/10.1186/1757-1146-4-4.
[177] A. Aboutorabi, M. Arazpour, S.W. Hutchins, S. Curran, M. Maleki, The efficacy of foot orthoses on alteration to center of pressure displacement in subjects with flat and normal feet: A literature review, Disabil. Rehabil. Assist. Technol. 10 (2015) 439–444. https://doi.org/10.3109/17483107.2014.913716.
[178] G.S. Murley, K.B. Landorf, H.B. Menz, Do foot orthoses change lower limb muscle activity in flat-arched feet towards a pattern observed in normal-arched feet?, Clin. Biomech. 25 (2010) 728–736. https://doi.org/10.1016/j.clinbiomech.2010.05.001.
[179] Y.C. Chen, S.Z. Lou, C.Y. Huang, F.C. Su, Effects of foot orthoses on gait patterns of flat feet patients, Clin. Biomech. 25 (2010) 265–270. https://doi.org/10.1016/j.clinbiomech.2009.11.007.
[180] M. Eslami, C. Tanaka, S. Hinse, M. Anbarian, P. Allard, Acute effect of orthoses on foot orientation and perceived comfort in individuals with pes cavus during standing, Foot. 19 (2009) 1–6. https://doi.org/10.1016/j.foot.2008.06.004.
[181] C.T.F. Tse, M.B. Ryan, M.A. Hunt, Influence of foot posture on immediate biomechanical responses during walking to variable-stiffness supported lateral wedge insole designs, Gait Posture. 81 (2020) 21–26. https://doi.org/10.1016/j.gaitpost.2020.06.026.
[182] H. Hermens, B. Freriks, R. Merletti, D. Stegeman, J. Blok, G. Rau, C. Disselhorst-Klug, G. Hägg, SENIAM - European recommendations for surface electromyography, (1999).
[183] K.M. Kruger, A. Graf, A. Flanagan, B.D. McHenry, H. Altiok, P.A. Smith, G.F. Harris, J.J. Krzak, Segmental foot and ankle kinematic differences between rectus, planus, and cavus foot types, J. Biomech. 94 (2019) 180–186. https://doi.org/10.1016/j.jbiomech.2019.07.032.
[184] R. Wang, E.M. Gutierrez-Farewik, The effect of subtalar inversion/eversion on the dynamic function of the tibialis anterior, soleus, and gastrocnemius during the stance phase of gait, Gait Posture. 34 (2011) 29–35. https://doi.org/10.1016/j.gaitpost.2011.03.003.
[185] A. Manoli, B. Graham, Clinical and new aspects of the subtle cavus foot: A review of an additional twelve year experience, Fuss Und Sprunggelenk. 16 (2018) 3–29. https://doi.org/10.1016/j.fuspru.2017.11.006.
[186] I. Arias-Martín, M. Reina-Bueno, P. V. Munuera-Martínez, Effectiveness of custom-made foot orthoses for treating forefoot pain: a systematic review, Int. Orthop. 42 (2018) 1865–1875. https://doi.org/10.1007/s00264-018-3817-y.
[187] J.L. McCrory, M.J. Young, A.J.M. Boulton, P.R. Cavanagh, Arch index as a predictor of arch height, Foot. 7 (1997) 79–81. https://doi.org/10.1016/S0958-2592(97)90052-3.
[188] H.B. Menz, Clinical hindfoot measurement: a critical review of the literature, Foot. 5 (1995) 57–64. https://doi.org/10.1016/0958-2592(95)90012-8.

[189] T. Prachgosin, D.Y.R. Chong, W. Leelasamran, P. Smithmaitrie, S. Chatpun, Medial longitudinal arch biomechanics evaluation during gait in subjects with flexible flatfoot, Acta Bioeng. Biomech. 17 (2015) 121–130. https://doi.org/10.5277/ABB-00296-2015-02.
[190] S. Angin, K.J. Mickle, C.J. Nester, Contributions of foot muscles and plantar fascia morphology to foot posture, Gait Posture. 61 (2018) 238–242. https://doi.org/10.1016/j.gaitpost.2018.01.022.
[191] K.M. Kruger, A. Graf, A. Flanagan, B.D. McHenry, H. Altiok, P.A. Smith, G.F. Harris, J.J. Krzak, Segmental foot and ankle kinematic differences between rectus, planus, and cavus foot types, J. Biomech. 94 (2019) 180–186. https://doi.org/10.1016/j.jbiomech.2019.07.032.
[192] S. Taş, N.Ö. Ünlüer, F. Korkusuz, Morphological and mechanical properties of plantar fascia and intrinsic foot muscles in individuals with and without flat foot, J. Orthop. Surg. 26 (2018) 1–6. https://doi.org/10.1177/2309499018802482.
[193] S. Taş, A. Çetin, An investigation of the relationship between plantar pressure distribution and the morphologic and mechanic properties of the intrinsic foot muscles and plantar fascia, Gait Posture. 72 (2019) 217–221. https://doi.org/10.1016/j.gaitpost.2019.06.021.
[194] K. Sakamoto, S. Kudo, Morphological characteristics of intrinsic foot muscles among flat foot and normal foot using ultrasonography, Acta Bioeng. Biomech. 22 (2020) 161–166. https://doi.org/10.37190/ABB-01713-2020-02.
[195] S. Angin, G. Crofts, K.J. Mickle, C.J. Nester, Ultrasound evaluation of foot muscles and plantar fascia in pes planus, Gait Posture. 40 (2014) 48–52. https://doi.org/10.1016/j.gaitpost.2014.02.008.
[196] K. Okamura, K. Egawa, T. Ikeda, K. Fukuda, S. Kanai, Relationship between foot muscle morphology and severity of pronated foot deformity and foot kinematics during gait: A preliminary study, Gait Posture. 86 (2021) 273–277. https://doi.org/10.1016/j.gaitpost.2021.03.034.
[197] P.O. McKeon, J. Hertel, D. Bramble, I. Davis, The foot core system: a new paradigm for understanding intrinsic foot muscle function, Br. J. Sports Med. 49 (2015) 1–9. https://doi.org/10.1136/bjsports-2013-092690.
[198] S. Delacroix, A. Lavigne, D. Nuytens, L. Cheze, Effect of custom foot orthotics on three-dimensional kinematics and dynamics during walking, Comput. Methods Biomech. Biomed. Engin. 17 (2014) 82–83.
[199] A. Stacoff, I.K. de Quervain, M. Dettwyler, P. Wolf, R. List, T. Ukelo, Biomechanical effects of foot orthoses during walking, Foot. 17 (2007) 143–153. https://doi.org/http://dx.doi.org/10.1016/j.foot.2007.02.004.
[200] D. Bonifácio, J. Richards, J. Selfe, S. Curran, R. Trede, Influence and benefits of foot orthoses on kinematics, kinetics and muscle activation during step descent task, Gait Posture. 65 (2018) 106–111. https://doi.org/10.1016/j.gaitpost.2018.07.041.
[201] R. Barn, M. Brandon, D. Rafferty, R.D. Sturrock, M. Steultjens, D.E. Turner, J. Woodburn, Kinematic, kinetic and electromyographic response to customized foot orthoses in patients with tibialis posterior tenosynovitis, pes plano valgus and rheumatoid arthritis, Rheumatol. (United Kingdom). 53 (2014) 123–130. https://doi.org/10.1093/rheumatology/ket337.
[202] A. Mündermann, B.M. Nigg, R.N.N. Humble, D. Stefanyshyn, Consistent immediate effects of foot orthoses on comfort and lower extremity kinematics, kinetics, and muscle activity, J. Appl. Biomech. 20 (2004) 71–84. http://libproxy.wlu.ca/login?url=http://search.ebscohost.com/login.aspx?direct=true&AuthType=ip,cookie,url,uid&db=sph&AN=12256275&site=ehost-live.
[203] G.S. Murley, A.R. Bird, M. GS, B. AR, G.S. Murley, A.R. Bird, M. G.S., The effect of three levels of foot orthotic wedging on the surface electromyographic activity of selected lower limb muscles during gait, Clin. Biomech. 21 (2006) 1074–1080. https://doi.org/10.1016/j.clinbiomech.2006.06.007.
[204] D. Hinkle, W. Wiersma, S. Jurs, Applied Statistics for the Behavioral Sciences, 5th ed., Houghton Mifflin, Boston, 2003.
[205] A.K. Buldt, P. Levinger, G.S. Murley, H.B. Menz, C.J. Nester, K.B. Landorf, Foot posture is associated with kinematics of the foot during gait: A comparison of normal, planus and cavus feet, Gait Posture. 42

(2015) 42–48. https://doi.org/10.1016/j.gaitpost.2015.03.004.
[206] P. Fiolkowski, D. Brunt, M. Bishop, R. Woo, M. Horodyski, L. Atc, Intrinsic Pedal Musculature Support of the Medial Longitudinal Arch : An Electromyography Study, 42 (2003). https://doi.org/10.1053/j.jfas.2003.10.003.
[207] K. Okamura, S. Kanai, M. Hasegawa, A. Otsuka, S. Oki, The effect of additional activation of the plantar intrinsic foot muscles on foot dynamics during gait, Foot. 34 (2018) 1–5. https://doi.org/10.1016/j.foot.2017.08.002.
[208] L.A. Kelly, A.G. Cresswell, S. Racinais, R. Whiteley, G. Lichtwark, Intrinsic foot muscles have the capacity to control deformation of the longitudinal arch, J. R. Soc. Interface. 11 (2014) 20131188. https://doi.org/10.1098/rsif.2013.1188.
[209] D.L. Headlee, J.L. Leonard, J.M. Hart, C.D. Ingersoll, J. Hertel, Fatigue of the plantar intrinsic foot muscles increases navicular drop, J. Electromyogr. Kinesiol. 18 (2008) 420–425. https://doi.org/10.1016/j.jelekin.2006.11.004.
[210] X. Zhang, K.H. Schütte, B. Vanwanseele, Foot muscle morphology is related to center of pressure sway and control mechanisms during single-leg standing, Gait Posture. 57 (2017) 52–56. https://doi.org/10.1016/j.gaitpost.2017.05.027.
[211] E.P. Mulligan, P.G. Cook, Effect of plantar intrinsic muscle training on medial longitudinal arch morphology and dynamic function, Man. Ther. 18 (2013) 425–430. https://doi.org/10.1016/j.math.2013.02.007.
[212] P.O. McKeon, F. Fourchet, Freeing the Foot Integrating the Foot Core System into Rehabilitation for Lower Extremity Injuries, Clin. Sports Med. 34 (2015) 347+. https://doi.org/10.1016/j.csm.2014.12.002.
[213] B.S. Neal, I.B. Griffiths, G.S. Murley, S.E. Munteanu, M.M. Franettovich Smith, N.J. Collins, C.J. Barton, Foot posture as a risk factor for lower limb overuse injury: a systematic review and meta-analysis, J. Foot Ankle Res. 7 (2014) 1–13. https://doi.org/10.1002/hon.2377.
[214] B.M. Nigg, M.M. Mohr, S.R. Nigg, Muscle tuning and preferred movement path – a paradigm shift, Curr. Issues Sport Sci. 2 (2017) 1–12. https://doi.org/10.15203/ciss_2017.007.
[215] P. Zehr, T. Nakajima, T. Barss, T. Klarner, S. Miklosovic, R.A. Mezzarane, M. Nurse, T. Komiyama, Cutaneous stimulation of discrete regions of the sole during locomotion produces “sensory steering” of the foot, BMC Sports Sci. Med. Rehabil. 6 (2014) 33. https://doi.org/10.1186/2052-1847-6-33.
[216] R. Collings, J. Paton, N. Chockalingam, T. Gorst, J. Marsden, Effects of the site and extent of plantar cutaneous stimulation on dynamic balance and muscle activity while walking, Foot. 25 (2015) 159–163. https://doi.org/10.1016/j.foot.2015.05.003.
[217] A.L. Hatton, J. Dixon, K. Rome, D. Martin, Standing on textured surfaces: effects on standing balance in healthy older adults, Age Ageing. 40 (2011) 363–368. https://doi.org/10.1093/ageing/afr026.
[218] C. Ritchie, K. Paterson, A.L. Bryant, S. Bartold, R.A. Clark, The effects of enhanced plantar sensory feedback and foot orthoses on midfoot kinematics and lower leg neuromuscular activation, Gait Posture. 33 (2011) 576–581. https://doi.org/10.1016/j.gaitpost.2011.01.012.
[219] K. a Stern, J.S. Gottschall, Altering footwear type influences gait during level walking and downhill transitions, J. Appl. Biomech. 28 (2012) 481–490. https://doi.org/10.1123/jab.28.5.481.
[220] K. Bapirzadeh, A. Jamali, S. Forghany, C. Nester, S. Tavakoli, F. Hemmati, The effect of three different insoles on balance in people with functional ankle instability, J. Foot Ankle Res. 7 (2014) A19. https://doi.org/10.1186/1757-1146-7-s1-a19.
[221] D.J. Clark, E.A. Christou, S.A. Ring, J.B. Williamson, L. Doty, Enhanced somatosensory feedback reduces prefrontal cortical activity during walking in older adults, Journals Gerontol. - Ser. A Biol. Sci. Med. Sci. 69 (2014) 1422–1428. https://doi.org/10.1093/gerona/glu125.
[222] A. Kalron, D. Pasitselsky, M. Greenberg-Abrahami, A. Achiron, Do textured insoles affect postural control and spatiotemporal parameters of gait and plantar sensation in people with multiple sclerosis?, PM R. 7 (2015) 17–25. https://doi.org/10.1016/j.pmrj.2014.08.942.

[223] E. Lirani-Silva, R. Vitório, F.A. Barbieri, A.M. Baptista, P.C.R. Dos Santos, L.T.B. Gobbi, Different types of additional somatosensory information do not promote immediate benefits on gait in patients with Parkinson’s disease and older adults, Motriz. Rev. Educ. Fis. 21 (2015) 244–249. https://doi.org/10.1590/S1980-65742015000300004.
[224] W.T. Lo, D.P. Wong, K.L. Yick, S.P. Ng, J. Yip, L. W.T., W. D.P., Y. K.L., N. S.P., Effects of custom-made textile insoles on plantar pressure distribution and lower limb EMG activity during turning, J. Foot Ankle Res. 9 (2016) 22. https://doi.org/http://dx.doi.org/10.1186/s13047-016-0154-5.
[225] N. Steinberg, G. Waddington, R. Adams, J. Karin, O. Tirosh, The effect of textured ballet shoe insoles on ankle proprioception in dancers, Phys. Ther. Sport. 17 (2016) 38–44. https://doi.org/10.1016/j.ptsp.2015.04.001.
[226] M.L. Wilson, K. Rome, D. Hodgson, P. Ball, Effect of textured foot orthotics on static and dynamic postural stability in middle-aged females, Gait Posture. 27 (2008) 36–42. https://doi.org/10.1016/j.gaitpost.2006.12.006.